

**Radical additions of hydrocarbons, ethers and acetals to alkenes via allyl transfer  
reaction: A new chain reaction for C-H bond functionalization**

Shradha V. Patil

Dissertation submitted to the faculty of the Virginia Polytechnic Institute and State  
University in partial fulfillment of the requirements for the degree of

**Doctor of Philosophy**

**In**

**Chemistry**

James M. Tanko, Chair

Paul R. Carlier

Neal Castagnoli Jr.

Karen J. Brewer

April 4, 2013

Blacksburg, Virginia

Keywords: Allyl transfer, Phthalimido-*N*-oxyl radical, Radical additions, Hydrocarbons,  
Ethers, Chain reactions, Kinetics

Copyright 2013, Shradha V. Patil

**Radical additions of hydrocarbons, ethers and acetals to alkenes via allyl transfer reaction: A new chain reaction for C-H bond functionalization**

Shradha V. Patil

ABSTRACT

Functionalization of hydrocarbons via a free-radical based allyl transfer reaction using various allyl bromide substrates has been previously studied. The work described in this dissertation focuses on the replacement of Br• by phthalimido-*N*-oxyl (PINO•) which helps make this chemistry environmentally friendly. To replace Br• with PINO•, replacement of previously used allyl-bromide substrates with new allyl-PINO substrates were necessary. Various allyl-PINO compounds were synthesized and the use of these allyl-phthalimido-*N*-oxyl (allyl-PINO) compounds for the functionalization of various alkyl aromatic hydrocarbons is demonstrated. Kinetic studies were performed to observe the efficiency of the new chain reaction compared to the previously reported studies with allyl-bromides.

We recently discovered that these allyl substrates are useful for the functionalization of ethers and acetals. The functionalization of various cyclic and acyclic ethers was performed using these allyl transfer reactions. This reaction was also performed in-solution, which allowed us to perform these reactions at low reagent concentrations. Kinetic chain lengths were measured for these reactions. High chain lengths were observed for all used ethers.

Kinetic studies to investigate the rate of radical addition-elimination processes were performed using laser flash photolysis and competition kinetics. These experiments helped us to measure the reactivity and selectivity of PINO• as a chain carrier in comparison with Br•. Additionally, a new competition experiment was designed to study the relative rate constant for the  $\beta$ -fragmentation process. For this experiment a novel substrate that contains two leaving

groups, Br• and PINO•, was synthesized, and the relative rates of elimination of Br• vs PINO• were compared.

## **Dedication**

*To my parents,  
who made me the person I am  
&  
To Neeraj,  
who loves me for all I am.*

## Acknowledgments

This journey would not have been possible without the help of so many people in so many ways. First and foremost, I would like to express my immense gratitude towards my parents, Mr. Vasant G. Patil and Dr. Rekha V. Patil, for their support and inspiration throughout my education. I would not have reached so far in my career without them behind me. There are no words that will express my love and respect for them. It is only their support, love and guidance that have made me the person that I am today.

I would like to thank my research advisor, Prof. James M. Tanko, for his infinite patience, guidance, and inspiration that he has given me throughout my Ph.D. career. I thank him for being a great teacher and mentor. I am truly indebted to him for inspiring me and keeping me motivated throughout my graduate career. I want to thank my committee members for mentoring me through my graduate school. First, I would like to thank Prof. Paul R. Carlier for providing the most interesting ideas and suggestions. I thank Prof. Neal Castagnoli for his inspiration and guidance. I specially thank Prof. Karen J. Brewer for her constant motivation, support and positive feedback that inspired me to work harder.

I would also like to thank past and present Tanko group members who were like my family during my time in Tanko group, Dr. Liang Chen, Jared Spencer, Dr. Susan Mitroka, Dr. Michelle Grimm, Dr. Amber Hancock, Secil Celebi, Akiko Nakamura, Justin Cutiss, Dr. Lesley Owens and Marwa Abdel Latif. I enjoyed working with all of you. I would like to give special thanks to Jared Spencer for all those helpful discussions on chemical kinetics. I would also like to thank my close circle of friends that have been my support during my time in Blacksburg.

Thank you Astha, Dr. Nipa Deora, Secil, Amrita Paul, Jimit Mehta, Dhruvi Naik, Sujit Nair, Asif. I will always remember the time we spent together.

A special expression of gratitude goes out to my brother Ashish Patil for all those phone conversations when I gave him large doses of free advice in order to feel better about myself. A special thanks to my mother-in-law Mrs. Nayana Patwardhan for being a great friend, support system and a great inspiration even though she was miles away from me. I also would like to thank my brother-in-law Ninad Patwardhan who made me laugh with his poorest possible jokes when I needed them the most, and sister-in-law Ela Joag-Patwardhan for being there for me to share my joys.

I would also like to thank my mentor and instructor at SynTech lab, Dr. Harry Gibson. His passion and enthusiasm for chemistry is contagious and has inspired me to work harder every day.

Last and by absolutely no means the least, I would like to extend my deepest gratitude to the one person who walked through every day of my graduate life with me, patiently listened to all my whines and shared all my joys and sorrows of the past decade: my best friend, strongest supporter, beloved husband, and literally my better half: Neeraj Patwardhan. You make my life beautiful and complete.

**Chapter 1 Review: Fundamental classes of free radical reactions involved in C-H bond functionalization and allyl transfer**

1.1 Introduction .....	1
1.2 Hydrocarbon functionalization.....	2
1.2.1 Metal-mediated C-H bond functionalization of hydrocarbons.....	2
1.2.2 Functionalization of hydrocarbons through oxidation reactions.....	3
1.2.3 Free radical based approaches to C-H bond functionalization.....	4
1.3 Functionalization of hydrocarbons via allyl transfer reaction.....	6
1.3.1 H-atom abstraction by chain carrier in allyl transfer reaction.....	7
1.4 Other nitroxyl radicals as H atom abstractors and chain carriers.....	12
1.5 Applications of PINO• in free radical mediated processes.....	15
1.6 Formation of Carbon-Carbon bonds through radical intermediates.....	20
1.6.1 Addition of carbon radicals to C=C bonds.....	20
1.6.2 Other allyl transfer reactions (Living/controlled polymerization processes).....	21
1.7 Radical initiators .....	25
1.7.1 Thermal initiator ( <i>t</i> -butyl peroxide) .....	25
1.7.2 Organoboranes as radical generators (trialkylborane).....	27
1.8 Conclusions and directions for research.....	29
1.9 References.....	31

**Chapter 2 Hydrocarbon functionalization via allyl transfer using PINO• as a chain carrier**

2.1 Introduction .....	36
2.2 Development of a “bromine-free” allyl transfer process based upon PINO•.....	38

2.3 Results and discussion.....	40
2.3.1 Synthesis of allyl-PINO substrates.....	40
2.3.2 Reactions of allyl-PINO substrates with hydrocarbons.....	42
2.3.3 Comparison of allyl bromides and allyl-PINO substrates with hydrocarbons.....	44
2.3.4 Low temperature reactions using triethylborane/O <sub>2</sub> .....	46
2.3.5 Low temperature reactions using triethylborane and a Lewis acid.....	50
2.4 Methods for determination of rate constant for addition-elimination process.....	56
2.4.1 Laser Flash Photolysis.....	56
2.4.2 Radical generation via photolabile radical precursor.....	57
2.4.2.1 Synthesis, mechanism and applications of photolabile thiohydroxamic esters.....	57
2.4.2.2 Direct radical generation using thermal initiator.....	61
2.4.3 Competition Experiment: Measurement of relative rate constant for $\beta$ -elimination step....	66
2.5 Conclusions.....	68
2.6 References.....	70

**Chapter 3 Radical additions of acyclic and cyclic ethers via allyl transfer using  
phthalimido-*N*-oxyl radical**

3.1 Review: Direct $\alpha$ -C-H activation and functionalization of ether.....	74
3.1.1 Radical addition-elimination reactions of ethers with alkenes and alkynes.....	75
3.1.2 Radical addition of alcohol and ether to alkene, alkyne, aldehyde and imine.....	76
3.1.3 Metal mediated carbenoid insertion to $\alpha$ -C-H of ether.....	79
3.1.4 Oxidative CDC reaction of ether with carbonyl compounds.....	82
3.1.5 Intramolecular annulation in ether via 1,5-hydride migration.....	84
3.2 Introduction to ether functionalization via allyl transfer.....	87

3.2.1 Direct functionalization of acyclic ethers via allyl transfer.....	88
3.2.2 Direct functionalization of cyclic ether.....	89
3.2.3 Competition for H-abstraction in Me-THF and 1,3-dioxane.....	92
3.2.3.1 Functionalization of 2-MeTHF via allyl transfer reaction.....	93
3.2.3.2 Functionalization of 1,3-dioxane via allyl transfer reaction.....	94
3.2.4 Allyl transfer in solution using low concentration of reagents.....	96
3.3 Kinetic chain length measurements.....	98
3.4 C-H functionalization of acetals.....	98
3.4.1 Chemistry of acyl intermediates .....	99
3.5 Amine C-H bond functionalization via allyl transfer.....	103
3.6 Conclusions.....	105
3.7 References.....	107

#### **Chapter 4: Experimental (For Chapter 2)**

4.1 General information.....	110
4.2 Materials and Purification (Hydrocarbon functionalization).....	110
4.3 Experimental procedure for the synthesis of allyl bromides ( <b>2-14</b> and <b>2-17</b> ).....	111
4.4 Experimental procedure for the synthesis of Allyl-PINO compounds.....	115
4.4.1 General procedure for allyl transfer reactions of hydrocarbons.....	120
4.4.2 General procedure for chain length calculations.....	120
4.4.3 Correction factors for allyl-bromides, allyl-PINO and hydrocarbon functionalized products.....	122
4.5 Kinetic chain lengths measurements for allyl transfer reactions of hydrocarbons with allyl-PINO substrate ( <b>2-11</b> ) using di- <i>t</i> -butylperoxide.....	123

4.6 Typical experimental procedure for low temperature allyl transfer reactions using triethylborane/O <sub>2</sub> .....	126
4.6.1 Typical experimental procedure for allyl transfer reactions using triethylborane/O <sub>2</sub> and Lewis acid (AlCl <sub>3</sub> ).....	126
4.6.2 Experimental procedure for the synthesis of di- <i>t</i> -butyl hyponitrite ( <b>2-31</b> ).....	126
4.7 Kinetic chain lengths measurements for allyl transfer reactions of hydrocarbons and allyl-PINO substrates using di- <i>t</i> -butylhyponitrite.....	127
4.8 Experimental procedure for the synthesis of 2-thioxopyridin-1(2H)-yl 2-phenylacetate ( <b>2-38</b> ).....	129
4.8.1 General procedure for competition experiments (Relative rate constant for addition-elimination process).....	129
4.9 Experimental procedure for the synthesis 2-((2-(bromomethyl)allyl)oxy)isoindoline-1,3-dione ( <b>2-45</b> ) .....	130
4.9.1 General experimental procedure for the competition experiments for relative rate constant for leaving group abilities.....	132
4.10 References.....	133

### Chapter 5: Experimental (For Chapter 3)

5.1 General procedure for allyl transfer reactions of ethers.....	134
5.2 Experimental data for ether products.....	134
5.3 Kinetic chain length calculations- Allyl transfer reactions of ethers.....	168
5.4 GC-MS evidences for regioisomers ( <b>3-96</b> and <b>3-98</b> ) in allyl transfer reaction of 2-MeTHF with <b>2-10</b> .....	176
5.4.1 GC-MS evidences for regioisomers ( <b>3-97</b> and <b>3-99</b> ) in allyl transfer reaction of 2-MeTHF with <b>2-11</b> .....	179
5.5 GC-MS analysis of <b>3-78</b> .....	182
5.6 References.....	183

## List of Schemes

<b>Scheme 1-1</b> Oxidation of cyclohexene using Mn and dioxygen.....	4
<b>Scheme 1-2</b> Oxidation of cyclohexene to cyclohexane epoxide using dioxygen and Pt.....	4
<b>Scheme 1-3</b> Oxidation of cyclohexane to cyclohexanone using dioxygen and NHPI.....	4
<b>Scheme 1-4</b> Propagation steps of the allyl transfer reaction.....	6
<b>Scheme 1-5</b> Polar effect on hydrogen atom abstraction from hydrocarbon.....	10
<b>Scheme 1-6</b> Reactivity of PINO• compared to HBr <sub>2</sub> •.....	10
<b>Scheme 1-7</b> Transition state for the reaction of PINO• with Phenols.....	11
<b>Scheme 1-8</b> Baciocchi's representation of reversible electron transfer from PINO•.....	12
<b>Scheme 1-9</b> Resonance stabilization in TEMPO radical.....	13
<b>Scheme 1-10</b> Isotopic labeling studies on cyclohexene.....	14
<b>Scheme 1-11</b> Reactions of indolinolic nitroxide with reactive radicals.....	15
<b>Scheme 1-12</b> NHPI catalyzed addition of diethyl ether to DEAD.....	16
<b>Scheme 1-13</b> Cu catalyzed C-O bond formation using NHPI.....	17
<b>Scheme 1-14</b> NHPI catalyzed oxidation of methyl aromatic hydrocarbons.....	17
<b>Scheme 1-15</b> Oxidation of alcohol catalyzed by NHPI and phosphomolybdic acid.....	18
<b>Scheme 1-16</b> Oxidation of isobutene using NHPI/Co catalyst .....	18
<b>Scheme 1-17</b> Radical chain mechanism for autoxidation of hydrocarbons.....	19
<b>Scheme 1-18</b> Addition of carbon radical to alkene.....	20
<b>Scheme 1-19</b> General atom transfer mechanism.....	21
<b>Scheme 1-20</b> Mechanism for metal catalyzed ATRP .....	22
<b>Scheme 1-21</b> General mechanism for nitroxide mediated polymerization.....	23
<b>Scheme 1-22</b> General mechanism for radical addition fragmentation transfer method .....	24
<b>Scheme 1-23</b> RAFT polymerization with reactive C=S bond .....	25

<b>Scheme 1-24</b> Generation of new radical using thermal initiators.....	25
<b>Scheme 1-25</b> Mechanism for autoxidation of trialkylboranes.....	28
<b>Scheme 1-26</b> Brown's mechanism for addition of trialkylborane to methyl vinyl ketone.....	29
<b>Scheme 2-1</b> Propagation steps and overall reaction in allyl transfer.....	36
<b>Scheme 2-2:</b> $\beta$ -bromo bridging interactions with intermediate carbon radical.....	37
<b>Scheme 2-3</b> Resonance contributors in phthalimido- <i>N</i> -oxyl radical (PINO•).....	39
<b>Scheme 2-4</b> New substrates (allyl-PINO) for allyl transfer reaction.....	40
<b>Scheme 2-5</b> Synthetic pathway for (2-10) 2-((2-phenylallyl)oxy)isoindoline-1,3-dione.....	40
<b>Scheme 2-5</b> Synthetic pathway for (2-11) ethyl 2-(((1,3-dioxoisoindoline-2-yl)oxy)methyl)acrylate.....	41
<b>Scheme 2-7:</b> Synthetic pathway for 2-12, 2-(((1,3-dioxoisoindolin-2-yl)oxy)methyl)acrylonitrile.....	41
<b>Scheme 2-8</b> Lewis acid catalyzed conjugate radical addition to chiral $\alpha,\beta$ -unsaturated <i>N</i> -enoyloxazolidinones.....	50
<b>Scheme 2-9:</b> Lewis acid catalyzed hydrocarbon functionalization using TEB/O <sub>2</sub> .....	51
<b>Scheme 2-10</b> Effect of Lewis acid on PINO• and hydrogen abstraction.....	53
<b>Scheme 2-11</b> Synthesis of di- <i>t</i> -butylhyponitrite (2-31).....	53
<b>Scheme 2-12</b> A) <i>N</i> -hydroxy-2-pyridone (2-31) B) 2-thiopyridin-1(2H)-yl 2-aryl/alkyl carboxylate ester (2-34).....	57
<b>Scheme 2-13</b> Synthetic pathway for 2-thioxopyridin-1(2H)-yl 2-phenylacetate.....	58
<b>Scheme 2-14</b> Mechanism for generation of a benzyl radical from 2-thioxopyridin-1(2H)-yl 2-phenyl acetate.....	59
<b>Scheme 2-15</b> Reaction of benzyl radical with 2-11 via LFP.....	60
<b>Scheme 2-16</b> Direct radical generation for LFP studies on benzyl radical addition-elimination process.....	61
<b>Scheme 2-17</b> Initial set up for competition experiment for relative rate constant measurement..	62

<b>Scheme 2-18</b> Modified competition experiment for the measurement of relative rate constant for radical addition-elimination processes.....	63
<b>Scheme 2-19</b> Synthesis of 2-((2-(bromomethyl)allyl)oxy)isoindolone-1,3-dione ( <b>2-45</b> ).....	66
<b>Scheme 2-20</b> Competition experiment for comparing leaving group abilities between Br• and PINO• .....	67
<b>Scheme 2-21</b> Proposed $\beta$ -bridging interactions of Br• with the intermediate carbon radical ( <b>2-48</b> ) .....	68
<b>Scheme 3-1</b> Peroxide or light initiated reaction of THF with alkynyl triflones.....	75
<b>Scheme 3-2</b> The alkenylation of esters using substituted vinyl triflones.....	76
<b>Scheme 3-3</b> Ether functionalization via reactions with alkene.....	77
<b>Scheme 3-4</b> Alcohol functionalization via reaction with alkyne.....	77
<b>Scheme 3-5</b> Radical addition of ethers to aldehydes and imines.....	78
<b>Scheme 3-6</b> Synthesis of (+)-myriocin via addition of methanol to ketoxime.....	79
<b>Scheme 3-7</b> Metal carbenoid insertion into the $\alpha$ -C-H bond of ether.....	80
<b>Scheme 3-8</b> Rh <sub>2</sub> (S-DOSP) <sub>4</sub> - catalyzed carbenoid insertion to methane $\alpha$ -C-H bond of phenyl methinyl ether.....	80
<b>Scheme 3-9</b> Microwave irradiated benzylic sp <sup>3</sup> C-H bond functionalization using the siloxycarbenes.....	81
<b>Scheme 3-10</b> Rh <sub>2</sub> (S-PTTL) <sub>4</sub> -catalyzed carbenoid insertion to $\alpha$ -C-H bond of phenyl ether.....	82
<b>Scheme 3-11</b> Cu-catalyzed carbenoid insertion into $\alpha$ -C-H of aliphatic ether.....	82
<b>Scheme 3-12</b> CDC reaction of $\alpha$ -C-H bond of ether and carbonyl compounds.....	82
<b>Scheme 3-13</b> CDC reaction of benzyl ethers with malonate derivatives.....	83
<b>Scheme 3-14</b> CDC reaction of benzyl ethers with ketones without metal-catalyst.....	83
<b>Scheme 3-15</b> Proposed single-electron transfer mechanism for CDC reaction.....	84
<b>Scheme 3-16</b> Intramolecular annulation of ether with alkene via 1,5-hydride migration.....	85

<b>Scheme 3-17</b> Comparison of aldehyde with acetal towards the intramolecular annulations.....	86
<b>Scheme 3-18</b> Intramolecular annulations of ethers with acetals.....	86
<b>Scheme 3-19</b> Reported mechanism for intramolecular annulation of ether with acetal.....	87
<b>Scheme 3-20</b> Resonance stabilization of $\alpha$ -alkoxyl radical in tetrahydrofuran (THF).....	88
<b>Scheme 3-21</b> Synthesized products from functionalization of acyclic ethers.....	88
<b>Scheme 3-22</b> Competition for H-abstraction in A) 2-MeTHF, B) 1,3-dioxane.....	92
<b>Scheme 3-23</b> Functionalization of 2-MeTHF via allyl transfer reaction.....	93
<b>Scheme 3-24</b> Functionalization of 1,3-dioxane via allyl transfer reaction.....	95
<b>Scheme 3-25</b> Comparison of BDEs between cyclic ether and acyclic dimethyl ether.....	99
<b>Scheme 3-26</b> Reactive intermediates: Acyl cation and acyl radical.....	99
<b>Scheme 3-27</b> General mechanism for Friedel-Craft acylation.....	100
<b>Scheme 3-28</b> Hayashi rearrangement for the synthesis of substituted o-benzyl benzoic acid....	100
<b>Scheme 3-29</b> Proposed pathway for functionalization of acyclic dimethyl acetal.....	101
<b>Scheme 3-30</b> Synthesis of dimethyl acetal of benzaldehyde.....	102
<b>Scheme 3-31</b> Functionalization of dimethyl acetal of benzaldehyde.....	102
<b>Scheme 3-32</b> Resonance stabilization of methyl radical in <i>N,N</i> -dimethylaniline.....	103
<b>Scheme 3-33</b> Attempted allyl transfer reaction of <i>N,N</i> -dimethylaniline with <b>2-10</b> .....	104
<b>Scheme 3-34</b> Predicted pathway for the dimerization of <i>N,N</i> -dimethylaniline.....	104

## List of Tables

<b>Table 1-1</b> Reactivities of halogens towards hydrogen atom abstraction.....	7
<b>Table 1-2</b> Relative C-H bond reactivity.....	7
<b>Table 1-3</b> BDEs and relative reactivities of C-H bonds with Br•.....	8
<b>Table 1-4</b> Reported rate constants for H-abstraction by various radicals.....	9
<b>Table 1-5</b> Sheldon's representation of BDE studies on various hydroxyamines.....	13
<b>Table 1-6</b> Activation parameters for t-butyl peroxide decomposition.....	27
<b>Table 2-1</b> Allyl transfer reactions of toluene, cumene and ethyl benzene with allyl-PINO substrates ( <b>2-10</b> , <b>2-11</b> ).....	42
<b>Table 2-2</b> Reactions of toluene with <b>2-11</b> at varying reaction time and concentration of initiator.....	44
<b>Table 2-3</b> Comparison: Reactions of allyl-PINO and allyl bromide substrates with hydrocarbons.....	45
<b>Table 2-4</b> Kinetic chain length comparison between allyl bromide and allyl-PINO substrates...46	
<b>Table 2-5</b> Reactions of <b>2-14</b> with hydrocarbons at low temperature using Et <sub>3</sub> B/O <sub>2</sub> .....	48
<b>Table 2-6</b> Reactions of <b>2-10</b> , <b>2-11</b> with hydrocarbons at low temperature using Et <sub>3</sub> B/O <sub>2</sub> .....	49
<b>Table 2-7</b> Reactions of <b>2-11</b> and <b>2-17</b> with hydrocarbons (neat) initiated by DTBHN.....	54
<b>Table 2-8</b> Kinetic chain length data with 10 mol% of <b>2-31</b> at 45 °C.....	55
<b>Table 2-9</b> Result of competition experiment: Relative rate constant measurement with varying substituents and leaving groups.....	64
<b>Table 2-10</b> Relative rate constants for the addition/elimination of benzyl radical to allyl-bromide vs. allyl-PINO substrates.....	65
<b>Table 3-1</b> Functionalization of acyclic ethers via allyl transfer reaction.....	89
<b>Table 3-2</b> Functionalization of cyclic ethers and benzo-1,3-dioxole via allyl transfer reaction...91	
<b>Table 3-3</b> Functionalization of 2-MeTHF via allyl transfer reaction.....	93

<b>Table 3-4</b> Ally transfer reaction of 1,3-dioxane leading to mixture of products.....	95
<b>Table 3-5</b> THF functionalization in solution (acetonitrile).....	96
<b>Table 3-6</b> Allyl transfer reaction in solution.....	97
<b>Table 3-7</b> Summarized kinetic chain length data for allyl transfer reactions on ethers.....	98
<b>Table 3-8</b> Results for the functionalization of dimethyl acetal of benzaldehyde in acetonitrile.....	102
<b>Table 4-1:</b> Correction factors and GC retention times for allyl-bromide substrates, allyl-PINO substrates and products.....	122
<b>Table 4-2:</b> Results of competition experiments (Reactions of benzyl radical with allyl-bromides and allyl-PINO substrates) .....	130

## List of Equations

<b>Equation 2-1</b> Reported rate constants for H-abstraction by PINO• and Br• from toluene at room temperature.....	55
--	----

## List of Figures

<b>Figure 1-1</b> Pathways of C-H activation.....	1
<b>Figure 1-2</b> Mechanisms for the metal-mediated activation of C-H bonds.....	2
<b>Figure 1-3</b> Bond dissociation energies (BDE) of several types of C-H bonds.....	5
<b>Figure 2-1</b> Triethylborane initiated reaction of cumene and <b>2-11</b> with Lewis acid (AlCl <sub>3</sub> ) compared to the reaction without Lewis acid.....	52
<b>Figure 2-2</b> Triethylborane initiated reaction of toluene and <b>2-11</b> with Lewis acid (AlCl <sub>3</sub> ) compared to the reaction without Lewis acid.....	52
<b>Figure 2-3</b> Transient absorption spectra for 2-thioxopyridin-1(2H)-yl 2-phenyl acetate.....	60
<b>Figure 2-4</b> Arithmetic derivation of the required relative rate constant using three measured relative rate constants.....	65
<b>Figure 3-1</b> Synthesized products from functionalization of cyclic ethers and thioether.....	90
<b>Figure 3-2:</b> GC analysis of 2-MeTHF functionalization showing all regioisomeric products.....	94
<b>Figure 4-1:</b> Reaction of toluene with <b>2-11</b> .....	123
<b>Figure 4-2:</b> Reaction of ethyl benzene with <b>2-11</b> .....	124
<b>Figure 4-3:</b> Reaction of cumene with <b>2-11</b> .....	125
<b>Figure 4-4:</b> Reaction of ethyl benzene with <b>2-11</b> using 10 mol% DTBHN at 45 °C.....	127
<b>Figure 4-5:</b> Reaction of toluene with <b>2-11</b> using 10 mol% DTBHN at 45 °C.....	128
<b>Figure 5-1:</b> Reaction of <b>2-10</b> with THF.....	168
<b>Figure 5-2:</b> Reaction of <b>2-10</b> with 2-MeTHF (for major product).....	169
<b>Figure 5-3:</b> Reaction of <b>2-10</b> with 1,4-dioxane.....	170
<b>Figure 5-4:</b> Reaction of <b>2-11</b> with THF.....	171
<b>Figure 5-5:</b> Reaction of <b>2-11</b> with 2-MeTHF (for major product).....	172
<b>Figure 5-6:</b> Reaction of <b>2-11</b> with 2-MeTHF.....	173
<b>Figure 5-7:</b> Reaction of <b>2-11</b> with 1,4-dioxane.....	174

<b>Figure 5-8:</b> Reaction of <b>2-11</b> with THF (3 eq.) in acetonitrile (0.8 M).....	175
<b>Figure 5-9:</b> GC-MS chromatogram showing products of the allyl transfer reaction of <b>2-10</b> with 2-MeTHF.....	176
<b>Figure 5-10:</b> GC-MS chromatogram showing products from the allyl transfer reaction of <b>2-11</b> with 2-MeTHF.....	179
<b>Figure 5-11:</b> GC-MS analysis of <b>3-78</b> .....	182

## List of Abbreviations

2-MeTHF	2-methyl tetrahydrofuran
9-BBN	9-Borabicyclo[3.3.1]nonane
AIBN	Azoisobutyronitrile
ATRP	Atom transfer radical polymerization
BDE	Bond dissociation energy
CDC	Cross-dehydrogenative coupling
CTR	Chain transfer reagents
DDQ	Dichloro dicyano benzoquinone
DMA	<i>N,N</i> -dimethylaniline
DMSO	Dimethylsulfoxide
DTBHN	Di- <i>t</i> -butyl hyponitrite
DTBPO	Di- <i>t</i> -butyl peroxide
EPR	Electron paramagnetic resonance
GC	Gas chromatography
HAT	Hydrogen atom transfer
HBr	Hydrobromic acid
LA	Lewis acid
LC-MS	Liquid chromatography mass spectrometry
NaOAc	Sodium acetate
NBS	<i>N</i> -bromosuccinimide
Nd-YAG	Neodymium-yttrium aluminium
NHPI	<i>N</i> -hydroxyphthalimide

NMP	Nitroxide mediated polymerization
NMR	Nuclear magnetic resonance
PCET	Proton coupled electron transfer
PINO	Phthalimido- <i>N</i> -oxyl
PINO-H	<i>N</i> -hydroxyphthalimide
RAFT	Radical addition-fragmentation transfer
TBHP	<i>t</i> -butyl hydroperoxide
TEB	Triethylborane
TEMPO	Tetramethyl piperidine oxide
THF	Tetrahydrofuran

## Chapter 1 Review: Fundamental classes of free radical reactions involved in C-H bond functionalization and allyl transfer

### 1.1 Introduction

Hydrocarbons are abundant in nature in the form of petroleum based products, natural gas and oil.<sup>1</sup> These compounds are simple in structure and relatively non-reactive towards electrophiles and nucleophiles. Due to this non-reactive nature, very few methods are available for their activation and functionalization.<sup>2</sup> Therefore effective, cost efficient, and atom economical methods are always needed in order to directly convert these compounds into complex and more useful functional groups. Although the functionalization of hydrocarbons into carbon based reactive intermediates such as electrophiles, nucleophiles and carbon radicals, are known in the literature, achieving such functionalizations under mild reaction conditions is still a topic of significant research.<sup>3</sup> (Figure 1-1)

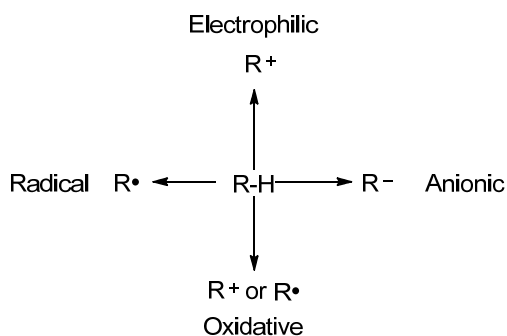


**Figure 1-1:** Pathways of C-H activation

A new free radical-based condensation reaction that achieved hydrocarbon functionalization and C-C bond formation in a single step was reported in our group in 1999.<sup>4</sup> In devising this process, several known radical reactions (hydrogen atom abstraction, radical additions, and  $\beta$ -cleavage) were tailored to develop a new propagation sequence that achieves the overall conversion  $R-H + CH_2=C(Z)CH_2X \rightarrow RCH_2C(Z)=CH_2 + H-X$  (for  $X = Br$ ). This review

chapter discusses each of these fundamental classes of free radical reactions, and their allied topics in order to introduce our efforts to modify this method into a greener process.

## 1.2 Hydrocarbon Functionalization

### 1.2.1 Metal-mediated C-H bond functionalization of hydrocarbons

The activation of C-H bonds in order to functionalize hydrocarbons into complex molecules has been known in the literature.<sup>5</sup> Such activation helps in the replacement of a strong C-H bond with a weaker bond, which is capable of undergoing further functionalization easily.<sup>6</sup> In this brief section, we will summarize a few examples of metal-mediated activation of hydrocarbons. There are several known pathways that have been employed in such activations (Figure 1-2).<sup>7</sup>

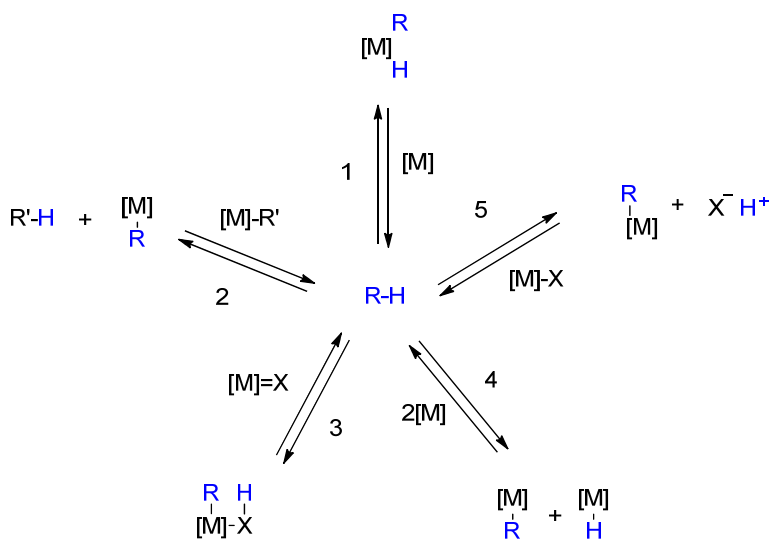
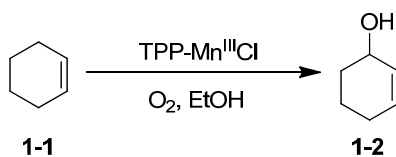


**Figure 1-2:** Mechanisms for the metal-mediated activation of C-H bonds<sup>7</sup>: (1) Oxidative addition-reductive elimination; (2) Deprotonative metalation; (3) 1,2-addition-elimination; (4) Two metal homolytic cleavage and (5) Electrophilic activation

A typical example of metal-mediated activation is based on the oxidative-addition/reductive-elimination pathway (1), in which the C-H bond adds to the metal center to generate new metal-carbon and metal-hydride bonds.<sup>7</sup> The deprotonative metalation pathway (2) activates the C-H bond leading to the corresponding organometallic compound. Pathway (3) involves the formal insertion of the C-H bond into an unsaturated metal-ligand bond. Such activation (4) can also be achieved with the intermediacy of two metal centers leading to separate metal-alkyl and metal-hydride complexes. Finally, the electrophilic activation (5) occurs via the displacement of a hydrogen atom by another group (X=halide) followed by the R group usually being displaced from the metal as a functionalized product. These activation pathways have been shown to be involved in a variety of processes reported for the activation of hydrocarbons. Apart from these pathways other metal-mediated activations involve acidic, basic or oxidative intermediates. The next section discusses hydrocarbon functionalization through direct oxidation of C-H bonds via various intermediates.

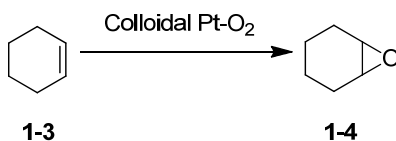
### **1.2.2 Functionalization of hydrocarbons through oxidation reactions**

Functionalization of C-H bonds of hydrocarbons to a C-X, C-O, C-N or C-C bond (oxidation), under mild reaction conditions, has been the main objective of this research in the recent past. However, achieving high selectivity and high yield is still a challenge.<sup>8</sup> In many such direct oxidation reactions, dioxygen serves as an oxidizing agent. Even though dioxygen is a triplet diradical in its ground state, this molecule is relatively inert towards strong C-H bonds. This low reactivity demands either homogeneous or heterogeneous catalysis that can operate under mild conditions.<sup>9</sup> Use of a catalyst may not only increase the reactivity but may reduce the formation of unwanted side products. Use of metal catalysts for such activation is well known in organic chemistry.

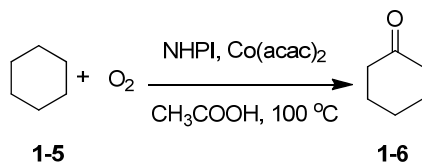


**Scheme 1-1:** Oxidation of cyclohexene using Mn and dioxygen.<sup>10</sup>

For example, Tabushi *et al.* reported the selective oxidation of cyclohexene **1-1** to cyclohexenol **1-2**. In this reaction TPP-Mn<sup>III</sup>Cl catalyst was used to activate dioxygen (Scheme 1-1).<sup>10</sup> Similarly, the conversion of cyclohexene **1-3** to cyclohexane epoxide **1-4** was reported where dioxygen was activated using colloidal Pt-catalyst.<sup>11</sup> (Scheme 1-2)



**Scheme 1-2:** Oxidation of cyclohexene to cyclohexane epoxide using dioxygen and Pt.<sup>11</sup>



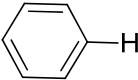
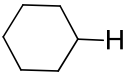
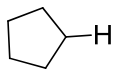
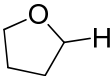
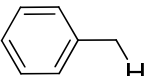
**Scheme 1-3:** Oxidation of cyclohexane to cyclohexanone using dioxygen and NHPI<sup>12</sup>

Similarly, the selective oxidation of cyclohexane **1-5** to cyclohexanone **1-6** was reported by Ishii and coworkers (Scheme 1-3). In this reaction a cobalt (Co) catalyst was used to activate dioxygen and NHPI (*N*-hydroxyphthalimide) was used as a hydrogen atom abstractor. In all the above mentioned experiments, transition metal catalyst was used to activate triplet dioxygen.

### 1.2.3 Free radical based approaches to C-H bond functionalization

As mentioned earlier, most of the reported processes for hydrocarbon functionalization involve the use of metals and/or harsh reaction conditions. But, green chemistry seeks to avoid

the use of metals because of their toxicity.<sup>13</sup> The free radical activation of hydrocarbons for such functionalizations affords a viable alternative for this purpose owing to its neutral conditions. Such functionalizations of hydrocarbons where the activating group weakens the desired C-H bond are well known in the literature.<sup>14</sup> However, hydrocarbons lacking activators rarely participate in such reactions. Activation in these cases strongly depends on the ability of hydrocarbons to form carbon radicals, which depends on the bond dissociation energy (BDE) of the C-H bond of these hydrocarbons. Figure 1-3 represents the BDE values for an array of C-H bonds.<sup>15</sup> The highest BDEs reported for methane and benzene are 105 and 113 kcal/mol, respectively. The BDE for ethane is slightly lower than methane at 100 kcal/mol. Other primary C-H bonds, such as toluene (benzylic C-H bond) or propene (allylic C-H bond) are at 90 and 88 kcal/mol, respectively. Secondary aliphatic alkanes are ca. 3 kcal/mol lower than primary alkane (98 kcal/mol for propane and butane) whereas the reported BDE for the tertiary C-H bond of 2-methylpropane is 96 kcal/mol.

		$\text{H}-\text{CH}_3$	$\text{H}-\overset{\text{H}_2}{\text{C}}-\text{CH}_3$	$\text{H}-\text{CH}(\text{CH}_3)_2$
BDE (kcal/mol)	113	105	101	98
<hr/>				
	$\text{H}-\text{CH}(\text{CH}_3)-\text{CH}_2-\text{CH}_3$			$(\text{H}_3\text{C})_3-\text{C}-\text{H}$
BDE (kcal/mol)	98	97	96.5	96
<hr/>				
		$\text{CH}_3-\text{CH}_2-\text{NH}_2$		$\text{H}-\text{CH}_2-\text{CH}=\text{CH}_2$
BDE (kcal/mol)	92	90	90	88

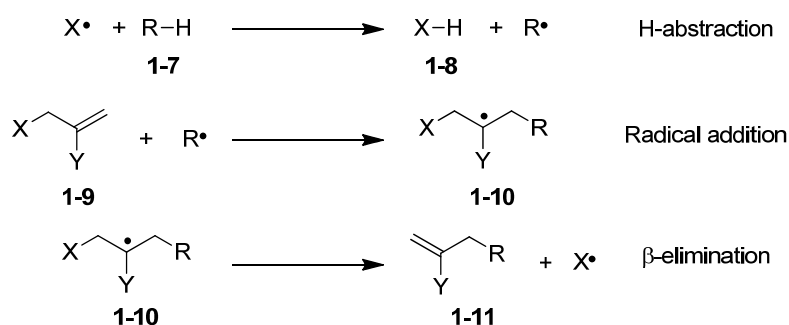
**Figure 1-3:** Bond dissociation energies (BDEs) of several types of C-H bonds.<sup>7</sup>

This number is slightly lower than the BDE for a C-H bond of cyclohexane (97 kcal/mol), and very similar to that of cyclopentane (96.5 kcal/mol). The BDEs for the R-C-H bond in ethers and

amines are also worth mentioning. As representative examples, BDE for the  $\alpha$ -C-H bond in tetrahydrofuran (THF) is reported as 92 kcal/mol, whereas in the case of ethylamine it is 90 kcal/mol. Through these values, it has been confirmed that the presence of a vicinal oxygen or nitrogen atom to a C-H bond weakens its BDE by ca. 4 kcal/mol compared to their homologues in a saturated hydrocarbon.<sup>16</sup> In this chapter we will discuss various methods for generation of carbon radicals through H atom abstraction and their radical addition reactions with alkenes.

### 1.3 Functionalization of hydrocarbons via allyl transfer reaction

As mentioned briefly in the introduction, functionalization of benzylic hydrocarbons via allyl transfer reaction was reported in our group. This reaction involved abstraction of H atom from alkyl aromatic hydrocarbons like toluene, cumene using a thermal initiator. The resulting carbon radical was functionalized via addition to a C=C bond of an allyl substrate **1-9** (Scheme 1-4, X=Br). The leaving group Br atom ( $\text{Br}\cdot$ ) also acts as a chain carrier which propagates the chain to yield final product **1-11**.

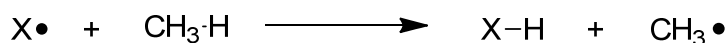


**Scheme 1-4:** Propagation steps of the allyl transfer reaction.<sup>4</sup>

In this section we will briefly discuss the fundamentals of C-H abstraction, halogen chain carriers and introduce nitroxyl radicals as a viable alternative to these halogen atoms.

### 1.3.1 H-atom abstraction by chain carrier in allyl transfer reaction

Weak C-H bonds at benzylic or allylic positions are reactive towards halogen radicals. A halogen atom, specifically Br•, is formed in the propagating sequence of allyl transfer reaction from allyl halide substrates. Therefore, reactivity and selectivity of these halide radicals towards hydrogen abstraction is of interest.



X•	ΔH(kcal/mol)	k <sub>H</sub> (M <sup>-1</sup> s <sup>-1</sup> )	E <sub>a</sub> (kcal/mol)
F	-20	1.3 x 10 <sup>10</sup>	1.2
Cl	2	4.1x 10 <sup>7</sup>	3.8
Br	+17	6.6x 10 <sup>3</sup>	18
I	+34	10 <sup>-14</sup> (est.)	34

**Table 1-1:** Reactivities of halogens toward hydrogen atom abstraction,<sup>17</sup>

X•	3°	2°	1°
Cl•	4.0	3.5	1.0
Br•	1,700	80	1.0

**Table 1-2:** Relative C-H bond reactivity<sup>17</sup> The Cl atom is more reactive and less selective compared to the Br atom.

Table 1-2 illustrates that F• and Cl• are extremely reactive and poorly selective in hydrogen atom abstraction whereas I• is extremely slow reacting. As a result, Br• is the best choice for H-atom abstraction because it shows the best balance of reactivity and selectivity towards hydrogen abstraction.

One of the goals of this research was to replace chain-carrying Br• used in the allyl transfer reaction with PINO• (phthalimido-N-oxyl, a nitroxyl radical). Nitroxyl radicals will be

discussed at length in section 1.4. The goal of this replacement was to attempt achieving better selectivity and provide a greener allyl transfer reaction. Studies have reported that PINO• is slightly less reactive and more selective than Br• in hydrogen abstraction.<sup>8</sup>

Rate constants for hydrogen atom abstraction and BDE of the C-H bond play an important role in homolytic cleavage of the C-H bond. This information was used to compare relative reactivity towards H-abstractions. To study reactivity differences between PINO• and Br•, hydrocarbons with significantly different C-H bond dissociation energies were selected and their BDEs were recorded by Espenson *et al.* (Table 1-3).<sup>17</sup>

Nature of resulting radical	R-H	BDE (kcal/mol)	$k_{rel}$ at 77 °C (per hydrogen)
1°	CH <sub>3</sub> CH <sub>3</sub>	98.2	1
2°	(CH <sub>3</sub> ) <sub>2</sub> CH <sub>2</sub>	95.1	220
3°	(CH <sub>3</sub> ) <sub>3</sub> CH	93.2	19,400
1° benzylic	C <sub>6</sub> H <sub>5</sub> CH <sub>3</sub>	88.0	64,000
2° benzylic	C <sub>6</sub> H <sub>5</sub> CH <sub>2</sub> CH <sub>3</sub>	85.4	1,600,000
3° benzylic	C <sub>6</sub> H <sub>5</sub> CH(CH <sub>3</sub> ) <sub>2</sub>	84.4	3,800,000

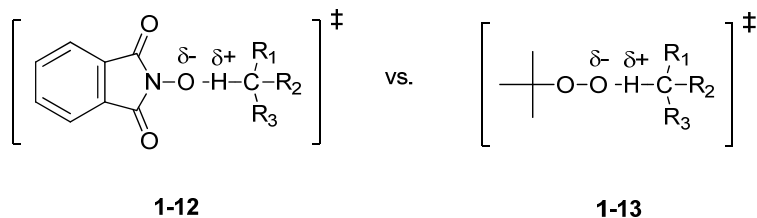
**Table 1-3:** BDEs<sup>18</sup> and relative reactivities<sup>19</sup> of C-H bonds with Br•.

The data in Table 1-3 demonstrate that the C-H BDE decreases with the increase in stabilization of resulting radical,<sup>18</sup> and the rate constant for H atom abstraction increases with radical stability (decreasing C-H BDE). In these examples, the radicals are stabilized by conjugation and/or hyperconjugation.

<b>R-H</b>	$k_{t\text{-BuOO}\cdot}^a$	$k_{\text{PINO}\cdot}^b$
Ph <sub>3</sub> CH	-	58.5
Isopropanol	-	1.89
Benzyl alcohol	0.065	5.65
Ph <sub>2</sub> CH <sub>2</sub>	0.25	6.63
Cumene	0.22	3.25
Ethylbenzene	0.10	1.12
Toluene	0.012	0.127
Cyclohexane	0.00026	0.0039
Cyclohexene	0.75	5.05
THF	0.085	0.72

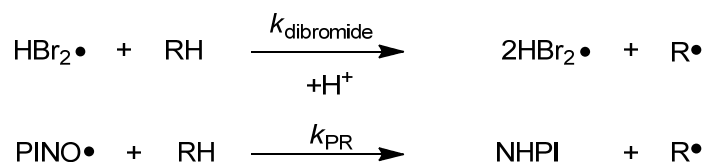
**Table 1-4:** Reported rate constants ( $\text{M}^{-1} \text{s}^{-1}$ ) for H-abstraction by various radicals (per hydrogen).<sup>17, 20</sup>

The data in Table 1-4 show a fair comparison between reactivity of two oxygen radicals. From the rate constant data, it appears that PINO• is 8- to 11-fold more reactive than *t*-BuOO•. This difference between reactivity is not resulting from O-H bond dissociation energies (PINO-H 89 kcal/mol, *t*-BuOO-H 84 kcal/mol)<sup>21</sup> but is due to the polar effects. Thus, the polar effect is more dominant on the rate of hydrogen abstraction with PINO•, because of the more stabilized transition state **1-12**, than **1-13** (Scheme 1-5).<sup>8</sup> In both structures a partial negative charge is developed on the oxygen. This partial negative charge is better stabilized in **1-12** due to the electron withdrawing carbonyl group attached to the nitrogen whereas in case of **1-13**, the partial negative charge is destabilized due to the electron donating oxygen. This negative charge is enhanced due to electron rich *t*-butyl group.



**Scheme 1-5 :** Polar effect on hydrogen atom abstraction from hydrocarbon<sup>8</sup>, A) Transition state for PINO• B) Transition state for *t*-BuOO•, R<sub>1</sub>, R<sub>2</sub>, R<sub>3</sub> = alkyl, aryl and/or H

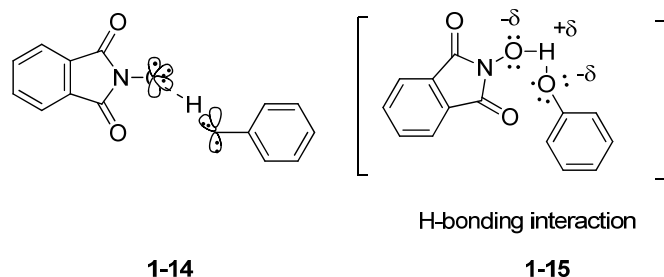
In order to measure the relative reactivity of Br• and PINO• towards hydrogen atom abstraction, Koshino *et al.* performed reactions of several aryl derivatives with PINO• and HBr<sub>2</sub>• to study their relative reactivity. The rate constant data for H-abstraction was used to study the relative reactivity.<sup>17</sup> The slope confirms that the HBr<sub>2</sub>• is more reactive and less selective compared to PINO• in H-abstraction. Redox potential studies concluded that the reactions with HBr<sub>2</sub>• are more exothermic than that with PINO•, which are nearly thermoneutral.<sup>17</sup> In this experiment (Scheme 1-6), HBr<sub>2</sub>• was used because of the convenient experimental procedures.



**Scheme 1-6:** Reactivity of PINO• compared to HBr<sub>2</sub>•.<sup>17</sup> (HBr<sub>2</sub> is used as a source of Br<sub>2</sub>•<sup>-</sup>)

PINO• abstracts hydrogen from benzylic C-H bonds<sup>22</sup> and phenolic C-H bonds via two different mechanisms.<sup>23</sup> In the former case, reaction follows a HAT (hydrogen atom transfer) pathway shown in **1-14**, whereas in the latter case it follows a PCET (proton coupled electron transfer) pathway shown in **1-15**. Based on the reported kinetic deuterium isotope effect studies in the PCET mechanism, the reactants form a “hydrogen-bonded complex,” **1-15** followed by

transfer of H to a sigma bonding orbital of PINO• and transfer of an electron from 2p-II orbital on the phenol to 2p orbital of the phenol (Scheme 1-7).<sup>22</sup>

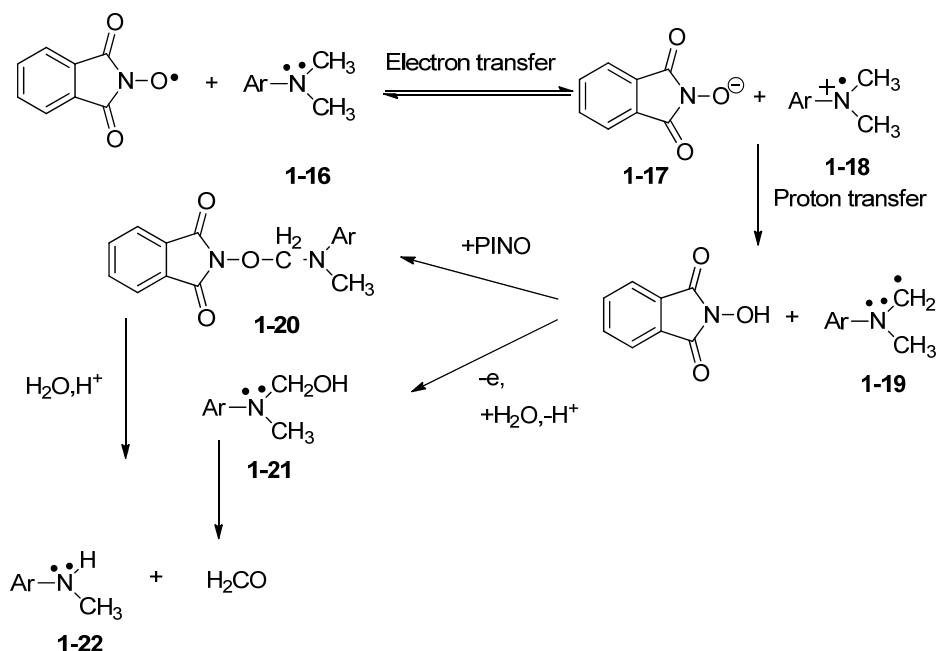


**Scheme 1-7:** Transition state for the reaction of PINO• with phenols.<sup>22</sup> **1-14:** Orbital picture,

**1-15:** Bonding interaction

Reactivity of PINO• with phenolic O-H bonds is much greater than that of benzylic C-H bonds because of the fact that, in this case, the hydrogen transfers between one O centered radical to another O-centered radical, making the transition state more symmetrical<sup>24</sup> (Scheme 1-7). To summarize, the transition state in the reaction of PINO• and phenol involves a symmetrical -O-H-O- bond whereas, in case of benzylic C-H bond it is -O-H-C- bond.

Similar to phenols and benzylic hydrocarbons, PINO• shows high reactivity in abstraction of H atom towards -N-C-H bonds of alkyl aromatic amines. H-abstraction from the  $\alpha$ -C-H bond of **1-16** by PINO • follows oxidative demethylation of N-CH<sub>3</sub> groups leading to **1-17**.<sup>25</sup> To investigate the mechanism of this process, *N,N*-dimethylanilines (DMA) were used, and their reaction with PINO• was analyzed. Kinetic data of reaction and oxidation potential studies of substrates concluded that the reaction follows a reversible electron transfer pathway<sup>25</sup> (Scheme 1-8).

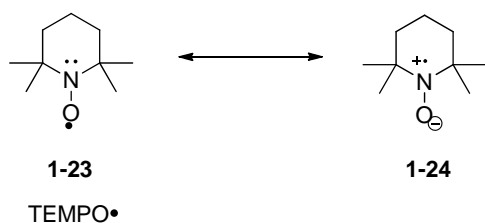


**Scheme 1-8:** Baciocchi's representation of reversible electron transfer from PINO•.<sup>25</sup>

#### 1.4 Other nitroxyl radicals as H atom abstractors and chain carriers

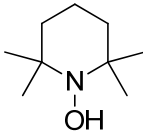
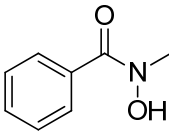
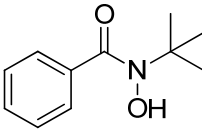
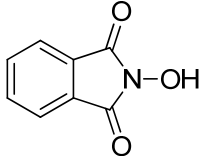
Generation of carbon-centered radicals using nitroxyl radical initiators has gained interest because of their wide applications in free radical reactions and “living” polymerization processes. One of the objectives of this research was to replace Br• with a suitable nitroxyl radical. Therefore, this section focuses on structure, mechanism and physical properties of nitroxyl radical initiators

Nitroxyl radicals can be divided into two main categories: Dialkylnitroxyl and diacylnitroxyl.<sup>26</sup> Alkylnitroxyl radicals are more stable than acylnitroxyl radicals because of the resonance stabilization over N-O bond (Scheme 1-9)<sup>27</sup>. These are used in the formation of carbon centered radicals, mainly through H-abstraction.



**Scheme 1-9:** Resonance stabilization in TEMPO radical,<sup>28</sup>

The reactivity of a nitroxyl radical depends on its structure and physical properties. For example, TEMPO• **1-23** (2,2,6,6-tetramethylpiperidinyloxy, a nitroxyl radical), is generally used as an autoxidation inhibitor whereas, PINO• (phthalimido-N-oxy, a nitroxyl radical) favors autoxidation reactions. To rationalize this contradictory behavior, BDEs of TEMPO-H and PINO-H (NHPI) were determined.<sup>17, 20c, 21</sup>

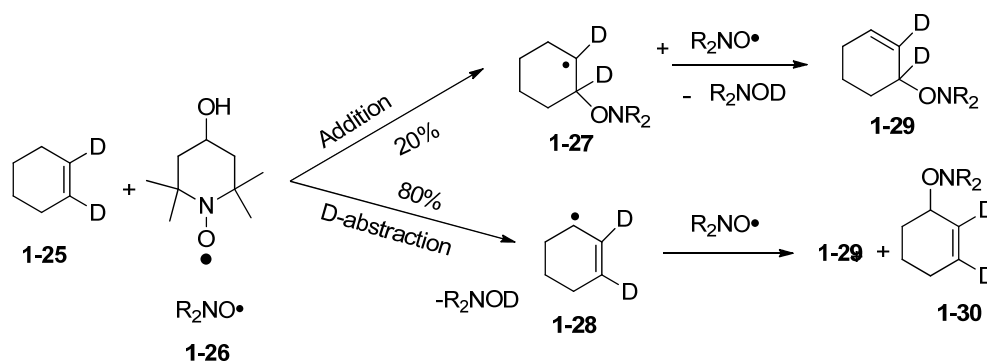
Structure				
BDE (O-H) kcal/mol	69.74 <sup>[a]</sup>	79.53 <sup>[b]</sup>	77.14 <sup>[c]</sup>	88.13 <sup>[b]</sup> 89.56 <sup>[c]</sup>
[a] <sup>21</sup> [b] <sup>20c</sup> [c] <sup>29</sup>				

**Table 1-5:** Sheldon's representation of BDE studies on various hydroxyamines,<sup>30</sup>

Various nitroxyl radicals in Table **1-5** show that the replacement of methyl group by acyl group in TEMPO• significantly increases the BDE. This increase in BDE is reported to be resulting from the intramolecular H-bonding with the carbonyl group and the resonance stabilization of the nitrogen lone pair over carbonyl groups.<sup>20c</sup>

Dialkyl nitroxyl radicals such as TEMPO• rarely participate in H abstraction. In fact, a completely different mechanism was reported for reactions of TEMPO• with unsaturated hydrocarbons. For example, TEMPO• react with cycloalkenes to form 3-substituted products

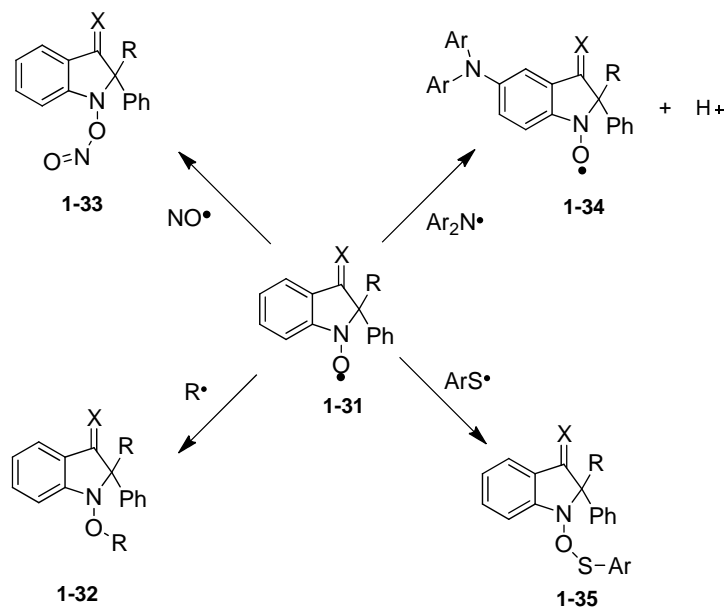
(Scheme 1-10). Jenkin *et al.* proposed that it follows an abstraction pathway<sup>31</sup> whereas Barbiarz *et al.* proposed that TEMPO• first adds to the cycloalkene followed by H-abstraction using another mole of TEMPO• leading to 3-substituted products.<sup>32</sup> Finally, Coseri *et al.* performed deuterium studies, which proved that rate of D-abstraction is 4X fold faster than the rate of radical addition. Product analysis<sup>33</sup> confirmed that the product **1-30** formed via D-abstraction followed by radical addition dominates the product **1-29** formed via initial addition followed by D-abstraction. Addition of R<sub>2</sub>NO• **1-26** to the product **1-28** of abstraction pathway forming **1-29** (Scheme 1-10) is not observed.



**Scheme 1-10:** Isotopic labeling studies on cyclohexene,<sup>33</sup>

Hydrogen abstraction by nitroxyl derivatives is an important process both in chemistry and biology.<sup>8</sup> Nitroxyl radicals play an important role in inhibiting oxidation processes via free radicals in biological systems.<sup>8</sup> Therefore, the study of oxygen radicals or other antioxidants are important. TEMPO• has the ability to react with not only carbon radicals<sup>34</sup> and sulfur radicals,<sup>35</sup> but also oxygen radicals<sup>36</sup> and displays much lower rates of hydrogen abstraction compared to other aromatic nitroxyl radicals. E. Damiani *et al.* reported that indolinonic (a derivative of indolinone) nitroxyl radicals (Scheme 1-11) show structure dependent H-abstraction ability and are more reactive than TEMPO• derivatives.<sup>37</sup> The antioxidant property also depends on

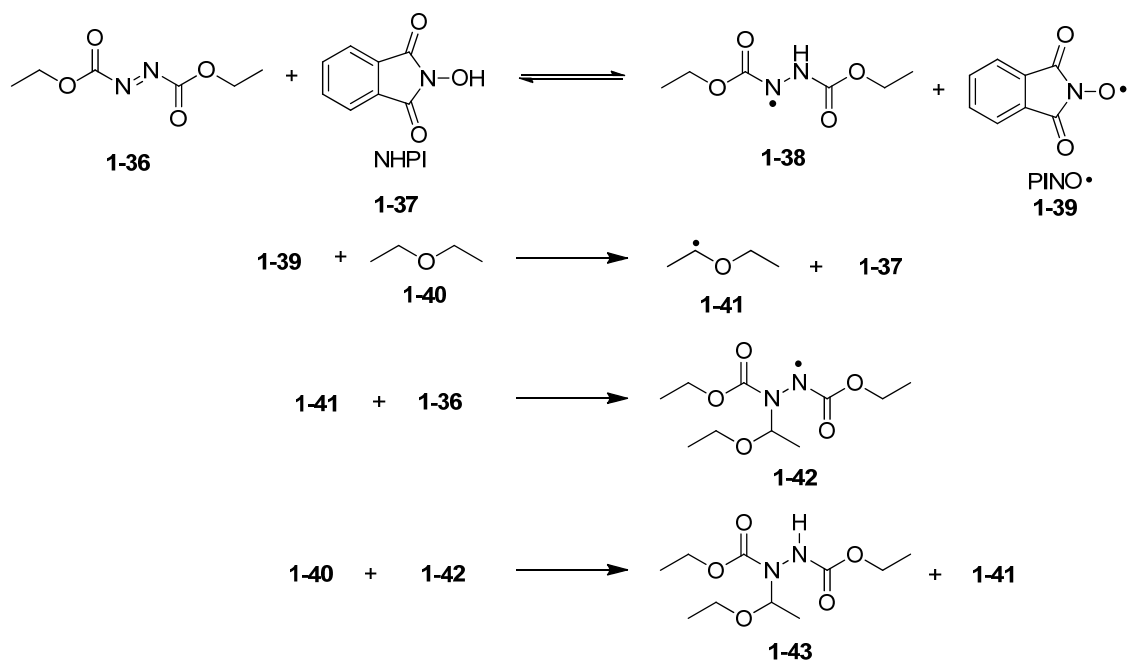
stereoelectronic effects, scavenging capacity, kinetics and thermodynamics of reaction. Since indolinonic radicals are better antioxidants than TEMPO• derivatives, their H- abstraction ability is worth mentioning.



**Scheme 1-11:** Reactions of indolinolic nitroxide with reactive radicals.<sup>37</sup>

### 1.5 Applications of PINO• in free radical mediated processes

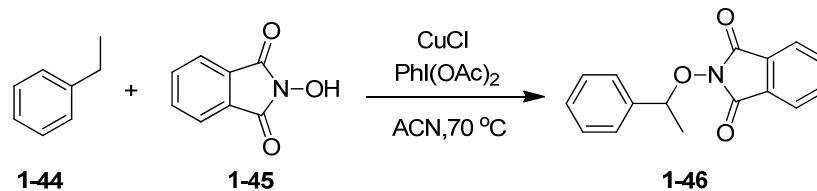
Recent developments in radical chemistry introduced phthalimido-*N*-oxyl (PINO•)<sup>8</sup> which has the potential to replace metals in functionalization of hydrocarbons.<sup>38</sup> In 1977, Grochowski *et al.* reported the catalytic use of NHPI for addition of diethyl ether to diethyl azodicarboxylate (DEAD) (Scheme 1-8).<sup>39</sup>



**Scheme 1-12:** NHPI catalyzed addition of diethyl ether to DEAD

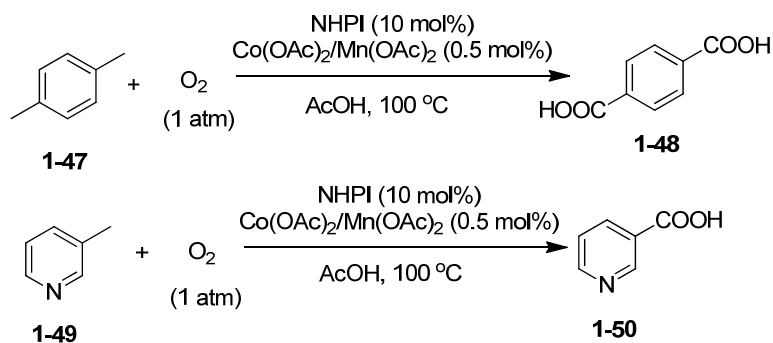
A detailed description of this reaction was not proven experimentally but since reaction did not progress in presence of a radical scavenger, this reaction was believed to proceed via mechanism depicted in Scheme 1-12. The hydrogen atom of *N*-hydroxyphthalimide (**1-37**) is added to diethyl azodicarboxylate (**1-36**), achieving an equilibrium between phthalimide *N*-oxyl (PINO•) (**1-39**) and **1-38**. PINO• (**1-39**) abstracts the hydrogen atom from the  $\alpha$ -C-H bond of ether (**1-40**) and generates a radical species (**1-41**), which adds to **1-36** resulting in the generation of a radical species **1-42**. This radical **1-42** abstracts the hydrogen atom from ether (**1-40**) to yield the product **1-43** and regenerates radical species **1-41**.

Lee *et al.* reported that the selective functionalization of allylic or benzylic C-H bonds can be achieved using *N*-hydroxyphthalimide and a copper catalyst (Scheme 1-13).<sup>40</sup> In this reaction PINO• abstracts H-atom from the hydrocarbon **1-44**. Interestingly, in this process, the H-abstraction is reported to be the rate limiting step.<sup>40</sup>

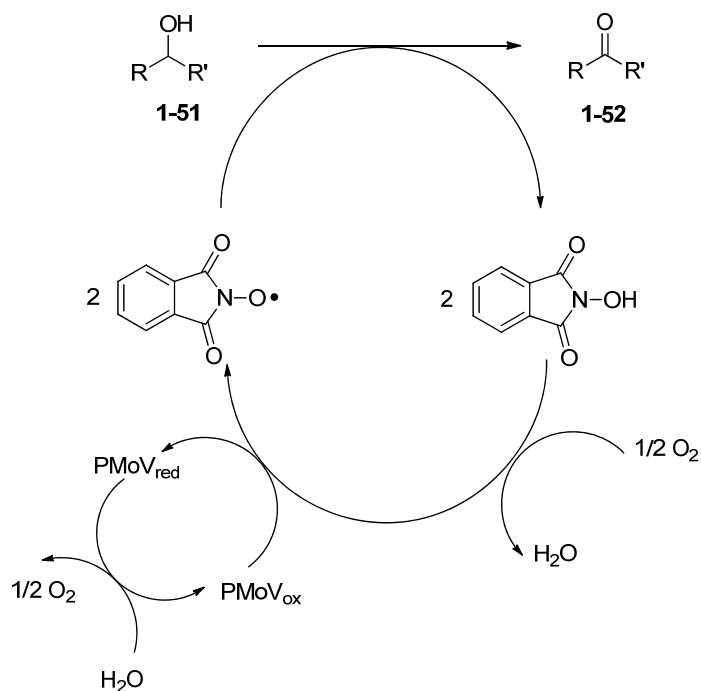


**Scheme 1-13:** Cu catalyzed C-O bond formation using NHPI<sup>40</sup>

PINO• has also been used as an oxidation catalyst in oxidation of alkanes,<sup>41</sup> alkylbenzenes (Scheme 1-14),<sup>23</sup> β-picoline to nicotinic acid,<sup>42</sup> unsaturated hydrocarbons,<sup>43</sup> cyclic ketones and alcohols (“K/A oil”),<sup>44</sup> carbonylation of alkanes,<sup>45</sup> one electron oxidation reactions,<sup>46</sup> reaction of aldehydes with alkenes to convert to corresponding ketones,<sup>47</sup> radical coupling between alkane and alkene,<sup>48</sup> etc. To summarize these applications, NHPI is used as a catalyst where homolytic cleavage of C-H bond is needed to generate carbon radicals.

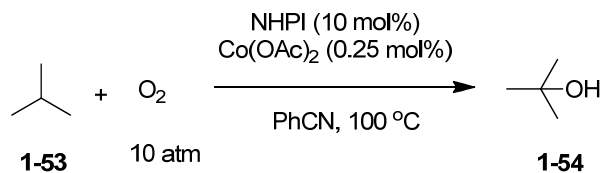


**Scheme 1-14:** NHPI catalyzed oxidation of methyl aromatic hydrocarbons.<sup>49</sup>



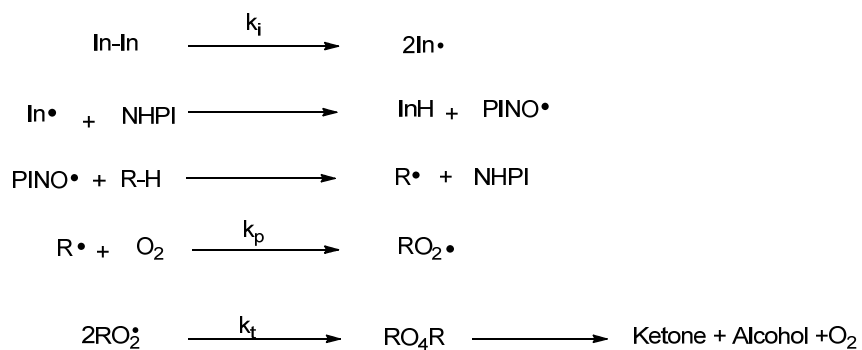
**Scheme 1-15:** Oxidation of alcohol catalyzed by NHPI and phosphomolybdic acid.<sup>12, 50</sup>

In the process of studying the NHPI catalyzed oxidation reaction of alcohols **1-51**, *Ishii et al.* proposed that the use of heteropoly acid (phosphomolybdic acid) would initiate the reaction. Surprisingly, it was observed that the reaction is successful in absence of heteropoly acid. Later on they proposed the mechanism that this oxidation occurred through the reaction of molecular oxygen with NHPI to generate PINO•, followed by PINO• abstracting the hydrogen atom from the alcohol to produce a ketone **1-52**. (Scheme 1-15).<sup>12, 50</sup> NHPI catalyzed oxidation of hydrocarbons were reported. For example, the oxidation of isobutane using NHPI and Co(OAc)<sub>2</sub> produced *t*-butyl alcohol in high yield.



**Scheme 1-16:** Oxidation of isobutene using NHPI/Co catalyst.<sup>51</sup>

Use of NHPI in the autoxidation of hydrocarbons is explained using a radical chain autoxidation mechanism. In this process, thermal initiators like peroxides initiate chain process and abstract H-atoms from hydrocarbons. In the initiation step, a reactive radical is generated which reacts with dioxygen and generates a peroxy radical. Finally, the peroxy radical abstracts a H-atom from the hydrocarbon in the propagation step to continue a chain reaction. This process has been used in the synthesis of ketones and alcohols from simple hydrocarbons (Scheme 1-17).<sup>52</sup>

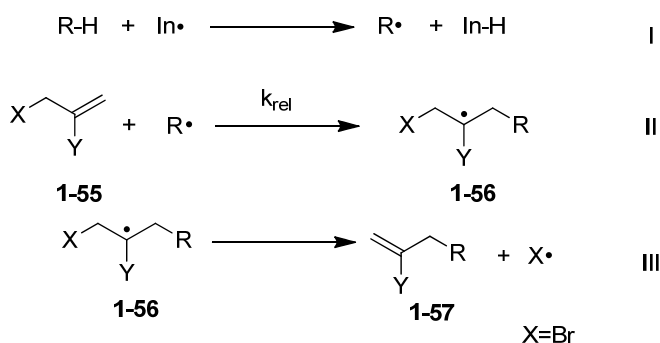


**Scheme 1-17:** Radical chain mechanism for autoxidation of hydrocarbons,<sup>19</sup>

## 1.6 Formation of Carbon-Carbon bonds through radical intermediates

### 1.6.1 Addition of carbon radicals to C=C bonds

Radical additions to C=C bonds are important in polymer synthesis and free radical mediated reactions in organic synthesis. Scheme 1-18 illustrates the mechanism of allyl transfer (addition of carbon radicals to C=C). In step (I) formation of R• is achieved using thermal initiators like *t*-butyl peroxide, benzoyl peroxide, or azoisobutyronitrile (AIBN). The X group must generate a reactive radical towards hydrogen abstraction such as bromine atom. In step (II) Y can be groups like Ph, CO<sub>2</sub>Et or CN that can stabilize the radical formed in the propagation step. R-H is a hydrocarbon which upon H-abstraction generates a carbon radical, R•. In the second step of the mechanism, the carbon radical adds to the allyl substrate **1-55**. There are various factors that could affect this addition. Sterics, polar, and enthalpic effects are important,<sup>17</sup> but sterics and polar effects seem to have a dominant effect on the transition state energy and rate of addition. As a result of this polar effect, the rate of addition of a carbon radical R• to an alkene **1-55** increases as Y substituent becomes more electron withdrawing.<sup>53</sup> (Scheme 1-18)

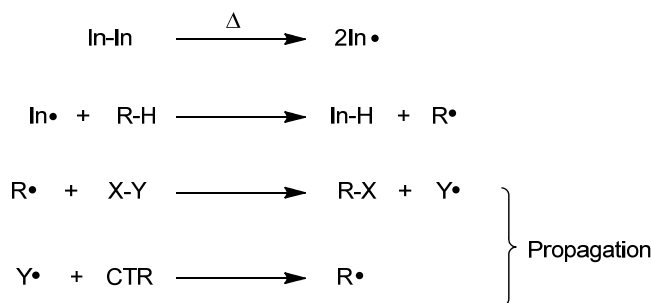


**Scheme 1-18:** Addition of carbon radical to alkene,<sup>53</sup> R=alkyl, benzyl radical, X=H,CH<sub>3</sub>

## 1.6.2 Other allyl transfer reactions (Living/controlled polymerization processes)

Part of the inspiration for the allyl transfer reaction, specifically the addition/elimination step, comes from the earlier work in the area of living/controlled radical polymerization (especially radical addition-fragmentation chain transfer (RAFT) which involves the transfer of an allyl group). Accordingly, this section focuses on some of that earlier chemistry.

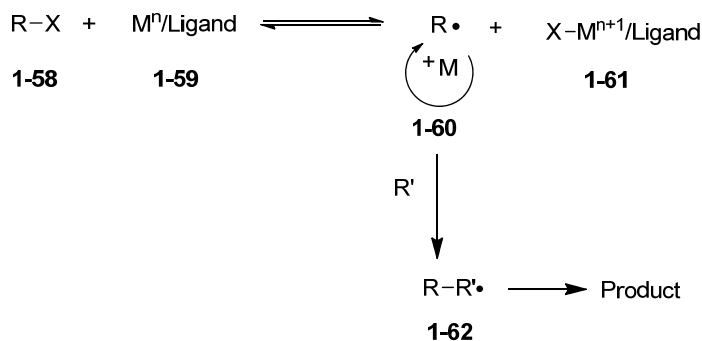
One of the processes that involve “allyl transfer” in which the allyl group is transferred by addition of a carbon radical to C=C (Scheme 1-10), is a living/controlled free radical polymerization process. This process is an effective way to accurately control molecular structure and molecular weight of a polymer and is categorized into three general mechanisms:<sup>54</sup> 1) atom transfer radical polymerization (ATRP) (Scheme 1-19) and ATRP mediated by a transition metal<sup>55</sup> (Scheme 1-20), 2) nitroxide-mediated polymerization (NMP,<sup>56</sup> Scheme 1-21) radical addition-fragmentation chain transfer (RAFT,<sup>57</sup> Scheme 1-22).



**Scheme 1-19:** General atom transfer mechanism, CTR=Chain transfer reagent,<sup>55</sup>

Atom transfer is a key step in metal-mediated atom transfer radical polymerization (ATRP). In this method, an alkyl halide is reduced by a metal to form a reactive radical.<sup>58</sup> Matyjaszewski *et al.* reported this to be a useful reaction for C-C bond formation in organic chemistry.<sup>55, 59</sup> In this reaction (Scheme 1-20), a metal/ ligand complex **1-60** abstracts the

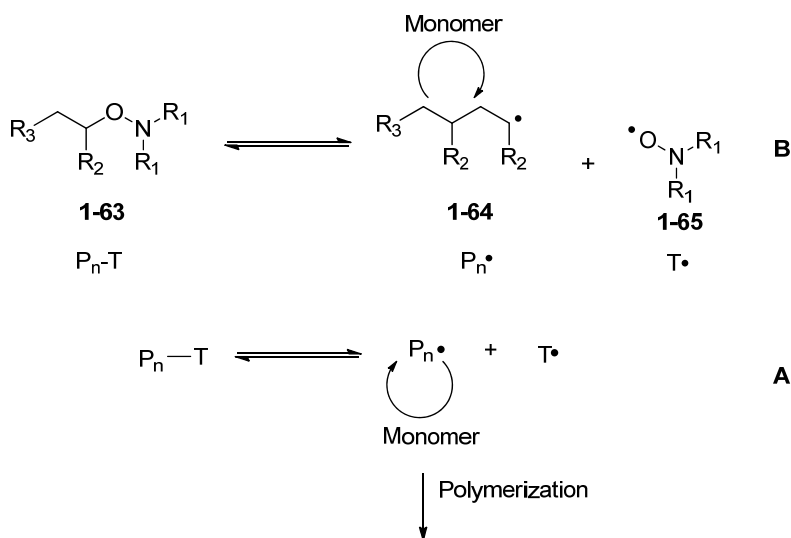
halogen (X) from an alkyl halide **1-58** and carries it until oxidized to a higher oxidation number **1-61** ( $X-M^{n+1}$ ).



**Scheme 1-20:** Mechanism for metal catalyzed ATRP (atom transfer radical polymerization)<sup>55</sup>

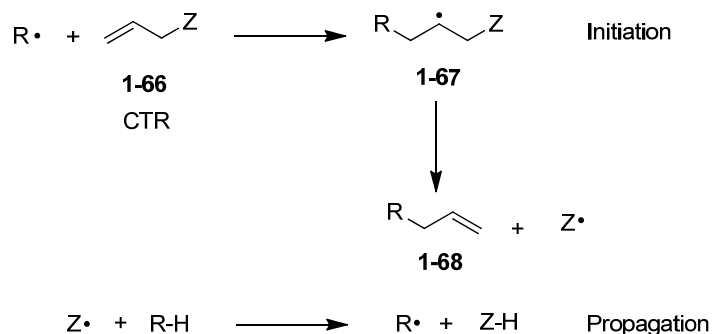
The resulting alkyl radical ( $R'$ ) adds to the alkene to form an adduct **1-62**. Finally, the adduct reacts with the oxidized halide-metal complex and undergoes termination or disproportionation to form final product. In this process, the metal reduces the alkyl halide ( $R-X$ ) and sets the stage for another redox cycle (Scheme 1-20).<sup>58</sup>

As the name implies, nitroxide-mediated radical polymerization (NMP) uses a nitroxide radical as an initiator. This method is highly efficient in achieving controlled stereochemistry, high chain length and a very low polydispersity index in polymerization.<sup>54</sup> In this method a nitroxyl radical is generated from an alkoxyamine **1-63** ( $R_2N-OH$ ) via thermally induced homolysis of the C-O bond ( $P_n-T$ , Scheme 1-21) generating a stable nitroxyl radical **1-65** and a carbon radical **1-64**.<sup>60</sup> For the best results, the  $R_1$  group attached to the nitrogen (Scheme 1-21, B) is preferred to be a sterically hindered group whereas the  $R_2$  group (Scheme 1-21, B) attached to oxygen is preferred to be a phenyl which helps in generating a stable benzyl radical. The lack of termination allows NMP polymerization to continue till long polymeric chains are generated.<sup>60</sup>



**Scheme 1-21:** A) General mechanism for nitroxide mediated polymerization<sup>56</sup> ( $\text{P}_n\cdot$  represents the growing polymer chain,  $\text{T}\cdot$  represents mediating nitroxyl radical), B) Mechanism using nitroxide and carbon radical, monomer used is either styrene or derivatives of styrene.

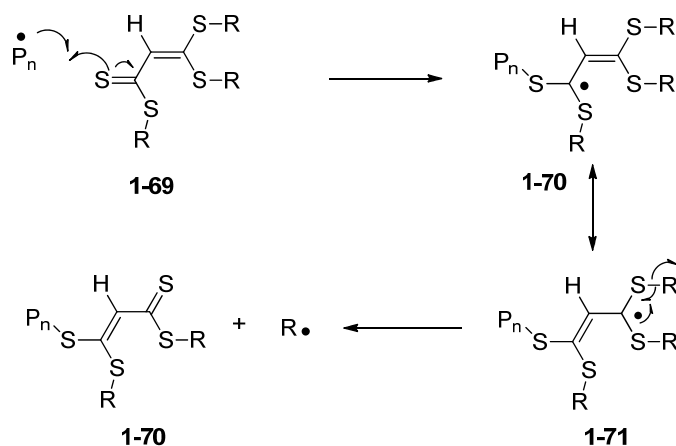
Nitroxyl mediated polymerizations (Scheme 1-21) work effectively with styrene type substrates.<sup>60</sup> However, the literature reports that the slower rate of the polymerization could be a problem in this method.<sup>61</sup> Since the rates of polymerization mainly depend on the BDE of the C-O bond of nitroxide/alkoxyamine, it is reported that the BDE significantly decreases with the increase in the ring size of alkoxyamines.<sup>54</sup> Moreover, Tordo *et al.* reported that the open chain  $\beta$ -phosphonylated nitroxyl radicals are better alternatives and this modification in structure significantly increases the rates of propagation and overcomes all control related problems.<sup>62</sup>



**Scheme 1-22:** General mechanism for radical addition-fragmentation transfer method,

CTR=Chain transfer reagent,<sup>63</sup> (Z = I, Br, SR, SnR<sub>3</sub>, etc.)

Radical addition-fragmentation chain transfer (RAFT) polymerization (Scheme 1-22) is an efficient method for radical addition especially for the substrates like xanthates,<sup>64</sup> thiocarbonylthio,<sup>65</sup> dithioesters<sup>66</sup> and thiocarbamates.<sup>57</sup> These substrates are used as a chain transfer agent (RAFT agent). The RAFT method provides excellent control over molecular weight and polydispersity indices.<sup>67</sup> Many synthetically useful radical addition processes depend on tin reagents. But, if substrates have weak bonds, then use of tin or any other heavy metal could be easily avoided. Based on this hypothesis, RAFT offers a suitable alternative to metal-mediated free radical addition reactions. Zard *et al.* studied xanthates (Scheme 1-23) and reported that the weak C-S bonds in xanthates undergoes cleavage easily to generate reactive free radicals.<sup>64a</sup> The xanthate group transfers reversibly in the propagation step.<sup>64a</sup> The reactive C=S bonds and weak C-S bonds are key factors involved in RAFT polymerization. Generally, thermal initiators like azoisobutyronitrile (AIBN) or benzoyl peroxide are used in RAFT polymerization.<sup>67</sup> RAFT polymerizations are used to design complex polymers such as linear block copolymers, comb-like, star, brush polymers etc.<sup>67</sup>



**Scheme 1-23:** RAFT polymerization with reactive C=S bond,<sup>68</sup>

## 1.7 Radical initiators

In this section we will briefly discuss about various thermal initiators that are known to be used in allyl transfer reactions

### 1.7.1 Thermal initiator (*t*-butyl peroxide)

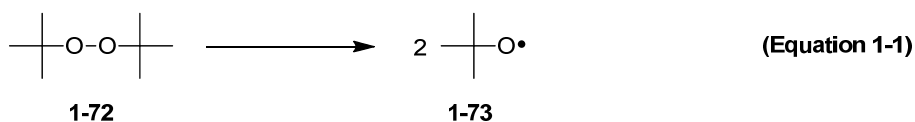
Thermal initiators are important in organic chemistry due to their wide applications. These are the compounds with weak bonds and electron stabilizing functional groups which can stabilize the generating radical. Commonly used thermal initiators are benzoyl peroxide (BzO)<sub>2</sub>, *t*-butyl peroxide (*t*-BuO)<sub>2</sub> and azobisisobutyronitrile (AIBN).



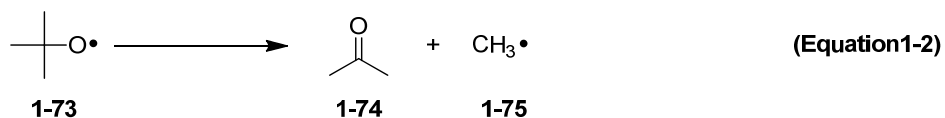
**Scheme 1-24:** Generation of new radical using thermal initiators,<sup>18</sup>

These radicals are formed *in situ*. The main problem with using these thermal initiators is that the reactions require high temperatures, often > 120° C, which results in loss of stereo-control.

Some of the earlier work in this research involves the use of a thermal initiator, *t*-butyl peroxide. This section is dedicated to a discussion of the mechanism and physical properties of this initiator. *t*-Butyl peroxide follows first-order decomposition in gas and solution phase.<sup>69</sup> The activation parameters at 116-350 °C were reported to be 38 kcal ( $E_a$ ) and  $7 \times 10^{15} \text{ s}^{-1}$  (pre-exponential factor).<sup>70</sup> The rate constants for decomposition in solution and in gas phase are essentially the same suggesting a simple unimolecular process.<sup>69</sup>



However, the mechanism for decomposition is complicated as it converts *t*-butoxyl radical **1-73** to acetone **1-74** and methyl radical **1-75** (**Equation 1-2**) followed by dimerization of methyl radical **1-75**, when in the gas phase.



In solution, *t*-butoxyl radical **1-73** may abstract hydrogen atom from solvent forming *t*-butanol and compete with reaction in (**Equation 1-2**), which is a radical decomposition process and expected to occur at a constant rate at a given temperature and be independent of the medium. The *t*-butyl alcohol/acetone ratio depends on the hydrogen atom-donating ability of the solvent.<sup>71</sup> Increasing hydrogen atom-donating ability will result in more *t*-butanol formation. Since, *t*-butyl alcohol/acetone ratio decreases with temperature in a given system, it is concluded that the activation energy for the *t*-butoxy radical **1-73** decomposition (**Equation 1-2**) is higher than that for hydrogen abstraction. An estimate for the activation energy of the  $\beta$ -scission step is ca. 11-16 kcal/ mol.<sup>72</sup> Thus, *t*-butoxy radical **1-73** decomposition is easy to circumvent and

almost any hydrogen donor will divert this intermediate away from acetone **1-74** to *t*-butyl alcohol product.

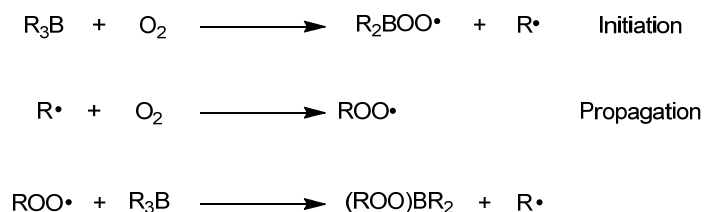
Reaction condition	E <sub>a</sub> (kcal/mol)	log A (s <sup>-1</sup> )
Gas phase	37.4	15.6
In <i>t</i> -butylbenzene	38.0	16
In Cumene	37.5	15.8

**Table 1-6:** Activation parameters for *t*-butyl peroxide decomposition.<sup>71</sup>

Although the activation enthalpy varies from 31 kcal/mol in acetonitrile to 40.8 kcal/mol in cyclohexane, there is not very much difference in the rates because of compensation in the apparent activation entropies.<sup>73</sup>

### 1.7.2 Organoboranes as radical generators (trialkylborane)

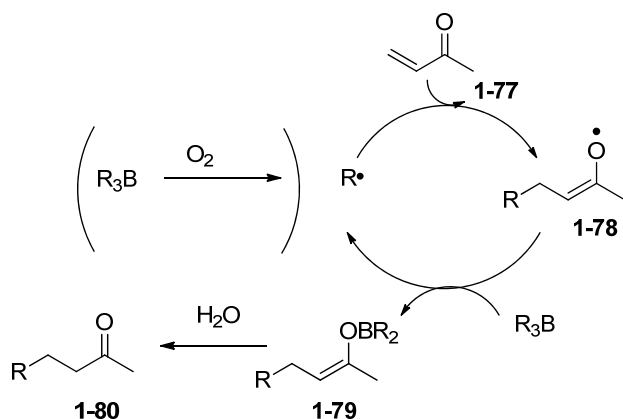
Trialkylborane and 9-BBN [9-borabicyclo(3.3.1)nonane] are used as radical initiators in many organic transformations.<sup>74</sup> These initiators are especially useful in stereoselective radical addition reactions,<sup>75</sup> where reaction conditions demand very low temperature (-78 °C). The proposed mechanism for autoxidation of trialkylborane to generate reactive radical suggests that in the initiation step this compound reacts with triplet oxygen and generates a peroxy and an alkyl radical. The alkyl radical reacts with another mole of triplet oxygen to generate another peroxy radical in the propagation step. Alkyl and/or peroxy radicals act as an initiator for H-atom abstraction (Scheme 1-25).<sup>76</sup> This chain reaction goes on until all the alkyl groups on boron atom have been utilized for peroxy radical generation.



**Scheme 1-25:** Mechanism of autoxidation of trialkylboranes,<sup>74</sup>

Oshima *et al.* reported that triethylborane serves as a good radical initiator and chain transfer reagent upon autoxidation.<sup>77</sup> This reagent can be successfully used at lower temperatures (-78 °C) and suitable for reactions involving thermally unstable products and poor stereochemical control at high temperature.<sup>74</sup> Triethylborane has been used as a replacement for several “tin hydride-mediated” processes such as, halogen atom abstraction,<sup>78</sup> addition to unsaturated hydrocarbons (with control of diastereoselectivity and enantioselectivity),<sup>79</sup> atom transfer reactions etc.<sup>74, 78, 80</sup> Whereas, 9-BBN has been used in the reduction of halogens, regioselective addition on alkenes and reported to be a better reagent than triethylborane.<sup>74</sup>

Brown *et al.* proposed the unusual behavior of trialkyl borane compound in presence of a  $\alpha,\beta$ -unsaturated ketone. Trialkylborane reacts with triplet oxygen to generate a reactive ethyl radical (R•) which then adds to the conjugated ketone **1-77** rather than reacting with another mole of triplet oxygen. The intermediate enolate radical **1-78** then reacts with trialkylborane to form **1-79**. Finally, **1-79** hydrolyzes to yield the final product **1-80**. (Scheme 1-26).<sup>81</sup>



**Scheme 1-26:** Brown's mechanism for the addition of trialkylborane to methyl vinyl ketone,<sup>81</sup>

Some other applications of triethylborane include radical inhibition for chain reactions, organocatalyst in polymerization processes,<sup>82</sup> and hydroboration reactions.<sup>83</sup>

## 1.8 Conclusions and directions for research

In this review chapter we discussed various methods of hydrocarbon functionalization, addition of carbon radicals to alkenes, allied polymerization processes that involve radical addition- fragmentation transfer, hydrogen atom abstraction and thermal initiation. We also discussed in detail the utility of PINO as an H-atom abstractor, and provided examples of its use in various reactions.

In the course of introducing this chemistry, we briefly reviewed an allyl transfer reaction introduced by Tanko *et al.*<sup>84</sup> This allyl transfer reaction has been reported using bromine as a chain carrier. In the current research we seek to replace the bromine atom by a nitroxyl radical (phthalimido-*N*-oxyl) which will help make this chemistry environmentally friendly. This new allyl transfer reaction will provide a convenient and metal-free way to hydrocarbon functionalization. In chapter 2 synthesis of these new allyl-PINO substrates will be discussed.

The hydrocarbon functionalization of alkyl aromatic hydrocarbons via allyl transfer using allyl-PINO substrates will be discussed. The kinetic studies will be performed to test the efficiency of these chain reactions via kinetic chain length measurement. Relative rate constant for radical addition elimination process will be discussed.

Through these investigations role of phthalimido-*N* oxyl radical as hydrogen abstractor and leaving group will be evaluated. This process will be compared to the earlier process involving bromine chemistry.

## 1.9 References

1. Hembre, R. T., Selective Hydrocarbon Activation. Edited by Julian A. Davies, Patricia L. Watson. *Photochem. Photobiol.* **1992**, *56* (1), 143-143.
2. Dagani, R. O. N., Hydrocarbon bonds activated by complexes. *Chemical & Engineering News Archive* **1982**, *60* (3), 59-63.
3. (a) Bergman, R. G., *Nature* **2007**, (446), 391; (b) Labinger, J. A.; Bercaw, J. E., *Nature* **2002**, *417*, 507.
4. Tanko, J. M.; Sadeghipour, M., Funktionalisierung von Kohlenwasserstoffen über eine neuartige, radikalische Kondensationsreaktion. *Angew. Chem.* **1999**, *111* (1-2), 219-222.
5. (a) Davies, J. A., *Selective hydrocarbon activation : principles and progress*. VCH Publishers: New York, N.Y., 1990; (b) Parkins, A. W., Activation and catalytic reactions of saturated hydrocarbons in the presence of metal complexes. A. E. Shilov and G. B. Shul'pin. Kluwer Academic Publishers, Dordrecht, 2000. xiv + 536 pages. £142 ISBN 0-7923-6101-6. *Appl. Organomet. Chem.* **2000**, *14* (11), 746-747.
6. Shilov, A. E.; Shul'pin, G. B., Activation of C–H Bonds by Metal Complexes. *Chem. Rev.* **1997**, *97* (8), 2879-2932.
7. Díaz-Requejo, M. M.; Pérez, P. J., Coinage Metal Catalyzed C–H Bond Functionalization of Hydrocarbons. *Chem. Rev.* **2008**, *108* (8), 3379-3394.
8. Recupero, F.; Punta, C., Free Radical Functionalization of Organic Compounds Catalyzed by N-Hydroxyphthalimide†. *Chem. Rev. (Washington, DC, U. S.)* **2007**, *107* (9), 3800-3842.
9. Simándi, L. I.; Central Research Institute for Chemistry, B. In *Dioxygen activation and homogeneous catalytic oxidation : 4th International symposium : Papers*, 1991; Elsevier.
10. Tabushi, I.; Koga, N., P-450 type oxygen activation by porphyrin-manganese complex. *J. Am. Chem. Soc.* **1979**, *101* (21), 6456-6458.
11. Tabushi, I.; Yazaki, A., P-450-type dioxygen activation using hydrogen/colloidal platinum as an effective electron donor. *J. Am. Chem. Soc.* **1981**, *103* (24), 7371-7373.
12. Ishii, Y.; Nakayama, K.; Takeno, M.; Sakaguchi, S.; Iwahama, T.; Nishiyama, Y., Novel Catalysis by N-Hydroxyphthalimide in the Oxidation of Organic Substrates by Molecular Oxygen. *J. Org. Chem.* **1995**, *60* (13), 3934-3935.
13. Beeson, T. D.; Mastracchio, A.; Hong, J.-B.; Ashton, K.; MacMillan, D. W. C., Enantioselective Organocatalysis Using SOMO Activation. *Science* **2007**, *316* (5824), 582-585.
14. Godula, K.; Sames, D., C-H Bond Functionalization in Complex Organic Synthesis. *Science* **2006**, *312* (5770), 67-72.
15. (a) Blanksby, S. J.; Ellison, G. B., Bond Dissociation Energies of Organic Molecules. *Acc. Chem. Res.* **2003**, *36* (4), 255-263; (b) Kranenburg, M.; Ciriano, M. V.; Cherkasov, A.; Mulder, P., Carbon–Oxygen Bond Dissociation Enthalpies in Peroxyl Radicals. *J. Phys. Chem. A* **2000**, *104* (5), 915-921.
16. Cruickshank, F. R.; Benson, S. W., Kinetics and mechanism of the reaction of iodine with tetrahydrofuran. Carbon-hydrogen bond dissociation energy in tetrahydrofuran. *J. Am. Chem. Soc.* **1969**, *91* (6), 1289-1292.
17. Koshino, N.; Cai, Y.; Espenson, J. H., Kinetic Study of the Phthalimide N-Oxyl (PINO) Radical in Acetic Acid. Hydrogen Abstraction from C–H Bonds and Evaluation of O–H Bond Dissociation Energy of N-Hydroxyphthalimide. *J. Phys. Chem. A* **2003**, *107* (21), 4262-4267.
18. Erlenmayer, H.; Schoenare, W., *Helv. Chim. Acta* **1936**, *19* (338).

19. Anderson, H. R. J.; Scherage, H. A.; VanArtsdalen, E. R., *J.Chem.Phys* **1953**, *21*, 1258.
20. (a) Howatd, J. A., In Peroxy Radicals. *Wiley & Sons,Chichester* **1997**; (b) Ueda, C.; Noyama, M.; Ohmori, H.; Masui, M., *Chem.Pharma.Bull.* **1987**, *35*, 1372; (c) Amorati, R.; Lucarini, M.; Mugnaini, V.; Pedulli, G. F.; Minisci, F.; Recupero, F.; Fontana, F.; Astolfi, P.; Greci, L., Hydroxylamines as Oxidation Catalysts: Thermochemical and Kinetic Studies. *J. Org. Chem.* **2003**, *68* (5), 1747-1754.
21. Mahoney, L. R.; Mendenhall, G. D.; Ingold, K. U., Calorimetric and equilibrium studies on some stable nitroxide and iminoxy radicals. Approximate oxygen-hydrogen bond dissociation energies in hydroxylamines and oximes. *J. Am. Chem. Soc.* **2002**, *95* (26), 8610-8614.
22. Baciocchi, E.; Gerini, M. F.; Lanzalunga, O., Reactivity of Phthalimide N-Oxyl Radical (PINO) toward the Phenolic O–H Bond. A Kinetic Study. *J. Org. Chem* **2004**, *69* (25), 8963-8966.
23. Yoshino, Y.; Hayashi, Y.; Iwahama, T.; Sakaguchi, S.; Ishii, Y., Catalytic Oxidation of Alkylbenzenes with Molecular Oxygen under Normal Pressure and Temperature by N-Hydroxyphthalimide Combined with Co(OAc)<sub>2</sub>. *J. Org. Chem* **1997**, *62* (20), 6810-6813.
24. Simonyi, M.; Fitos, I.; Kardos, J.; Lukovits, I., *J.chem.Soc.Chem.Comm.* **1975**, 252.
25. Baciocchi, E.; Bietti, M.; Gerini, M. F.; Lanzalunga, O., Electron-Transfer Mechanism in the N-De methylation of N,N-Dimethylanilines by the Phthalimide-N-oxyl Radical. *J. Org. Chem* **2005**, *70* (13), 5144-5149.
26. Lebedev, O. L.; Kazarnovskii, S. N., *Chem.Abstr.* **1961**, *55*, 1473a.
27. Rozatsev, E. G., Free Nitroxyl radicals. *plenum press.* **1970**, *New York* (Ed.: H.Ulrich).
28. Sheldon, R. A.; Arends, I. W. C. E., Organocatalytic Oxidations Mediated by Nitroxyl Radicals. *Adv. Synth. Catal.* **2004**, *346*, 1051-1071.
29. Jenkins, T. C.; Perkins, M. J.; Siew, N. P. Y., *J.chem.Soc.Perkin Trans.* **1983**, *2*, 717.
30. Sheldon, Roger A.; Arends, Isabel W. C. E., Organocatalytic Oxidations Mediated by Nitroxyl Radicals. *Advanced Synthesis & Catalysis* **2004**, *346* (9-10), 1051-1071.
31. Bottle, S. E.; Busfield, W. K.; Jenkins, I. D., *J.chem.Soc.Perkin Trans.* **1992**, *2*, 2145.
32. Babiarz, J. E.; Cunkle, G. T.; DeBellis, A. D.; Eveland, D.; Pastor, S. D.; Shum, S. P., The Thermal Reaction of Sterically Hindered Nitroxyl Radicals with Allylic and Benzylic Substrates: Experimental and Computational Evidence for Divergent Mechanisms. *J. Org. Chem* **2002**, *67* (19), 6831-6834.
33. Coseri, S.; Ingold, K. U., Distinguishing between Abstraction and Addition as the First Step in the Reaction of a Nitroxyl Radical with Cyclohexene. *Org. Lett.* **2004**, *6* (10), 1641-1643.
34. (a) Carloni, P.; Greci, L.; Stipa, P.; Ebersson, L., Electron-transfer reactions. Oxidation of Grignard reagents in the presence of an aminoxyl as a radical-trapping agent. *J. Org. Chem* **2002**, *56* (15), 4733-4737; (b) Stipa, P.; Greci, L.; Carloni, P.; Damiani, E., "Synthesis and thermal stability of alkoxyamines". *Polym.Degrad.Stab* **1997**, *55*, 323-327.
35. Damiani, E.; Carloni, P.; Iacussi, M.; Stipa, P.; Greci, L., "Reactivity of sulfur-centered radicals with indolonic and quinolinic aminoxyls. *Euro.J.Org.Chem.* **1999**, *1*, 2405-2412.
36. Greci, L., "Homolytic substitution in indolinone nitroxide radicals". *Gazz.Chim.Ital* **1982**, *119*, 621-625.
37. Damiani, E.; Astolfi, P.; Benaglia, M.; Alberti, A.; Greci, L., Hydrogen Abstraction Ability of Different Aromatic Nitroxides. *Free Radical Res.* **2004**, *38* (1), 67-72.
38. Ishii, Y.; Sakaguchi, S.; Iwahama, T., Innovation of Hydrocarbon Oxidation with Molecular Oxygen and Related Reactions. *Adv. Synth. Catal.* **2001**, *343* (5), 393-427.

39. Grochowski, E. B., T.; Jurczak, J., Reaction of Diethyl Azodicarboxylate with Ethers in the Presence of N-Hydroxyimides as Catalysts *Synthesis* **1977**, 718.
40. Lee, J. M.; Park, E. J.; Cho, S. H.; Chang, S., Cu-Facilitated C–O Bond Formation Using N-Hydroxyphthalimide: Efficient and Selective Functionalization of Benzyl and Allylic C–H Bonds. *J. Am. Chem. Soc.* **2008**, *130* (25), 7824-7825.
41. Ishii, Y.; Iwahama, T.; Sakaguchi, S.; Nakayama, K.; Nishiyama, Y., Alkane Oxidation with Molecular Oxygen Using a New Efficient Catalytic System: N-Hydroxyphthalimide (NHPI) Combined with Co(acac)<sub>n</sub> (n = 2 or 3)<sup>†</sup>. *The Journal of Organic Chemistry* **1996**, *61* (14), 4520-4526.
42. Shibamoto, A.; Sakaguchi, S.; Ishii, Y., *Org. Process Res. Dev.* **2000**, *4*, 505.
43. (a) Iwahama, T.; Sakaguchi, S.; Ishii, Y., *Chem. Comm.* **1999**, 727; (b) Sakaguchi, S.; Takase, T.; Iwahama, T.; Ishii, Y., *Chem. Comm.* **1998**, 2037.
44. Fukuda, O.; Iwahama, T.; Sakaguchi, S.; Ishii, Y., *Tetrahedron Lett.* **2001**, *42*, 3479.
45. Kato, S.; Iwahama, T.; Sakaguchi, S.; Ishii, Y., N-Hydroxyphthalimide-Catalyzed Carboxylation of Polycyclic Alkanes with Carbon Monoxide in the Presence of Dioxygen. *J. Org. Chem* **1998**, *63* (2), 222-223.
46. Sakaguchi, S.; Hirabayashi, T.; Ishii, Y., *Chem. Comm.* **2002**, 516.
47. Tsujimoto, S.; Iwahama, T.; Sakaguchi, S.; Ishii, Y., *Chem. Comm.* **2001**, 2352.
48. Hara, T.; Iwahama, T.; Sakaguchi, S.; Ishii, Y., Catalytic Oxyalkylation of Alkenes with Alkanes and Molecular Oxygen via a Radical Process Using N-Hydroxyphthalimide. *J. Org. Chem* **2001**, *66* (19), 6425-6431.
49. Ullmann, F.; Gerhartz, W.; Yamamoto, Y. S.; Campbell, F. T.; Pfefferkorn, R.; Rounsaville, J. F., *Ullmann's encyclopedia of industrial chemistry*. VCH: Weinheim, Federal Republic of Germany; Deerfield Beach, FL, USA, 1985.
50. Masui, M.; Ueshima, T.; Ozaki, S., *J. chem. Soc. Chem. Commun.* **1983**, 479.
51. S. Sakaguchi; S. Kato; T. Iwahama; Ishii, Y., *Bull. Chem. Soc. Jpn.* **1998**, *71*, 1237.
52. Sheldon, R. A.; Kochi, J. K., Metal Catalysed Oxidations of Organic Compounds. *Academic Press* **1981**, New York.
53. Russell, G. A.; Kochi, J. K., In free Radicals. *Wiley & Sons, New York* **1973**, *1* (1A), Chapter 7.
54. Moad, G.; Rizzardo, E., Alkoxyamine-Initiated Living Radical Polymerization: Factors Affecting Alkoxyamine Homolysis Rates. *Macromolecules* **2002**, *28* (26), 8722-8728.
55. Matyjaszewski, K.; Xia, J., Atom Transfer Radical Polymerization. *Chem. Rev.* **2001**, *101* (9), 2921-2990.
56. Hawker, C. J.; Bosman, A. W.; Harth, E., New Polymer Synthesis by Nitroxide Mediated Living Radical Polymerizations. *Chemical Reviews* **2001**, *101* (12), 3661-3688.
57. Chiefari, J.; Chong, Y. K.; Ercole, F.; Krstina, J.; Jeffery, J.; Le, T. P. T.; Mayadunne, R. T. A.; Meijs, G. F.; Moad, C. L.; Moad, G.; Rizzardo, E.; Thang, S. H., Living Free-Radical Polymerization by Reversible Addition–Fragmentation Chain Transfer: The RAFT Process. *Macromolecules* **1998**, *31* (16), 5559-5562.
58. Wang, J.-S.; Matyjaszewski, K., Controlled/"living" radical polymerization. atom transfer radical polymerization in the presence of transition-metal complexes. *J. Am. Chem. Soc.* **2002**, *117* (20), 5614-5615.
59. Matyjaszewski, k., Advances in Living/Controlled Radical Polymerization. *American Chemical Society* **2003**, 854.

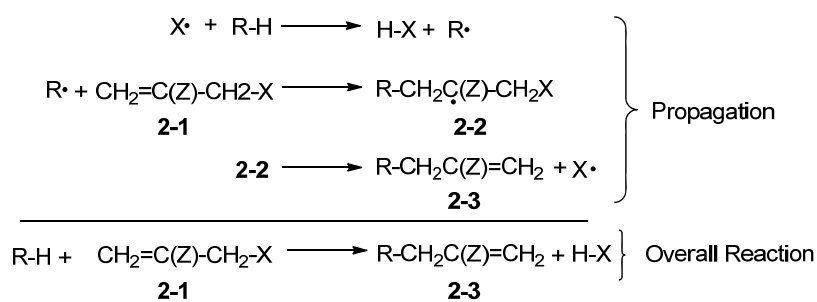
60. Hawker, C. J.; Bosman, A. W.; Harth, E., New Polymer Synthesis by Nitroxide Mediated Living Radical Polymerizations. *Chem. Rev.* **2001**, *101* (12), 3661-3688.
61. Rizzardo, E., *Chem.Aust.* **1987**, *54* (32).
62. Grimaldi, S.; Finet, J.-P.; Le Moigne, F.; Zeghdaoui, A.; Tordo, P.; Benoit, D.; Fontanille, M.; Gnanou, Y., Acyclic  $\beta$ -Phosphonylated Nitroxides: A New Series of Counter-Radicals for "Living"/Controlled Free Radical Polymerization. *Macromolecules* **2000**, *33* (4), 1141-1147.
63. Barson, C. A., "Chain Transfer" in comprehensive polymer science Eastmond G.C Ledwith A. **1989**, *171* (Ed 3th).
64. (a) Zard, S. Z., On the Trail of Xanthates: Some New Chemistry from an Old Functional Group. *Angewandte Chemie International Edition in English* **1997**, *36* (7), 672-685; (b) Destarac, M.; Bzducha, W.; Taton, D.; Gauthier-Gillaizeau, I.; Zard, S. Z., Xanthates as Chain-Transfer Agents in Controlled Radical Polymerization (MADIX): Structural Effect of the O-Alkyl Group. *Macromol. Rapid Commun.* **2002**, *23* (17), 1049-1054.
65. Mikolajczyk, M.; Luczak, J., Organosulfur compounds. 14. Dimethyl selenoxide oxidation of trivalent phosphorus compounds, thio- and selenophosphoryl compounds, and thiocarbonyl compounds. Stereochemical studies and selective modification of the thiocarbonyl-containing nucleic acid components. *J. Org. Chem* **1978**, *43* (11), 2132-2138.
66. Hua, D.; Ge, X.; Bai, R.; Lu, W.; Pan, C., Dithioester (ZC(S)SR) mediated 'controlled/living' free-radical polymerization of methyl acrylate under  $^{60}\text{Co}$   $\gamma$ -ray irradiation. Structure effect of Z-group. *Polymer* **2005**, *46* (26), 12696-12702.
67. O'Donnell, J. M., Reversible addition-fragmentation chain transfer polymerization in microemulsion. *Chem. Soc. Rev.* **2012**, *41* (8), 3061-3076.
68. Destarac, M.; Gauthier-Gillaizeau, I.; Vuong, C.-T.; Zard, S. Z., Vinylogous Thionothio Compounds for RAFT Polymerization. *Macromolecules* **2005**, *39* (3), 912-914.
69. Raley, J. H.; Rust, F. F.; Vaughan, W. E., Decompositions of Di-t-Alkyl Peroxides. I. Kinetics. *J. Am. Chem. Soc.* **1948**, *70* (1), 88-94.
70. Lossing, F.; Tickner, A. W., *J. Chem. Phys.* **1952**, *20*, 907.
71. Lamb, R. C.; Pacifici, J. G., Organic Peroxides. III. The Behavior of Cyclohexaneformyl Peroxide in the Presence of Excess Stable Radicals. The Simultaneous Determination of Kinetics and Free Radical Efficiencies in the Thermal Decompositions of Free Radical Initiators. *J. Am. Chem. Soc.* **1964**, *86* (5), 914-918.
72. Gray, P.; Williams, A., The Thermochemistry And Reactivity Of Alkoxy Radicals. *Chem. Rev.* **1959**, *59* (2), 239-328.
73. Huyser, E. S.; VanScoy, R. M., Effects of solvent on the unimolecular decomposition of t-butyl peroxide. *J. Org. Chem.* **1968**, *33* (9), 3524-3527.
74. Ollivier, C.; Renaud, P., Organoboranes as a Source of Radicals. *Chem. Rev.* (Washington, DC, U. S.) **2001**, *101* (11), 3415-3434.
75. Sibi, M. P.; Porter, N. A., Enantioselective Free Radical Reactions. *Acc. Chem. Res.* **1998**, *32* (2), 163-171.
76. (a) Krusic, P. J.; Kochi, J. K., Electron spin resonance studies of homolytic substitution reactions. Organoboron, -aluminum, and -gallium compounds. *J. Am. Chem. Soc.* **2002**, *91* (14), 3942-3944; (b) Snyder, H. R.; Kuck, J. A.; Johnson, J. R., Organoboron Compounds, and the Study of Reaction Mechanisms. Primary Aliphatic Boronic Acids I. *J. Am. Chem. Soc.* **2002**, *60* (1), 105-111.
77. Oshima, K., *Bull. Chem. Soc. Jpn* **1989**, *62*, 143.

78. Curran, D. P.; Chen, M. H.; Spletzer, E.; Seong, C. M.; Chang, C. T., Atom-transfer addition and annulation reactions of iodomalونات. *J. Am. Chem. Soc.* **2002**, *111* (24), 8872-8878.
79. Nozaki, K.; Oshima, K.; Uchimoto, K., Et<sub>3</sub>B-induced radical addition of R<sub>3</sub>SnH to acetylenes and its application to cyclization reaction. *J. Am. Chem. Soc.* **2002**, *109* (8), 2547-2549.
80. Curran, D. P.; Chang, C. T., Atom transfer cyclization reactions of .alpha.-iodo esters, ketones, and malonates: examples of selective 5-exo, 6-endo, 6-exo, and 7-endo ring closures. *J. Org. Chem.* **2002**, *54* (13), 3140-3157.
81. Kabalka, G. W.; Brown, H. C.; Suzuki, A.; Honma, S.; Arase, A.; Itoh, M., Inhibition of the reaction of organoboranes with .alpha.,.beta.-unsaturated carbonyl derivatives by galvinoxyl. Evidence for a free-radical chain mechanism. *J. Am. Chem. Soc.* **2002**, *92* (3), 710-712.
82. Busch, B. B.; Paz, M. M.; Shea, K. J.; Staiger, C. L.; Stoddard, J. M.; Walker, J. R.; Zhou, X.-Z.; Zhu, H., The Boron-Catalyzed Polymerization of Dimethylsulfoxonium Methylide. A Living Polymethylene Synthesis. *J. Am. Chem. Soc.* **2002**, *124* (14), 3636-3646.
83. Brown, H. C.; Midland, M. M., Facile photochemical or oxygen initiated free-radical chain reactions of trialkylboranes with organic disulfides. Convenient new synthesis of organic sulfides via hydroboration. *J. Am. Chem. Soc.* **2002**, *93* (13), 3291-3293.
84. Tanko, J. M.; Sadeghipour, M., Functionalization of Hydrocarbons by a New Free Radical Based Condensation Reaction. *Angew. Chem., Int. Ed.* **1999**, *38* (1-2), 159-161.

## Chapter 2: Hydrocarbon functionalization via allyl transfer using PINO• as a chain carrier

### 2.1 Introduction

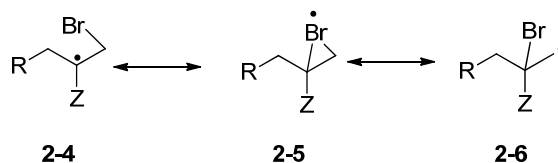
A new free radical-based condensation method that achieves hydrocarbon functionalization and C-C bond formation in a single step was reported in our group.<sup>1</sup> Utilizing an appropriately substituted allyl bromide as the key reactant, the net result of this transformation is the transfer of an allyl group to the hydrocarbon:  $\text{RH} + \text{CH}_2=\text{C}(\text{Z})\text{CH}_2\text{Br} \rightarrow \text{RCH}_2\text{C}(\text{Z})=\text{CH}_2 + \text{HBr}$ . This allyl transfer reaction was especially fascinating because, unlike other methods that effect this transformation, this functionalization was accomplished without the use of heavy metals such as tri-n-butyl tin hydride, distannanes, or alkyl mercuric halides,<sup>2</sup> which are often needed in such radical-based synthetic methods. Similarly, strong acidic or basic reaction conditions which are needed in electrophilic or nucleophilic methods are not needed. This method demonstrates that high chemical yields do not necessarily have to be compromised with the adoption of green chemical technologies.<sup>3</sup>



**Scheme 2-1:** Propagation steps and overall reaction in allyl transfer

The mechanism of this reaction is depicted in Scheme 2-1 ( $\text{X} = \text{Br}$ ). The bromine atom ( $\text{Br}^\bullet$ ) abstracts a hydrogen atom from a hydrocarbon  $\text{R-H}$  such as toluene (which has a relatively weak, benzylic, C-H bond) generating an intermediate benzyl radical,  $\text{R}^\bullet$ . Addition of  $\text{R}^\bullet$  to the alkene of allyl bromide **2-1** generates a  $\beta$ -bromo radical **2-2**, which undergoes subsequent  $\beta$ -cleavage to form the final product **2-3** and regenerates  $\text{X}^\bullet$ . The bromine atom proved particularly effective in

this reaction because it abstracts a hydrogen atom from the benzylic position with high selectivity,<sup>4</sup> (for example, the Ziegler bromination<sup>5</sup>) and the intermediate  $\beta$ -bromo radicals readily undergo  $\beta$ -cleavage. Reaction yields and kinetic chain lengths (i.e., the rate of product formation relative to the rate of initiator disappearance) are both improved when the substituent Z was electron withdrawing, and the relative rates for radical addition were found to be 180 (Z = CN) > 110 (Z=CO<sub>2</sub>R) > 65 (Z=Ph) >> 1 (Z=H).<sup>1b</sup> This reactivity order parallels the relative rates of addition of PhCH<sub>2</sub>• to substituted alkenes.<sup>6</sup> It is likely that the reactivity of the allyl bromides towards radical addition is enhanced compared to the other alkenes because of either  $\beta$ -bromo bridging interactions (Scheme 2-2) that stabilize the intermediate radical **2-4**,<sup>7</sup> or simply the addition of an electronegative Br atom which makes the double bond even more electrophilic facilitating addition of the nucleophilic benzyl radical.<sup>6, 8</sup> (This enhanced reactivity of the substrate is required to achieve high yields of **2-3** because **2-3** also possesses a reactive double bond.)



**Scheme 2-2:**  $\beta$ -bromo bridging interactions with intermediate carbon radical

Although this chemistry was a step forward in the development of new, environmentally benign synthetic methods, there were some drawbacks:

**1) The chemistry is based upon bromine.** Allyl bromides are hygroscopic and difficult to handle, and inevitably, a strong acid (HBr) is formed as a side product which must be scavenged. This reaction could be drastically improved if a suitable replacement for the bromine atom could be identified.

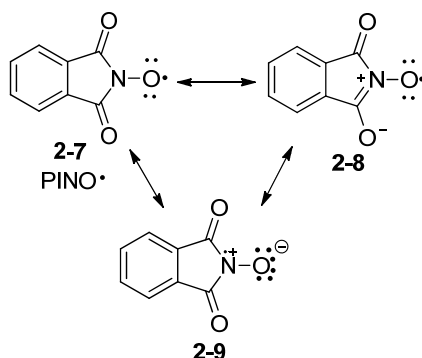
**2) High reaction temperatures are needed (120 °C).** Di-*t*-butyl peroxide<sup>9</sup> (DTBPO) proved to be an excellent initiator for this reaction, because the resulting *t*-butoxyl radical does not readily add to double bonds. This is not true for radicals generated from lower-temperature initiators such as AIBN or benzoyl peroxide.<sup>10</sup> Any attempts to develop this reaction into a stereoselective C-C bond forming reaction,<sup>11</sup> either through use of a prochiral radical or an  $\alpha$ -substituted allyl compound, will require lower reaction temperatures.

**3) A large excess (i.e., solvent quantities) of R-H is used.** This reaction would be “greener” if it used stoichiometric quantities of starting materials. Points 1) and 2) are addressed herein; Chapter 3 will address point 3), and expand the diversity of “R-H” to include alcohols, ethers, amines and other substrates with relatively weak C-H bonds.

## 2.2 Development of a “bromine-free” allyl transfer process based upon PINO•

To replace the Br• as the chain carrier in this reaction, a suitable radical must be found which both abstracts a hydrogen atom with good selectivity, and acts as a good leaving group for  $\beta$ -cleavage. Nitroxyl radicals were chosen owing to their established use in living radical polymerizations and reversible addition-fragmentation chain transfer processes.<sup>12</sup> Phthalimido-*N*-oxyl radical (PINO•) was chosen for its higher reactivity as compared to dialkyl nitroxyl radicals as the carbonyl groups effectively tie up the lone electron pair in resonance,<sup>13</sup> thus diminishing the contribution of resonance form **2-9** which removes spin density from oxygen (Scheme 2-3). In the past few years, new methods for hydrocarbon functionalization have been reported based on the chemistry of the phthalimido-*N*-oxyl radical (PINO•). For example, *N*-hydroxyphthalimide (as discussed in Chapter 1) has been shown to catalyze the autoxidation of

hydrocarbons ( $R-H \rightarrow ROOH$ ),<sup>14</sup> and in this process, PINO• serves as the a hydrogen atom abstractor.<sup>15</sup>



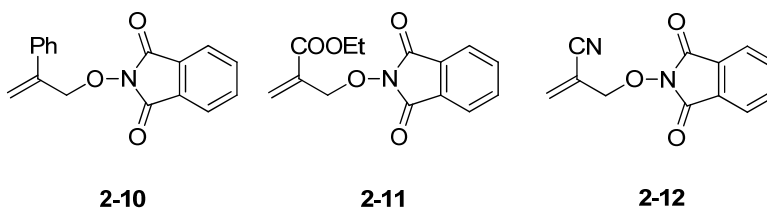
**Scheme 2-3:** Resonance contributors in phthalimido-*N*-oxyl radical (PINO•)

More importantly, as a hydrogen atom abstractor, PINO• has been shown to be even less reactive and more selective than the bromine atom.<sup>16</sup> This suggests that PINO• might be a suitable replacement for Br• in the allyl transfer reaction—if the corresponding allyl-PINO compounds are as reactive towards radical addition as allyl bromides, and if PINO• is a suitable leaving group for  $\beta$ -cleavage. The results in this chapter demonstrate that both conditions are met. Allyl-PINO compounds **2-10** and **2-11** (Scheme 2-4) are superb substrates for this chemistry, offering several advantages over the corresponding allyl bromides. This chapter also discusses our efforts to lower the temperature of this reaction and the results provide insight into the issues related to the propagation step/s (e.g., a hydrogen abstraction by PINO•, leaving group ability of PINO• etc.) in the allyl transfer process.

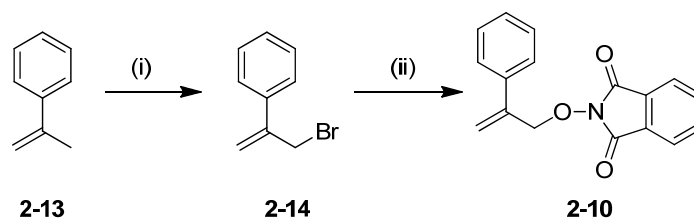
## 2.3 Results and discussion

### 2.3.1 Synthesis of allyl-PINO substrates

New “Allyl-PINO” compounds **2-10**, **2-11** and **2-12** were prepared following modified literature procedures,<sup>17</sup> via a pathway that involves an allyl bromide substrate as an intermediate. Since this research also demands the comparative study of Br• vs. PINO• chemistry, these pathways were chosen because they yield both set of compounds (allyl bromide and allyl-PINO) easily in one synthetic route. In addition to this, a “*proof of concept*” was required before more work could be done on the greener synthesis of allyl-PINO compounds that do not involve bromine.



**Scheme 2-4:** New substrates (allyl-PINO) for allyl transfer reaction

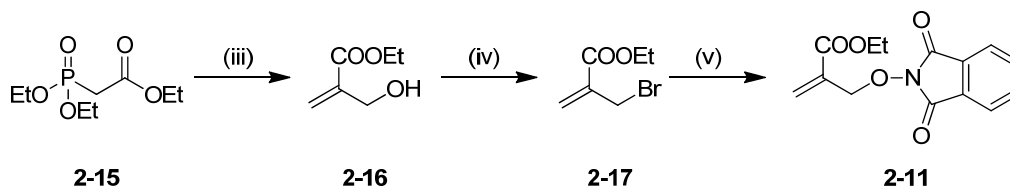


(i) NBS, CCl<sub>4</sub>, rt, 68% (ii) DMSO, NaOAc, NHPI, 65%

**Scheme 2-5:** Synthetic pathway for **2-10** (2-((2-phenylallyl)oxy)isoindoline-1,3-dione)

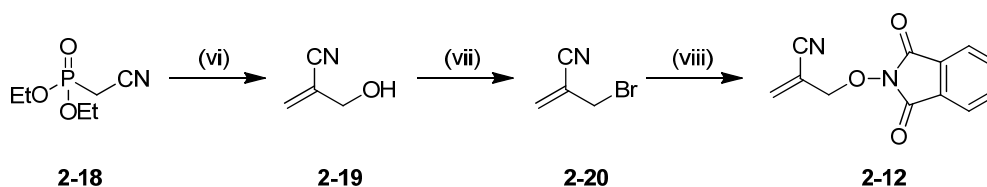
Allyl-PINO substrate **2-10** (a white crystalline solid) was synthesized from α-methyl styrene **2-13** via allylic bromination<sup>17b</sup> followed by the substitution strategy<sup>17c</sup> shown in Scheme 2-5. Similarly, **2-11** was synthesized in three steps from triethyl phosphonoacetate, **2-15** as

shown in Scheme 2-6. **2-15** was converted to alcohol **2-16** via a Wittig-Horner reaction,<sup>17a</sup> which was then converted to the corresponding allyl bromide **2-17** through a PBr<sub>3</sub> bromination reaction. **2-17** was then converted to **2-11** (a white crystalline solid) by a substitution reaction.<sup>18</sup>



(iii) HCHO (4 eq.) K<sub>2</sub>CO<sub>3</sub>, 65% (iv) PBr<sub>3</sub>, ether, -10 °C, 70% (v) DMSO, NaOAc, NHPI, 65%

**Scheme 2-6:** Synthetic pathway for **2-11** (ethyl 2-(((1,3-dioxoisindolin-2-yl)oxy)methyl)acrylate)

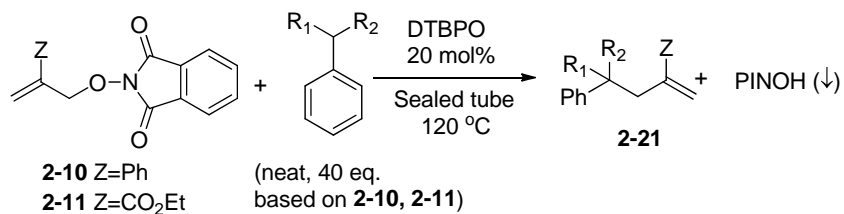


(vi) HCHO (4 eq.) K<sub>2</sub>CO<sub>3</sub>, 65% (vii) PBr<sub>3</sub>, ether, -10 °C, 70% (viii) DMSO, NaOAc, NHPI, 65%

**Scheme 2-7:** Synthetic pathway for **2-12**, 2-(((1,3-dioxoisindolin-2-yl)oxy)methyl)acrylonitrile

Allyl-PINO compound **2-12** was synthesized in three steps from diethyl cyanomethylphosphonoacetate, **2-18** (Scheme 2-7). **2-18** was converted to alcohol **2-19** via a Wittig-Horner reaction,<sup>17a</sup> which was then converted to the corresponding allyl bromide **2-20** through a PBr<sub>3</sub> bromination reaction. **2-20** was then converted to **2-12** (a white crystalline solid) by a substitution reaction.<sup>18</sup> These novel compounds (**2-10**, **2-11** and **2-12**) were characterized by <sup>1</sup>H NMR and <sup>13</sup>C NMR spectroscopy and HRMS analysis.

### 2.3.2 Reactions of allyl-PINO substrates with hydrocarbons



Entry	R <sup>1</sup>	R <sup>2</sup>	Z	Time (h)	% GC yield <b>2-21</b>	% Unreacted <b>2-10, 2-11</b>	% Mass balance
1	H	H	Ph	24	77 (±2)	23	100
2	H	H	CO <sub>2</sub> Et	42	48 (±3), 43 <sup>a</sup> (±2)	21, 30 <sup>a</sup>	69
3	H	CH <sub>3</sub>	Ph	29	89 (±3)	9	98
4	H	CH <sub>3</sub>	CO <sub>2</sub> Et	17	85 (±1)	7	92
5	CH <sub>3</sub>	CH <sub>3</sub>	Ph	29	76 (±2)	22	98
6	CH <sub>3</sub>	CH <sub>3</sub>	CO <sub>2</sub> Et	24	91 (±1)	9	100

Reactions were performed in sealed pressure tubes at 120 °C, using di-*t*-butyl peroxide, in neat hydrocarbons. Reported yields were determined using GC (internal standard= diphenylmethane).

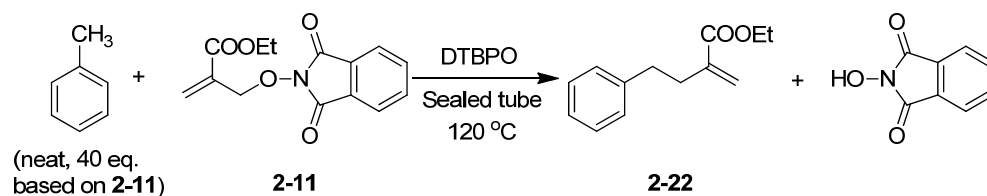
Mass balance=**2-21**+**2-10** or **2-11**. <sup>a</sup>Reaction time= 24 h, (Hydrocarbon 6.0 M, **2-10**, **2-11**- 0.15 M, DTBPO 0.03 M)

**Table 2-1:** Allyl transfer reactions of toluene, cumene and ethyl benzene with allyl-PINO substrates (**2-10**, **2-11**).

Allyl-PINO substrates **2-10** and **2-11** were allowed to react with neat toluene, ethyl benzene, and cumene under specific reaction conditions (Table 2-1). Optimized product yields ranged from 50 – 90%. Moreover, the obligatory side product, *N*-hydroxyphthalimide (PINO-H) precipitated from solution and was easily separated by filtration at the end of the reaction.

In Table 2-1, Entry 1 and entries 3-6 demonstrate that the reactions of **2-10** and **2-11** with alkyl aromatic hydrocarbons work efficiently with high yields (up to 91%) and high mass balances (up to 100%). These high mass balances suggest that the reactions are clean and negligible side products are formed. However, entry 2 (where Z=CO<sub>2</sub>Et) showed relatively lower yield. This lower yield could be attributed to further addition of benzyl radical to product **2-21**. This multiple addition was observed previously in the case of reaction of benzyl radical with allyl bromides.<sup>1a</sup>

To further study this behavior of toluene with **2-11**, a separate set of experiments was performed (Table 2-2, entry 2). In these experiments, the concentration of initiator and reaction time was varied and product yield was monitored by GC. In the first experiment, a moderate yield of **2-22** was observed at long reaction time (42 h) and when 20 mol% of initiator was used (Entry 1). The experiment in entry 2 confirmed that the product yields could not be improved by reducing the concentration of initiator (DTBPO) below 20 mol%. Although the reaction mixture was fed with extra 10 mol% of initiator after 24 h, (note that the half-life for this initiator (di-*t*-butyl peroxide) at 120 °C is 10<sup>3</sup> min), further drop in the product yields were observed (Entry 3). Even at high initiator concentrations (Entry 4 and 5), no significant increase in product yields was observed. It was concluded that neither adjusting the quantity of initiator nor the reaction time could solve this issue.



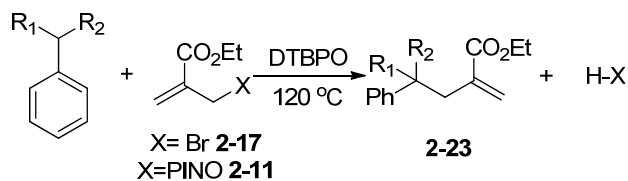
Entry	Initiator ( <i>t</i> -BuO) <sub>2</sub> mol %	Time (h)	<b>2-22</b> GC yield (%)	Unreacted <b>2-11</b> (%)	Mass balance (%)
1	20%	42	48 (±3)	21	69
2	10%	24	43 (±2)	30	73
3	10% <sup>a</sup> +10% <sup>b</sup>	24 <sup>a</sup> +24 <sup>b</sup>	32 (±1)	0	32
4	30%	16	45 (±3)	15	60
5	5%	16	42 (±3)	49	91

Reactions were performed in sealed pressure tubes at 120 °C, using di-*t*-butyl peroxide, in neat hydrocarbons. Mass balance=% **2-22**+% **2-11**, <sup>a</sup>10 mol% of initiator was added at t=0, <sup>b</sup>10 mol% of initiator was added at t=24 h (Toluene: 6.0 M, **2-11**: 0.15 M)

**Table 2-2:** Reactions of toluene with **2-11** at varying reaction time and concentration of initiator

### 2.3.3 Comparison of allyl bromides and allyl-PINO substrates with hydrocarbons

To confirm whether the replacement of PINO• with Br• leads to cleaner and efficient reactions, reactions of allyl bromide (**2-17**) and allyl-PINO substrate (**2-11**) with hydrocarbons were studied. The results are summarized in Table 2-3. For each of these experiments, the reaction conditions were identical with regard to time, temperature, etc. High mass balances were observed for the reactions of **2-11** with hydrocarbons. Overall, the reactions utilizing the allyl-PINO substrates were considerably cleaner than the analogous reactions with allyl bromides. Although the allyl bromides tended to react faster under comparable conditions leading to higher product yields, the mass balances were lower and undesirable side-products were formed.

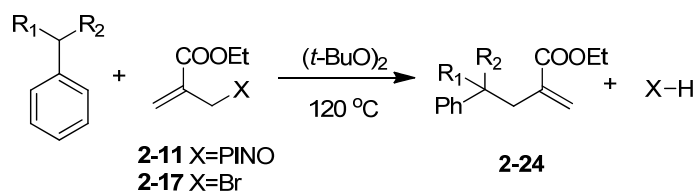


Entry	R <sub>1</sub>	R <sub>2</sub>	X = Br			X = PINO		
			% 2-17	% 2-23	Mass balance (%)	% 2-11	% 2-23	Mass balance (%)
1 <sup>a</sup>	H	H	0	35	35	21	48	69
2 <sup>b</sup>	H	CH <sub>3</sub>	0	70	70	44	56	100
3 <sup>b</sup>	CH <sub>3</sub>	CH <sub>3</sub>	41	36	77	75	20	95

Reactions performed at 120 °C using 20 mol% di-*t*-butyl peroxide in neat hydrocarbons. %Mass balance= %**2-11** or **2-17**+%**2-23** <sup>a</sup>Reaction time 42 h <sup>b</sup>Reaction time 3h (Hydrocarbon: 6.0 M, **2-17** or **2-11**: 0.15 M, DTBPO- 0.03 M)

**Table 2-3:** Comparison: Reactions of allyl- PINO and allyl bromide substrates with hydrocarbons

To probe this further, kinetic chain lengths (i.e., the rate of product formation relative to the rate of initiator disappearance,  $(\partial[\text{product}]/\partial t)/(-\partial[\text{DTBPO}]/\partial t)$ <sup>19</sup> were determined by following product yields as a function of time for Z = CO<sub>2</sub>Et (Table 2-4). The initial chain lengths for the allyl-PINO compounds were consistently lower than for the allyl bromides, although the reduced chain lengths for the allyl-PINO substrates do not have a deleterious effect on the product yield or mass balance for the reaction. These results, and others (vide infra) lead to the suspicion that for X = PINO, the hydrogen abstraction or β-fragmentation step may not be as efficient as is the case for X = Br.



Kinetic chain length			
X	$\text{R}^1=\text{H}, \text{R}^2=\text{H}$	$\text{R}^1=\text{H}, \text{R}^2=\text{CH}_3$	$\text{R}^1=\text{CH}_3, \text{R}^2=\text{CH}_3$
Br <sup>[b]</sup>	800	-	60
PINO	270(±70)	130(±30)	12(±4)

<sup>[b]</sup>Reported chain lengths (120 °C)<sup>1a</sup> (Hydrocarbon: 6.0 M, **2-11** or **2-17** 0.15 M, DTBPO 0.03 M)

**Table 2-4:** Kinetic chain length comparison between allyl bromide and allyl PINO substrates

As noted, one of advantages of using DTBPO as an initiator was that *t*-butoxyl radical does not readily add to double bonds, but is an excellent hydrogen atom abstractor. On the other hand, the disadvantage is the high temperature (120 °C) required for initiation which does not allow exploring regio- and stereoselectivity. To address this issue, initiators which are known to work effectively at low temperatures such as triethylborane, di-*t*-butylhyponitrite were considered for allyl transfer reactions at low temperatures.

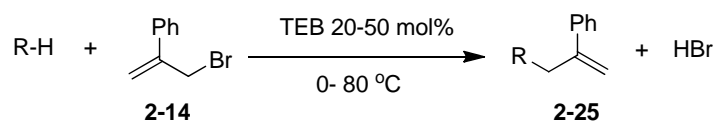
### 2.3.4 Low temperature reactions using triethylborane/O<sub>2</sub>

The primary goal behind performing the allyl transfer reaction at low temperature was to investigate regio- and stereoselectivity of the radical addition step. As observed in various cases, stereoselectivity depends directly on the temperature of the reaction and is generally found to be enhanced at lower temperatures.<sup>20</sup> In case of allyl transfer processes, low temperature might provide an opportunity to achieve enantioselective radical addition if a prochiral radical or chiral auxiliary on the electrophile is used.<sup>21</sup> But the biggest challenge for the radical processes at low

temperatures is finding an initiator which works efficiently at those temperatures. There are few reported initiators like triethylborane/O<sub>2</sub><sup>22</sup> and dimethylzinc/O<sub>2</sub><sup>23</sup> in the literature which has been successfully used at very low temperatures. Triethylborane (a precursor of Et• and/or EtOO•) was selected for allyl transfer reactions at low temperature owing to its established use in free radical reactions at low temperatures.<sup>22, 24</sup>

In this subsection, we discuss the reactions of allyl-PINO substrates with hydrocarbons using triethylborane/O<sub>2</sub> as an initiator. Allyl-PINO substrates **2-10**, **2-11** and allyl-bromide substrate **2-14** were allowed to react with neat toluene, ethyl benzene and cumene in presence of triethylborane.

The low temperature reactions were first performed with allyl-bromide substrate **2-14** and hydrocarbons at varying concentration of initiator and reaction temperature (Table 2-5). The reaction of toluene with **2-14** (Entry 1) using 20 mol % of initiator at 0 °C led to no formation of product **2-25**. Increasing the temperature of this reaction to room temperature led to a negligible 1% product formation (Entry 2). Similarly, gradually increasing the concentration of initiator and reaction temperature (Entries 2, 3, 4) led to a slight improvement in product yield (up to 10%). Finally, increasing the reaction temperature to 80 °C led to respectable product formation (Entry 5). Use of ethyl benzene and cumene (Entries 6 and 7) showed similar results, which led to the conclusion that a respectable product yields could only be achieved at high temperatures (80 °C).

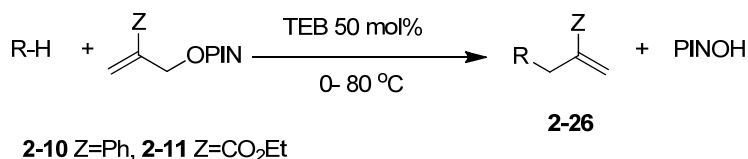


Entry	R-H Hydrocarbon	Initiator (TEB) (eq.)	Temperature °C	Time (h)	GC yield % (2-25)
1	Toluene	0.2-0.5	0	24	N/O
2	Toluene	0.2	rt	24	1 (±0)
3	Toluene	0.5	rt	24	2 (±0)
4	Toluene	0.5	50	12	10 (±1)
5	Toluene	0.5	80	12	30 (±1)
6	Cumene	0.5	80	12	40 (±1)
7	Ethyl benzene	0.5	80	12	35 (±3)

**Table 2-5:** Reactions of **2-14** with hydrocarbons at low temperature using Et<sub>3</sub>B/O<sub>2</sub>.

(Hydrocarbon 11.0 M, **2-14** 0.36 M, TEB (0.5 eq.): 0.18 M)

The data in Table 2-6 show reactions of the allyl-PINO substrates **2-10** and **2-11** with hydrocarbons. However, even in this case, no product formation was observed at low temperatures (0 °C). Similar to the allyl bromides, significant product yields were observed only at high temperatures.



Entry	Substrate	R-H Hydrocarbon	Initiator (TEB) (eq.)	Temp. °C	Time h	GC yield % (2-26)
1	2-10	Toluene	0.5	0	12	N/O
2	2-10	Toluene	0.5	rt	24	5 (±1)
3	2-10	Toluene	0.5	50	12 /24	35 (±1)
4	2-10	Toluene	0.5	80	12	40 (±2)
5	2-10	Cumene	0.5	80	12	45 (±1)
6	2-10	Ethyl benzene	0.5	80	12	42 (±1)
7	2-11	Toluene	0.5	80	12	36 (±2)
8	2-11	Cumene	0.5	80	12	40 (±1)
9	2-11	Ethyl benzene	0.5	80	12	36 (±1)

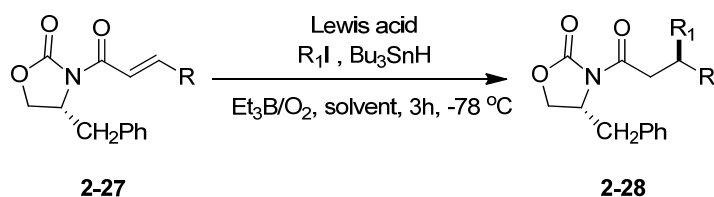
**Table 2-6:** Reactions of **2-10**, **2-11** with hydrocarbons at low temperature using Et<sub>3</sub>B/O<sub>2</sub>.

(Hydrocarbon 10.0 M, **2-10**, **2-11** 0.3 M, TEB 0.15 M)

Since Et<sub>3</sub>B/O<sub>2</sub> generates an Et• and EtOO•,<sup>24e, 25</sup> it was conceivable that the mediocre results obtained with this initiator were because of these possibilities; 1) either Et• and/or EtOO• does not abstract a hydrogen at the rate sufficient enough to efficiently initiate the reaction, 2) hydrogen atom abstraction by PINO• is very slow at low temperature, or 3) radical addition step is slow at low temperature. Based on the hypothesis that a Lewis acid could be used to activate the substrate (especially **2-11**) and accelerate the radical addition step, we decided to explore the possible Lewis acid catalyzed allyl transfer reaction and address the issue related to possibility 3) mentioned above.

### 2.3.5 Low temperature reactions using triethylborane and a Lewis acid

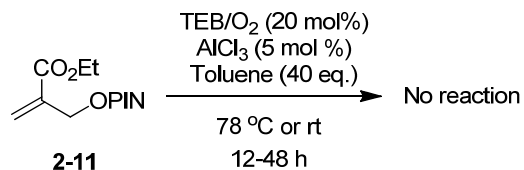
Lewis acids have been reported to activate various functionalities and accelerate the rate of radical reactions. In 1999, Sibi *et al.* developed a highly stereoselective method for the conjugate addition of carbon radicals to chiral  $\alpha,\beta$ -unsaturated *N*-enoyloxazolidinones **2-27** using tributyltin hydride ( $\text{Bu}_3\text{SnH}$ ) as a chain carrier and triethylborane/ $\text{O}_2$  ( $\text{Et}_3\text{B}/\text{O}_2$ ) as radical initiator (Scheme 2-8).<sup>26</sup> In the presence of a Lewis acid ( $\text{Yb}(\text{OTf})_3$ ) optimized results for both chemical yield and diastereoselectivity were observed. It was confirmed that the Lewis acid ( $\text{Yb}(\text{OTf})_3$ ) plays an important role in controlling the conformation by chelation to both carbonyl groups and greatly activate the substrate reactivity at low temperature ( $-78\text{ }^\circ\text{C}$ ).<sup>26</sup> In this case, the Lewis acid also makes the alkene more electrophilic and accelerates the addition of the nucleophilic alkyl radical to an alkene.



**Scheme 2-8:** Lewis acid catalyzed conjugate radical addition to chiral  $\alpha,\beta$ -unsaturated *N*-enoyloxazolidinones.<sup>26</sup>

Based on the literature precedent, a commercially available Lewis acid, aluminum chloride ( $\text{AlCl}_3$ ) was selected for this acceleration of the radical addition step. A series of experiments were performed using  $\text{AlCl}_3$  at low temperatures ( $-78\text{ }^\circ\text{C}$ ,  $0\text{ }^\circ\text{C}$ , and room temperature). Unfortunately, no improvement in yields was observed (Scheme 2-9). Once again the allyl transfer reaction was observed to work effectively only at high temperatures ( $120\text{ }^\circ\text{C}$ ). High mass balances and high yields were observed in all reactions at  $120\text{ }^\circ\text{C}$ , but it was

noteworthy that reactions in the presence of a Lewis acid at high temperature were much cleaner than reactions without the Lewis acid under similar conditions.



**Scheme 2-9:** Lewis acid catalyzed hydrocarbon functionalization using TEB/O<sub>2</sub>

To investigate the exact role of the Lewis acid in the allyl transfer process at high temperature, reactions were performed with and without AlCl<sub>3</sub> at 120 °C. If the Lewis acid is participating in the process and facilitating the radical addition by activating **2-11**, then a dramatic difference may be observed in product yields. Finally, significant improvement in product yields were observed for the reactions *with* added Lewis acid. This data suggested that the Lewis acid accelerates the rate of the reaction by activating **2-11** at high temperature only. The reactions were cleaner, with negligible side products, and higher chain lengths when Lewis acid was used. The product yield was determined using GC, and plot of % product yield as a function of time for the reaction of **2-11** with cumene (Figure 2-1) and **2-11** with toluene (Figure 2-2) was used to observe the role of AlCl<sub>3</sub>.

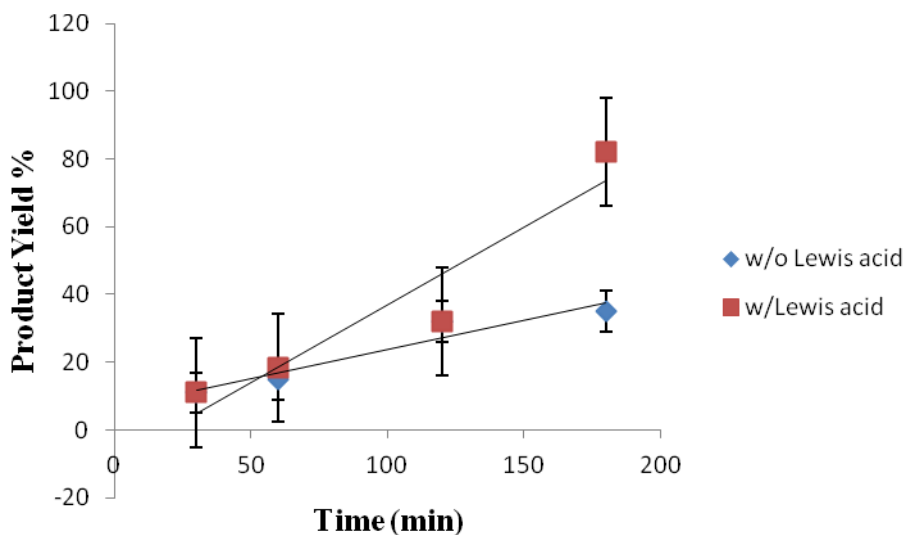


**Figure 2.1:** Triethylborane initiated reaction of cumene and **2-11** with Lewis acid ( $\text{AlCl}_3$ ) compared to the reaction without Lewis acid (**2-11** 0.15 M, TEB 0.07 M, cumene 6.0 M,  $\text{AlCl}_3$  0.007 M)

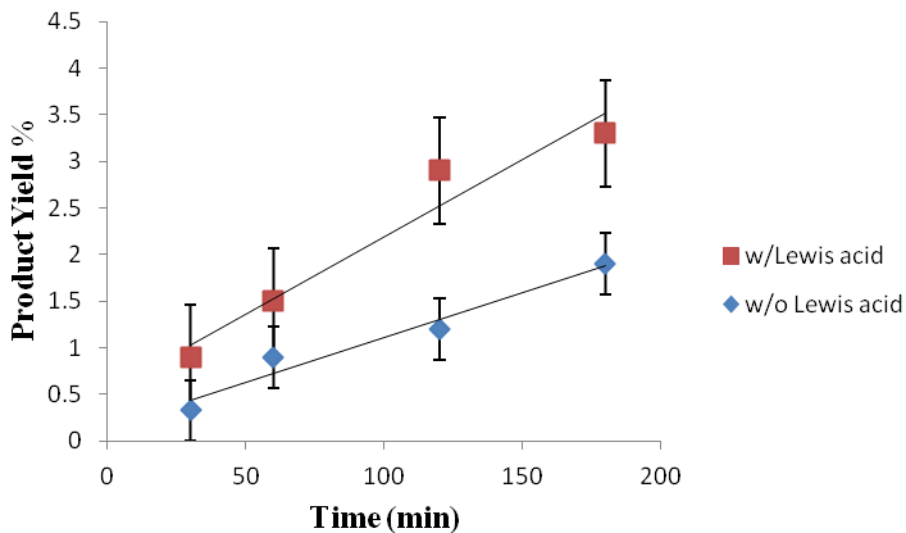
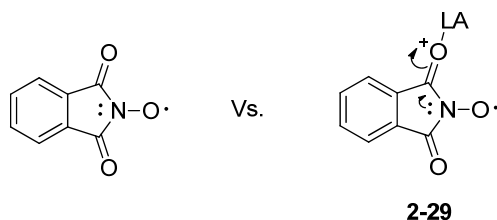
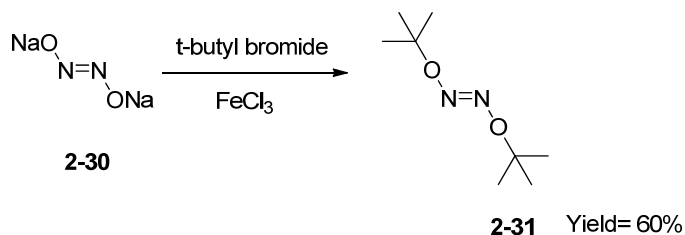


**Figure 2-2:** Triethylborane initiated reaction of toluene and **2-11** with Lewis acid ( $\text{AlCl}_3$ ) compared to the reaction without Lewis acid. (**2-11** 0.15 M, TEB 0.07 M, toluene 6.0 M,  $\text{AlCl}_3$  0.007 M)

Although these reactions showed rapid product formation in presence of a Lewis acid, they still might be good chain reactions even in absence of a Lewis acid. Especially from Figure 2-2, the effect of Lewis acid can be quantitated approximately. From slopes, it can be postulated that the formation of the product as a function of time is accelerated twice as much with the Lewis acid than the product formation without the Lewis acid. This data also led to a speculation that the Lewis acid probably forms a complex **2-29** with PINO• which forces the lone pair on nitrogen to tie up even better in the resonance. This effect stabilizes the spin density on oxygen making PINO• more reactive towards a hydrogen atom abstraction. (Scheme 2-10)



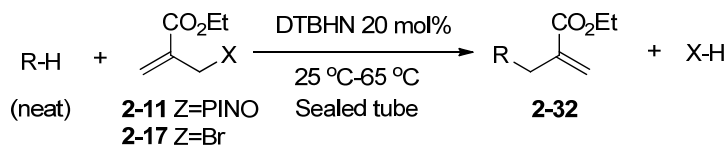
**Scheme 2-10:** Effect of Lewis acid on PINO• and hydrogen abstraction



**Scheme 2-11:** Synthesis of di-*t*-butylhyponitrite (**2-31**)

As mentioned earlier, one of the reasons for poor yields at low temperature, was inefficient initiation by TEB/O<sub>2</sub> initiator (EtOO• or Et•). To investigate this further, we employed a new initiator di-*t*-butylhyponitrite<sup>27</sup> (**2-31**) which was synthesized using a literature procedure (Scheme 2-11). Fortunately, through the use of di-*t*-butylhyponitrite (**2-31**), it was possible to

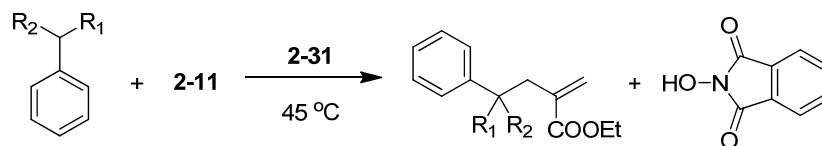
generate *t*-butoxyl radical at room temperature<sup>28</sup> and allyl transfer reactions were performed using **2-31** at low temperature (Table 2-7).



Entry	R-H	Substrate	Temperature (°C)	Time (h)	% yield <b>2-32</b>	% unreacted <b>2-11, 2-12</b>
1	PhCH <sub>3</sub>	<b>2-11</b>	25	96	31 (±1)	41
2	PhCH <sub>2</sub> CH <sub>3</sub>	<b>2-11</b>	25	96	36 (±2)	39
3	PhCH(CH <sub>3</sub> ) <sub>2</sub>	<b>2-11</b>	25	168	23 (±3)	45
4	PhCH <sub>2</sub> CH <sub>3</sub>	<b>2-11</b>	65	12	65 (±1)	35
5	PhCH <sub>3</sub>	<b>2-17</b>	25	96	48 (±3)	-
6	PhCH <sub>3</sub>	<b>2-17</b>	65	12	69 (±3)	-

**Table 2-7:** Reactions of **2-11**, **2-17** (CH<sub>2</sub>=C(COOEt)CH<sub>2</sub>Br) with hydrocarbons (neat) initiated by DTBHN, (**2-11**, **2-17** 0.15M, DTBHN 0.03 M, R-H 6.0 M)

The product yields for the reaction of **2-11** with the alkyl aromatic hydrocarbons at room temperature were poor. At longer reaction time (168 h), further drop in the product yields was observed. (Entry 3) A respectable yield was only obtained when the reaction temperature was elevated to 65 °C (Entry 4 and 6). To address this further, the kinetic chain lengths for the reaction of **2-11** with toluene and ethyl benzene, initiated by **2-31** at 45 °C, were measured. This temperature was chosen for the chain lengths calculation because of the known decomposition rate constant for triethylborane at that temperature.



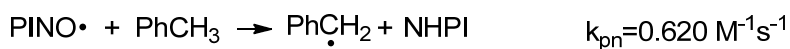
Entry	Substrate	R-H	Kinetic chain length
1	<b>2-11</b>	R <sub>1</sub> =R <sub>2</sub> =H	1.4 (±1)
2	<b>2-11</b>	R <sub>1</sub> =H, R <sub>2</sub> =CH <sub>3</sub>	1.9 (±1)

<sup>a</sup>Kinetic chain length measurement at 45 °C

(**2-11** 0.37 M, **2-31** 0.03 M, hydrocarbon 9.0 M)

**Table 2-8** Kinetic chain length data with 10 mol% of **2-31** at 45 °C

In both cases, the chain lengths were slightly greater than unity: PhCH<sub>3</sub>, 1.4 (Entry 1); PhCH<sub>2</sub>CH<sub>3</sub>, 1.9 (Entry 2, Table 2-8). For all practical purposes, these results show that at lower temperatures, this is not an efficient free radical chain process. Di-*t*-butylhyponitrite (**2-31**) generates *t*-butoxyl radical which is known to abstract hydrogen readily at room temperature ( $k = 1.9 \times 10^5 \text{ M}^{-1} \text{ s}^{-1}$ ) for hydrogen abstraction from toluene at 25 °C;  $E_a = 3.5 \text{ kcal/mol}$ ).<sup>29</sup> This rules out the problem with the initiation step. Consequently, at low temperatures, there must be a problem with one of the propagation steps, presumably hydrogen abstraction by PINO• or β-elimination. To investigate this, reported rate constants for a hydrogen atom abstraction by Br• and PINO• were compared.<sup>30</sup>



**Equation 2-1** Reported rate constants for hydrogen abstraction by PINO• and Br• from toluene at room temperature.<sup>16</sup>

From Equation 1-1, it is clear that hydrogen atom abstraction by Br• is faster than PINO• which may explain the lower chain lengths with allyl-PINO substrates. From the results shown

in Table 2-7 and the respectable product formation at low temperature, it is clear that radical addition and  $\beta$ -fragmentation steps work efficiently at low temperature. In contrast, the hydrogen abstraction step, which is critical in order to achieve good chain lengths, may be slow at low temperature. Finally, using these results, it was concluded that the hydrogen abstraction is the rate limiting step.

## **2.4 Methods for determination of rate constant for addition-elimination process**

The most successful method for absolute rate constant measurement is laser flash photolysis which involves the instantaneous generation of a high concentration of the radical in the presence of a large excess of reactive substrate.<sup>31</sup> If radical reacts principally with this reactive substrate, it will decay following pseudo first-order kinetics. Its decay can be monitored by available methods used for radical reactions.<sup>32</sup> The resulting pseudo-first order rate constant is converted to a true bimolecular rate constant by dividing the molar concentration of the reactive substrate. This method has been successfully applied in flash photolysis technique since the 1960s.<sup>19</sup>

### **2.4.1 Laser flash photolysis**

Flash photolysis is a technique that is typically used for photochemical reactions. The most important feature of this technique is the the flash lamp.<sup>33</sup> For reactions proceeding at a moderate rate, xenon lamp is an excellent choice but, for very fast reactions it probably is a poor choice because of its microsecond pulse.<sup>34</sup> In principal, time of the light emission from the lamp must be much faster than the reaction being monitored. Generally, the pulse width of the light source must be much shorter than the half-time of the chemical reaction.<sup>35</sup> Lasers with the nanosecond pulse width are generally used for very fast reactions.<sup>35</sup> These lasers can work

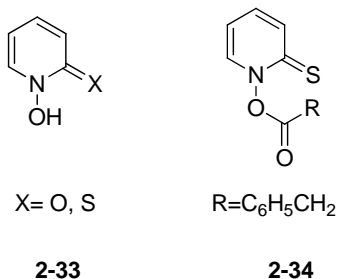
effectively up to femtosecond time scale. In our laboratory, the laser flash-photolysis system operates with Nd-YAG laser.<sup>36</sup> Nd-YAG (neodymium-yttrium aluminum garnet) is a synthetic material that is excited by flash lamp to generate light in the IR region. To convert the IR light into the UV region special arrangement of optics is used<sup>37</sup> which triples the photon frequency to yield output at 355 nm, which works effectively for many organic conjugated systems.

For the rate constant measurement for the radical addition-elimination step, two methods were chosen: a) Radical generation via photolabile radical precursor, and b) Direct radical generation using a thermal initiator.

## 2.4.2 Radical generation via photolabile radical precursor

### 2.4.2.1 Synthesis, mechanism and applications of photolabile thiohydroxamic esters

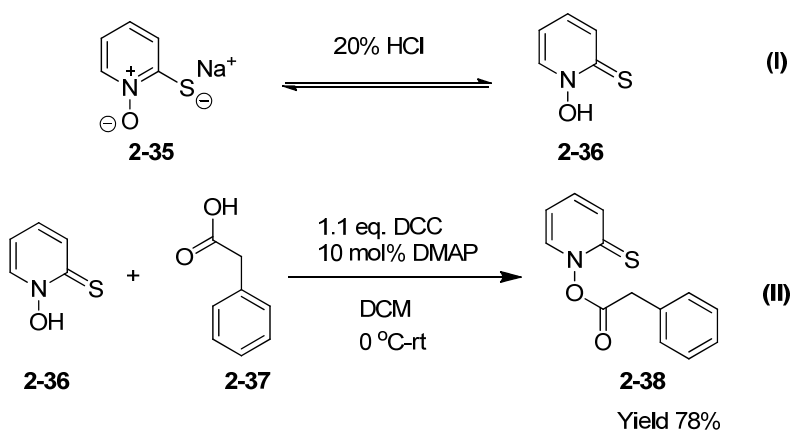
Homolytic cleavage of nitrogen-oxygen bonds induced by heat or light has been reported in the literature.<sup>38</sup> Compounds like *N*-hydroxy-2-pyridone, thiohydroxamic esters containing weak N-O bond, are commonly used for such homolytic cleavage. These compounds are widely used in radical chemistry because of their efficiency in generation of desired reactive radicals. These radicals are trapped by various trapping techniques and used for elucidation of mechanism in radical reactions.



**Scheme 2-12:** *N*-hydroxy-2-pyridone (**2-33**), 2-thioxopyridin-1(2H)-yl 2-aryl/alkyl carboxylate ester (**2-34**)

This section discusses one of the derivative of 2-thioxopyridin-1(2H)-yl 2-arylcarboxylate esters developed by Barton, *et al.* Derivatives of 2-thioxopyridin-1(2H)-yl 2-arylcarboxylate esters are reported to be a convenient and controlled source of carbon radicals. 2-thioxopyridin-1(2H)-yl 2-aryl/alkyl carboxylate esters are known to undergo a chain reaction. Under continuous irradiation, the major product was reported to be 2-pyridyl thioether via decarboxylative rearrangement. The reaction mechanism was reported to involve photochemically induced homolytic cleavage of the N-O bond, followed by the formation of a 2-pyridylthiyl radical and an acyloxy radical (RCOO•). When R is an aliphatic group, decarboxylation is expected to occur rapidly to give a carbon radical (R•).

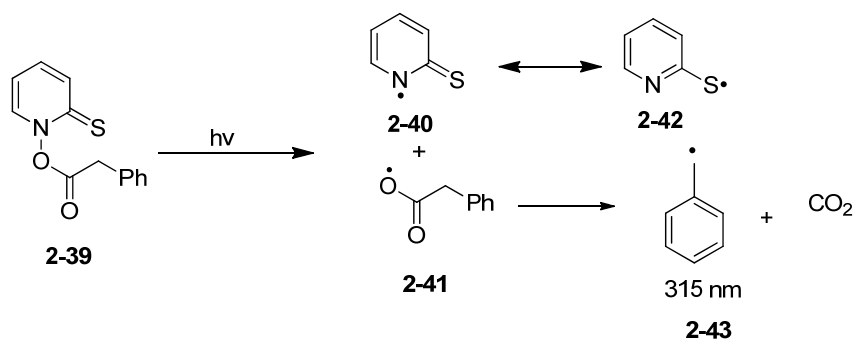
Despite the wide synthetic applications of photolabile precursors for kinetic investigation, the primary photochemistry and subsequent reactions of the 2-thioxopyridin-1(2H)-yl 2-aryl/alkyl carboxylate esters have not been explored thoroughly. Reported studies on these precursors used EPR and laser flash photolysis studies to detect the free radicals generated from thiohydroxamic esters.



**Scheme 2-13:** Synthetic pathway for 2-thioxopyridin-1(2H)-yl 2-phenylacetate **2-38**.<sup>39</sup>

In this section, we will discuss the synthesis, mechanism and laser flash photolysis studies of 2-thioxopyridin-1(2H)-yl 2-aryl/alkyl carboxylate esters. The desired compound (2-

thioxopyridin-1(2H)-yl 2-phenyl acetate ester) **2-38**, a precursor of a benzyl radical, was synthesized using a literature procedure of a coupling reaction between an acid **2-37** and an alcohol **2-36** (Scheme 2-13). Upon photolysis, this substrate is reported to generate a carboxyl radical  $\text{PhCH}_2\text{CO}_2\cdot$  (**2-41**) and the 2-pyridylthiyl radical (**2-42**) (Scheme 2-14). The decarboxylation of **2-41** to the benzyl radical **2-43** is rapid and may allow **2-43** to participate in subsequent reactions. Our goal was to (a) confirm the generation of benzyl radical (b) study the addition-elimination reaction of benzyl radical to alkene (**2-11**), and (c) measure the absolute rate constant for this process.



**Scheme 2-14:** Mechanism for generation of benzyl radical from 2-thioxopyridin-1(2H)-yl 2-phenyl acetate.

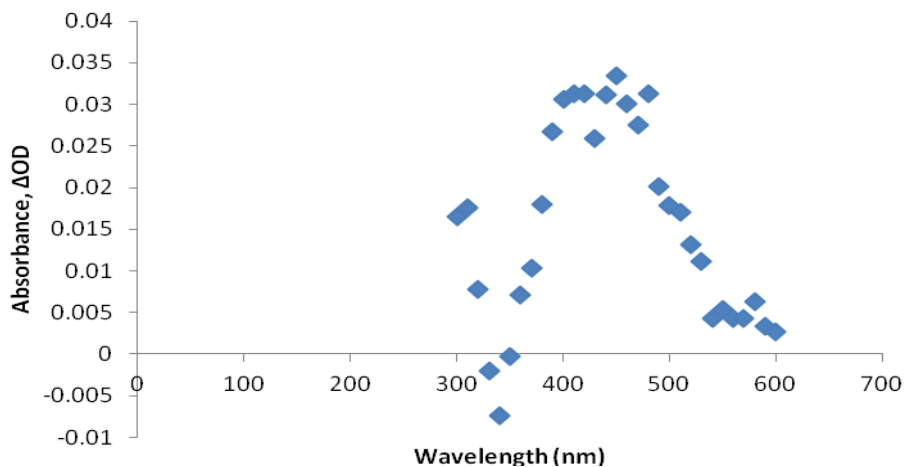
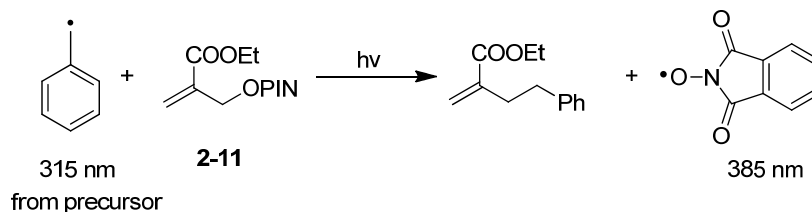


**Figure 2-3:** Transient absorption spectra for 2-thioxopyridin-1(2H)-yl 2-phenyl acetate, 0.5mM in acetonitrile,  $\lambda_{\text{exc}}=355\text{nm}$ , absorption maxima at 450-460 nm showing benzenethiyl radical formation.<sup>39</sup>

2-thioxopyridin-1(2H)-yl 2-phenyl acetate was photoionized in the presence of compound **2-11** utilizing nanosecond laser flash photolysis. Transient absorption spectrum showed maxima in the region 450-460 nm indicating the benzene thiyl radical formation (Figure 2-3). No absorption maximum was detected at 315 nm where benzyl radical is expected to appear or at 380-385 nm region where PINO• was expected to appear. These results lead to some speculations; 1) Either benzyl radical generation is unsuccessful using this technique so there is no addition-elimination reaction, or 2) the radical addition-elimination process is too slow ( $k < 10^4 \text{ s}^{-1}$ ) to measure via the LFP method.

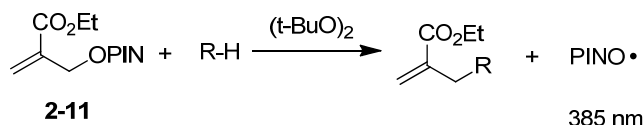


**Scheme 2-15:** Reaction of benzyl radical with **2-11** via LFP

## 2.4.2 Direct radical generation using thermal initiator

In this method, standard reaction conditions were used to generate the benzyl radical from a thermal initiator, di-*t*-butyl peroxide, using toluene as a solvent. The thermal initiator was expected to undergo homolytic cleavage at O-O bond to generate *t*-BuO•. This reactive radical could easily abstract the H-atom from toluene to generate benzyl radical. Similar to Scheme 2-15, if benzyl radical undergoes addition-elimination reaction with the substrate, the absorption for PINO• at 382-385 nm is expected. But in this experiment too, no such absorption for PINO• was observed.

Although according to the literature precedence,<sup>40</sup> this method is known to generate PhCH<sub>2</sub>• efficiently at the concentrations and timescale (tens of microseconds) used in the experiment, the observed failure in this case is likely due to the slow radical addition-elimination process.



**Scheme 2-16:** Direct radical generation for LFP studies on benzyl radical addition-elimination process, 60% solution of di-*t*-butyl peroxide in toluene (3 mM), **2-11** 0.5 mM, R-H=Toluene)

After the laser flash photolysis experiments, we decided to measure the relative rate constants for the same process via competition experiments. The initial plan for the competition experiment was to generate benzyl radical using di-*t*-butyl peroxide and allow it to react with allyl bromide and allyl-PINO substrate with same Z substituent (Scheme 1-17). This experiment was designed to compare radical addition-elimination reaction of benzyl radical that would measure the relative reactivity of allyl bromide vs. allyl-PINO substrates. The only problem with



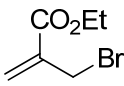
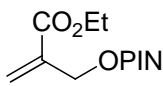
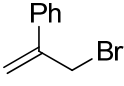
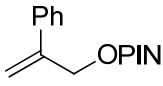
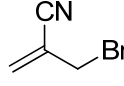
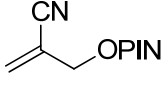


Ratio	Relative rate constant
$\frac{k_{Br}^{COOEt}}{k_{PINO}^{Ph}}$	3.40 ( $\pm 0.03$ )
$\frac{k_{Br}^{Ph}}{k_{PINO}^{COOEt}}$	1.20 ( $\pm 0.01$ )
$\frac{k_{Br}^{COOEt}}{k_{PINO}^{CN}}$	2.60 ( $\pm 0.02$ )
$\frac{k_{Br}^{CN}}{k_{Br}^{COOEt}}$	1.10 ( $\pm 0.01$ )
$\frac{k_{Br}^{Ph}}{k_{PINO}^{CN}}$	2.70 ( $\pm 0.02$ )
$\frac{k_{Br}^{CN}}{k_{PINO}^{Ph}}$	2.30 ( $\pm 0.05$ )

**Table 2-9:** Result of the competition experiment: Relative rate constant measurements with varying substituents and leaving groups. (120 °C)

$$\begin{array}{l}
 \frac{k_{Br}^{COOEt}}{k_{PINO}^{Ph}} = X \\
 \frac{k_{Br}^{Ph}}{k_{PINO}^{COOEt}} = Y \\
 \frac{k_{Br}^{COOEt}}{k_{PINO}^{CN}} = Z
 \end{array}
 \quad
 \begin{array}{l}
 \frac{k_{Br}^{CN}}{k_{Br}^{COOEt}} = X' \\
 \frac{k_{Br}^{Ph}}{k_{PINO}^{CN}} = Y' \\
 \frac{k_{Br}^{CN}}{k_{PINO}^{Ph}} = Z'
 \end{array}
 \quad
 \begin{array}{l}
 \frac{k_{Br}^{COOEt}}{k_{PINO}^{Ph}} = X \\
 k_{Br}^{COOEt} = Z k_{PINO}^{CN} \\
 = Z \frac{k_{Br}^{Ph}}{Y'} \\
 Z \frac{k_{Br}^{Ph}}{Y'} = X \\
 \frac{k_{Br}^{Ph}}{k_{PINO}^{Ph}} = \frac{XY'}{Z}
 \end{array}$$

**Figure 2-4:** Arithmetic derivation of the required relative rate constant using three measured relative rate constants.

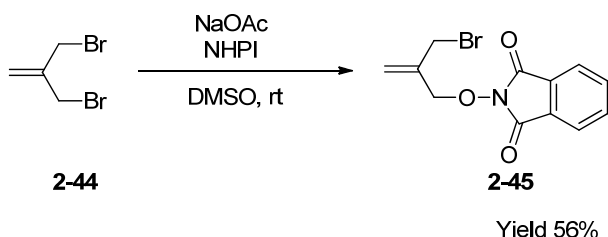
Bromide substrate	PINO substrate	Relative rate constant Br/PINO
		1.1(±0.3)
		3.6(±1.5)
		2.5(±1.0)

**Table 2-10:** Relative rate constants for the addition/elimination of benzyl radical to allyl-bromide vs. allyl-PINO substrates (120 °C)

From the results of competition experiment and relative rate constant values, it can be concluded that the allyl bromide substrates are slightly more reactive than allyl-PINO substrates in radical addition-elimination step of the allyl transfer reaction.

### 2.4.3 Competition experiment: Measurement of relative rate constant for $\beta$ -elimination step

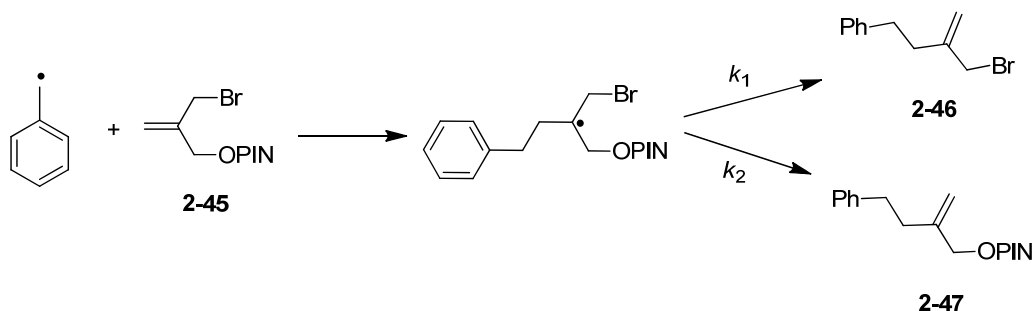
In this last section, we discuss the in-depth analysis for the  $\beta$ -fragmentation step. An exclusive competition experiment was designed to compare the leaving group abilities of  $\text{Br}\cdot$  and  $\text{PINO}\cdot$ . For this experiment a substrate having these two leaving group at the allylic position was a requirement. The synthesis of this substrate was a challenging task because the product alkene shows high susceptibility for the further radical addition. The substrate **2-45** was synthesized from **2-44** by a substitution reaction with *N*-hydroxyphthalimide (Scheme 2-19). This reaction was carried out under careful observation and reaction mixture was quenched well before its completion in order to achieve good yield of the required product. **2-45** was separated using column chromatography and isolated as a white solid in a moderate yield (56%) The structure was confirmed using  $^1\text{H}$  and  $^{13}\text{C}$  NMR analysis. We expected this experiment to provide the opportunity to determine the relative rate constant for elimination of two leaving groups.



**Scheme 2-19:** Synthesis of 2-((2-(bromomethyl)allyl)oxy)isoindoline-1,3-dione (**2-45**)

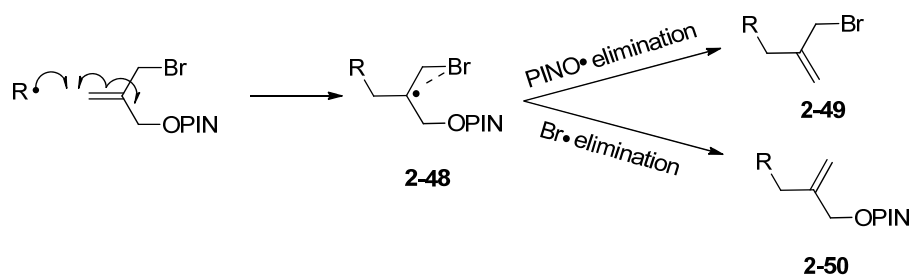
In the competition experiment (Scheme 2-20), the benzyl radical was generated using di-*t*-butyl peroxide as initiator and it was allowed to react with **2-45**. Both products formed in the

reaction were isolated using column chromatography and then each product was analyzed using  $^1\text{H}$  NMR analysis. The reaction time for this competition experiment was a critical factor in order to maintain the product and the reactant conversion below 10%. The low conversions allow comparing initial rate for the radical addition-elimination process and avoiding the reaction from participating into a chain process. Finally, the experiment was repeated in order to measure the relative rates for the formation of products shown in Scheme 2-20. From the ratio of the yields of **2-46** and **2-47**, the ratio for the relative rates for  $\beta$ -elimination process ( $k_1/k_2 = 3 (\pm 1)$ ) was calculated. From this data it was observed that the rate for the  $\beta$ -elimination of PINO• is probably slightly faster than the rates for the  $\beta$ -elimination of Br•.



**Scheme 2-20:** Competition experiment for comparing leaving group abilities between Br• and PINO• at 120 °C. (% yield of product **2-46**= 7.5, **2-47**= 2.3) (Toluene 10 M, **2-45** 0.34 M, DTBPO 0.07 M)

In the detail analysis of the experiment shown in Scheme 2-21 we proposed that the Br• probably participates in the  $\beta$ -bridging interactions with the intermediate carbon radical **2-48**. These interactions probably engage the Br• resulting in more **2-49** product formation than **2-50**.



**Scheme 2-21** Proposed  $\beta$ -bridging interactions of  $\text{Br}\cdot$  with the intermediate carbon radical (**2-48**)

The relative rate constant observed for this elimination process ( $k_1/k_2 = 3 (\pm 1)$ ) is a small number and negligible on a logarithmic scale. In conclusion, this result shows that  $\text{PINO}\cdot$  and  $\text{Br}\cdot$  are comparable leaving groups.

## 2.5 Conclusions

The results show that allyl-PINO compounds are excellent substrates for the free radical based allylation of hydrocarbons. High reaction yields and the mass balances are observed. Moreover, the side product of the reaction, *N*-hydroxyphthalimide (NHPI) precipitates from solution making these reactions operatively simple. NHPI was recycled which can be used again in the synthesis of allyl-PINO substrates making this a cost efficient process. Although kinetic chain lengths are shorter, the replacement of allyl bromides with allyl-PINO compounds is a major advance in making this chemistry more environmentally friendly.

Attempts to reduce the temperature of the reaction were less successful. Use of  $\text{BEt}_3/\text{O}_2$  as initiator only gave acceptable results at elevated temperatures, and it is unlikely that it is the nature of the initiating radical that is causing the problem. This was confirmed with the use of  ${}^t\text{BuON}=\text{NO}{}^t\text{Bu}$  (**2-31**) as initiator, which just like DTBPO, generates *t*-butoxyl but at much lower temperatures. Because *t*-butoxyl radical readily abstracts hydrogen from alkylaromatics at

lower temperature, benzyl radicals are being produced that can enter the propagation steps of this reaction. Reactions conducted in the presence of a Lewis acid confirmed that allyl transfer process is chain reaction with or without Lewis acid, as long as reactions are performed at high temperature (120 °C). Even at low temperatures, it seemed unlikely that addition of these radicals to the allyl-PINOs is sluggish, leading to the hypothesis that the hydrogen abstraction step might be controlling the rate and kinetic chain length of the reaction. Experiments with the pertinent relative rate constants to study the addition-elimination process, confirmed that the allyl bromide substrates are slightly more reactive than allyl-PINO (**2-10**, **2-11**, **2-12**) substrates.

In this chapter, we discussed the hydrocarbon functionalization via allyl transfer reaction using phthalimido-*N*-oxyl radical. Although this reaction was successful, the substrate scope was limited to the alkyl aromatic hydrocarbons (toluene, ethyl benzene, cumene) because of their weak C-H bonds at benzylic positions. The hydrocarbons with strong C-H bonds might be difficult to functionalize via this method because of their high BDEs. Therefore, to expand the substrate scope of the reaction, other substrates with weak  $\alpha$ -C-H bonds such as ethers, thioethers, acetals and amines were considered. Unlike many hydrocarbons, these substrates possess a weak C-H bond because of the vicinal heteroatom (O, S, N etc.). The vicinal heteroatom atom helps in lowering BDE, stabilizes the resulting radical via resonance and provides a site for complexation with chiral auxiliaries. In Chapter 3 we will discuss the functionalization of these substrates and our efforts to perform the allyl transfer reaction using low reagent concentrations of these substrates.

## 2.6: References:

1. (a) Tanko, J. M.; Sadeghipour, M., Functionalization of Hydrocarbons by a New Free Radical Based Condensation Reaction. *Angew. Chem., Int. Ed.* **1999**, *38* (1-2), 159-161; (b) Struss, J. A.; Sadeghipour, M.; Tanko, J. M., Radical additions to allyl bromides. A synthetically useful, [ ]Tin-Free' method for carbon-carbon bond formation. *Tetrahedron Lett.* **2009**, *50* (18), 2119-2120.
2. Baguley, P. A.; Walton, J. C., Flight from the Tyranny of Tin: The Quest for Practical Radical Sources Free from Metal Encumbrances. *Angew. Chem., Int. Ed.* **1998**, *37* (22), 3072-3082.
3. (a) Quiclet-Sire, B.; Seguin, S.; Zard, S. Z., A New Radical Allylation Reaction of Dithiocarbonates. *Angew. Chem., Int. Ed.* **1998**, *37* (20), 2864-2866; (b) Le Guyader, F.; Quiclet-Sire, B.; Seguin, S.; Zard, S. Z., New Radical Allylation Reaction of Iodides. *J. Am. Chem. Soc.* **1997**, *119* (31), 7410-7411; (c) Charrier, N.; Zard, S. Z., Radical Allylation with  $\alpha$ -Branched Allyl Sulfones. *Angew. Chem.* **2008**, *120* (49), 9585-9588.
4. Russell, G. A.; Kochi, J. K., In free Radicals. *Wiley & Sons, New York* **1973**, *1* (1A), Chapter 7.
5. Wang, Z., Wohl-Ziegler Bromination. In *Comprehensive Organic Name Reactions and Reagents*, John Wiley & Sons, Inc.: 2010.
6. Walbiner, M.; Wu, J. Q. F., *H. Helv. Chim. Acta* **1995**, *78*, 910 - 924.
7. Skell, P. S.; Traynham, J. G., *Acc. Chem. Res* **1984**, *17*, 160 - 166.
8. Ghosez-Giese, A.; Giese, B., in Controlled Radical Polymerization. *ACS Symposium Series, American Chemical Society* **1998**.
9. Protasiewicz, J.; Mendenhall, G. D., Di-tert-butyl hyponitrite as a source of alkoxy radicals for dimerization. *J. Org. Chem.* **1985**, *50* (17), 3220-3222.
10. Billmeyer, F., Textbook of Polymer Science *Wiley: New York* **1971**, Chapter 9 (2nd Ed.), 280.
11. (a) Sibi, M. P.; Porter, N. A., Enantioselective Free Radical Reactions. *Acc. Chem. Res.* **1998**, *32* (2), 163-171; (b) Sibi, M. P.; Ji, J., Practical and Efficient Enantioselective Conjugate Radical Additions. *J. Org. Chem* **1997**, *62* (12), 3800-3801.
12. (a) Moad, G.; Rizzardo, E.; Thang, S. H., Toward Living Radical Polymerization. *Acc. Chem. Res.* **2008**, *41* (9), 1133-1142; (b) Moad, G.; Rizzardo, E.; Thang, S. H., Radical addition-fragmentation chemistry in polymer synthesis. *Polymer* **2008**, *49* (5), 1079-1131.
13. Rozatsev, E. G., Free Nitroxyl radicals. *plenum press.* **1970**, *New York* (Ed.: H.Ulrich).
14. (a) Ishii, Y.; Nakayama, K.; Takeno, M.; Sakaguchi, S.; Iwahama, T.; Nishiyama, Y., Novel Catalysis by N-Hydroxyphthalimide in the Oxidation of Organic Substrates by Molecular Oxygen. *J. Org. Chem.* **1995**, *60* (13), 3934-3935; (b) Ishii, Y.; Iwahama, T.; Sakaguchi, S.; Nakayama, K.; Nishiyama, Y., Alkane Oxidation with Molecular Oxygen Using a New Efficient Catalytic System: N-Hydroxyphthalimide (NHPI) Combined with Co(acac)<sub>n</sub> (n = 2 or 3)<sup>†</sup>. *J. Org. Chem.* **1996**, *61* (14), 4520-4526; (c) Hara, T.; Iwahama, T.; Sakaguchi, S.; Ishii, Y., Catalytic Oxyalkylation of Alkenes with Alkanes and Molecular Oxygen via a Radical Process Using N-Hydroxyphthalimide. *J. Org. Chem* **2001**, *66* (19), 6425-6431; (d) Kato, S.; Iwahama, T.; Sakaguchi, S.; Ishii, Y., N-Hydroxyphthalimide-Catalyzed Carboxylation of Polycyclic Alkanes with Carbon Monoxide in the Presence of Dioxygen. *J. Org. Chem* **1998**, *63* (2), 222-223; (e) Yoshino, Y.; Hayashi, Y.; Iwahama, T.; Sakaguchi, S.; Ishii, Y., Catalytic Oxidation of Alkylbenzenes with Molecular Oxygen under Normal Pressure and Temperature by N-

- Hydroxyphthalimide Combined with Co(OAc)<sub>2</sub>. *J. Org. Chem.* **1997**, *62* (20), 6810-6813; (f) Sheldon, R. A.; Arends, I. W. C. E., Organocatalytic Oxidations Mediated by Nitroxyl Radicals. *Adv. Synth. Catal.* **2004**, *346*, 1051-1071.
15. Recupero, F.; Punta, C., Free Radical Functionalization of Organic Compounds Catalyzed by N-Hydroxyphthalimide†. *Chem. Rev. (Washington, DC, U. S.)* **2007**, *107* (9), 3800-3842.
16. Koshino, N.; Saha, B.; Espenson, J. H., Kinetic Study of the Phthalimide N-Oxyl Radical in Acetic Acid. Hydrogen Abstraction from Substituted Toluenes, Benzaldehydes, and Benzyl Alcohols. *J. Org. Chem.* **2003**, *68* (24), 9364-9370.
17. (a) Villieras, J.; Rambaud, M., Wittig-Horner Reaction in Heterogeneous Media; 1. An Easy Synthesis of Ethyl  $\alpha$ -Hydroxymethylacrylate and Ethyl  $\alpha$ -Halomethylacrylates using Formaldehyde in Water. *Synthesis* **1982**, *1982* (11), 924-926; (b) Pines, H.; Alul, H.; Kolobielski, M., Notes - Bromination of  $\alpha$ -Methylstyrene with N-Bromosuccinimide. *J. Org. Chem.* **1957**, *22* (9), 1113-1114; (c) Péguier, C.; Morellato, L.; Chahed, E.; Andrieux, J.; Nicolas, J.-P.; Boutin, J. A.; Bennejean, C.; Delagrangé, P.; Langlois, M.; Mathé-Allainmat, M., Synthesis of new arylalkoxy amido derivatives as melatonergic ligands. *Bioorg. Med. Chem.* **2003**, *11* (5), 789-800.
18. Albrecht, S.; Defoin, A.; Tarnus, C., Simple Preparation of O-Substituted Hydroxylamines from Alcohols. *Synthesis* **2006**, *2006* (EFirst), 1635-1638.
19. Espenson, J. H., *Chemical kinetics and reaction mechanisms*. McGraw-Hill: New York, 1995.
20. (a) Friestad, G. K.; Shen, Y.; Ruggles, E. L., Enantioselective Radical Addition to N-Acyl Hydrazones Mediated by Chiral Lewis Acids. *Angew. Chem.* **2003**, *115* (41), 5215-5217; (b) Sibi, M. P.; Petrovic, G.; Zimmerman, J., Enantioselective Radical Addition/Trapping Reactions with  $\alpha,\beta$ -Disubstituted Unsaturated Imides. Synthesis of anti-Propionate Aldols. *J. Am. Chem. Soc.* **2005**, *127* (8), 2390-2391; (c) Wu, J. H.; Radinov, R.; Porter, N. A., Enantioselective Free Radical Carbon-Carbon Bond Forming Reactions: Chiral Lewis Acid Promoted Acyclic Additions. *J. Am. Chem. Soc.* **1995**, *117* (44), 11029-11030; (d) Cho, D. H.; Jang, D. O., Enantioselective radical addition reactions to the C=N bond utilizing chiral quaternary ammonium salts of hypophosphorous acid in aqueous media. *Chem. Commun. (Cambridge, U. K.)* **2006**, *0* (48), 5045-5047.
21. (a) Kitamura, M.; Okada, S.; Suga, S.; Noyori, R., Enantioselective addition of dialkylzincs to aldehydes promoted by chiral amino alcohols. Mechanism and nonlinear effect. *J. Am. Chem. Soc.* **1989**, *111* (11), 4028-4036; (b) Sibi, M. P.; Liu, P.; Ji, J.; Hajra, S.; Chen, J.-x., Free-Radical-Mediated Conjugate Additions. Enantioselective Synthesis of Butyrolactone Natural Products: (-)-Enterolactone, (-)-Arctigenin, (-)-Isoarctigenin, (-)-Nephrosteranic Acid, and (-)-Roccellaric Acid. *J. Org. Chem.* **2002**, *67* (6), 1738-1745.
22. Johnson, J. R.; Campen, M. G. V., Organoboron Compounds. IV. Reaction of Tri-n-butylborane with Peroxides and with Oxygen. Mechanism of Autooxidation. *J. Am. Chem. Soc.* **2002**, *60* (1), 121-124.
23. Bazin, S.; L'Féray; Bertrand, M. P., Dialkylzinc in Radical Reactions. *Chimia* **2006**, *60*, 260-265.
24. (a) Busch, B. B.; Paz, M. M.; Shea, K. J.; Staiger, C. L.; Stoddard, J. M.; Walker, J. R.; Zhou, X.-Z.; Zhu, H., The Boron-Catalyzed Polymerization of Dimethylsulfoxonium Methylide. A Living Polymethylene Synthesis. *J. Am. Chem. Soc.* **2002**, *124* (14), 3636-3646; (b) Kabalka,

- G. W.; Brown, H. C.; Suzuki, A.; Honma, S.; Arase, A.; Itoh, M., Inhibition of the reaction of organoboranes with .alpha.,.beta.-unsaturated carbonyl derivatives by galvinoxyl. Evidence for a free-radical chain mechanism. *J. Am. Chem. Soc.* **2002**, *124* (3), 710-712; (c) Miyabe, H.; Yamaoka, Y.; Takemoto, Y., Triethylborane-Induced Intermolecular Radical Addition to Ketimines. *J. Org. Chem* **2005**, *70* (8), 3324-3327; (d) Nozaki, K.; Oshima, K.; Uchimoto, K., Et<sub>3</sub>B-induced radical addition of R<sub>3</sub>SnH to acetylenes and its application to cyclization reaction. *J. Am. Chem. Soc.* **2002**, *124* (8), 2547-2549; (e) Ollivier, C.; Renaud, P., Organoboranes as a Source of Radicals. *Chem. Rev. (Washington, DC, U. S.)* **2001**, *101* (11), 3415-3434.
25. Zhang, Z.-C.; Chung, T. C. M., Reaction Mechanism of Borane/Oxygen Radical Initiators during the Polymerization of Fluoromonomers. *Macromolecules* **2006**, *39* (16), 5187-5189.
26. Sibi, M. P.; Ji, J.; Sausker, J. B.; Jasperse, C. P., Free Radical-Mediated Intermolecular Conjugate Additions. Effect of the Lewis Acid, Chiral Auxiliary, and Additives on Diastereoselectivity. *J. Am. Chem. Soc.* **1999**, *121* (33), 7517-7526.
27. (a) Kiefer, H.; Traylor, T. G., Di-*t*-butyl hyponitrite. A convenient source of *t*-butoxy radicals. *Tetrahedron Lett.* **1966**, *7* (49), 6163-6168; (b) Protasiewicz, J.; Mendenhall, G. D., Di-*t*-butyl hyponitrite as a source of alkoxy radicals for dimerization. *J. Org. Chem* **1985**, *50* (17), 3220-3222.
28. Ogle, C. A.; Martin, S. W.; Dziobak, M. P.; Urban, M. W.; Mendenhall, G. D., Decomposition rates, synthesis, and spectral properties of a series of alkyl hyponitrites. *J. Org. Chem* **1983**, *48* (21), 3728-3733.
29. Finn, M.; Friedline, R.; Suleman, N. K.; Wohl, C. J.; Tanko, J. M., Chemistry of the *t*-Butoxy Radical: Evidence that Most Hydrogen Abstractions from Carbon are Entropy-Controlled. *J. Am. Chem. Soc.* **2004**, *126* (24), 7578-7584.
30. Koshino, N.; Cai, Y.; Espenson, J. H., Kinetic Study of the Phthalimide N-Oxyl (PINO) Radical in Acetic Acid. Hydrogen Abstraction from C-H Bonds and Evaluation of O-H Bond Dissociation Energy of N-Hydroxyphthalimide. *J. Phys. Chem. A* **2003**, *107* (21), 4262-4267.
31. Hair, S. R.; Taylor, G. A.; Schultz, L. W., An easily implemented flash photolysis experiment for the physical chemistry laboratory: The isomerization of 4-anilino-4'-nitroazobenzene. *J. Chem. Educ.* **1990**, *67* (8), 709.
32. Porter, G.; Topp, M. R., *Nature* **220**, 1228 - 1229
33. Yu, X. Kinetics of free radical reactions generated by laser flash photolysis of OH+Cl- and SO<sub>4</sub>+Cl- in the aqueous phase -chemical mechanism, kinetics data and their implications. 2001.
34. Kaplan, J. H.; Somlyo, A. P., Flash photolysis of caged compounds: New tools for cellular physiology. *Trends Neurosci.* **1989**, *12* (2), 54-59.
35. Scaiano, J. C., Nanosecond Laser Flash Photolysis: A Tool for Physical Organic Chemistry. In *Reactive Intermediate Chemistry*, John Wiley & Sons, Inc.: 2005; pp 847-871.
36. Elsayed, K.; Imam, H.; Harfoosh, A.; Hassebo, Y.; Elbaz, Y.; Aziz, M.; Mansour, M., Design and construction of Q-switched Nd:YAG laser system for LIBS measurements. *Optics & Laser Technology* **2012**, *44* (1), 130-135.
37. Li, H.; van 't Hag, L.; Yousef, Y. A.; Melo, T. B.; Razi Naqvi, K., Single shot laser flash photolysis with a fibre-coupled reference beam monitor. *Photochem. Photobiol. Sci.* **2013**, *12* (2), 404-406.

38. Wang, Z., Barton Reaction. In *Comprehensive Organic Name Reactions and Reagents*, John Wiley & Sons, Inc.: 2010.
39. Aveline, B. M.; Kochevar, I. E.; Redmond, R. W., Photochemistry of N-Hydroxypyridine-2-thione Derivatives: Involvement of the 2-Pyridylthiyl Radical in the Radical Chain Reaction Mechanism. *J. Am. Chem. Soc.* **1995**, *117* (38), 9699-9708.
40. Sanjuan, A.; Aguirre, G.; Alvaro, M.; Garcia, H.; Scaiano, J. C.; Chretien, M. N.; Focsaneanu, K.-S., Product studies and laser flash photolysis of direct and 2,4,6-triphenylpyrylium-zeolite Y photocatalyzed degradation of fenvalerate. *Photochem. Photobiol. Sci.* **2002**, *1* (12), 955-959.

## Chapter 3

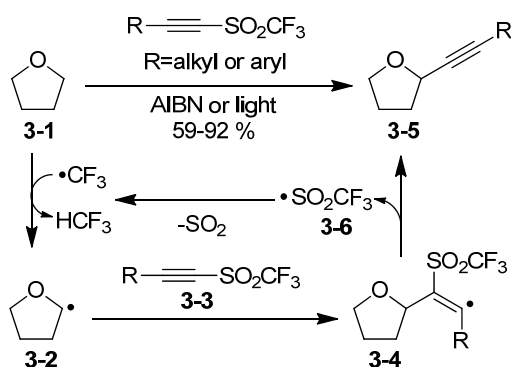
### Radical additions of acyclic and cyclic ethers via allyl transfer using phthalimido-*N*-oxyl radical

#### 3.1 Review: Direct $\alpha$ -C-H activation and functionalization of ether

Direct C-H bond activation and functionalization reactions have been interesting to organic chemists, as they provide easily accessible, economical and novel routes for interesting synthetic applications. Various high efficiency and versatile methods have been reported for such activations and functionalizations.<sup>1</sup> These reactions could be categorized mainly into: 1)  $sp^2$   $\alpha$ -C-H reactions of arene, alkene, aldehyde, imine; 2)  $sp^3$   $\alpha$ -C-H reactions of allyl, benzyl, carbonyl compounds; 3)  $sp^3$   $\alpha$ -C-H reactions of heteroatomic compounds containing oxygen, nitrogen and sulfur. The third type,  $sp^3$   $\alpha$ -C-H activation followed by new C-C bond formation reactions of alcohol, ether and amine are synthetically useful because of the direct conversion of these relatively unreactive compounds into novel substrates of varying complexity. This chapter specifically discusses reported methods for  $sp^3$   $\alpha$ -C-H activation and functionalization of ethers, and our contribution to this area through ether and acetal functionalization via allyl transfer reaction.

### 3.1.1 Radical addition-elimination reactions of ethers with alkenes and alkynes

In this section we discuss the representative examples of reactions of  $sp^3$  radicals of ethers with alkenes and alkynes. In 1990, Fuchs, *et al.* reported the radical addition-elimination reaction of ethers with various alkenyl or alkynyl triflones.<sup>2</sup> In this method, various cyclic and acyclic aliphatic ethers were reacted with alkenyl or alkynyl triflones to yield  $\alpha$ -acetylenic ethers in good yields.

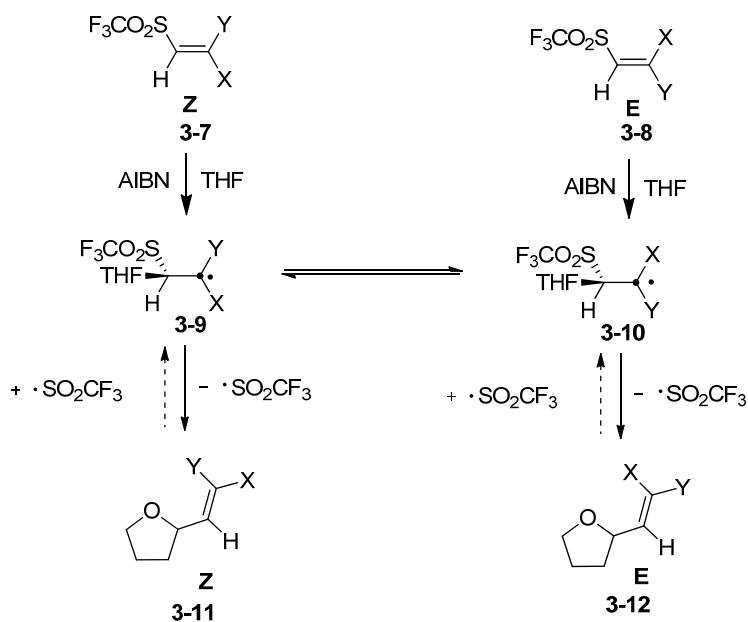


**Scheme 3-1:** Peroxide or light initiated reaction of THF with alkynyl triflones.

These reactions were initiated thermally or photochemically using high concentrations of the substrate ethers. The proposed radical addition-elimination mechanism for this reaction is shown in (Scheme 3-1). The thermal initiator or light triggered the initiation to generate a carbon radical **3-2** which added to the triflone **3-3**. The elimination of  $SO_2CF_3$  **3-6** from **3-4**, led to the  $\alpha$ -acetylenic ether product **3-5**. In addition to this, further fragmentation of  $SO_2CF_3$  **3-6** with the release of  $SO_2$  propagated the chain reaction by generating  $CF_3$ • as a chain carrier.

The alkenylation of ethers with substituted vinyl triflones **3-7** and **3-8** have also been reported.<sup>2c</sup> However, in this case, the free rotation of single bond of the radical intermediates **3-9** and **3-10** led to a mixture of E- isomer **3-12** and Z-isomer **3-11** of products (Scheme 3-2). To

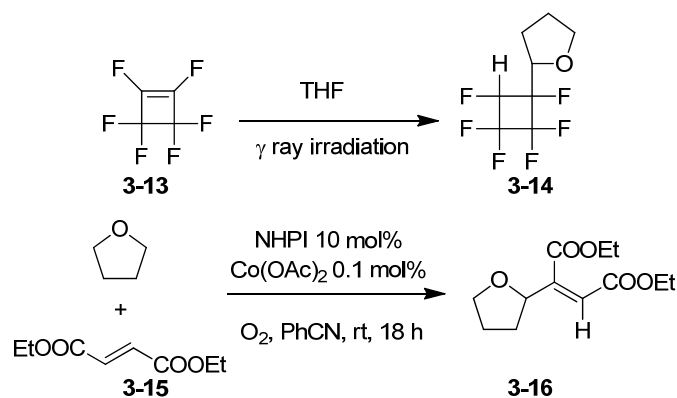
improve stereochemical control, 1,2-disubstituted vinyl triflones were used which led to the sterically preferred E- $\alpha$ -vinyl products.



**Scheme 3-2:** The alkenylation of ethers using substituted vinyl triflones

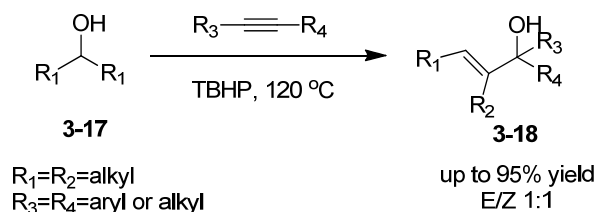
### 3.1.2 Radical addition of alcohol and ether to alkene, alkyne, aldehyde and imine

The addition-elimination reactions of radicals generated from ethers via  $\alpha$ -C-H activation-functionalization have been extensively studied.<sup>3</sup> Initial efforts were focused on the reactions of ether with polyfluoro-alkenes, initiated thermally or by  $\gamma$ -ray irradiation to synthesize  $\alpha$ -polyfluoroalkyl ethers. Similarly, the coupling reactions of THF with perfluorinated cyclobutene **3-13** were also reported. Ishii, *et al.* reported the NHPI (*N*-hydroxyphthalimide)/Co(OAc)<sub>2</sub> catalyzed radical addition of ethers to electrophilic alkenes **3-15** (Scheme 3-3).<sup>4</sup> Various cyclic ethers (like THF) were proved to be effective and high yields of the resulting products were obtained.



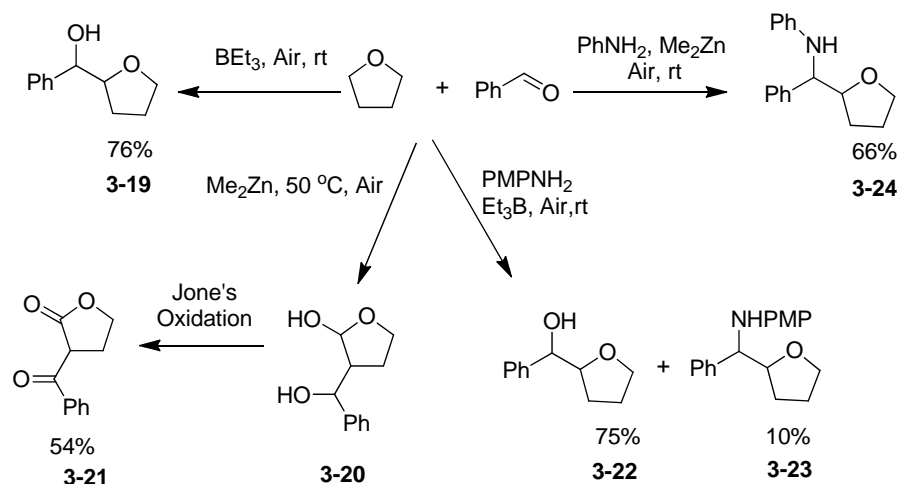
**Scheme 3-3:** Ether functionalization via reactions with alkene

In 2009, Liu, *et al.* succeeded in the radical addition of alcohols **3-17** to the alkynes using TBHP at 120 °C, which afforded the corresponding allylic alcohols **3-18** in excellent yields (Scheme 3-4).<sup>5</sup> A wide range of substrates including aliphatic alcohols, cyclic ethers and electron rich alkynes were reported to be effective in this reaction.



**Scheme 3-4:** Alcohol functionalization via reaction with alkyne

In 2003, Yoshimitsu, *et al.* developed a new method initiated by  $\text{BET}_3/\text{air}$  or  $t\text{-BuO}_2\text{H}$  for the radical addition of ethers to aldehydes to obtain  $\alpha$ -hydroxylalkyl ethers (Scheme 3-5). Cyclic ethers and aromatic aldehydes were reported to be more effective than the other substrates in this reaction.

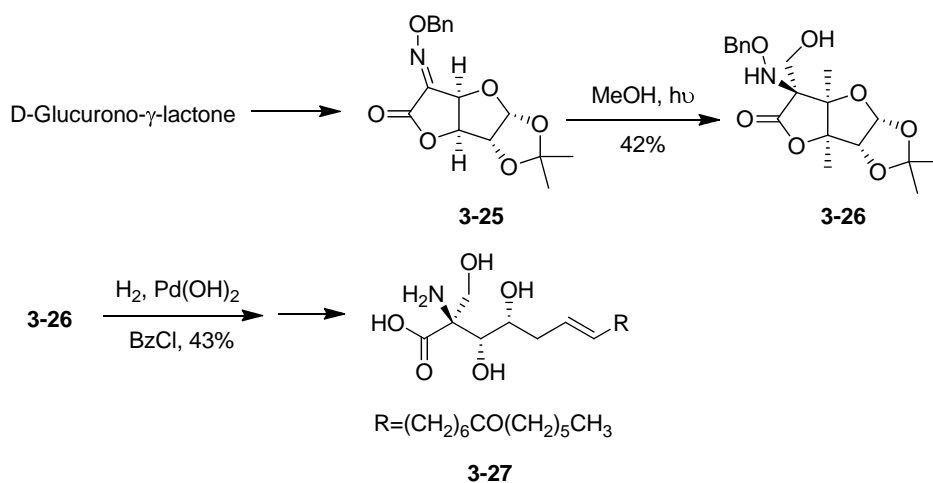


**Scheme 3-5:** Radical addition of ethers to aldehydes and imines. (PMP=*p*-methoxyphenyl)

However, an interesting observation was reported by Tomioka, *et al.* that the chemoselectivity of this radical addition was dependent on the initiator and replacement of  $\text{BEt}_3/\text{air}$  with  $\text{Me}_2\text{Zn}/\text{air}$  led to the formation of  $\beta$ -hydroxyalkyl- $\alpha$ -hydroxyl ether (**3-20**) rather than the  $\alpha$ -hydroxy alkyl ether (**3-19**).<sup>6</sup> Also, **3-20** could be further oxidized to  $\alpha$ -acyl lactones by Jones' oxidation (Scheme 3-5). Similarly, they carried out the  $\text{Me}_2\text{Zn}/\text{air}$  initiated radical addition of ether to aldimine (generated in-situ from aldehyde and amine). This reaction was used to synthesize the  $\alpha$ -aminoalkyl ethers (**3-24**) in good to high product yields<sup>6b, 7</sup> (Scheme 3-5). A wide range of substrates like formic acetals, and aldimines (generated from aryl aldehydes and aryl or toluenesulfonyl amines) were also reported to be effective in this reaction. Porta, *et al.* developed another catalytic system (Ti(III)/TBHP) for the direct three-components (ether, aldehyde and amine) coupling reaction to yield the similar product.<sup>8</sup> This procedure was used to synthesize  $\alpha,\alpha'$ -di (aminoalkyl)-substituted ether derivatives.

This method not only provided a new pathway to synthesize chiral amino alcohols and ethers using chiral C=N bond donors but also provided an alternative approach to chiral  $\alpha$ -amino

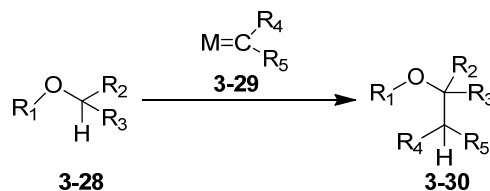
acids. For example, Alonso and coworkers reported the photoinitiated asymmetric synthesis of amino alcohol and acid derivatives through the radical addition of MeOH and formic acetal to chiral ketoximes and aldehydrazones, respectively.<sup>9</sup> Later on, based on this methodology, Alonso *et al.* reported a short synthesis of (+)-myriocin (**3-27**) using D-glucurono-g-lactone that involved key step of photoinduced addition of MeOH to a chiral ketoxime ether.<sup>9a, 10</sup> (Scheme 3-6)



**Scheme 3-6** : Synthesis of (+)-myriocin via addition of MeOH to ketoxime.<sup>11</sup>

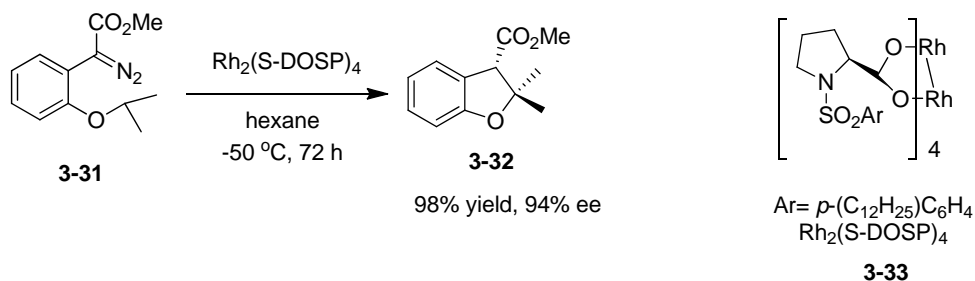
### 3.1.3 Metal mediated carbenoid insertion to $\alpha\text{-C-H}$ of ether

Metal carbenoid insertion into a C–H bond was reported to be an alternative approach to the metal-mediated C–H activation and C–H functionalization pathways. Although few review articles have already summarized various methods of carbenoid insertion,<sup>12</sup> this section discusses the recent progress in the carbenoid insertion to the C–H bond vicinal to oxygen atom (Scheme 3-7).



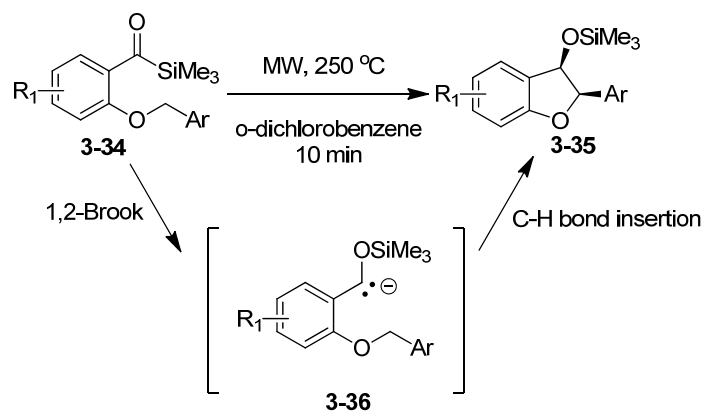
**Scheme 3-7:** Metal carbenoid insertion into the  $\alpha$ -C–H bond of ether,  $\text{R}_1$ – $\text{R}_3$ = alkyl, aryl.

The metal-carbenoid **3-29** insertion into the C–H bond vicinal to the oxygen atom in **3-28** was reported to be an effective methodology.<sup>13</sup> Over the past decade, several new catalysts have been reported for stereoselective syntheses of oxygen heterocycles. For example, Davies, *et al.* developed a novel catalyst ( $\text{Rh}_2(\text{S-DOSP})_4$ ) (**3-33**) for intramolecular insertion of carbenoid (derived from aryl diazoacetates) to the C–H bond adjacent to phenylether oxygen **3-31**, leading to substituted dihydrobenzofuran (**3-32**) in high yields (up to 94%) and good enantioselectivity (Scheme 3-8).<sup>14</sup>



**Scheme 3-8:**  $\text{Rh}_2(\text{S-DOSP})_4$ -catalyzed carbenoid insertion to methine  $\alpha$ -C–H bond of phenyl methinyl ether

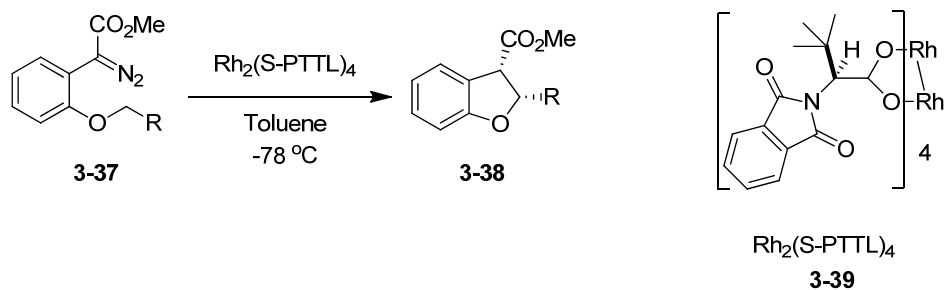
Recently, a novel, convenient and metal-free procedure for benzylic  $\text{sp}^3$  C–H bond functionalization was reported by Dong, *et al.*<sup>15</sup>



**Scheme 3-9:** Microwave irradiated benzylic  $\text{sp}^3$  C–H bond functionalization using the siloxycarbenes

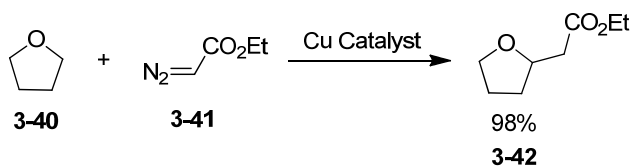
In this method, siloxycarbenes were used, which were generated from acylsilane using microwave irradiation. It was based on the hypothesis that a thermally induced Brook rearrangement would generate a siloxycarbene **3-36** that could undergo rapid insertion to a C–H bond. This method allowed a rapid and easy access to important oxygen heterocycle dihydrobenzofurans. After screening of several solvents and optimization of reaction conditions, this method showed high yield and good selectivity when *o*-dichlorobenzene was used at 250 °C for 5–10 min. Remarkably, by replacing *o*-dichlorobenzene with DMSO, a new variant of the process was developed to synthesize the benzofuran derivatives efficiently via the distinct Brook rearrangement. Various substituents on the aromatic ring were tolerated and the corresponding benzofurans were synthesized in up to good (up to 67%) yields (Scheme 3-9).

In addition to this, recently, two new catalysts,  $\text{Rh}_2(\text{S-DOSP})_4$  **3-33** and  $\text{Rh}_2(\text{S-PTTL})_4$  **3-39**, were reported for the asymmetric intermolecular  $\alpha$ -C–H carbenoid insertion to synthesize derivatives of cyclic ether (THF) and benzylic ether (Scheme 3-10).<sup>16</sup>



**Scheme 3-10:**  $\text{Rh}_2(\text{S-PTTL})_4$ -catalyzed carbenoid insertion to  $\alpha$ -C–H of phenyl ether.

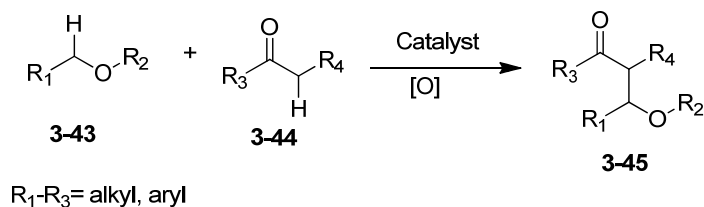
In 2002, Perez, *et al.* developed a bulky copper catalyst for intermolecular  $\alpha$ -C–H insertion carbenoid of ethyl diazoacetate **3-41** to cyclic ether **3-40**.<sup>17</sup> Thus, as an example, the  $\alpha$ -THF-substituted product **3-42** was afforded in 98% yield (Scheme 3-11).



**Scheme 3-11:** Cu-catalyzed carbenoid insertion into  $\alpha$ -C–H of aliphatic ether.

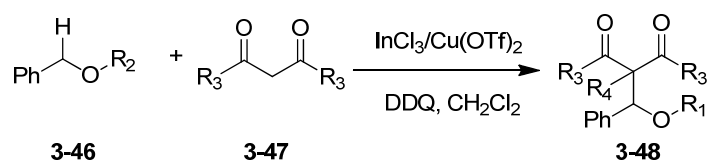
### 3.1.4 Oxidative CDC reaction of ether with carbonyl compounds

The cross-dehydrogenative coupling (CDC) reaction has provided an excellent approach to activate inert C–H bonds to react with nucleophiles. By definition, the CDC reaction is a C–C bond coupling that involves an oxidative dehydrogenation of  $\alpha$ -C–H bonds of ether **3-43** and carbonyl compounds **3-44** (Scheme 3-12).



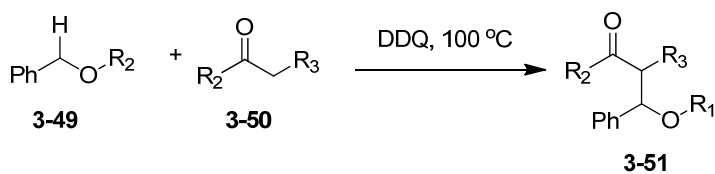
**Scheme 3-12:** CDC reaction of  $\alpha$ -C–H bond of ether and carbonyl compounds.

Li, and other research groups have reported a series of CDC reactions for  $\alpha$ -C-H functionalization of amines, allylic and benzylic compounds.<sup>18</sup> Although C-H bonds vicinal to oxygen are difficult to activate, the C-C bond coupling between ether **3-46** and carbonyl substrate **3-47** were successfully achieved via this method (Scheme 3-13).<sup>19</sup> Several combinations of In and Cu catalysts were screened and InCl<sub>3</sub>/Cu(OTf)<sub>2</sub> in 5 : 5 (mol%) with 1.2 eq. of DDQ (2,3-dichloro-5,6-dicyanobenzoquinone) in CH<sub>2</sub>Cl<sub>2</sub> was optimized as the best catalysis system. However, the above In/Cu/DDQ-promoted CDC reaction was limited to benzyl ethers and malonate derivatives.



**Scheme 3-13:** CDC reactions of benzyl ethers with malonate derivatives. R<sub>1</sub>= alkyl, R<sub>2</sub>, R<sub>3</sub>=OMe, R<sub>4</sub>=H, Me, Cl

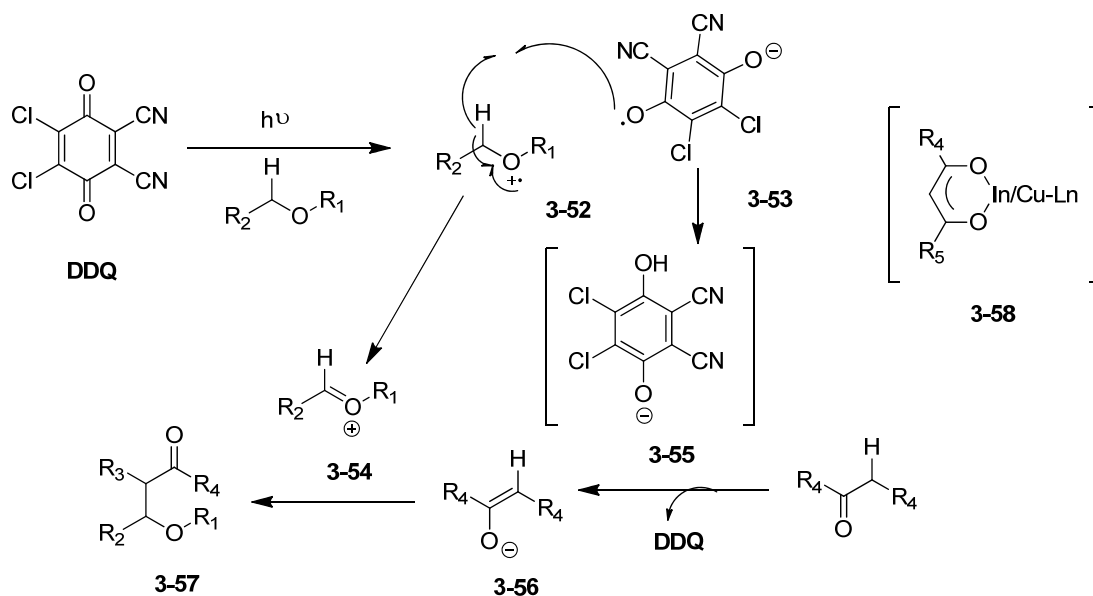
Li, *et al.* also extended the substrate scope to ketones **3-50** and succeeded in the metal-free CDC reaction using convenient reaction condition using just DDQ at 100 °C.<sup>20</sup> A series of coupling products were obtained in moderate yields in most cases (Scheme 3-14)



**Scheme 3-14:** CDC reaction of benzyl ethers with ketones without metal-catalyst.

Later on, a tentative single-electron transfer mechanism of this CDC as illustrated in Scheme 3-15 was proposed.<sup>19-20</sup> In the first step, a single-electron transfer from the benzyl ether

to DDQ generated a radical cation **3-52** and a DDQ radical anion **3-53**. DDQ radical anion abstracted a H-atom from **3-52** and generated a benzoyl cation **3-54** and a DDQ radical anion **3-55**. The latter abstracted H-atom from the ketone to give an enolate **3-56**, which added to benzoyl cation C to give the final product **3-57** with the release of DDQ. For the former work<sup>19</sup> (Scheme **3-15**), the role of  $\text{InCl}_3/\text{Cu}(\text{OTf})_2$  was probably to accelerate the enolization of malonates as shown in **3-58**. In addition, an  $\text{In}/\text{Cu}/\text{NHPI}/\text{O}_2$  promoted CDC reaction between cyclic benzyl ethers with malonates was reported recently.<sup>21</sup>

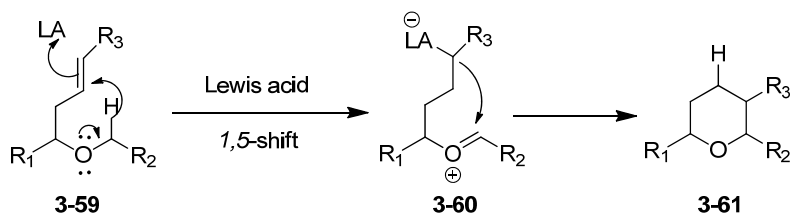


**Scheme 3-15:** Proposed single-electron transfer mechanism for CDC reaction

### 3.1.5 Intramolecular annulation in ether via 1,5-hydride migration

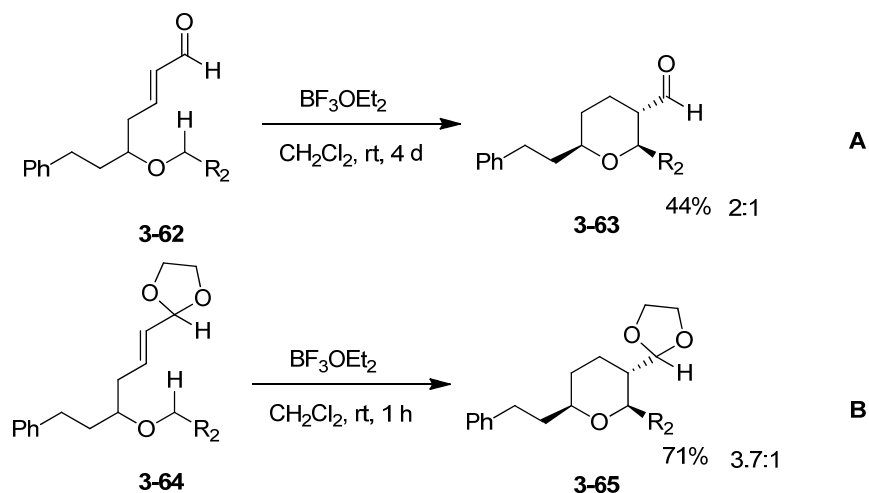
This section discusses syntheses of cyclic ethers via intramolecular ring annulations of acyclic ethers. Sames, *et al.* have reported annulations in ethers and have made an important contribution to this area.<sup>22</sup> In 2005, they reported a new method for Lewis acid catalyzed  $\alpha$ -C–H 1,5-hydride migration and annulation of unsaturated ethers.<sup>23</sup> The general mechanism for this

reaction is described in Scheme 3-16. This mechanism was reported to go through the following steps; 1) Lewis acids activation of unsaturated compound **3-59**, 2) cleavage of  $\alpha$ -C–H bond of ether to trigger a 1,5-hydride migration to form the zwitterionic pair **3-60**, and 3) intramolecular ion pair coupling to form the final product **3-61**.



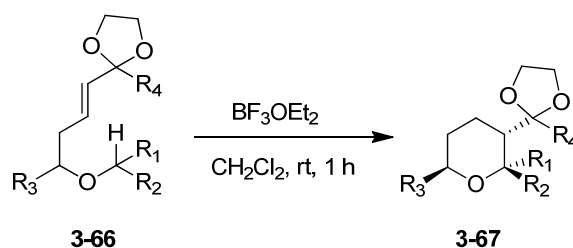
**Scheme 3-16:** Intramolecular annulation of ether with alkene via 1,5-hydride migration

The substrate scope of this reaction was investigated using several unsaturated compounds. These compounds were treated with 30 mol%  $\text{BF}_3 \cdot \text{OEt}_2$  and a series of products polysubstituted spiroether with an oxo-quaternary center, were synthesized. Through this reaction a new method was accomplished to access biologically significant spiroether<sup>24</sup> products. Further investigation of the substrate studies revealed that the  $\alpha,\beta$ -unsaturated aldehydes and ketones were effective to  $\text{BF}_3 \cdot \text{OEt}_2$  promoted reactions, whereas the  $\alpha,\beta$ -unsaturated esters were not. A new catalyst was used ( $\text{Sc}(\text{OTf})_3$ ) and reported to be an efficient catalyst for the reactions of  $\alpha,\beta$ -unsaturated esters. However, the limitation of this reaction was that only the aliphatic cyclic ethers were effective and acyclic ethers usually reacted very slowly under the same reaction conditions ( $\text{BF}_3 \cdot \text{OEt}_2$  at RT). This problem was solved recently via the conversion of the  $\alpha,\beta$ -unsaturated aldehydes **3-62**, **3-64** to corresponding acetals **3-63**, **3-65**.<sup>25</sup> As indicated in Scheme 3-17, this conversion made a huge difference and a dramatic increase of reactivity and chemical yields were observed.



**Scheme 3-17:** Comparison of aldehyde with acetal toward the intramolecular annulations

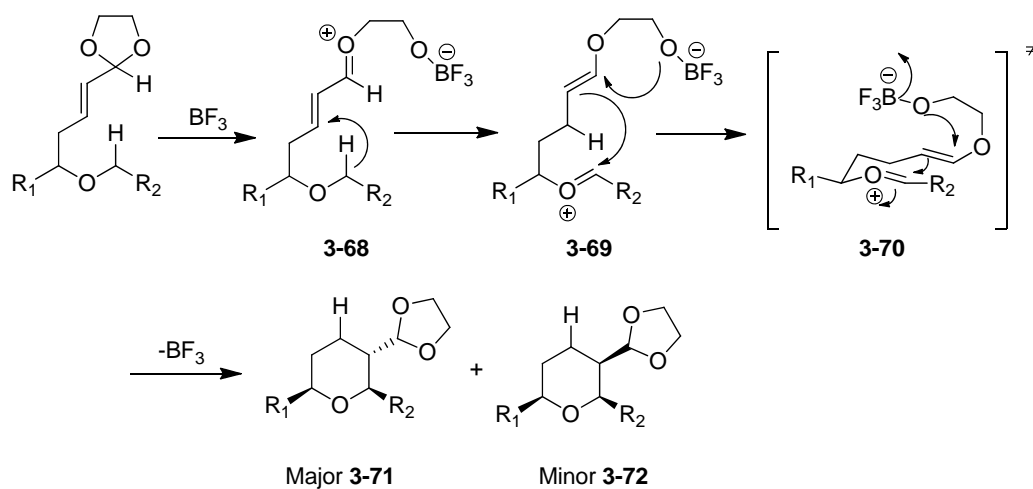
This method was extended to intramolecular annulation of ethers with acetals and ketals using various substituents as indicated in Scheme 3-18 below. The observed high product yields suggest that this method could be used efficiently for the synthesis of complex cyclic ethers derivative with aryl substituents.



**Scheme 3-18:** Intramolecular annulations of ethers with acetals  $R_1=H$ ,  $R_2=Ph$ .

The reaction mechanism for the acetal and ketal was proposed by Sames *et al.*<sup>25</sup> depicted in Scheme 3-19. In the first step, a Lewis acid opened the cyclic acetal to generate the oxocarbenium intermediate **3-68**. This intermediate activated the conjugated double bond for hydride abstraction. The shift in hydride resulted in oxocarbenium-enolether intermediate **3-69**, followed by C–C coupling in **3-69** to form the products **3-71** and **3-72** and Lewis acid catalyst

was regenerated. The observed stereoselectivity leading to **3-71** as a major product could be explained by most favorable transition state **3-70**, in which all substituents are in equatorial positions.



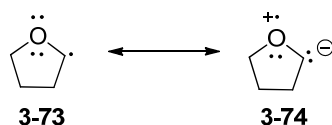
**Scheme 3-19:** Reported mechanism for intramolecular annulation of ether with acetal.

### 3.2 Introduction to ether functionalization via allyl transfer

As discussed in chapters 1 and 2, a wide variety of methods have been reported for the generation of carbon radicals.<sup>26</sup> However, only a few methods are known for the generation of  $\alpha$ -alkoxy carbon radicals under neutral, metal-free, and mild reaction conditions.<sup>27</sup> The generation of such carbon radicals from ethers is limited to either photoinitiation<sup>28</sup> or metal-mediated processes.<sup>27</sup> From the review of the reported methods, it can be concluded that the photoinduced methods were less selective and metal mediated processes generally showed limited substrate scope.

Ethers have weak C-H bonds<sup>29</sup> (THF (BDE) 93.8 kcal/mol, 1,3-dioxane (BDE) 93.3 kcal/mol) owing to the resonance stabilization of resulting radical **3-73** by the vicinal oxygen atom (Scheme 3-20). Ethers are thus a suitable choice for H-abstraction followed by radical

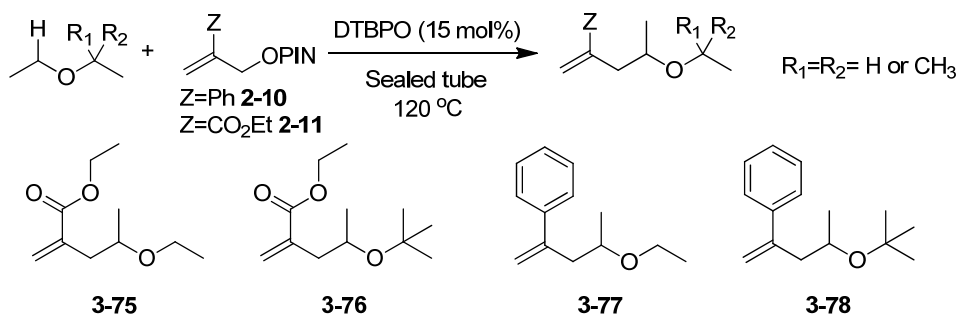
addition reactions. In this chapter, we will discuss in detail, this method of  $\alpha$ -alkoxyl C-H bond functionalization via allyl transfer using phthalimido-*N*-oxyl radical (PINO•). The reaction proceeds via the abstraction of  $\alpha$ -hydrogen from ether and the subsequent addition of the carbon radical to allyl-PINO substrates. Finally, elimination of the PINO• followed by hydrogen abstraction from ether lead to propagation of the chain.



**Scheme 3.20:** Resonance stabilization of  $\alpha$ -alkoxyl radical in tetrahydrocarbon (THF)

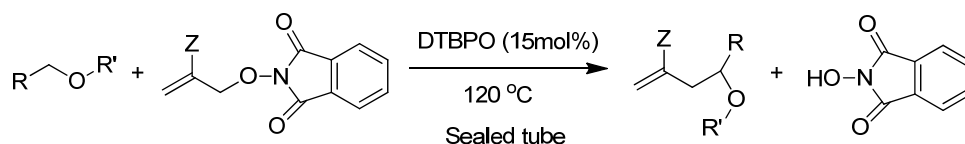
### 3.2.1 Direct functionalization of *acyclic* ethers via allyl transfer

Direct functionalization of acyclic ethers such as ethyl ether, and *t*-butyl ethyl ether has been discussed in section 3.1.3 and 3.1.4. We report here a metal-free and convenient procedure for functionalization of diethyl ether and *t*-butyl ethyl ether via the allyl transfer reaction. (Scheme 3-21) Since diethyl ether and *t*-butyl ethyl ether, both possess equivalent reactive hydrogens, each of these reactions led to a single product formation (Scheme 3-21, **3-75** - **3-78**).



**Scheme 3-21:** Synthesized products from functionalization of acyclic ethers

Both acyclic ethers were allowed to react with allyl-PINO substrates **2-10** and **2-11** in neat ethers at 120 °C in sealed pressure tubes (Scheme 3-21). Table 3-1 discusses the results of these reactions. The side product, NHPI precipitated out at the end of the reaction, which was recycled making this a cost effective synthetic method.



Entry	Ether	Z	Time (h)	Product	Isolated Yield (%)	GC Yield (%)
1		CO <sub>2</sub> Et	4	<b>3-75</b>	83	90
2		Ph	24	<b>3-77</b>	85	90
3		CO <sub>2</sub> Et	4	<b>3-76</b>	85	90
4		Ph	24	<b>3-78</b>	85	90

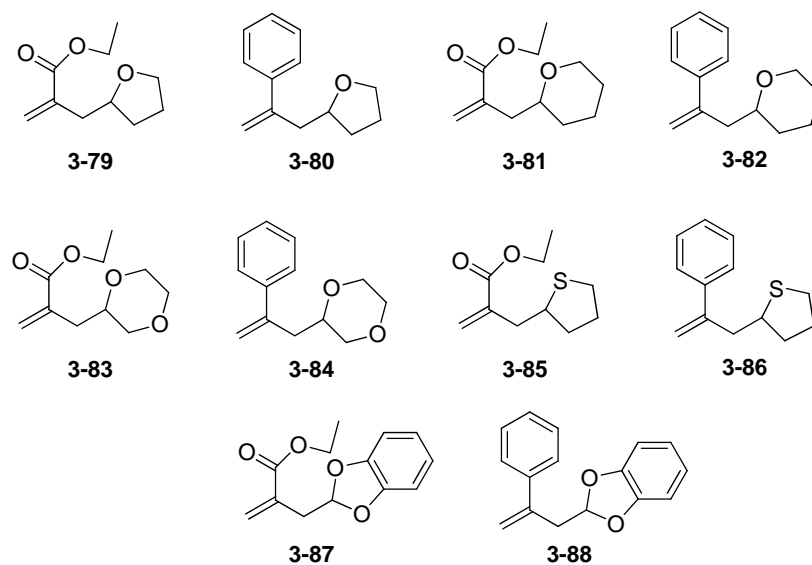
**Table 3-1:** Functionalization of acyclic ethers via allyl transfer reaction (Allyl-PINO substrate 0.45 M, DTBPO 0.07 M, ether 13.0 M)

Reactions of diethyl ether and t-butyl ethyl ether both led to products **3-75**, **3-77** and **3-76**, **3-78** respectively in high yields.

### 3.2.2 Direct functionalization of cyclic ethers

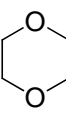
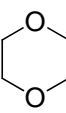
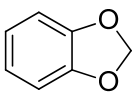
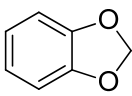
Cyclic ethers such as tetrahydrofuran (THF), 2-MeTHF are key structural motifs in a large number of biologically active compounds and natural products.<sup>30</sup> Thus, direct functionalization of THF has long been fascinating to organic chemists.<sup>31</sup> In connection with our work on acyclic ethers, we speculated that the same functionalization could be possible with cyclic ethers and thioethers. We screened a set of ethers containing THF, THP (tetrahydropyran), 1,4-dioxane, THT (tetrahydrothiophene) and 1,3-benzodioxole in the allyl transfer reaction with

substrates **2-10** and **2-11**. The conditions for these reactions are similar to those in Scheme 3-21. Similar to acyclic ethers, these compounds have only one functionalizable C-H bond owing to its symmetry. The expected products for these reactions are shown in Figure 3-1.



**Figure 3-1:** Synthesized products from functionalization of cyclic ethers and thioether

Table 3-2 demonstrates the results of cyclic ether and thioether functionalization. In the case of THF (Entry 1), the observed yield was relatively lower than the other ethers. This may be because of the high nucleophilicity of the THF radical which may undergo subsequent addition reactions with the product. This might result in the consumption of formed product and reduction in overall product yield. High isolated yields were observed for reactions of THP and 1,4-dioxane (Entry 2 and 3). THT (Entry 4) could also be easily functionalized using this method. Similarly, the 1,3-benzodioxane (Entry 5) which is an important building block for biologically active heterocycles, was also functionalized using this method.

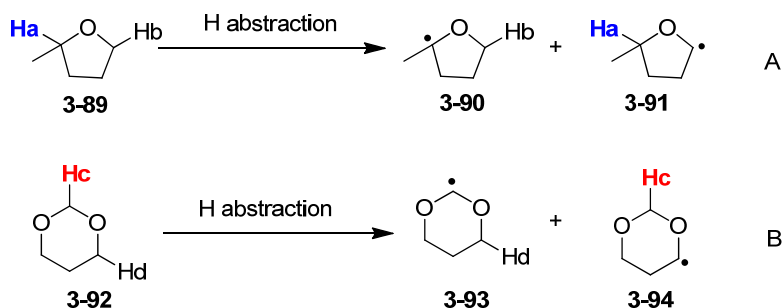
Entry	Ether	Z	Time (h)	Product	Isolated Yield (%)	GC Yield (%)
1		CO <sub>2</sub> Et	1	<b>3-79</b>	60	65(±3)
2		Ph	16	<b>3-80</b>	75	70(±2)
3		CO <sub>2</sub> Et	2	<b>3-81</b>	85	85(±3)
4		Ph	16	<b>3-82</b>	84	90(±2)
5		CO <sub>2</sub> Et	1	<b>3-83</b>	88	88(±2)
6		Ph	18	<b>3-84</b>	85	90(±1)
7		CO <sub>2</sub> Et	2	<b>3-85</b>	85	88(±1)
8		Ph	18	<b>3-86</b>	85	90(±2)
9		CO <sub>2</sub> Et	8	<b>3-87</b>	80	86(±3)
10		Ph	14	<b>3-88</b>	75	81(±2)

**Table 3-2:** Functionalization of cyclic ethers and benzo-1,3-dioxole via allyl transfer reaction.

(Sealed tube, 120 °C) (**2-10**, **2-11** 0.45 M, DTBPO 0.007 M, ether 13.0 M)

### 3.2.3 Competition for H-abstraction in Me-THF and 1,3-dioxane

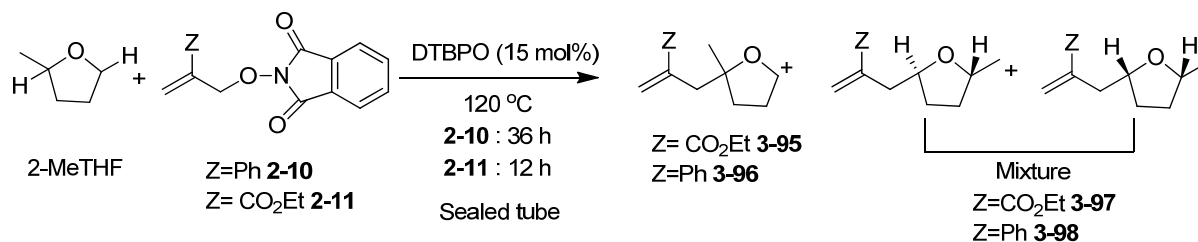
Cyclic ethers such as the unsymmetrical 2-MeTHF and, 1,3-dioxane which have more than one reactive hydrogen were also studied. In these cases, we speculated that the allyl transfer reaction might lead to multiple products, owing to the competition in hydrogen abstraction. To investigate this further, BDEs of competitive C-H bonds and nature of resulting radical were analyzed.



**Scheme 3-22:** Competition for H abstraction in A) 2-MeTHF, B) 1,3-dioxane

In case of 2-MeTHF **3-89**, the most reactive C-H bond (**H<sub>a</sub>**) leads to the tertiary radical **3-90** whereas the second-most reactive C-H bond leads to the secondary radical **3-91**. Thus, we expected a significant difference in their reactivities towards hydrogen abstraction since **3-90** is expected to be more stable than **3-91**. However, in case of 1,3-dioxane **3-92**, both hydrogens (**H<sub>c</sub>** and **H<sub>d</sub>**) are secondary leading to radicals **3-93** and **3-94**. BDE of the C-H bond vicinal to two oxygen atoms (**H<sub>c</sub>**) in 1,3-dioxane was reported to be 93.3 kcal/mol and the C-H bond vicinal to only one oxygen (**H<sub>d</sub>**) was reported to be 93.8 kcal/mol. These similar BDE values suggest that competition in hydrogen abstractions might be significant enough to scramble the ratios of observed products.

### 3.2.3.1 Functionalization of 2-MeTHF via allyl transfer reaction



**Scheme 3-23:** Functionalization of 2-MeTHF via allyl transfer reaction

Functionalization of 2-MeTHF was performed using di-*t*-butyl peroxide (15 mol%) in neat 2-MeTHF. This reaction led to the formation of mixture of products as shown in Scheme 3-23.

Entry	Substrate	Time (h)	Overall reaction yield (%)	Products	GC Yield %	Integrated NMR Yield (%)
1	<b>2-10</b>	36	80	<b>3-96</b>	80	79
				<b>3-98</b> (cis+trans)	20	21
2	<b>2-11</b>	12	82	<b>3-95</b>	-	70
				<b>3-97</b> (cis+trans)	-	30

Reactions were performed in sealed pressure tubes using neat 2-MeTHF. (Sealed tube, 120 °C)  
 (**2-10**, **2-11** 0.4 M, DTBPO 0.06 M, 2-MeTHF 10.0 M)

**Table 3-3:** Functionalization of 2-MeTHF via allyl transfer reaction.

Table 3-3 shows the results of 2-MeTHF functionalization. Entry 1 shows, the reaction of **2-10** with 2-MeTHF leading to products **3-96** and **3-98** and entry 2 shows the reaction of **2-11** with 2-MeTHF leading to products **3-95** and **3-97**. For entry 1, Gas chromatographic analysis was used to calculate the relative ratios of **3-98** to **3-96**. Figure 3-2 shows the GC trace showing

all products formed in this reaction. The product ratios were calculated using gas chromatography using diphenylmethane as an internal standard. From calculation of peak area it was observed that this ratio is 80:20 (Figure 3-2). The major product is speculated to be compound **3-96** whereas the minor product which exist in the form of a mixture of cis and trans isomers forms the rest of 20%. This was further confirmed using  $^1\text{H}$  NMR analysis in which methyl protons signal from the major product appear as a singlet at 1.12 whereas methyl proton signals from cis and trans isomers of **3-98** appear as doublets at 1.20 and 1.25.

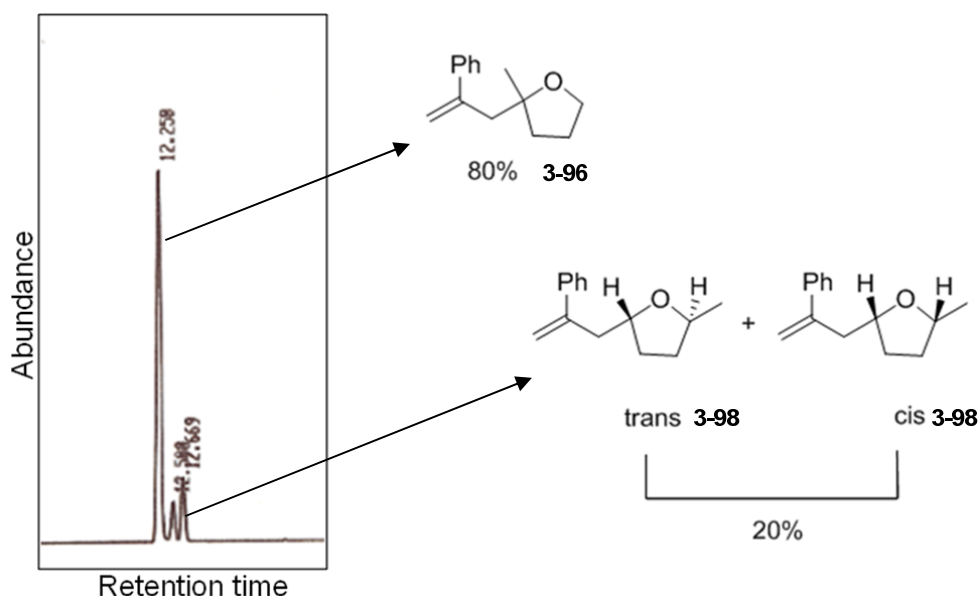
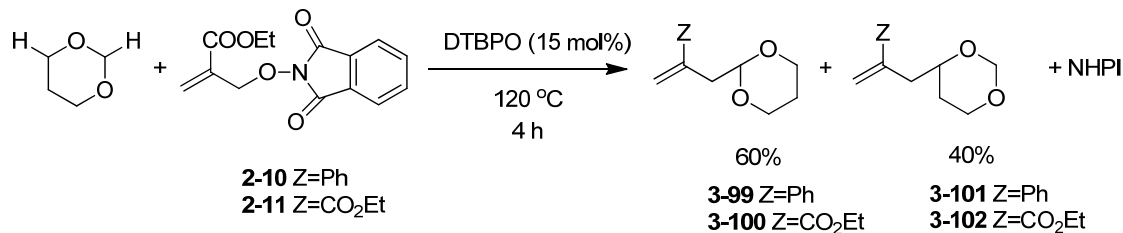


**Figure 3-2:** GC analysis of 2-MeTHF functionalization showing all regioisomeric products

### 3.2.3.2 Functionalization of 1,3-dioxane via allyl transfer reaction

As mentioned above, similar to 2-MeTHF, 1,3-dioxane has more than one functionalizable C-H bonds. Functionalization of 1,3-dioxane was performed using di-*t*-butyl peroxide (15 mol%) in neat 1,3-dioxane. This reaction led to the formation of a mixture of products as shown in Scheme 3-23. The ratio of products in this case was measure using  $^1\text{H}$

NMR spectroscopy. A close competition in hydrogen abstraction was observed in this case that led to major:minor (**3-99:3-100**) product ratio of 60:40 (Scheme 3-24)



**Scheme 3-24:** Functionalization of 1,3-dioxane via allyl transfer reaction

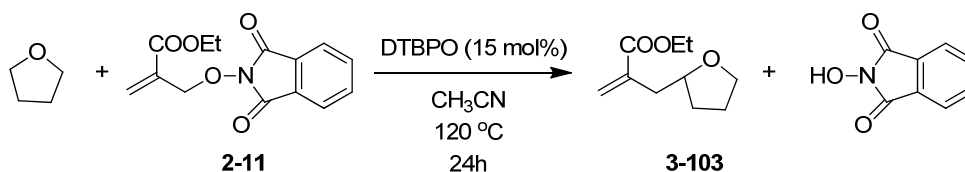
Entry	Substrate	Time (h)	Overall reaction yield (%)	Products	Integrated NMR Yield (%)
1	<b>2-10</b>	4	88	<b>3-99</b> <b>3-101</b>	60 40
2	<b>2-11</b>	24	85	<b>3-100</b> <b>3-102</b>	62 38

**Table 3-4:** Allyl transfer reaction of 1,3-dioxane leading to mixture of products. (Sealed tube, 120 °C) (**2-11** 0.4 M, DTBPO 0.06 M, 1,3-dioxane 10.0 M)

This competition is expected, knowing the relatively close BDEs of the two C-H bonds. (Scheme 3-22). We postulated that, this poor selectivity in hydrogen abstraction by PINO•, could be improved A) by reducing the concentration of initiator, or B) by using low concentration of 1,3-dioxane (i.e by performing reaction in solution). The next subsection discusses our efforts to test these hypotheses.

### 3.2.4 Allyl transfer in solution using low concentration of reagents

To test the hypothesis that the regioselectivity could be improved at low concentration of ethers, we first studied these reactions at varying concentrations of THF in reaction with 2-11. Table 3-5 shows the results of this study. Acetonitrile was used as a solvent in the experiments. In these experiments concentration of THF in acetonitrile is gradually increased from 0.07 M to 0.71 M and the resulting product yield was measured. Significant product yields were observed in entries 3 and 4 where the concentration of THF is reduced to around 0.2-0.3 M without compromising a lot on product yields. From this data it was concluded that 3 to 4 equivalents of THF might be enough for a successful reaction in solution.

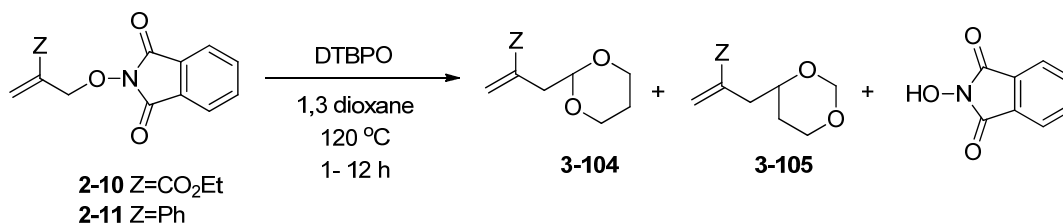


Entry	THF (equiv.)	Conc. of THF (M)	Yield (%) 3-103
1	1	0.07	30
2	2	0.14	45
3	3	0.21	60
4	4	0.28	62
5	10	0.71	65

**Table 3-5:** THF functionalization in solution (acetonitrile) (2-11 0.07 M, DTBPO 0.010 M)

To test the regioselectivity in solution, a set of experiments was performed at varying concentration of 1,3-dioxane. The resulting product mixture was analyzed using NMR

spectroscopy to determine ratios of the major:minor product (Table 3-6). As seen in Entry 1 and 2, reducing the concentration of 1,3-dioxane from 18 M to 0.8 M did not improve selectivity of this reaction.



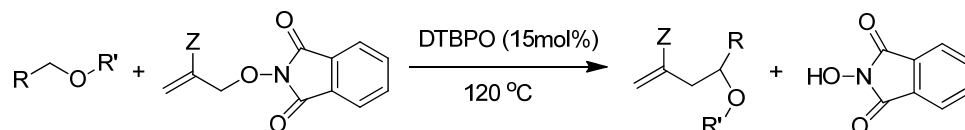
Entry	Substrate	DTBPO (mol %)	1,3-dioxane (eq.)	1,3-dioxane (M)	GC Yield (%) <sup>a</sup> (3-104+3-105)	Ratio (3-104:3-105) <sup>b</sup>
1	<b>2-10</b>	15	30	2.1	85	60:40
2 <sup>a</sup>	<b>2-10</b>	15	3 in CH <sub>3</sub> CN	0.21	66	60:40
3 <sup>a</sup>	<b>2-10</b>	10	3 in CH <sub>3</sub> CN	0.21	62	67:33
4	<b>2-11</b>	15	30	2.1	82	59:41
5 <sup>a</sup>	<b>2-11</b>	10	3 in CH <sub>3</sub> CN	0.21	60	66:34

**Table 3-6:** Allyl transfer reaction in solution. <sup>a</sup>GC yield was calculated using internal standard diphenylmethane. <sup>b</sup>Product ratios were determined using <sup>1</sup>H-NMR spectroscopy. <sup>a</sup>(**2-10**, **2-11** 0.07 M, DTBPO 0.010 M, THF 0.21 M)

Similarly, to test if reducing the amount of initiator (DTBPO) increases selectivity, the concentration of initiator was reduced to 10 mol % (Entry 3). However, this change did not lead to significant improvement of selectivity. A similar trend was observed when **2-11** was used as the substrate. (Entry 4 and 5)

### 3.3 Kinetic chain length measurements

Data in Table 3-7 illustrates that allyl transfer reactions are highly efficient chain reactions with kinetic chain length as high as 15,000. Kinetic chain lengths for THF and 1,4-dioxane both were observed to be very high whereas, they were significantly shorter for 2-MeTHF. This decrease in chain length can be attributed to the competition in hydrogen abstraction and the steric crowding in the radical addition step. Although chain lengths in solution were significantly lower than the reactions with neat ethers, data shows that it is still an efficient chain reaction in solution.



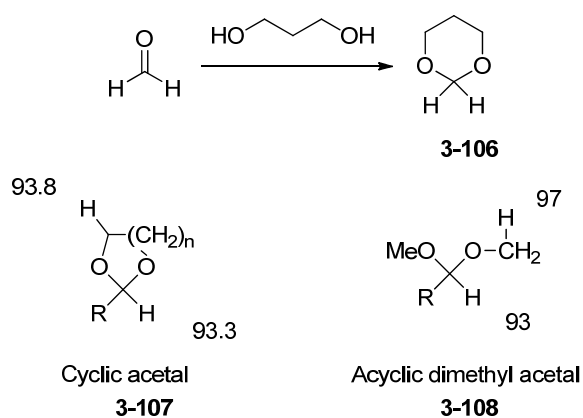
Z	THF	THF <sup>a</sup> (3eq. In ACN)	2-MeTHF (Major product)	2-MeTHF (All products: mixture)	1,4-dioxane
CO <sub>2</sub> Et	15000(±5000)	40 (±20)	300(±70)	1200(±400)	8000(±2500)
Ph	1200(±600)	N/D	N/D	80(±20)	1300(±300)

**Table 3-7:** Summarized kinetic chain length data for allyl transfer reactions on ethers. <sup>a</sup>(**2-11** and **2-12** 3.5 mM, DTBPO 0.53 mM,)

### 3.4 C-H functionalization of acetals

In this chapter, we have discussed the reaction of 1,3-dioxane with allyl-PINO substrates via allyl transfer. Since, 1,3 dioxane is a cyclic acetal of formaldehyde (**3-106**), this inspired us to

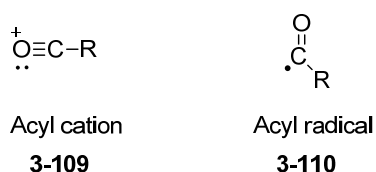
work on the extension of this method to various acetals. Previous results suggested that the cyclic acetals (like 1,3-dioxane) might lead to multiple products owing to the competition in hydrogen abstraction (Section 3.2.3). On the other hand, in case of acyclic dimethyl acetals (**3-108**), this difference in BDEs is large and could potentially assist in selective hydrogen abstraction leading to a single product. Through the use of such acyclic dimethyl acetal, we proposed to generate an acyl radical equivalent in-situ, which can then be used in an allyl transfer reaction.



**Scheme 3-25:** Comparison of BDEs between cyclic ether and acyclic dimethyl ether.

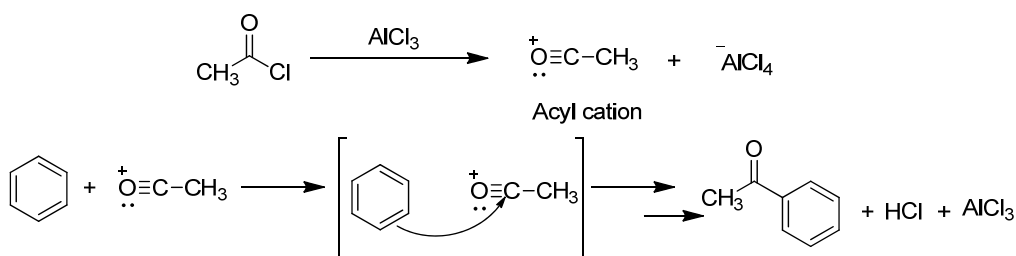
### 3.4.1 Chemistry of acyl intermediates

Acyl cations **3-109** or acyl radicals **3-110** are important reactive intermediates because of their strong electrophilic nature (Scheme 3-26) and their use in synthetic organic chemistry, biochemistry, and catalysis.<sup>32</sup>



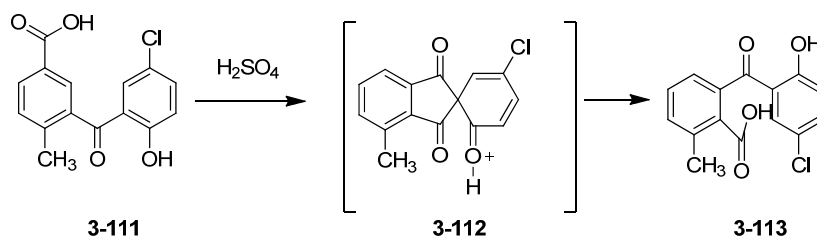
**Scheme 3-26:** Reactive intermediates: Acyl cation and acyl radical

Generally, acyl cation **3-109** is generated in-situ via the reaction of an acyl chloride with Lewis acid ( $\text{AlCl}_3$ ).<sup>33</sup> This intermediate has linear geometry at the electrophilic carbon because of the triple bond between carbon and oxygen. The acyl cation is more stable than other carbocation intermediates because the octet rule is satisfied for all of the atoms involved. Such intermediates are known to be involved in Friedel-Craft acylation reactions<sup>33</sup> (Scheme 3-27).



**Scheme 3-27:** General mechanism for Friedel-Craft acylation

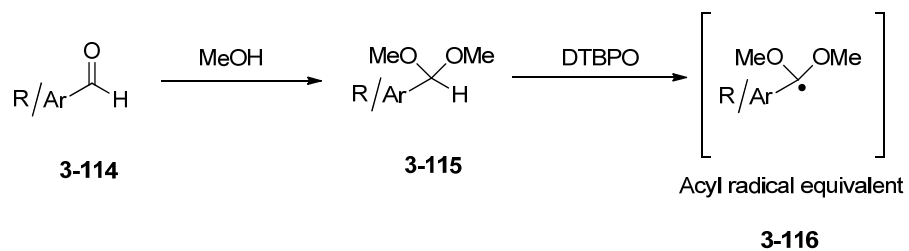
Newman et al. reported a very interesting work on the reaction of o-benzoyl benzoic acid **3-111** in sulfuric acid.<sup>34</sup> In this reaction, intramolecular acylation occurs through the cyclic carbonium ion intermediate which on heating yields the acyl carbonium ion. Using this precedence, later on, Hayashi et al. proposed another mechanism that involved the intramolecular rearrangement of an acyl carbonium ion **3-112**.<sup>35</sup> This rearrangement was reported to take place in such a way that there is an increase in conjugation. Finally, a rearranged substituted product, o-benzoyl benzoic acid **3-113**, was achieved via the attack of electrophilic acylium ion with a spiro intermediate (Scheme 3-28).



**Scheme 3-28:** Hayashi rearrangement for the synthesis of substituted o-benzoyl benzoic acid.<sup>35</sup>

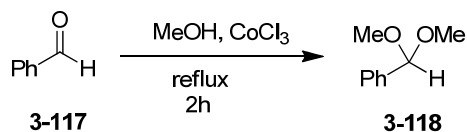
Although formation of acyl anion and acyl radical is very rare in organic synthesis, there are a few reported methods, which have been reported to generate acyl radical intermediates. For example, acyl selenides have been reported to be excellent precursors for the in-situ generation of acyl radicals under strong basic conditions.<sup>36</sup> In this process hydrogen abstraction from the tin hydride was reported to be an essential reductive step in propagation sequence. To avoid tin and this reductive step, phosphite deoxygenation of acyloxy radical were replaced by selenides and acyl radical was generated using the acyl thiohydroxamate method.<sup>36-37</sup> In 1992, Crich *et al.* reported the reactions of acyl and aryl tellurides as an efficient method for the generation of acyl radicals.<sup>38</sup> In all the reported methods harsh reaction conditions were used to generate the acyl radical.

We proposed the in-situ generation of acyl radical equivalent shown in Scheme 3-29. In this method we chose aromatic aldehydes which can easily undergo acetal formation reaction with methanol to yield the corresponding dimethyl acetal.



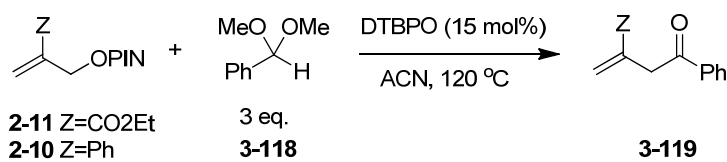
**Scheme 3-29:** Proposed pathway for functionalization of acyclic dimethyl acetal.

The dimethyl acetal of benzaldehyde was synthesized using a literature procedure (Scheme 3-30).<sup>39</sup> A convenient and efficient method was used for acetalization of benzaldehyde with methanol using the inexpensive and water tolerant  $\text{CoCl}_2$  as a catalyst. This method did not involve strong acidic or basic conditions and the metal catalyst was recycled without the loss of activity.



**Scheme 3-30:** Synthesis of dimethyl acetal of benzaldehyde.<sup>39</sup>

Reactions of dimethyl acetal of benzaldehyde with **2-10** and **2-11** were optimized in such a way that minimum concentration of the ether reagents and initiator could be used.



**Scheme 3-31:** Functionalization of dimethyl acetal of benzaldehyde

Entry	Z	Product	Time (h)	Yield % (Isolated)
1	CO <sub>2</sub> Et		24	84
2	Ph		24	89

**Table 3-8** Results for the functionalization of dimethyl acetal of benzaldehyde in acetonitrile.

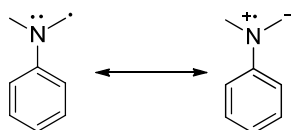
(Sealed tube, 120 °C) (**2-10** and **2-11** 0.35 M, **3-118** 1.07 M, DTBPO 0.05 M)

In both cases of reactions of **3-118** with **2-10** and **2-11**, high yields were observed for the in-situ hydrolyzed ketone product **3-119** (Table 3-8). This type of functionalization is not known under mild and metal-free reaction conditions. These products are stable and do not isomerize to

the conjugated ketone. Especially in Entry 2, where the alkene double bond is not in conjugation with the ketone carbonyl and neither does it to isomerizes to the  $\alpha,\beta$ -unsaturated ketone isomer.

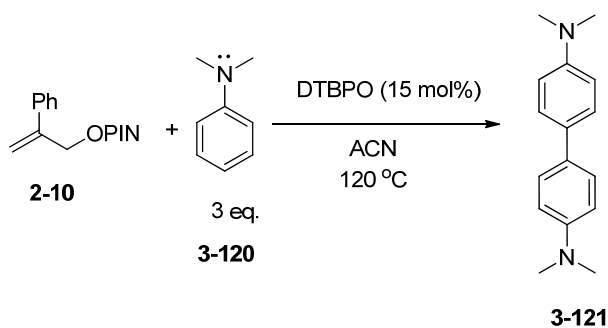
### 3.5 Amine C-H bond functionalization via allyl transfer

Similar to alkyl aromatic hydrocarbons and ethers, we envisioned that the allyl transfer reaction would work for the selective functionalization of  $\alpha$ -C-H bond containing tertiary amines. Since BDEs of  $\alpha$ -C-H bonds of amines like triethylamine (93.9 kcal/mol) or *N,N*-dimethylaniline (93.1 kcal/mol) are similar to the BDEs of hydrocarbons and ethers, we speculated them to undergo the same chain reaction via allyl transfer. Especially, the hydrogen abstraction from the methyl C-H bond of alkyl aromatic amines (for example, *N,N*-dimethylaniline) could potentially lead to the corresponding carbon radical, which is in resonance with the lone pair of the electrons on the nitrogen (Scheme 3-32). This stable radical might lead to the efficient allyl transfer with the appropriate substrate. Functionalization of *N,N*-dimethylaniline via allyl transfer was attempted as a pilot reaction.



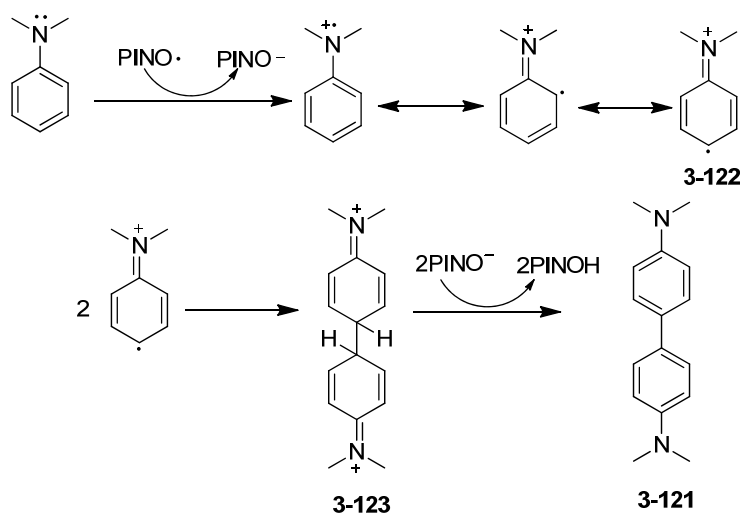
**Scheme 3-32:** Resonance stabilization of methyl radical in *N,N*-dimethylaniline.

In this experiment, an interesting result was observed along with <10% of desired product formation was recorded. Major product of the reaction was separated and identified as a dimer of *N,N*-dimethyl aniline (Scheme 3-33).



**Scheme 3-33:** Attempted allyl transfer reaction of *N,N*-dimethylaniline with **2-10**

The possible mechanistic pathway for this product formation was proposed (Scheme 3-33). We postulated that PINO• could participate in single electron oxidation of aniline leading to aniline radical cation **3-122**. **3-122** can potentially undergo a dimerization to form the intermediate **3-123** which on deprotonation by PINO• undergoes re-aromatization leading to the dimer product **3-121**.



**Scheme 3-34:** Predicted pathway for dimerization of *N,N*-dimethylaniline.

In 2005, Baciocchi, *et al.* reported the similar single electron transfer from *N,N*-dimethylaniline to PINO•<sup>40</sup> leading to demethylation of *N,N*-dimethylaniline. This confirms that

such single electron transfer pathway is possible with the alkyl aromatic amines and partially supports the proposed pathway for dimerization of *N,N*-dimethylaniline.

### 3.6 Conclusions

In conclusion, we have successfully demonstrated an efficient method for functionalization of various ethers and dimethyl acetal of benzaldehyde via an allyl transfer reaction using phthlimido-*N*-oxyl radical as a chain carrier. The utility of this method is established by the observed high yields and high mass balances under metal-free, mild and neutral reaction conditions. A wide substrate scope, as established by several acyclic and cyclic ethers and acetals is demonstrated for this transformation. The reported allyl transfer reaction was successfully carried out in-solution using acetonitrile as solvent, which allowed successful implementation at low concentration of reagents, thus making this a cost-effective and environmentally friendly method of ether functionalization.

The PINO• shows good selectivity in hydrogen abstraction especially in case of 2-MeTHF, leading to 80% tertiary C-H functionalization (major product), and 20% secondary C-H functionalization (minor products). However, in case of 1,3-dioxane moderate selectivities were observed due to the competition between two active secondary C-Hs present. These two experiments provided a valuable insight in selectivity/ reactivity of PINO• in hydrogen abstraction, thus helping us in designing a similar protocol with acetals, which in turn can be used as a method to functionalize aldehydes. A dimethyl acetal of benzaldehyde was tried as a template for this reaction, which showed high yield of the desired functionalized product. Selective functionalization of the tertiary C-H bond was observed, supporting our hypotheses of reactivity in these reactions. Application of this protocol in the functionalization of substituted

aryl and alkyl aldehydes is currently under development as a part of our efforts to establish the substrate scope of this reaction. Since, the allyl transfer reaction of *N,N*-dimethylaniline yielded the unexpected dimerized product **3-121**, we envisioned that the non-aromatic amines would be a better choice for functionalization of amines via allyl transfer reaction.

### 3.7 References:

1. Frontmatter. In *Handbook of C–H Transformations*, Dyker, G., Ed. Wiley-VCH Verlag GmbH: 2008; pp I-XXVI.
2. (a) Gong, J.; Fuchs, P. L., Alkynylation of C–H Bonds via Reaction with Acetylenic Triflones. *J. Am. Chem. Soc.* **1996**, *118* (18), 4486-4487; (b) Xiang, J.; Fuchs, P. L., Alkenylation of C–H Bonds via Reaction with Vinyl and Dienyl Triflones. Stereospecific Synthesis of Trisubstituted Vinyl Triflones via Organocopper Addition to Acetylenic Triflones. *J. Am. Chem. Soc.* **1996**, *118* (47), 11986-11987; (c) Xiang, J.; Jiang, W.; Gong, J.; Fuchs, P. L., Stereospecific Alkenylation of C–H Bonds via Reaction with  $\beta$ -Heteroatom-Functionalized Trisubstituted Vinyl Triflones. *J. Am. Chem. Soc.* **1997**, *119* (18), 4123-4129.
3. (a) Muramatsu, H.; Moriguchi, S.; Inukai, K., The Addition Reactions of Aldehydes, Alcohols, and Ethers to Perfluorocyclobutene. *J. Org. Chem.* **1966**, *31* (4), 1306-1309; (b) H. Muramatsu; K. Inukai; Ueda, T., *Bull. Chem. Soc. Jpn* **1967**, *40*, 903; (c) R. D. Chambers; R. W. Fuss; Jones, M., *J. Fluorine Chem* **1990**, *49*, 409; (d) J. Chen; R. L. Krichmeier; Shreeve, J. M., *Inorg. Chem* **1996**, *35*, 6676.
4. K. Hirano; S. Sakaguchi; Ishii, Y., *Tetrahedron Lett.* **2002**, *43*, 3617.
5. Z.-Q. Liu; L. Sun; J.-G. Wang; J. Han; Y.-K. Zhao; Zhou, B., *Org. Lett.* **2009**, *11*, 1437.
6. (a) Y. Yamamoto; K.-i. Yamada; Tomioka, K., *Tetrahedron Lett.* **2004**, *45*, 795; (b) K.-i. Yamada; Y. Yamamoto; Tomioka, K., *Org. Lett.* **2003**, (5), 1797.
7. (a) K.-i. Yamada; Y. Yamamoto; M. Maekawa; K. Tomioka, *J. Org. Chem.* **2004**, (69), 1531; (b) Y. Yamamoto; M. Maekawa; T. Akindele; K.-i. Yamada; Tomioka, K., *Tetrahedron Lett.* **2005**, *61*, 379.
8. A. Clerici; R. Cannella; N. Pastori; W. Panzeri; Porta, O., *Tetrahedron Lett.* **2006**, *62*, 5986.
9. (a) S. Torrente; Alonso, R., *Org. Lett.* **2001**, *3*, 1985; (b) M. Ferná'ndez; Alonso, R., *Org. Lett.* **2003**, *5* (2461).
10. A. V. R. Rao; M. K. Gurjar; T. R. Devi; Kumar, K. R., *Tetrahedron Lett.* **1993**, *34*, 1653.
11. Banfi, L.; Beretta, M. G.; Colombo, L.; Gennari, C.; Scolastico, C., 2-Benzoylamino-2-deoxy-2-hydroxymethyl-D-hexono-1,4-lactones: synthesis from D-fructose and utilization in the total synthesis of thermozytocidin (myriocin). *J. Chem. Soc., Perkin Trans. 2* **1983**, *0* (0), 1613-1619.
12. (a) H. M. L. Davies; Manning, J. R., *Nature* **2008**, 451-417; (b) C. G. Espino; DuBois, J., *Modern Rhodium-Catalyzed Organic Reactions Wiley-VCH, Weinheim* **2005**.
13. P. Wang; Adams, J., *J. Am. Chem. Soc.* **1994**, *116*, 3296.
14. H. M. L. Davies; M. V. A. Grazini; Aouad, E., *Org. Lett.* **2001**, *3*, 1475.
15. Z. Shen; Dong, V. M., *Angew. Chem., Int. Ed.* **2009**, *48*, 784.
16. (a) H. M. L. Davies; J. Yang; Nikolai, J., *J. Organomet. Chem.* **2005**, *690*, 6111; (b) H. M. L. Davies; S. J. Hedley; Bohall, B. R., *J. Org. Chem.* **2005**, *70*, 10737; (c) H. M. L. Davies; R. E. J. Beckwith; E. G. Antoulinakis; Jin, Q., *J. Org. Chem.* **2003**, *68*, 6126; (d) H. M. L. Davies; T. Hansen; Churchill, M. R., *J. Am. Chem. Soc.* **2000**, *122*, 3063; (e) H. M. L. Davies; Hansen, T., *J. Am. Chem. Soc.* **1997**, *119*, 9075.
17. (a) M. M. Di'az-Requejo; T. R. Belderrai'n; M. C. Nicasio; S. Trofimenko; Pe'rez, P. J., *J. Am. Chem. Soc.* **2002**, *124*, 896; (b) J. M. Fraile; J. I. Garc'ia; J. A. Mayoral; Rolda'n, M., *Org. Lett.* **2007**, *9*, 731.

18. Z. Li; D. S. Bohle; C.-J. Li; Natl., P., *Natl. Acad. Sci. U. S. A* **2006**, *103*, 8928.
19. Y. Zhang; Li, C.-J., *Angew. Chem., Int. Ed.* **2006**, *45*, 1949.
20. Y. Zhang; C.-J. Li, *J. Am. Chem. Soc.* **2006**, *128*, 4242.
21. W.-J. Yoo; C. A. Correia; Y. Zhang; Li, C.-J., *Synlett* **2009**, 138.
22. M. Tobisu; Chatani, N., *Angew. Chem., Int. Ed.* **2006**, *45*, 1683.
23. S. J. Pastine; K. M. McQuaid; Sames, D., *J. Am. Chem. Soc.* **2005**, *127*, 12180.
24. N. Haddad; Z. Abramovich; Ruhman, I., Recent Research Developments in Organic Chemistry. **1997**, *1*, 35.
25. K. M. McQuaid; Sames, D., *J. Am. Chem. Soc.* **2009**, *131*, 402.
26. (a) Beckwith, A. L. J., Radicals in organic synthesis: Formation of carbon—carbon bonds. Von B. Giese, Pergamon Press, Oxford 1986. XIII, 294 S., Paperback \$ 25.00. — ISBN 0-08-032494-0. *Angew. Chem* **1987**, *99* (8), 824-825; (b) Curran, D. P., The Design and Application of Free Radical Chain Reactions in Organic Synthesis. *Synthesis* **1988**, *Part 1*, 417-439; (c) Motherwell, W. B.; Crich, D., *Free radical chain reactions in organic synthesis*. Acad. Press: London [u.a.], 1992; (d) Renaud, P.; Sibi, M. P., *Radicals in organic synthesis*. Wiley-VCH: Weinheim; New York, 2001; (e) Ryu, I.; Sonoda, N.; Curran, D. P., Tandem Radical Reactions of Carbon Monoxide, Isonitriles, and Other Reagent Equivalents of the Geminal Radical Acceptor/Radical Precursor Synthons. *Chem. Rev.* **1996**, *96* (1), 177-194.
27. Hirano, K.; Sakaguchi, S.; Ishii, Y., Radical addition of ethers to alkenes under dioxygen catalyzed by N-hydroxyphthalimide (NHPI)/Co(OAc)<sub>2</sub>. *Tetrahedron Lett.* **2002**, *43* (20), 3617-3620.
28. Yilmaz, G.; Beyazit, S.; Yagci, Y., Visible light induced free radical promoted cationic polymerization using thioxanthone derivatives. *J. Polym. Sci., Part A: Polym. Chem.* **2011**, *49* (7), 1591-1596.
29. Koshino, N.; Saha, B.; Espenson, J. H., *J. Org. Chem* **2003**, *68*, 9364.
30. (a) Jaenicke, L., Ionophore Polyether Antibiotics – Naturally Occurring Acid Ionophores. Bd. 1: Biology. Von J. W. Westley. Marcel Dekker, Inc., New York – Basel 1982. XVII, 465 S., SFr. 185,-. *Nachrichten aus Chemie, Technik und Laboratorium* **1983**, *31* (9), 724-724; (b) Alali, F. Q.; Liu, X.-X.; McLaughlin, J. L., Annonaceous Acetogenins: Recent Progress. *J. Nat. Prod.* **1999**, *62* (3), 504-540; (c) Harmange, J.-C.; Figadère, B., Synthetic routes to 2,5-disubstituted tetrahydrofurans. *Tetrahedron: Asymmetry* **1993**, *4* (8), 1711-1754.
31. (a) Wolfe, J. P.; Rossi, M. A., Stereoselective Synthesis of Tetrahydrofurans via the Palladium-Catalyzed Reaction of Aryl Bromides with  $\gamma$ -Hydroxy Alkenes: Evidence for an Unusual Intramolecular Olefin Insertion into a Pd(Ar)(OR) Intermediate. *J. Am. Chem. Soc.* **2004**, *126* (6), 1620-1621; (b) Qian, H.; Han, X.; Widenhofer, R. A., Platinum-Catalyzed Intramolecular Hydroalkoxylation of  $\gamma$ - and  $\delta$ -Hydroxy Olefins to Form Cyclic Ethers. *J. Am. Chem. Soc.* **2004**, *126* (31), 9536-9537; (c) Sromek, A. W.; Kel'in, A. V.; Gevorgyan, V., A Novel 1,2-Migration of Acyloxy, Phosphatyloxy, and Sulfonyloxy Groups in Allenes: Efficient Synthesis of Tri- and Tetrasubstituted Furans. *Angew. Chem., Int. Ed.* **2004**, *43* (17), 2280-2282; (d) Antoniotti, S.; Genin, E.; Michelet, V.; Genêt, J.-P., Highly Efficient Access to Strained Bicyclic Ketals via Gold-Catalyzed Cycloisomerization of Bis-homopropargylic Diols. *J. Am. Chem. Soc.* **2005**, *127* (28), 9976-9977.
32. Magnuson, R. H.; Zulu, S.; T'Sai, W.-M.; Giering, W. P., Detection and characterization of radical cations resulting from the oxidation of methyl and acetyl iron complexes. *J. Am. Chem. Soc.* **1980**, *102* (22), 6887-6888.

33. Olah, G. A.; Kobayashi, S., Aromatic substitution. XXIX. Friedel-Crafts acylation of benzene and toluene with substituted acyl halides. Effect of substituents and positional selectivity. *J. Am. Chem. Soc.* **1971**, *93* (25), 6964-6967.
34. Newman, M. S., A Mechanism for the Formation of Anthraquinone from o-Benzoylbenzoic Acid. *J. Am. Chem. Soc.* **1942**, *64* (10), 2324-2325.
35. Sandin, R. B.; Melby, R.; Crawford, R.; McGreer, D., The Hayashi Rearrangement of Substituted o-Benzoylbenzoic Acids. *J. Am. Chem. Soc.* **1956**, *78* (15), 3817-3819.
36. Perchyonok, V. T.; Lykakis, I.; Postigo, A.; Royal Society of, C., *Streamlining free radical green chemistry*. RSC Publishing: Cambridge, 2012.
37. Benati, L.; Calestani, G.; Leardini, R.; Minozzi, M.; Nanni, D.; Spagnolo, P.; Strazzari, S., Generation and Intramolecular Reactivity of Acyl Radicals from Alkynylthiol Esters under Reducing Tin-Free Conditions. *Org. Lett.* **2003**, *5* (8), 1313-1316.
38. Chen, C.; Crich, D.; Papadatos, A., The chemistry of acyl tellurides: generation and trapping of acyl radicals, including aryltellurium group transfer. *J. Am. Chem. Soc.* **1992**, *114* (21), 8313-8314.
39. Velusamy, S.; Punniyamurthy, T., Cobalt(II)-catalyzed chemoselective synthesis of acetals from aldehydes. *Tetrahedron Lett.* **2004**, *45* (25), 4917-4920.
40. Baciocchi, E.; Bietti, M.; Gerini, M. F.; Lanzalunga, O., Electron-Transfer Mechanism in the N-Demethylation of N,N-Dimethylanilines by the Phthalimide-N-oxyl Radical. *J. Org. Chem.* **2005**, *70* (13), 5144-5149.

## Chapter 4: Experimental

### (For Chapter 2)

#### 4.1 General information

NMR spectra were recorded in  $\text{CDCl}_3$  (unless stated otherwise) on Bruker Advance II 500 or Varian Inova 400 NMR Spectrometers. The corresponding  $^{13}\text{C}$  NMR resonance frequencies for these spectrometers were 126 MHz and 101 MHz respectively. Coupling constants were reported in Hertz and chemical shifts were reported in ppm using the known chemical shift of the solvent used as an internal reference. Deuterated solvents were purchased from Cambridge Isotope Laboratories Inc. and used as is. The abbreviations used to indicate coupling are as follows: s (singlet), d (doublet), t (triplet), q (quartet), dd (doublet of doublet), m (multiplet) etc. GC was performed and recorded on a Hewlett Packard HP 5890A instrument equipped with FID detector, and an HP 3393A reporting integrator, DB-5 column (30x0.32 m). HRMS (TOF) was performed using a JEOL HX110 dual focusing mass spectrometer and (ESI) Agilent 6220 Accurate Mass TOF MS LC/MS. Thin layer chromatography was performed on 250  $\mu\text{m}$  silica gel 60-F silica plates (observed at  $\text{UV}_{254}$ ) purchased from EMD chemicals Inc. Flash chromatography was performed on silica gel (grade 60, 230- 400 mesh, 40-63  $\mu\text{m}$  silica gel) from VWR.

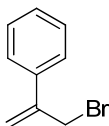
#### 4.2 Materials and Purification (Hydrocarbon functionalization)

Toluene (Sigma-Aldrich) and ethyl benzene (Sigma-Aldrich) were washed with  $\text{H}_2\text{SO}_4$  followed by purification using simple distillation. Purification of cumene was similar except it was done under an inert atmosphere (Argon) followed by vacuum distillation. After purification, all of the above reagents were stored over molecular sieves

under Argon. The following reagents were used without purification as is: hexanes, methylene chloride, acetonitrile (HPLC grade), water (distilled), ethyl acetate, carbon tetrachloride,  $\alpha$ -methylstyrene, NBS, formaldehyde (37% aqueous solution), ammonium chloride, potassium carbonate, triethyl phosphonoacetate, diethyl cyanomethylphosphonate, ethyl ether, phosphorus tribromide, sodium chloride, magnesium sulfate and sodium sulfate.

### 4.3 Experimental procedure for the synthesis of allyl bromides (2-14 and 2-17)

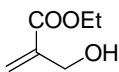
#### Synthesis of (3-bromoprop-1-en-2-yl)benzene (2-14)



**2-12**

**(3-bromoprop-1-en-2-yl)benzene:** Based on a literature procedure.<sup>1</sup> To a mixture of  $\alpha$ -methylstyrene (125 mL, 0.96 mol), *N*-bromosuccinimide (50 g, 0.28 mol), carbon tetrachloride (20 mL) was added. This solution was heated just to boil and the flask was quickly immersed in an ice bath. Pentane was added to the cold reaction mixture to remove the side product succinimide. Precipitate of succinimide was then separated by filtration. Additional 50 mL of pentane was added to ensure the removal of the side product. The filtrate was collected and remaining solvent was evaporated on rotary evaporator. The crude product (40 g) was purified by flash chromatography using 10% ethyl acetate in hexane. This purification yielded the pure product (2-12) as colorless liquid (25 g) in 68% yield. Purity was confirmed using <sup>1</sup>H NMR analysis. **<sup>1</sup>H NMR:** (400 MHz, CDCl<sub>3</sub>), 7.47 (5 H, m), 5.55 (1 H, s), 5.49 (1 H, s), 4.38 (2 H, s)

### Synthesis of ethyl 2-(hydroxymethyl)acrylate (2-16)

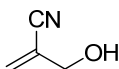


2-16

**Ethyl 2-(hydroxymethyl)acrylate:** Based on a literature procedure.<sup>2</sup> Mixture of triethyl phosphonoacetate (22.4 g, 0.1 mol) and 37% aqueous solution of formaldehyde (32.4 g, 0.4 mol) was stirred at room temperature. Saturated solution of potassium carbonate (24.15 g, 0.175 mol) was added to the above mixture over 30 min. At the end of addition reaction mixture reached 30 °C- 35 °C. Stirring was continued for 2 h. Reaction was quenched with saturated solution of ammonium chloride (35 mL). Reaction mixture was extracted with ethyl ether (3X12.5 mL). Organic layers were combined and dried over sodium sulfate. Solvent was evaporated using rotary evaporator and remaining colorless oil was purified using flash chromatography using 20% ethyl acetate in hexane. This purification yielded the pure product as colorless oil (8 g) in 70% yield.

<sup>1</sup>H NMR (400 MHz, CDCl<sub>3</sub>) 6.25 (1 H, s), 5.82 (1 H, s), 4.74 (1 H, s), 4.32 (2 H, s), 4.30 – 4.18 (2 H, m), 1.31 (3 H, t). <sup>13</sup>C NMR (101 MHz, CDCl<sub>3</sub>) 166.29, 139.34, 125.87, 62.65, 60.77, 13.92.

### Synthesis of 2-(hydroxymethyl)acrylonitrile (2-19)



2-19

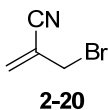
**2-(hydroxymethyl)acrylonitrile (2-19):** Based on a literature procedure.<sup>2</sup> Mixture of diethyl cyanomethylphosphonoacetate (22.4 g, 0.1 mol) and 37% aqueous solution of

formaldehyde (32.4 g, 0.4 mol) were stirred at room temperature. Saturated solution of potassium carbonate (24.15 g, 0.175 mol) was added to the above mixture over 30 min. At the end of addition reaction mixture reached 30 °C- 35 °C. Stirring was continued for 2 h. Reaction was quenched with saturated solution of ammonium chloride (35 mL). Reaction mixture was extracted with ethyl ether (3X12.5 mL). Organic layers were combined and dried over sodium sulfate. Solvent was evaporated using rotary evaporator and remaining colorless oil was purified using flash chromatography using 20% ethyl acetate in hexane. This purification yielded the pure product as colorless oil (8 g) in 70% yield.

<sup>1</sup>H NMR (400 MHz, CDCl<sub>3</sub>) 6.21 (1 H, s), 5.98 (1 H, s), 4.20 (2 H, s), 3.65 (1 H, s).

<sup>13</sup>C NMR (101 MHz, CDCl<sub>3</sub>) 131.3, 120.4, 117.3, 66.1.

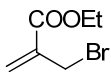
#### Synthesis of 2-(bromomethyl)acrylonitrile (2-20)



**2-(bromomethyl)acrylonitrile (2-20):** To the mixture of ethyl 2-(hydroxymethyl)acrylonitrile (4 g, 0.030 mol) and dry ethyl ether (20 mL), phosphorus tribromide (1.4 mL, 0.015 mol) was added drop wise at -10 °C while stirring. After addition was completed the solution was stirred at room temperature for 3 h. Water (20 mL) was added at -10 °C and the mixture was extracted with hexane (3X 10 ml) and washed with a saturated solution of sodium chloride (2X 10 mL). After drying the organic layer over magnesium sulfate, the solvent was evaporated under reduced pressure and the crude product (4.7 g) was purified using flash column chromatography; Product

yield: 4.1 g (70 %)  $^1\text{H NMR}$ : (400 MHz,  $\text{CDCl}_3$ ), 6.26 (1 H, s), 5.87 (1 H, s), 3.97 (2 H, s).

### Synthesis of ethyl 2-(bromomethyl) acrylate (2-17)

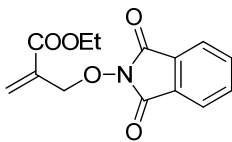


**2-13**

**Ethyl 2-(bromomethyl)acrylate:** To the mixture of ethyl 2-(hydroxymethyl) acrylate (4 g, 0.030 mol) and dry ethyl ether (20 mL), phosphorus tribromide (1.4 mL, 0.015 mol) was added drop wise at  $-10\text{ }^\circ\text{C}$  while stirring. After addition was completed the solution was stirred at room temperature for 3 h. Water (20 mL) was added at  $-10\text{ }^\circ\text{C}$  and the mixture was extracted with hexane (3X 10 ml) and washed with a saturated solution of sodium chloride (2X 10 mL). After drying the organic layer over magnesium sulfate, the solvent was evaporated under reduced pressure and the crude product (4.7 g) was purified using vacuum distillation; Product yield: 4.1 g (70 %); b.p.  $54\text{-}58\text{ }^\circ\text{C}/ 2\text{ torr}$ . Purity was confirmed using  $^1\text{H NMR}$  analysis.  $^1\text{H NMR}$ : (400 MHz,  $\text{CDCl}_3$ ), 6.22 (1 H, s), 5.87 (1 H, s), 4.22 (2 H, s), 4.24 (2 H, q), 1.31 (3 H, t)

#### 4.4 Experimental procedure for the synthesis of Allyl-PINO compounds

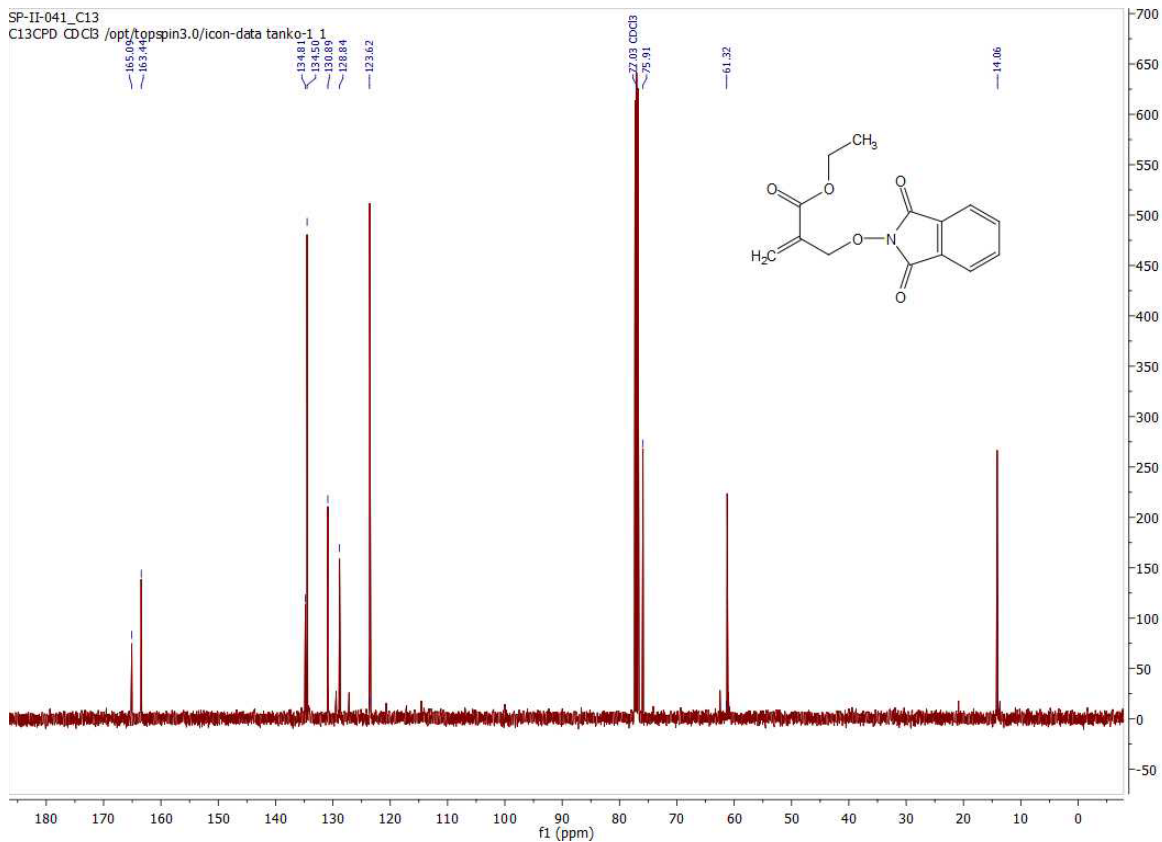
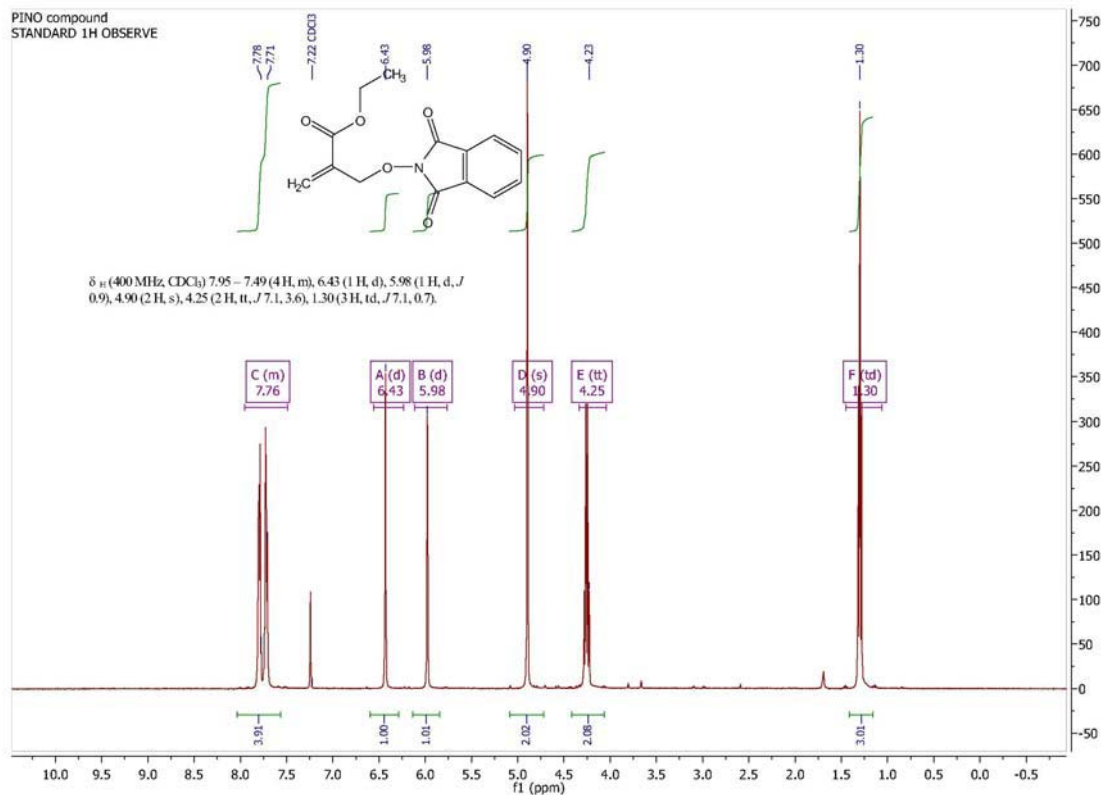
##### Synthesis of Ethyl 2-(((1,3-dioxoisindolin-2-yl)oxy)methyl)acrylate (2-11)



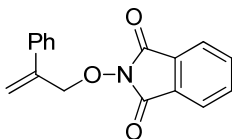
**2-11**

**Ethyl 2-(((1,3-dioxoisindolin-2-yl)oxy)methyl)acrylate:** Based on a literature procedure.<sup>3</sup> *N*-hydroxyphthalimide (3.2 g, 0.020 mol) was added to DMSO (110 mL). Sodium acetate (1.71 g, 0.020 mol) was added to the above mixture solution. (Solution turns dark red) then, ethyl 2-(bromomethyl) acrylate (4 g, 0.020 mol) in 35 mL DMSO was added drop wise to the mixture. The mixture was refluxed for an hour. The mixture was extracted with chloroform (50 mL 4X). The organic solution was washed 2X with saturated solution of NaCl and dried over sodium sulfate (Na<sub>2</sub>SO<sub>4</sub>). The solvents were evaporated under pressure. The solid residue was purified using flash column chromatography. The crude solid product was recrystallized in EtOAc/ hexane to yield **2-11** as white crystalline solid. (m.p: 76-78 °C).

**<sup>1</sup>H NMR**, (400 MHz, CDCl<sub>3</sub>) 7.95 – 7.49 (4 H, m), 6.43 (1 H, d), 5.98 (1 H, d, *J* 0.9), 4.90 (2 H, s), 4.25 (2 H, tt, *J* 7.1, 3.6), 1.30 (3 H, td, *J* 7.1, 0.7). **<sup>13</sup>C NMR**, (126 MHz, CDCl<sub>3</sub>) 165.09, 163.44, 134.50, 130.89, 128.84, 123.62, 75.91, 61.32, 14.06. **HRMS:** Calculated for C<sub>14</sub> H<sub>13</sub> NO<sub>5</sub>- 275.0788; observed 275.0782 (-2.23 ppm)



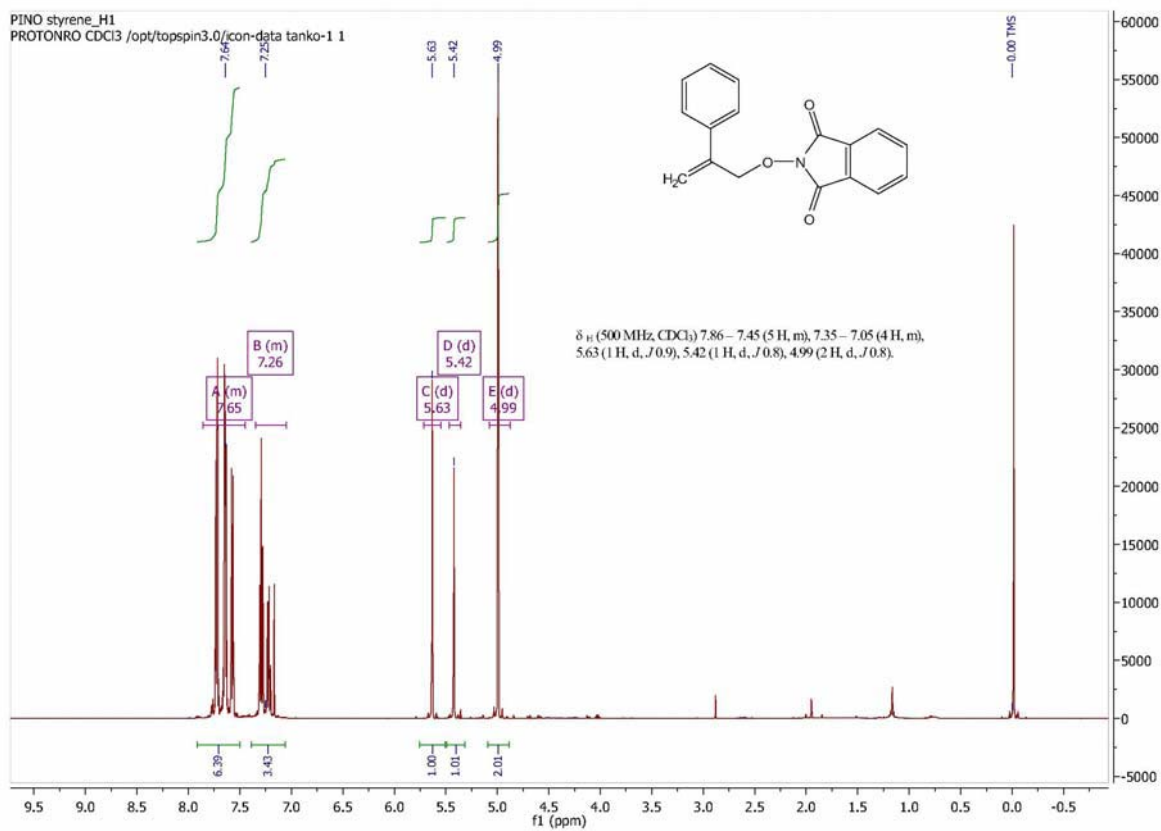
## Synthesis of 2-((2-phenylallyl)oxy)isoindoline-1,3-dione (**2-10**)

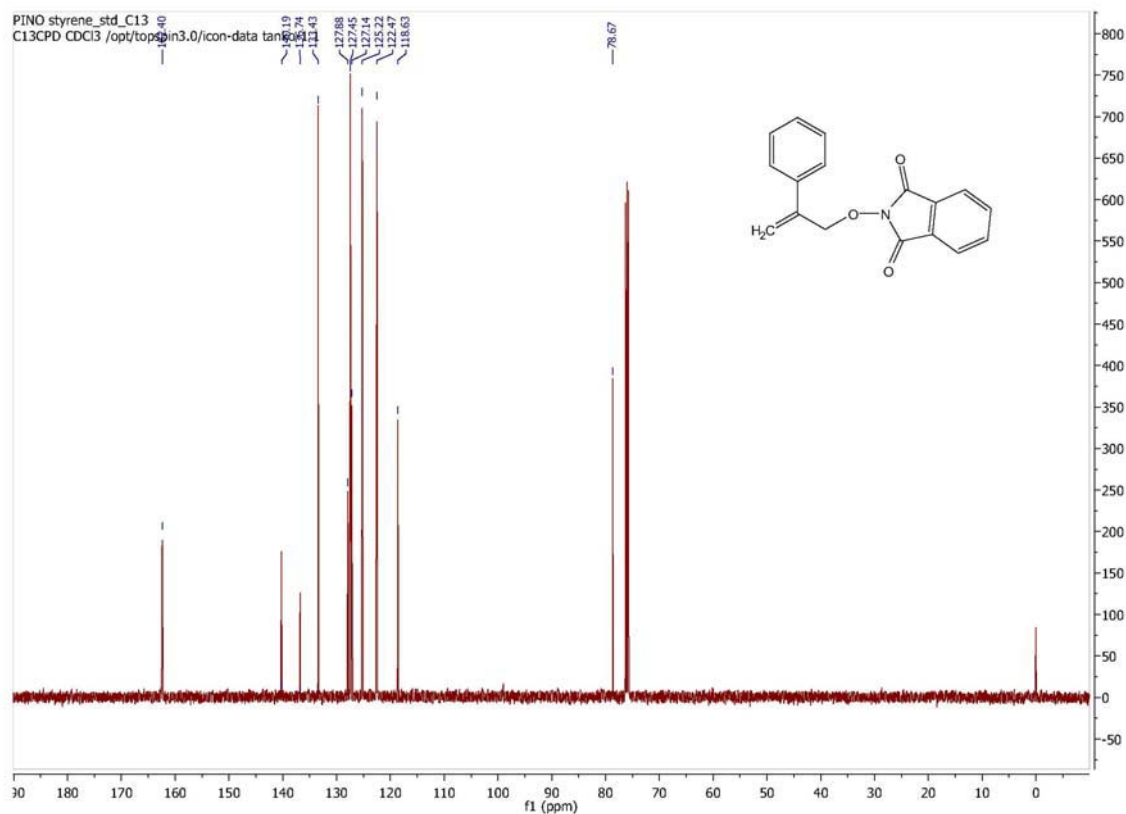


**2-10**

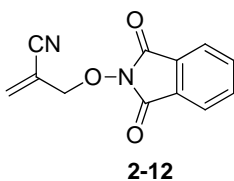
**2-((2-phenylallyl)oxy)isoindoline-1,3-dione:** Based on a literature procedure.<sup>3</sup> Repeated from the procedure for the synthesis of **2-11**. (m.p for **2-10**: 82-84 °C)

**<sup>1</sup>H NMR**, (500 MHz, CDCl<sub>3</sub>) 7.86 – 7.45 (5 H, m), 7.35 – 7.05 (4 H, m), 5.63 (1 H, d, *J* 0.9), 5.42 (1 H, d, *J* 0.8), 4.99 (2 H, d, *J* 0.8). **<sup>13</sup>C NMR**, (126 MHz, CDCl<sub>3</sub>) 162.40, 140.19, 136.74, 133.43, 127.88, 127.45, 127.14, 125.22, 122.47, 118.63, 78.67. **HRMS:** Calculated for C<sub>17</sub> H<sub>13</sub>NO<sub>3</sub>- 280.0968; observed 280.0988 (+ 7.09 ppm)



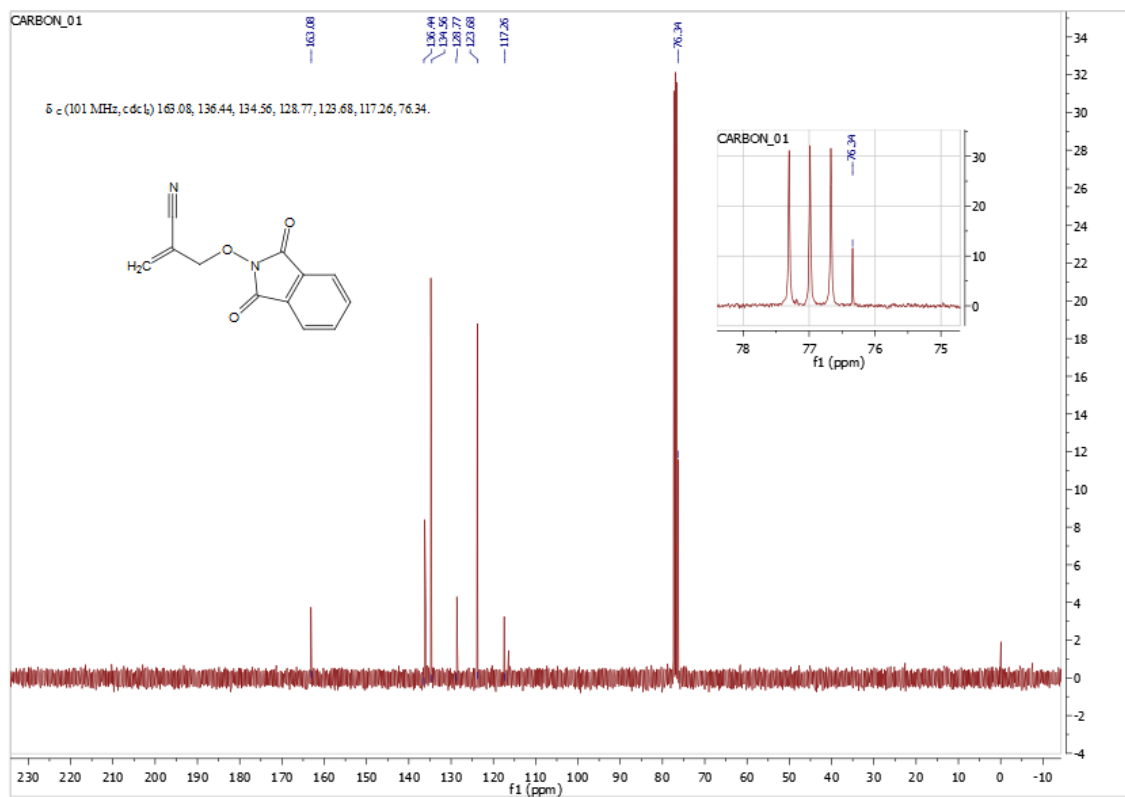
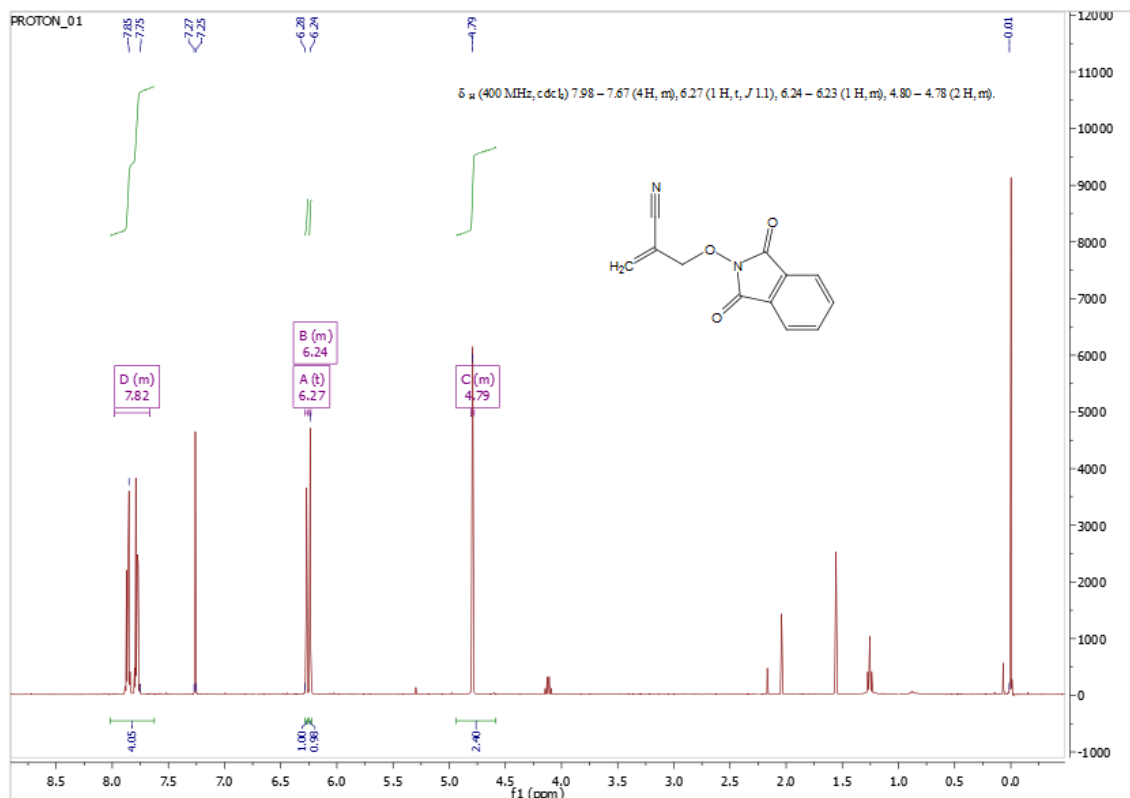


### Synthesis of 2-(((1,3-dioxisoindolin-2-yl)oxy)methyl)acrylonitrile (**2-12**)



Based on a literature procedure.<sup>3</sup> Repeated from the procedure for the synthesis of **2-11**.

**<sup>1</sup>H NMR** (400 MHz, CDCl<sub>3</sub>) 7.98 – 7.67 (4 H, m), 6.27 (1 H, t, *J* 1.1), 6.24 – 6.23 (1 H, m), 4.80 – 4.78 (2 H, m). **<sup>13</sup>C NMR** (101 MHz, CDCl<sub>3</sub>) 163.08, 136.44, 134.56, 128.77, 123.68, 117.26, 76.34. **HRMS:** Calculated for C<sub>12</sub> H<sub>8</sub> N<sub>2</sub> O<sub>3</sub> 229.0608, observed [M+H]<sup>+</sup> 229.0598 (-4.37 ppm); m.p 151-153 °C.



#### 4.4.1 General procedure for allyl transfer reactions of hydrocarbons

Allyl transfer reactions of hydrocarbon functionalization were run in 20 mL Pyrex pressure tubes in high vacuum line system. In a 20 mL Pyrex tube, the allyl-PINO or allyl bromide substrate (0.000716 mol) was mixed with the desired hydrocarbon substrate (0.00179 mol). Initiator, di-*t*-butyl peroxide (0.000143 mol) was added to the above mixture. This reaction mixture was degassed using high vacuum by freeze-pump-thaw (3X) and it was heated at the appropriate temperature while stirring. The temperature fluctuation was  $\pm 5$  °C and the time of the reaction run has the accuracy of  $\pm 1$  min. At the end of each reaction, the pressure tube was cooled down under tap water followed by solvent evaporation (if necessary) or liquid-liquid extraction to yield crude product. Reaction yields were determined by GC-MS using diphenylmethane as an internal standard and GC correction factor.

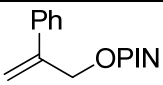
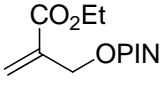
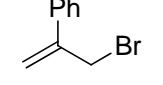
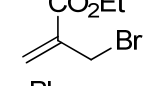
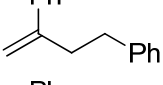
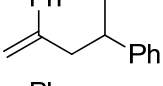
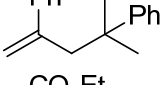
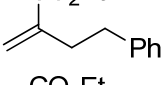
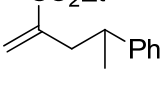
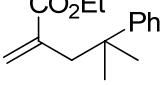
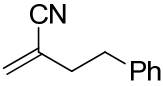
#### 4.4.2 General procedure for chain length calculations

In a 25 mL volumetric flask, allyl-PINO substrate **2-10** or **2-11** ( $1.818 \times 10^{-4}$  mol), di-*t*-butyl peroxide (20 mol %,  $3.636 \times 10^{-5}$  mol) were added. These compounds were diluted with the hydrocarbon (25 mL). 4 mL of solution was taken from the volumetric flask and transferred to a sealed tube. This sealed tube was heated at 120 °C for time (t). Product yield at time t was measured using GC. The experiment was repeated several times at varying (increasing but maintaining the reaction time below 1 h) time (t) and product yield was measured for each reaction at corresponding reaction times. 10  $\mu$ L of di-phenyl methane was added as an internal reference to each reaction tube and 1  $\mu$ L of the reaction mixture was used for injection/GC analysis. The amount of initiator (*t*-butoxyl radical)

was calculated based upon the first order rate constant (i.e.,  $k=1.72 \times 10^{-6} \text{ s}^{-1}$  at 120 °C) and the initial concentration of the initiator (DTBPO). To measure the initial chain length of the reaction, the product yield at time  $t$  (in mol) was divided by the total amount of radical produced from the initiator (mol) at time  $t$  (P/R) as a function of time. Then the  $\log(P/R)$  was plotted against time. And using the first three or five data points (less than an hour reaction time), the equation for linear regression approximation was derived. By extrapolating the regression line to  $t=0$ , the intercept was assumed to be the log of the initial chain length. Error in chain length was calculated using the formula= std. error in inverse log function  $(2.303) \times \text{initial chain length} \times \text{std. error in intercept}$ .

#### 4.4.3 Correction factors for allyl-bromides, allyl-PINO and hydrocarbon functionalized products

Correction factors and product yield measurements were performed using the following GC conditions.

Compound	Correction factor	Retention time
	1.3698	15.1
	1.0135	12.7
	0.5892	5.7
	0.2358	4.0
	0.7838	9.9
	0.8253	10.0
	1.1383	-
	0.8197	7.6
	0.7448	8.1
	0.9214	7.6
	0.7879	-
$\text{Ph}_2\text{CH}_2$		7.1

**Table 4-1:** Correction factors and GC retention times for allyl-bromide substrates, allyl-PINO substrates and products. (GC Conditions: Injector temp. 280 °C, detector temp. 325 °C, initial temp. 120 °C, initial time 2 min, rate 15 deg/min, final temp. 380 °C)

**4.5 Kinetic chain lengths measurements for allyl transfer reactions of hydrocarbons with allyl-PINO substrate (2-11) using di-*t*-butylperoxide.**

Time (min)	Log P/R
15	2.5
30	2.2
60	2.05
20	1.83
80	1.59

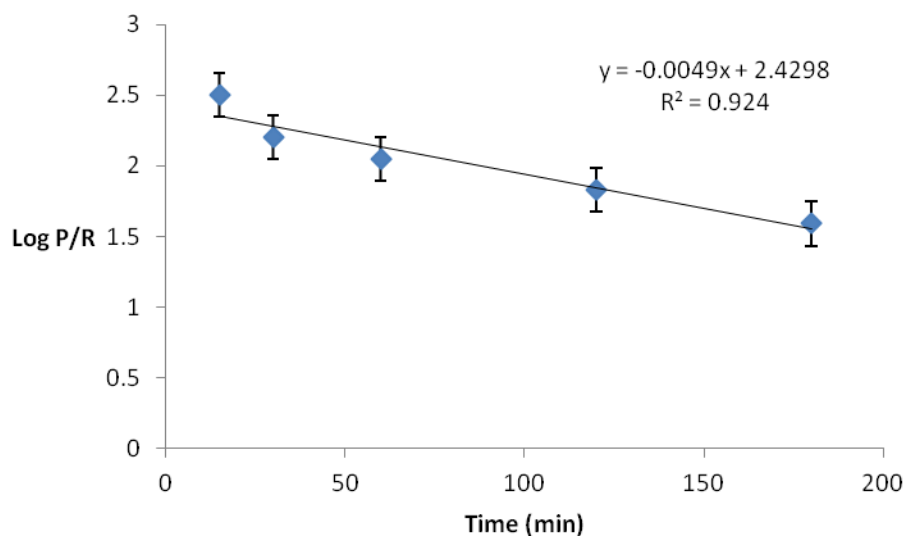


**Figure 4-1:** Reaction of toluene with **2-11**, initiator DTBPO (20mol%), 120 °C, Initial chain length= 270 ( $\pm 70$ ) (**2-11** 0.032 M, DTBPO 0.006 M, toluene 10 M)

Time (min)	Log P/R
15	2.11
30	2.09
60	2.08
20	2.0
80	1.98

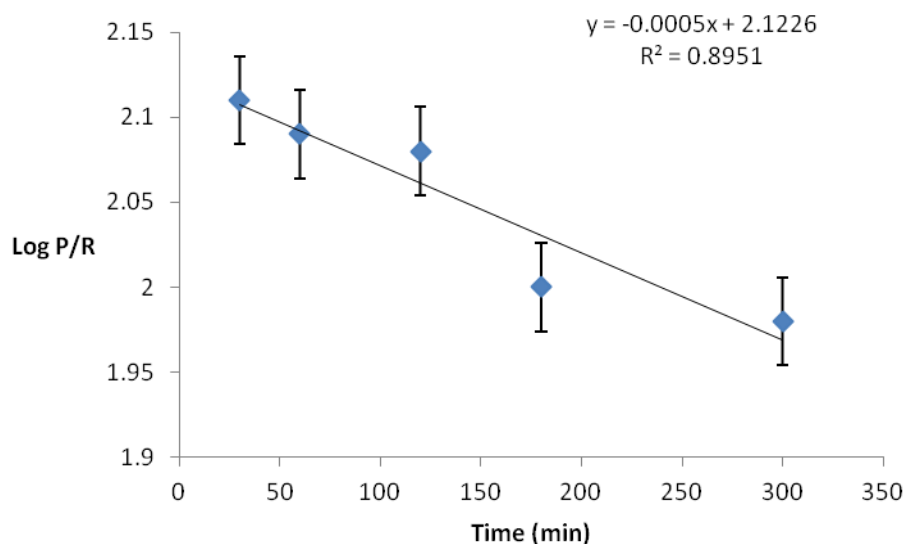


**Figure 4-2:** Reaction of ethyl benzene with **2-11**, initiator DTBPO (20 mol%) 120 °C

Initial chain length= 130( $\pm$ 30) (**2-11** 0.032 M, DTBPO 0.006 M, ethyl benzene 11 M)

Time (min)	Log P/R
15	1.12
30	1.11
60	1.10
20	0.9
80	0.9

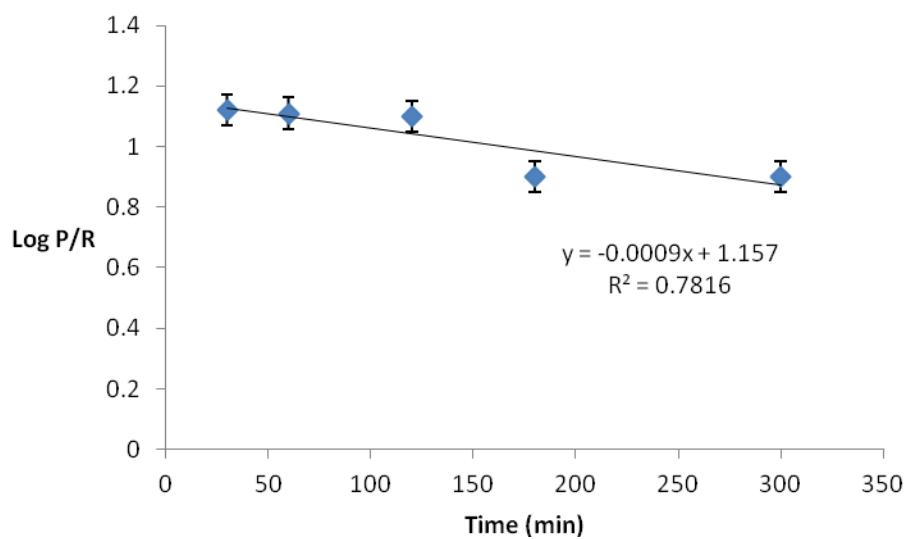


**Figure 4-3:** Reaction of cumene with **2-11**, initiator DTBPO 20 mol%, 120 °C.

Initial chain length= 12( $\pm$ 4) (**2-11** 0.032 M, DTBPO 0.006 M, cumene 11M)

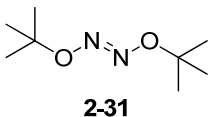
#### 4.6 Typical experimental procedure for low temperature allyl transfer reactions using triethylborane/O<sub>2</sub>

Reactions were run in 20 mL pyrex pressure tubes with air in it. At the end of each reaction, the pressure tube was cooled down under tap water followed by solvent evaporation (if necessary) or liquid-liquid extraction to yield crude product. Reaction yields were determined by GC-MS using diphenylmethane as an internal standard.

##### 4.6.1 Typical experimental procedure for allyl transfer reactions using triethylborane/O<sub>2</sub> and Lewis acid (AlCl<sub>3</sub>)

Reactions were run in 20 mL pyrex pressure tubes with air in it. At the end of each reaction, the pressure tube was cooled down under tap water followed by solvent evaporation (if necessary) or liquid-liquid extraction to yield crude product. Reaction yields were determined by GC-MS using diphenylmethane as an internal standard.

##### 4.6.2 Experimental procedure for the synthesis of di-*t*-butyl hyponitrite (2-31)



Sodium hyponitrite (0.4 g, 0.0038 mol) was slowly added to a solution of anhydrous ferric chloride (0.6 g, 0.0037 mol), 4 ml ether and 4 ml *t*-butyl bromide while stirring and maintaining the temperature below 45° C using water bath. The reaction mixture was stirred for 2 h at room temperature and then stirred overnight at 5 °C using ice bath. Reaction mixture was filtered to remove side product NaBr. Remaining filtrate was extracted using ethyl ether. The combined organic layers were dried over anhydrous sodium sulfate and concentrated using rotary evaporator to obtain 0.5 g (82%) of di-*t*-

butyl hyponitrite as white solid. Crude product was recrystallized using methanol. (m.p 80 °C-81 °C) Purity was confirmed using  $^1\text{H}$  NMR analysis.  $^1\text{H}$  NMR: (400 MHz,  $\text{CDCl}_3$ ), 1.38 (18 H, s).

#### 4.7 Kinetic chain lengths measurements for allyl transfer reactions of hydrocarbons and allyl-PINO substrates using di-*t*-butylhyponitrite

Time (min)	Log P/R
360	0.27
720	0.26
1440	0.25
2160	0.24

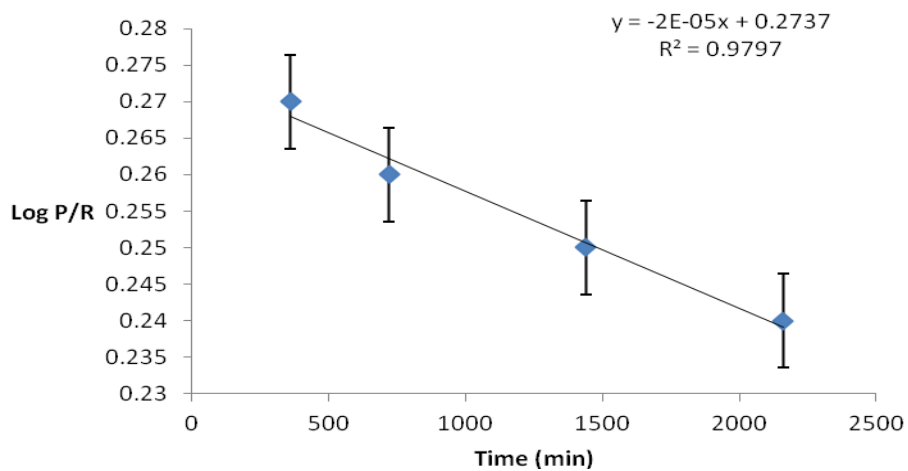


**Figure 4-4:** Reaction of ethyl benzene with **2-11** using 10 mol% DTBHN at 45 °C  
Initial chain length= 1.86( $\pm$ 1) (**2-11** 0.032 M, DTBPO 0.003 M, ethyl benzene 10 M)

Time (min)	Log P/R
360	0.12
720	0.11
1440	0.1
2160	0.08

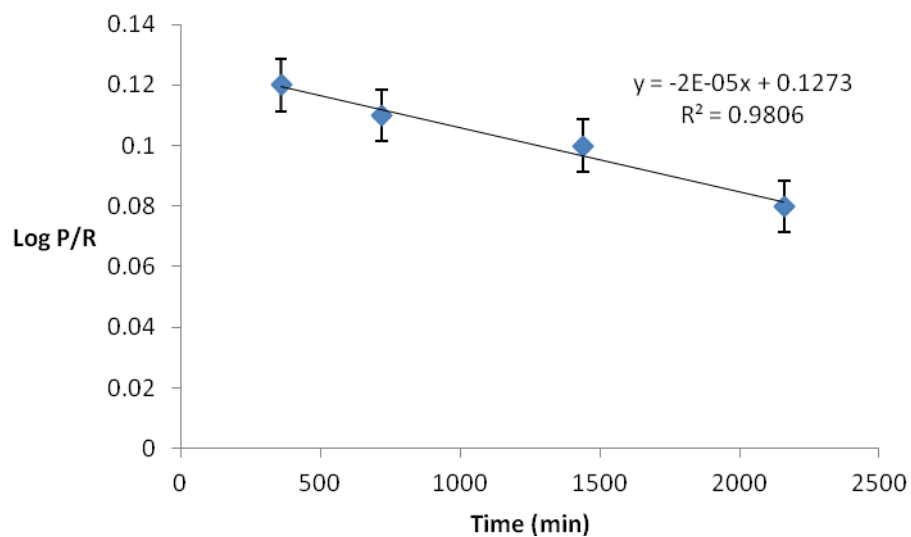
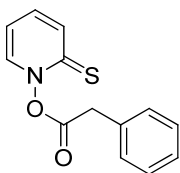


**Figure 4-5:** Reaction of toluene with **2-11** using 10 mol% DTBHN at 45 °C  
 Initial chain length= 1.34( $\pm$ 1) (**2-11** 0.032 M, DTBPO 0.003 M, toluene 10 M)

#### 4.8 Experimental procedure for the synthesis of 2-thioxopyridin-1(2H)-yl 2-phenylacetate (2-38)



2-38

**2-thioxopyridin-1(2H)-yl 2-phenylacetate:** Based on a literature procedure.<sup>4</sup> Phenyl acetic acid (0.21 g, 0.0015 mol) was added to the mixture of *N*-hydroxy pyridinethione (0.8 g, 0.0062 mol), dicyclohexylcarbodiimide (DCC) (0.27 mL, 0.0017 mol), 4-*N,N*-dimethyl aminopyridine (DMAP) (0.02 g, 0.00015 mol) and 3 mL methylene chloride at 0 °C. Reaction mixture was then stirred at room temperature for 3 h. Reaction mixture was washed with brine and organic layer of methylene chloride was evaporated on rotary evaporator to obtain crude product. Crude product was recrystallized using hexane to obtain white solid.

##### 4.8.1 General procedure for competition experiments (Relative rate constant for addition-elimination process)

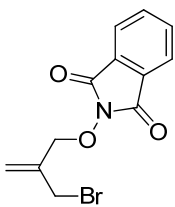
In a 20 mL Pyrex tube, allyl bromide (0.0148 g, 10  $\mu$ L, 0.0000779 mol), allyl-PINO (0.0000779 mol), di-*t*-butyl peroxide (0.00227g, 2.8  $\mu$ L, 0.0000155 mol) and toluene (2 mL) were added. 1,2 epoxy butane (0.0056 g, 0.0000779 mol) was added to neutralize the side product HBr. Reaction mixture was heated at 120 °C for 25 min. After 25 min reaction tube was quickly immersed in water bath to bring the temperature down to room temperature and stop the reaction. Diphenylmethane (10  $\mu$ L) was added to reaction mixture and used for GC analysis for product identification and quantitative analysis.

Errors in relative rate constants were calculated using the standard formula for propagation.<sup>5</sup>

Allyl-bromide	Allyl-PINO	Product from allyl bromide substrate (%)	Product from allyl-PINO substrate (%)	Relative rate constant from product yield (allyl bromide/allyl PINO)
Z=CO <sub>2</sub> Et	Z=Ph	1.13	0.33	3.42 (±0.03)
Z=Ph	Z=CO <sub>2</sub> Et	0.58	0.49	1.18 (± 0.01)
Z=CO <sub>2</sub> Et	Z=CN	8.0	3.1	2.58 (± 0.02)
Z=CN	Z=CO <sub>2</sub> Et	1.26	1.20	1.05 (± 0.01)
Z=Ph	Z=CN	15.05	1.20	2.70 (± 0.02)
Z=CN	Z=Ph	11.11	4.89	2.27 (± 0.05)

**Table 4-2:** Results of competition experiments (Reactions of benzyl radical with allyl-bromides and allyl-PINO substrates)

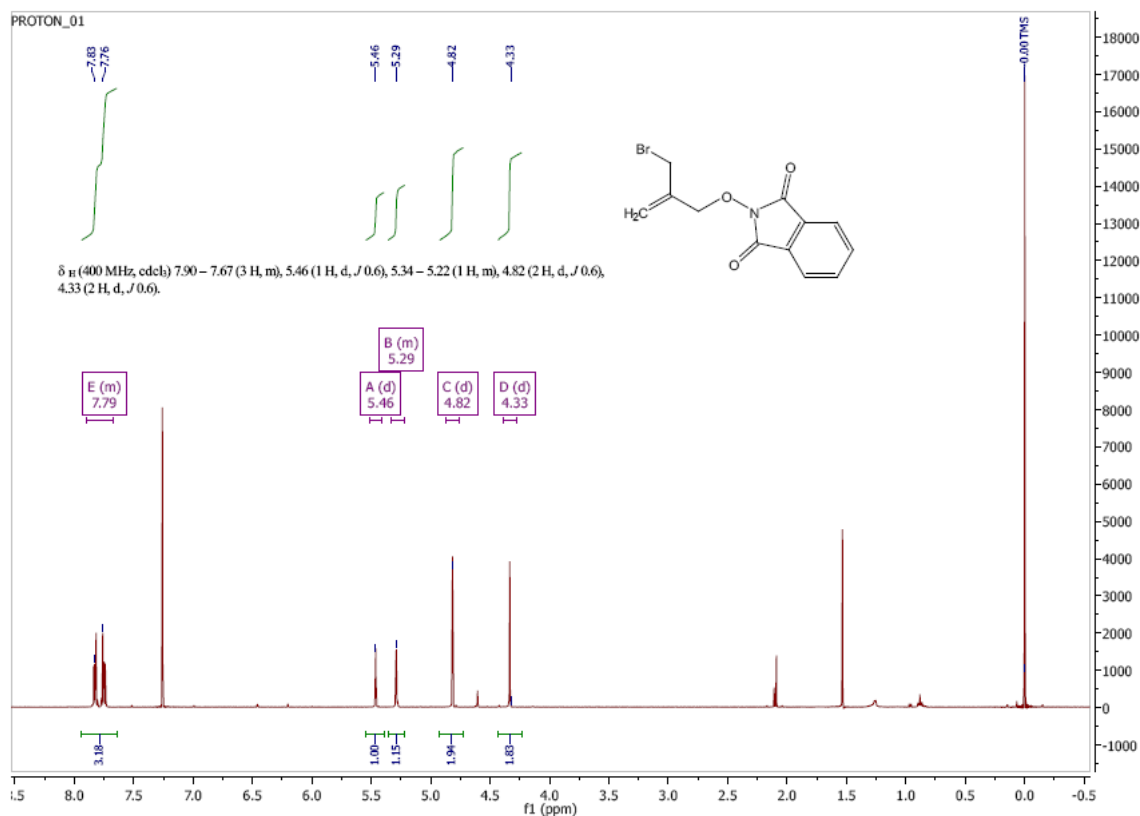
#### 4.9 Experimental procedure for the synthesis 2-((2-(bromomethyl)allyl)oxy)isoindoline-1,3-dione (2-45)

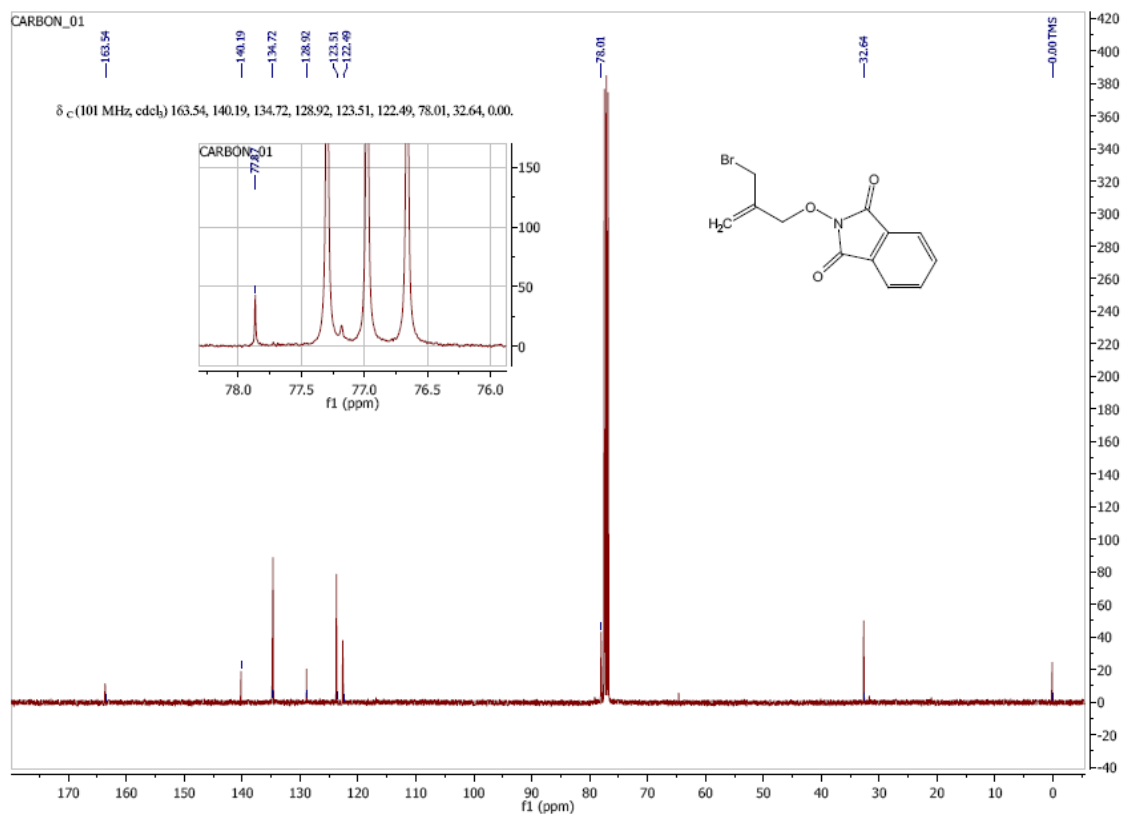


**2-45**

**2-((2-(bromomethyl)allyl)oxy)isoindoline-1,3-dione:** A solution of 3-bromo-2-(bromomethyl)prop-1-ene (0.5 g, 0.00237 mol) and DMSO (10 mL) was added drop wise

to the mixture of sodium acetate (0.16 g, 0.00118 mol), *N*-hydroxyphthalimide (0.19 g, 0.00118 mol) and DMSO (20 mL). Reaction mixture was stirred at room temperature for 30 min. Reaction mixture was extracted with chloroform and brine solution. Combined organic layers were dried over sodium sulfate. Solvent was evaporated using rotary evaporator and crude product was obtained in 55% yield, 0.38 g. The crude product was purified using flash chromatography using 20% ethyl acetate in hexane solvent system. Purified product was obtained as a white solid.  $^1\text{H NMR}$  (400 MHz,  $\text{CDCl}_3$ ) 7.90 – 7.67 (3 H, m), 5.46 (1 H, d,  $J$  0.6), 5.34 – 5.22 (1 H, m), 4.82 (2 H, d,  $J$  0.6), 4.33 (2 H, d,  $J$  0.6).  $^{13}\text{C NMR}$  (101 MHz,  $\text{CDCl}_3$ ) 163.54, 140.19, 134.72, 128.92, 123.51, 122.49, 78.01, 32.64, 0.00. **HRMS**: Calculated for  $\text{C}_{12}\text{H}_{10}\text{NO}_3\text{Br}$ : 295.9917 and 297.9897, observed 295.9912 and 297.9895 (-1.62 ppm). m.p 73-75 °C.





#### 4.9.1 General experimental procedure for the competition experiments for relative rate constant for leaving group abilities

In a 20 mL pyrex tube, toluene (0.4 mL) was added to the mixture of 3-bromo-2-(bromomethyl)prop-1-ene (0.1 g, 0.00034 mol) and di-*t*-butyl peroxide (0.0074g, 0.000051 mol). 1,2 epoxy butane (0.021g, 0.000017 mol) was added to neutralize the side product HBr. The reaction mixture was heated at 120 °C for 25 min. After 25 min reaction tube was quickly immersed in water bath to bring the temperature down to room temperature and stop the reaction. Diphenylmethane (10  $\mu\text{L}$ ) was added to reaction mixture and used for GC analysis for product identification and quantitative analysis. Error in relative rate constant was calculated using standard error in propagation.<sup>5</sup> Result: ( $k_1$  for elimination of PINO $\bullet$ ,  $k_2$  for elimination of Br $\bullet$   $k_1/k_2 = 7.5/3.3 = 3(\pm 1)$ ).

#### 4.10 References:

1. H. Pines, H. Alul and M. Kolobielski, *J. Org. Chem.*, 1957, **22**, 1113-1114.
2. J. Villieras and M. Rambaud, *Synthesis*, 1982, **1982**, 924-926.
3. C. Pégurier, L. Morellato, E. Chahed, J. Andrieux, J.-P. Nicolas, J. A. Boutin, C. Bennejean, P. Delagrangé, M. Langlois and M. Mathé-Allainmat, *Bioorg. Med. Chem.*, 2003, **11**, 789-800.
4. B. M. Aveline, I. E. Kochevar and R. W. Redmond, *J. Am. Chem. Soc.*, 1995, **117**, 9699-9708.
5. J. Andraos, *J. Chem. Educ.*, 1996, **73**, 150.

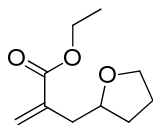
## Chapter 5: Experimental

### (For Chapter 3)

#### 5.1 General procedure for allyl transfer reactions of ethers

Allyl transfer reactions of ethers were run in 20 mL Pyrex pressure tubes. In 20 mL Pyrex tube, allyl-PINO substrate (**2-10** or **2-11**, 0.00090 mol) was mixed with the desired ether substrate (approx. 2-3 mL). Initiator, di-*t*-butyl peroxide (0.000136 mol) was added to the above mixture. This reaction mixture was degassed using high vacuum by freeze-pump-thaw (3X) method and it was heated at 120 °C while stirring. The temperature fluctuation was  $\pm 5$  °C and the time of the reaction run has the accuracy of  $\pm 1$  min. At the end of each reaction, the pressure tube was cooled down under tap water followed by solvent evaporation (if necessary) or liquid-liquid extraction to yield crude product. Crude product was then purified using flash chromatography (20% ethyl acetate: 80% hexanes). Reaction yields were determined by GC using diphenylmethane as internal standard.

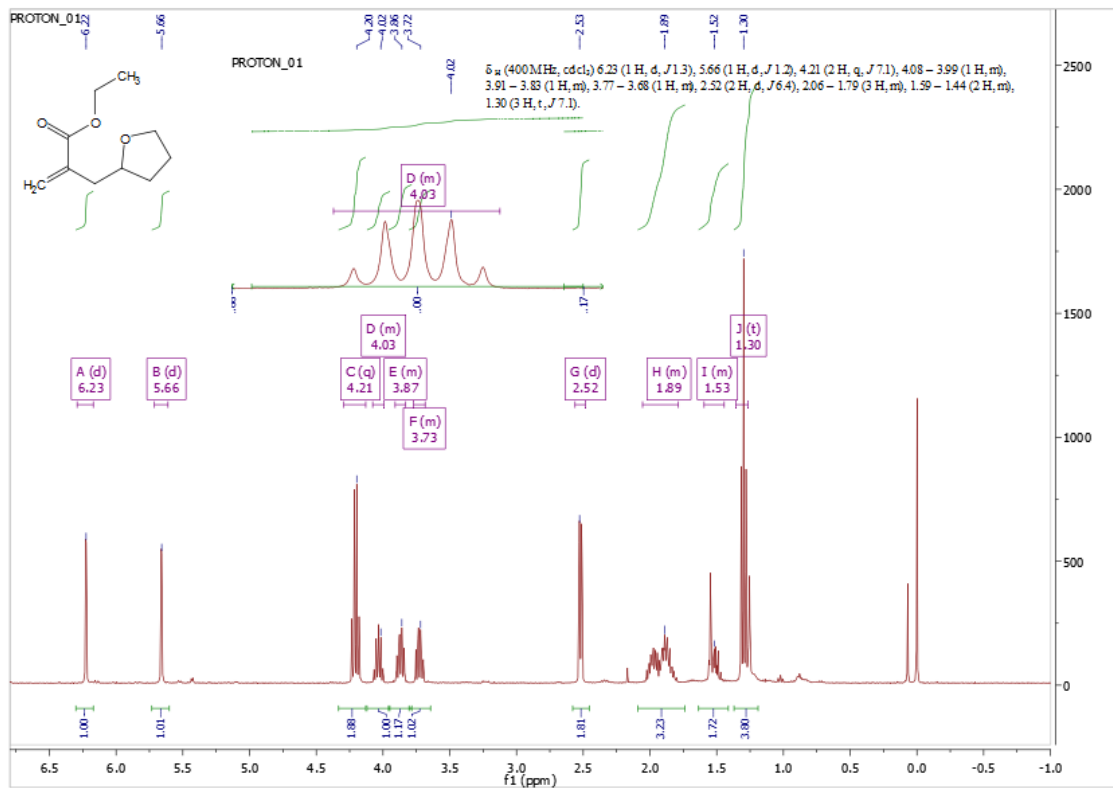
#### 5.2 Experimental data for ether products

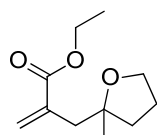
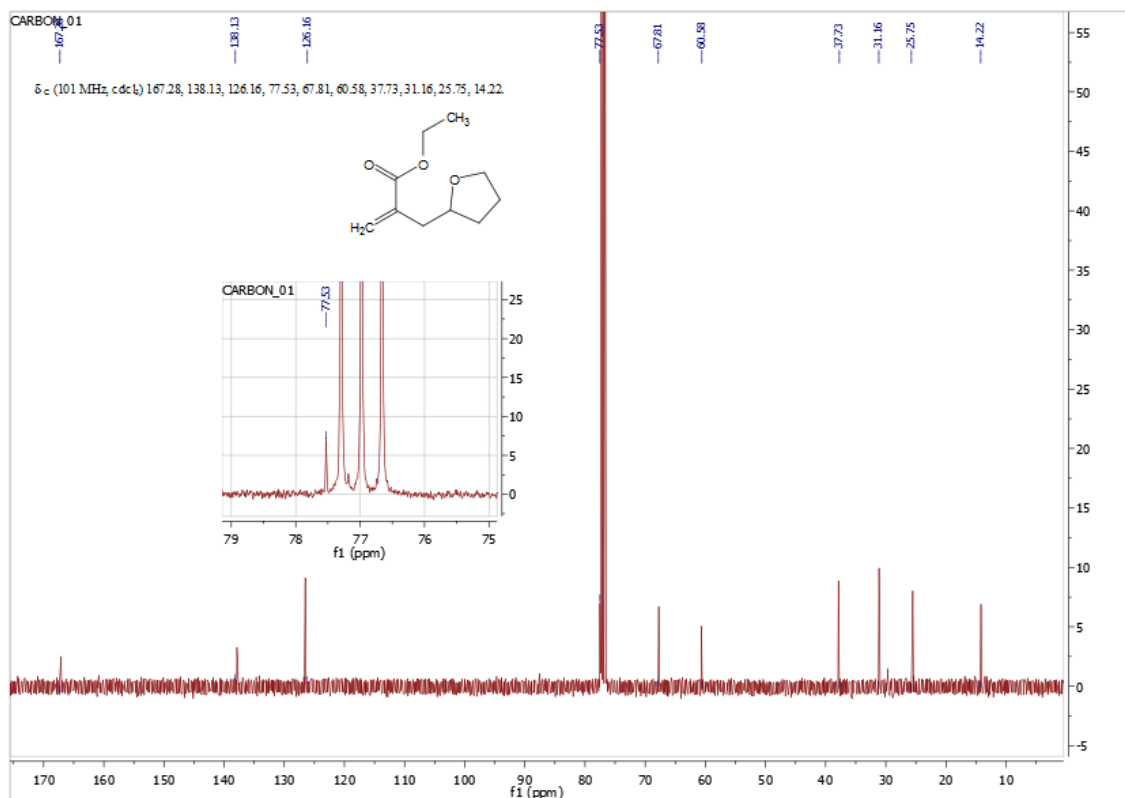


**3-79**

**Ethyl 2-((tetrahydrofuran-2-yl)methyl)acrylate (3-79):**  $^1\text{H NMR}$  (400 MHz,  $\text{CDCl}_3$ ) 6.23 (1 H, d,  $J$  1.3), 5.66 (1 H, d,  $J$  1.2), 4.21 (2 H, q,  $J$  7.1), 4.08 – 3.99 (1 H, m), 3.91 – 3.83 (1 H, m), 3.77 – 3.68 (1 H, m), 2.52 (2 H, d,  $J$  6.4), 2.06 – 1.79 (3 H, m), 1.59 – 1.44 (2 H, m), 1.30 (3 H, t,  $J$  7.1).  $^{13}\text{C NMR}$  (101 MHz,  $\text{CDCl}_3$ ) 167.31, 137.78, 126.19, 100.56, 67.20, 60.45, 37.66, 32.18,

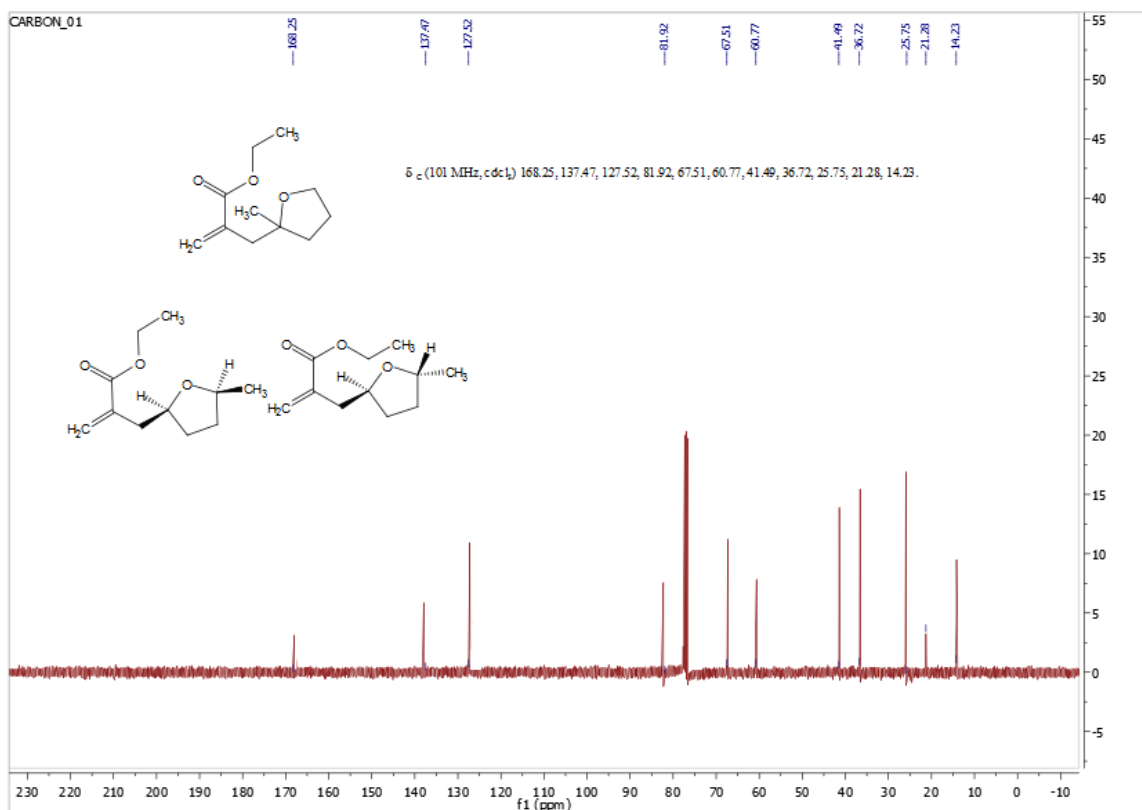
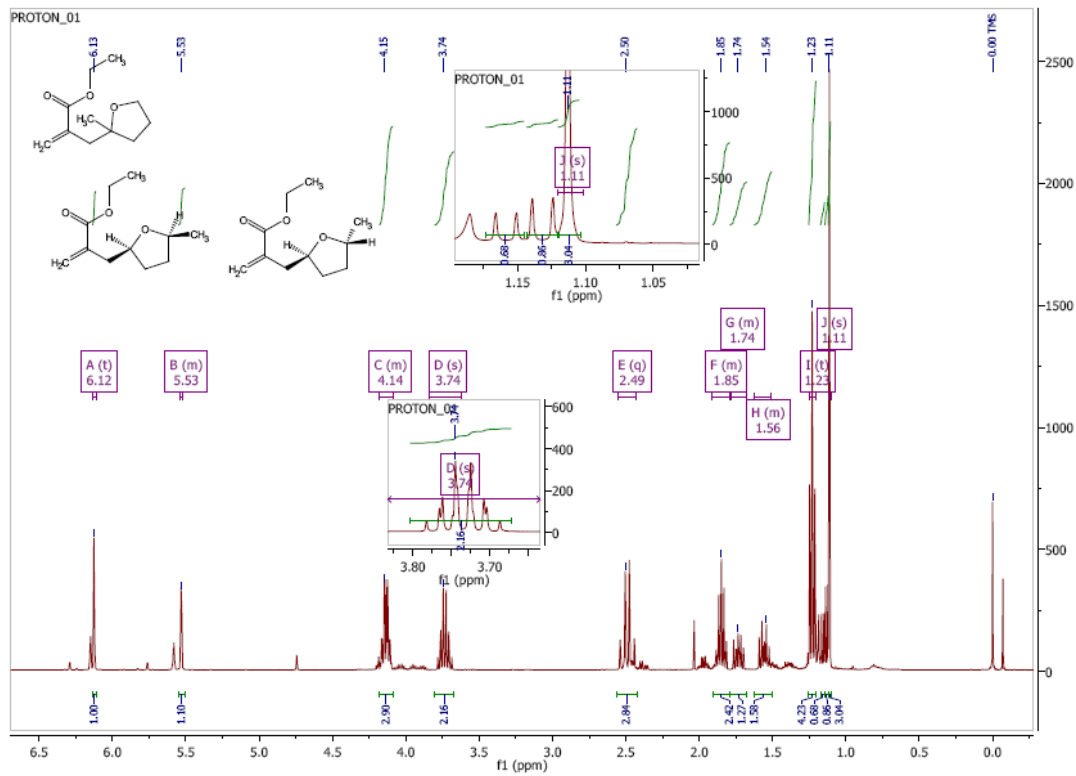
24.18, 14.21. **HRMS:** Calculated for C<sub>10</sub> H<sub>16</sub>O<sub>3</sub> 185.1172, observed [M+H] 185.1180 (+4.41 ppm).

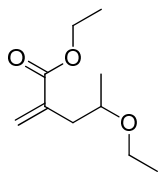




**3-95 + 3-97**

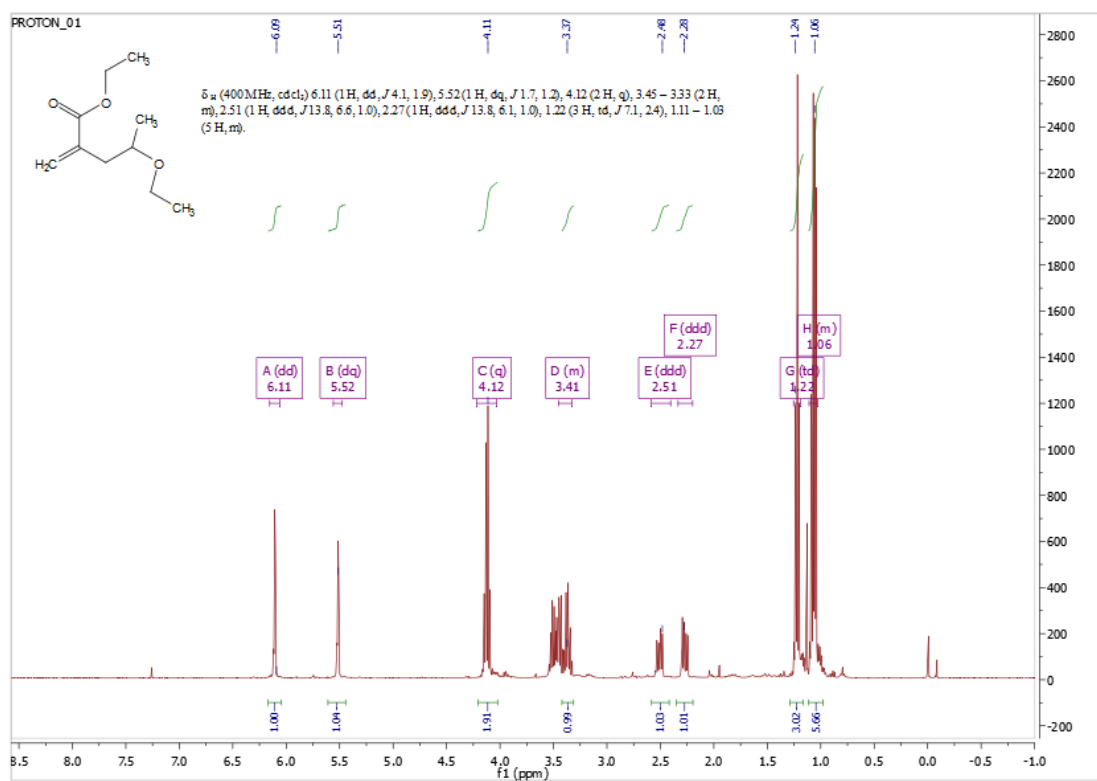
**Ethyl 2-((2-methyltetrahydrofuran-2-yl)methyl)acrylate (3-95) + mixture of 3-97: <sup>1</sup>H NMR** (400 MHz, CDCl<sub>3</sub>) 6.19 (1 H, d, *J* 1.8), 5.60 – 5.59 (1 H, m), 4.25 – 4.15 (3 H, m), 3.80 (2 H, dd, *J* 14.7, 6.8), 2.55 (3 H, q, *J* 13.5), 1.98 – 1.86 (2 H, m), 1.84 – 1.74 (1 H, m), 1.68 – 1.57 (2 H, m), 1.29 (4 H, td, *J* 7.1, 1.6), 1.18 (3 H, s). (Expansion in the 1.31-1.39 region shows evidence of regioisomers (cis and trans **3-97**) in the form of 3H, d). **<sup>13</sup>C NMR** (101 MHz, CDCl<sub>3</sub>) 168.25, 137.47, 127.52, 81.92, 67.51, 60.77, 41.49, 36.72, 25.75, 21.28, 14.23. **HRMS:** Calculated for C<sub>11</sub>H<sub>18</sub>O<sub>3</sub> (3-95) 199.1329, observed [M+H] 199.1325 (-2.06 ppm)

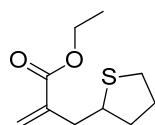
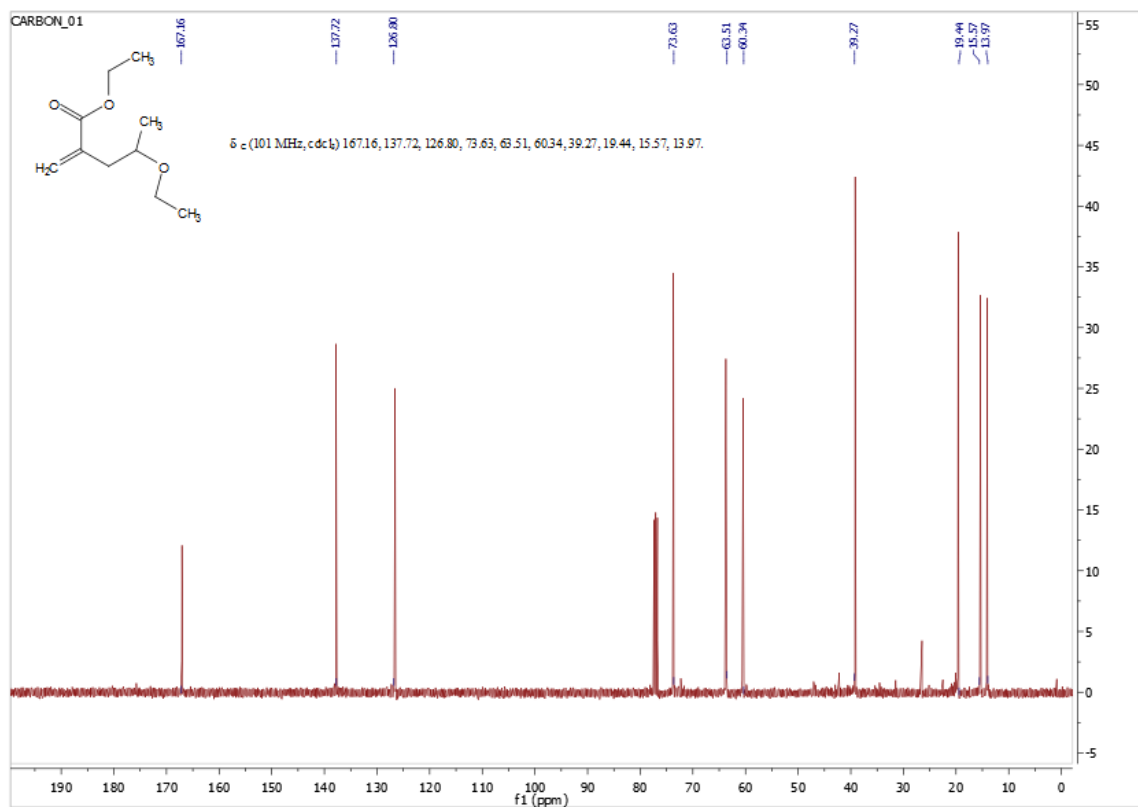




**3-75**

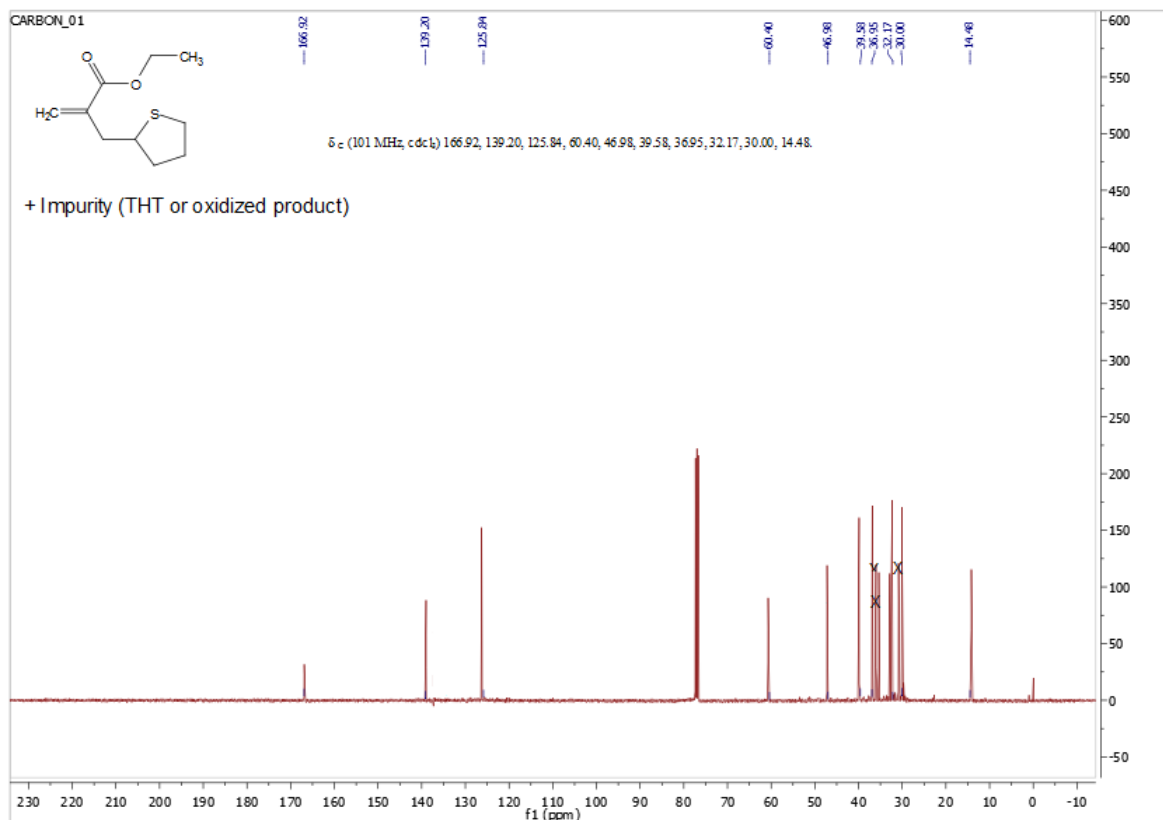
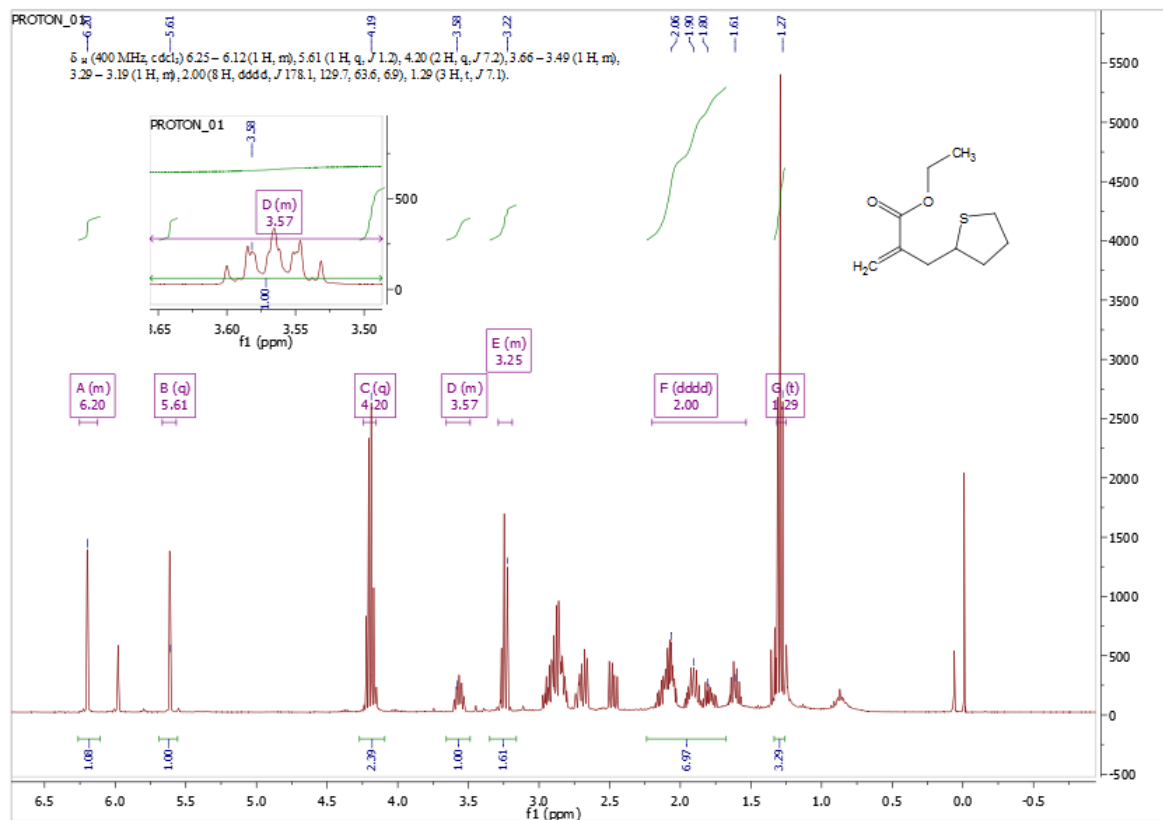
**Ethyl 4-ethoxy-2-methylenepentanoate (3-75):**  $^1\text{H}$  NMR (400 MHz,  $\text{CDCl}_3$ ) 6.11 (1 H, dd,  $J$  4.1, 1.9), 5.52 (1 H, dq,  $J$  1.7, 1.2), 4.12 (2 H, q), 3.45 – 3.33 (2 H, m), 2.51 (1 H, ddd,  $J$  13.8, 6.6, 1.0), 2.27 (1 H, ddd,  $J$  13.8, 6.1, 1.0), 1.22 (3 H, td,  $J$  7.1, 2.4), 1.11 – 1.03 (5 H, m).  $^{13}\text{C}$  NMR (101 MHz,  $\text{CDCl}_3$ ) 167.16, 137.72, 126.80, 73.63, 63.51, 60.34, 39.27, 19.44, 15.57, 13.97. **HRMS:** Calculated for  $\text{C}_{10}\text{H}_{18}\text{O}_3$  187.1329, observed  $[\text{M}+\text{H}]$  187.1325 (-1.82 ppm).

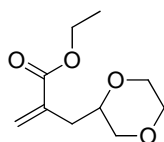




**3-85**

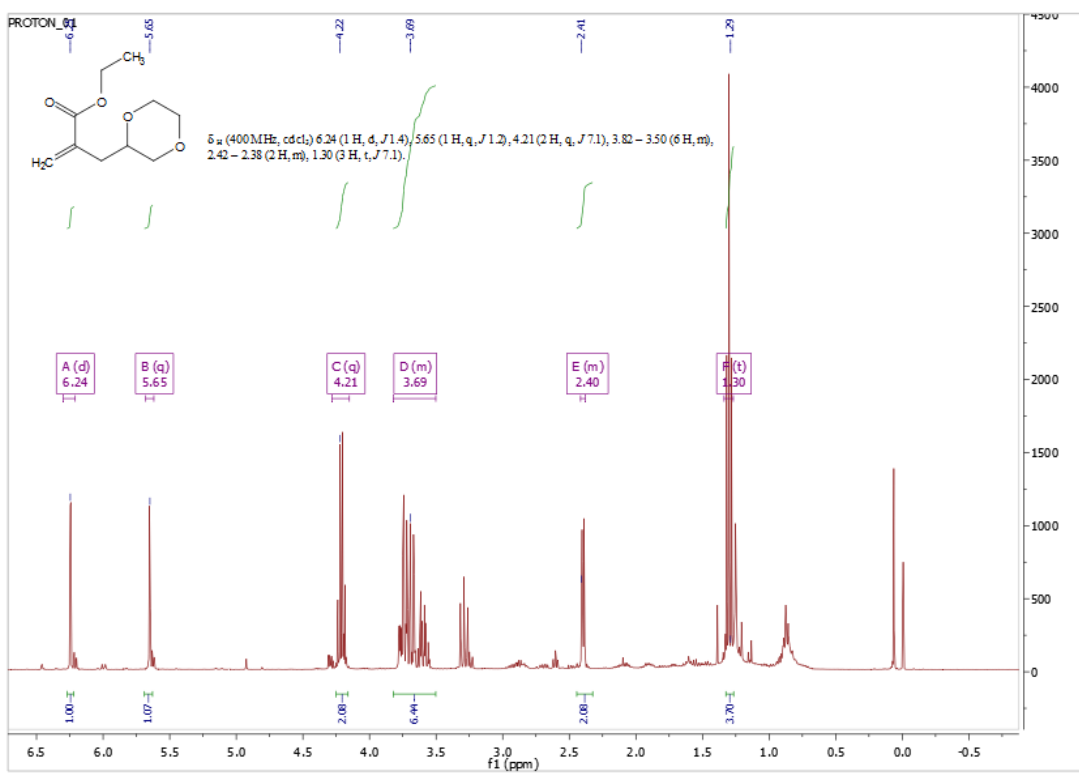
**Ethyl 2-((tetrahydrothiophen-2-yl)methyl)acrylate (3-85):**  $^1\text{H}$  NMR (400 MHz,  $\text{CDCl}_3$ ) 6.25 – 6.12 (1 H, m), 5.61 (1 H, q,  $J$  1.2), 4.20 (2 H, q,  $J$  7.2), 3.66 – 3.49 (1 H, m), 3.29 – 3.19 (1 H, m), 2.00 (8 H, dddd,  $J$  178.1, 129.7, 63.6, 6.9), 1.29 (3 H, t,  $J$  7.1).  $^{13}\text{C}$  NMR (101 MHz,  $\text{CDCl}_3$ ) 166.92, 139.20, 125.84, 60.40, 46.98, 39.58, 36.95, 32.17, 30.00, 14.48. **HRMS:** Calculated for  $\text{C}_{10}\text{H}_{16}\text{O}_2\text{S}$  201.0944, observed  $[\text{M}+\text{H}]$  201.0946 (+1.27)

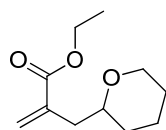
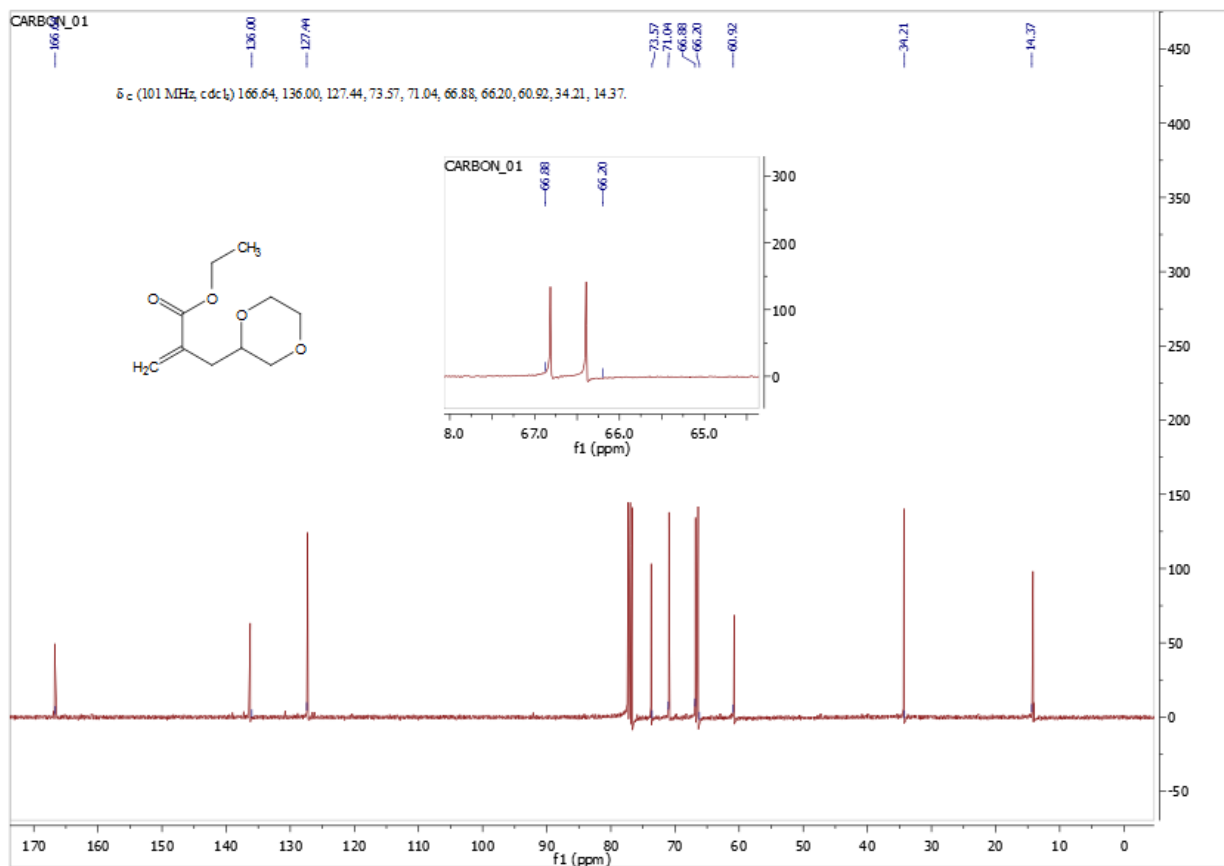




3-83

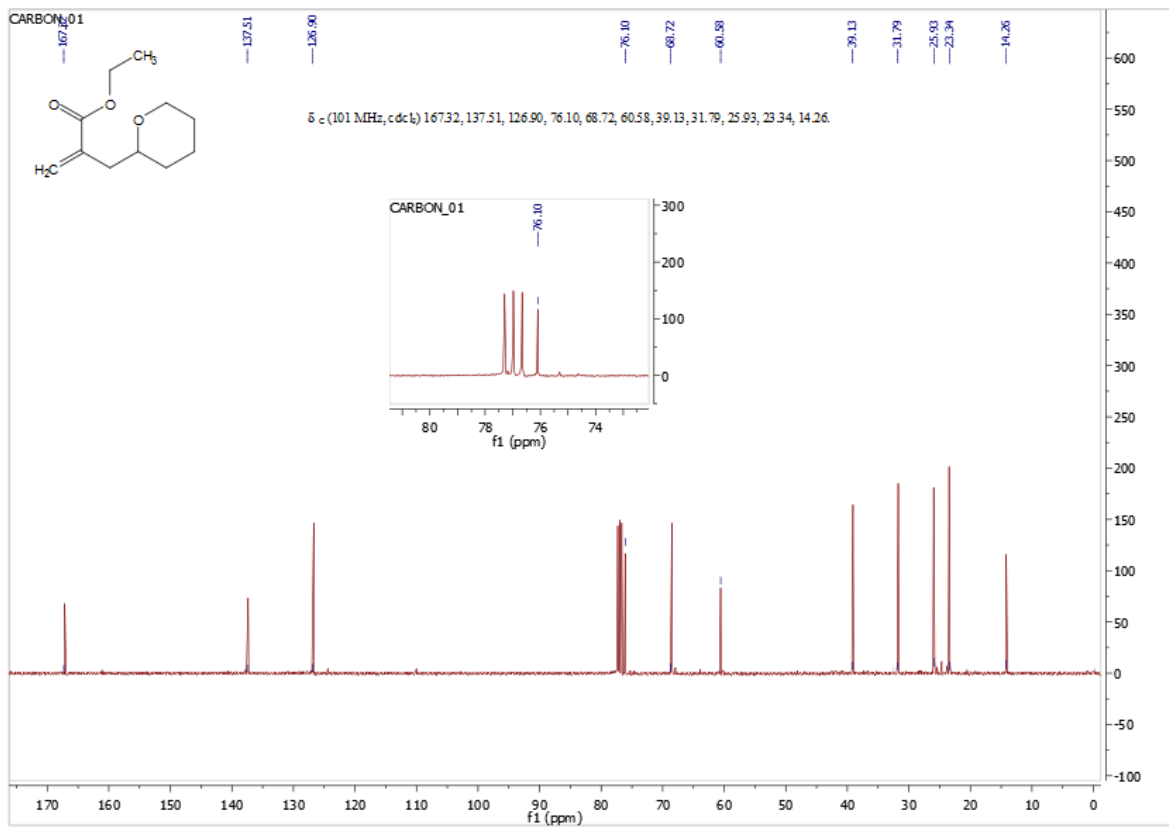
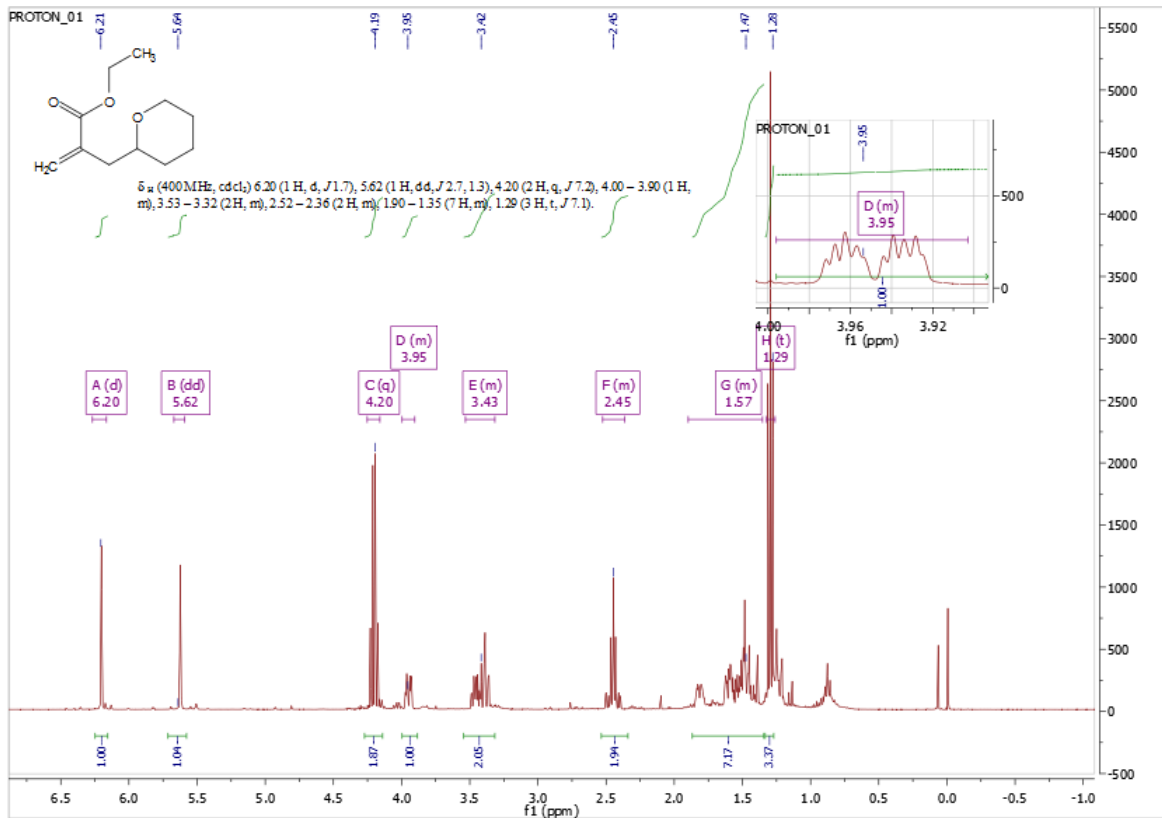
**Ethyl 2-((1,4-dioxan-2-yl)methyl)acrylate (3-83):**  $^1\text{H NMR}$  (400 MHz,  $\text{CDCl}_3$ ) 6.24 (1 H, d,  $J$  1.4), 5.65 (1 H, q,  $J$  1.2), 4.21 (2 H, q,  $J$  7.1), 3.82 – 3.50 (6 H, m), 2.42 – 2.38 (2 H, m), 1.30 (3 H, t,  $J$  7.1).  $^{13}\text{C NMR}$  (101 MHz,  $\text{CDCl}_3$ ) 166.64, 136.00, 127.44, 73.57, 71.04, 66.88, 66.20, 60.92, 34.21, 14.37. **HRMS:** Calculated for  $\text{C}_{10}\text{H}_{16}\text{O}_4$  201.1121, observed  $[\text{M}+\text{H}]$  201.1127 (+2.78)

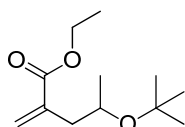




**3-81**

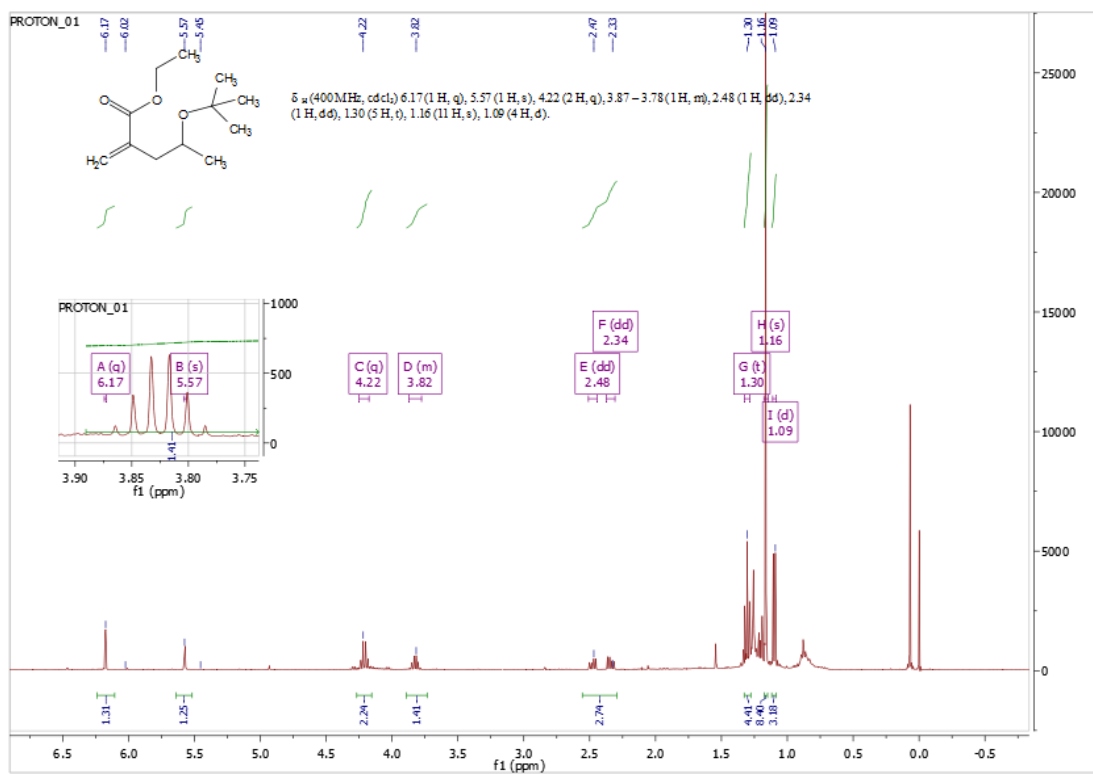
**Ethyl 2-((tetrahydro-2H-pyran-2-yl)methyl)acrylate:**  $^1\text{H}$  NMR (400 MHz,  $\text{CDCl}_3$ ) 6.20 (1 H, d,  $J$  1.7), 5.62 (1 H, dd,  $J$  2.7, 1.3), 4.20 (2 H, q,  $J$  7.2), 4.00 – 3.90 (1 H, m), 3.53 – 3.32 (2 H, m), 2.52 – 2.36 (2 H, m), 1.90 – 1.35 (7 H, m), 1.29 (3 H, t,  $J$  7.1).  $^{13}\text{C}$  NMR (101 MHz,  $\text{CDCl}_3$ ) 167.32, 137.51, 126.90, 76.10, 68.72, 60.58, 39.13, 31.79, 25.93, 23.34, 14.26. **HRMS:** Calculated for  $\text{C}_{11}\text{H}_{18}\text{O}_3$  199.1329, observed  $[\text{M}+\text{H}]$  199.1322 (-3.17 ppm).

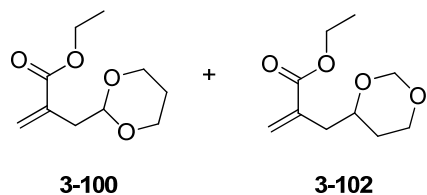
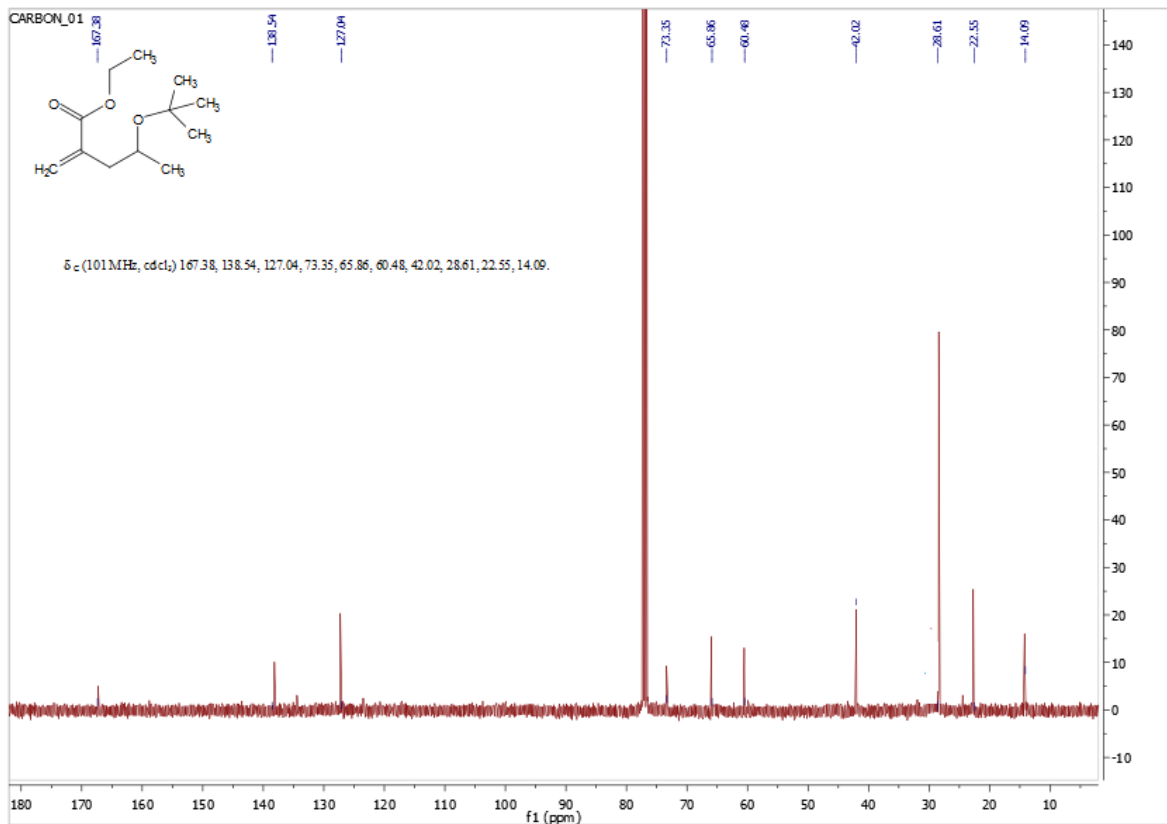




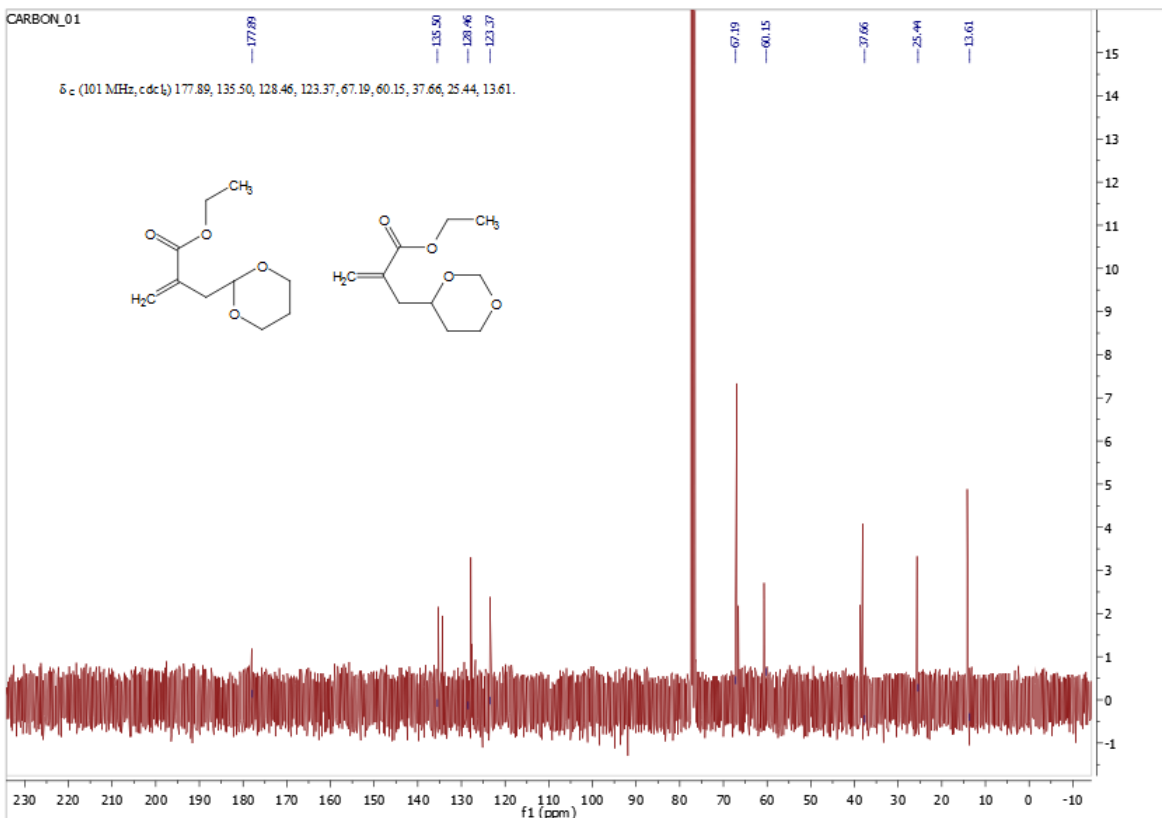
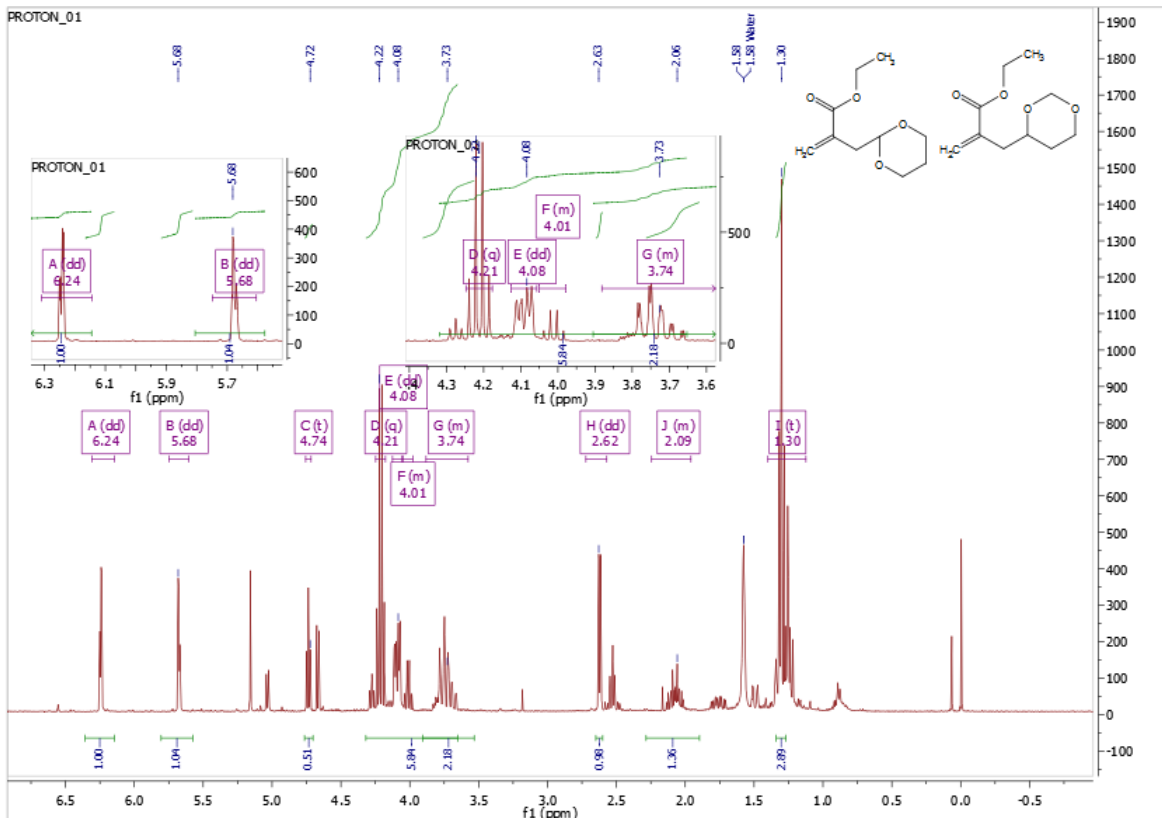
3-76

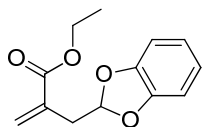
**Ethyl 4-(tert-butoxy)-2-methylenepentanoate:**  $^1\text{H NMR}$  (400 MHz,  $\text{CDCl}_3$ ) 6.17 (1 H, q), 5.57 (1 H, s), 4.22 (2 H, q), 3.87 – 3.78 (1 H, m), 2.48 (1 H, dd), 2.34 (1 H, dd), 1.30 (5 H, t), 1.16 (11 H, s), 1.09 (4 H, d).  $^{13}\text{C NMR}$  (101 MHz,  $\text{CDCl}_3$ ) 167.38, 138.54, 127.04, 73.35, 65.86, 60.48, 42.02, 28.61, 22.55, 14.09. **HRMS:** Calculated for  $\text{C}_{12}\text{H}_{22}\text{O}_3$  215.1642, observed  $[\text{M}+\text{H}]$  215.1626 (-7.36).





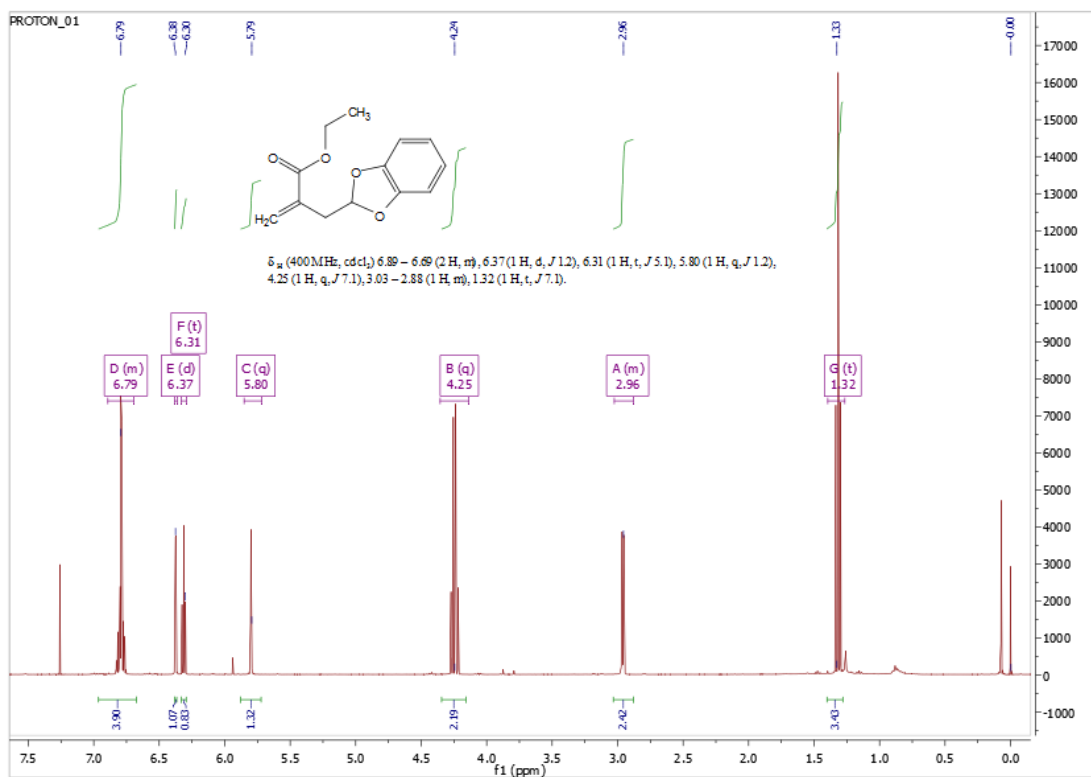
**Ethyl 2-((1,3-dioxan-2-yl)methyl)acrylate (3-100 + 3-102):**  $^1\text{H NMR}$  (400 MHz,  $\text{CDCl}_3$ ) 6.24 (2 H, dd,  $J$  3.8, 1.5), 5.68 (2 H, dd,  $J$  3.1, 1.2), 4.74 (1 H, t), 4.21 (3 H, q,  $J$  7.1), 4.08 (3 H, dd,  $J$  6.0, 4.7), 4.05 – 3.98 (1 H, m), 3.88 – 3.58 (4 H, m), 2.62 (3 H, dd,  $J$  5.4, 0.9), 2.24 – 1.96 (2 H, m), 1.30 (10 H, s).  $^{13}\text{C NMR}$  (101 MHz,  $\text{CDCl}_3$ ) 177.89, 135.50, 128.46, 123.37, 67.19, 60.15, 37.66, 25.44, 13.61. **HRMS:** Calculated for  $\text{C}_{10}\text{H}_{16}\text{O}_4$  201.1112, observed 201.110 (+2.17 ppm).

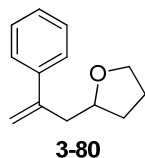
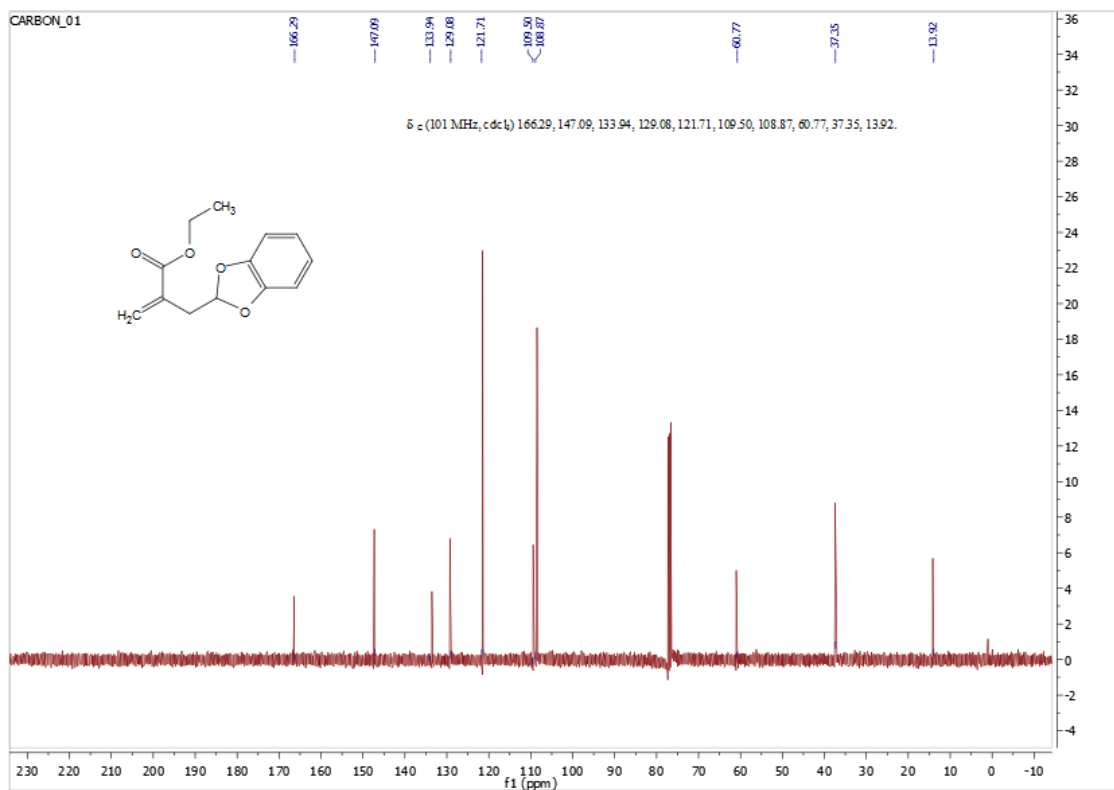




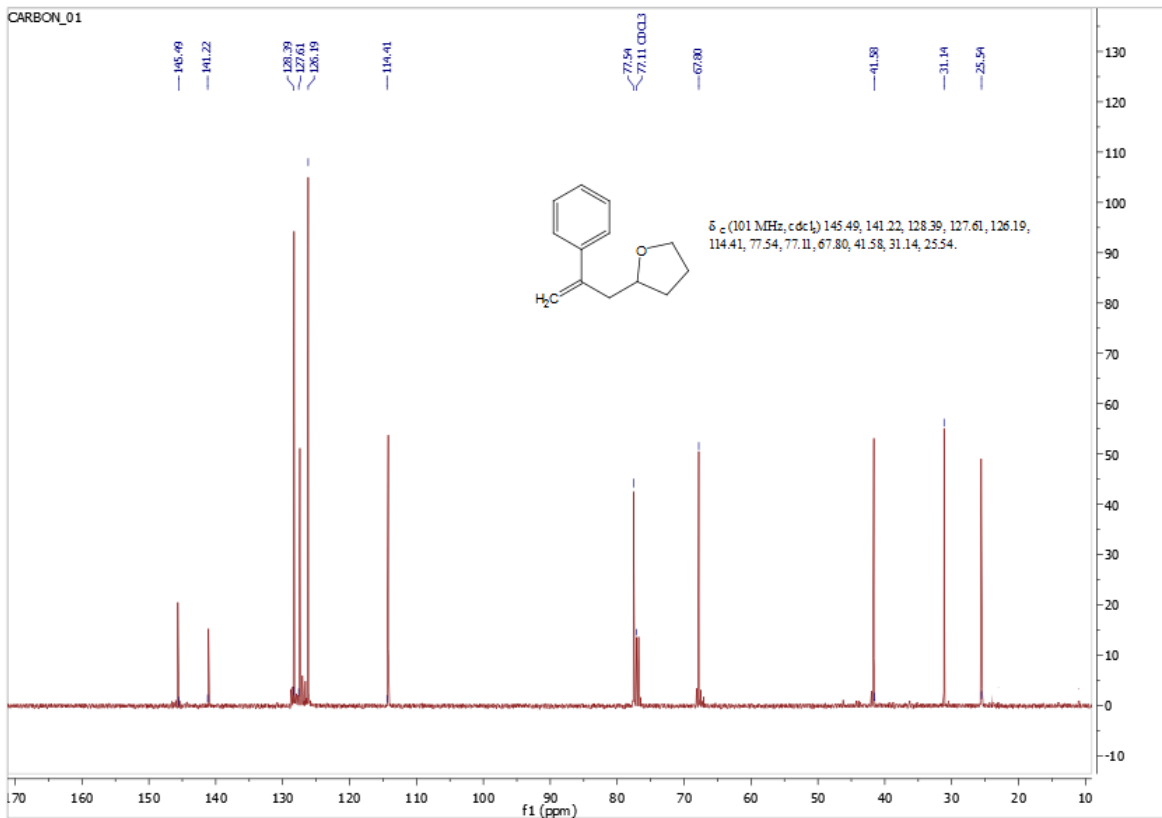
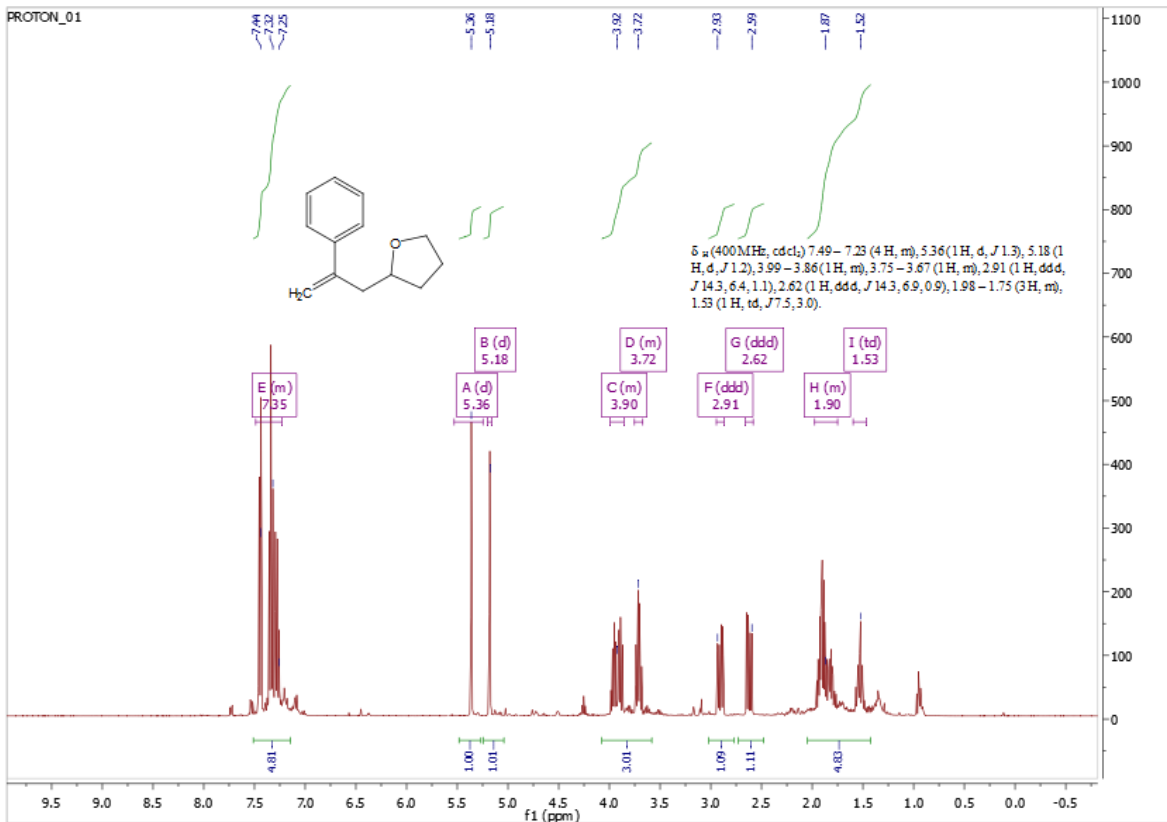
**3-87**

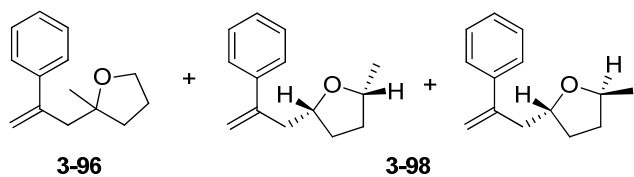
**Ethyl 2-(benzo[1,3]dioxol-2-ylmethyl)acrylate (3-87):**  $^1\text{H}$  NMR (400 MHz,  $\text{CDCl}_3$ ) 6.89 – 6.69 (2 H, m), 6.37 (1 H, d,  $J$  1.2), 6.31 (1 H, t,  $J$  5.1), 5.80 (1 H, q,  $J$  1.2), 4.25 (1 H, q,  $J$  7.1), 3.03 – 2.88 (1 H, m), 1.32 (1 H, t,  $J$  7.1).  $^{13}\text{C}$  NMR (101 MHz,  $\text{CDCl}_3$ ) 166.29, 147.09, 133.94, 129.08, 121.71, 109.50, 108.87, 60.77, 37.35, 13.92. **HRMS:** Calculated for  $\text{C}_{13}\text{H}_{14}\text{O}_4$  235.0965, observed  $[\text{M}+\text{H}]$  235.0975 (+4.5 ppm)



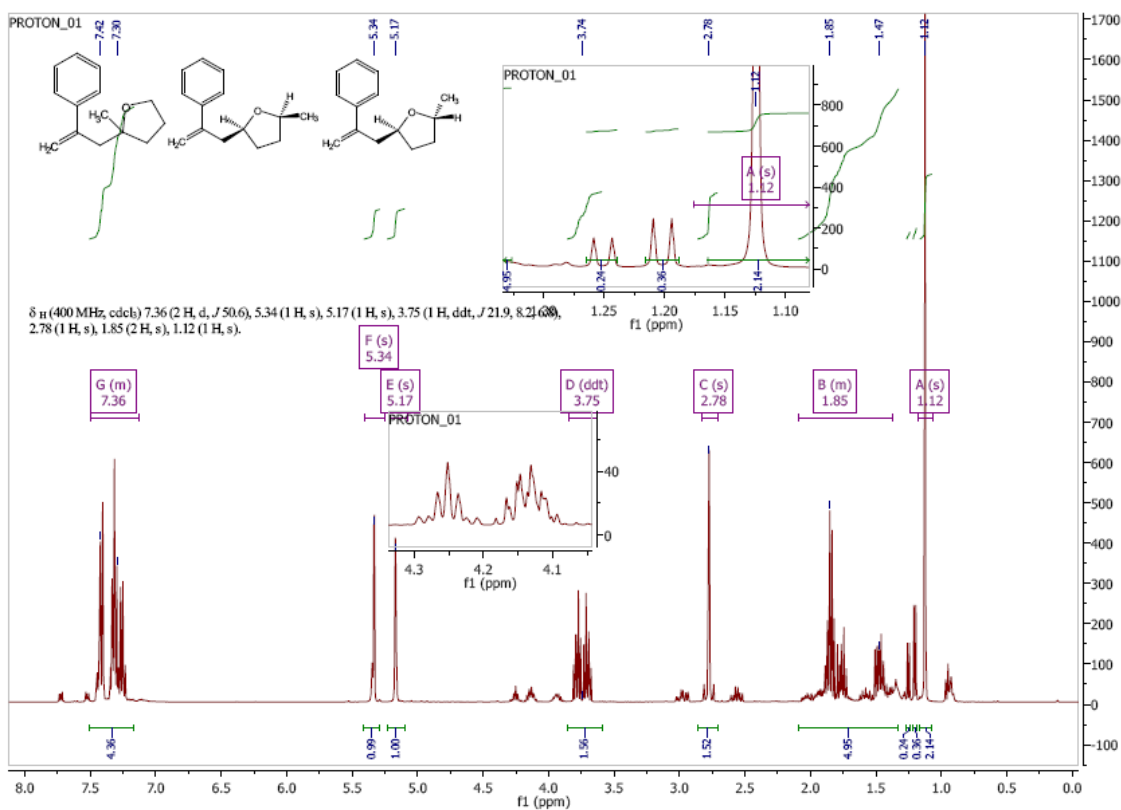


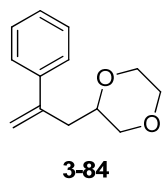
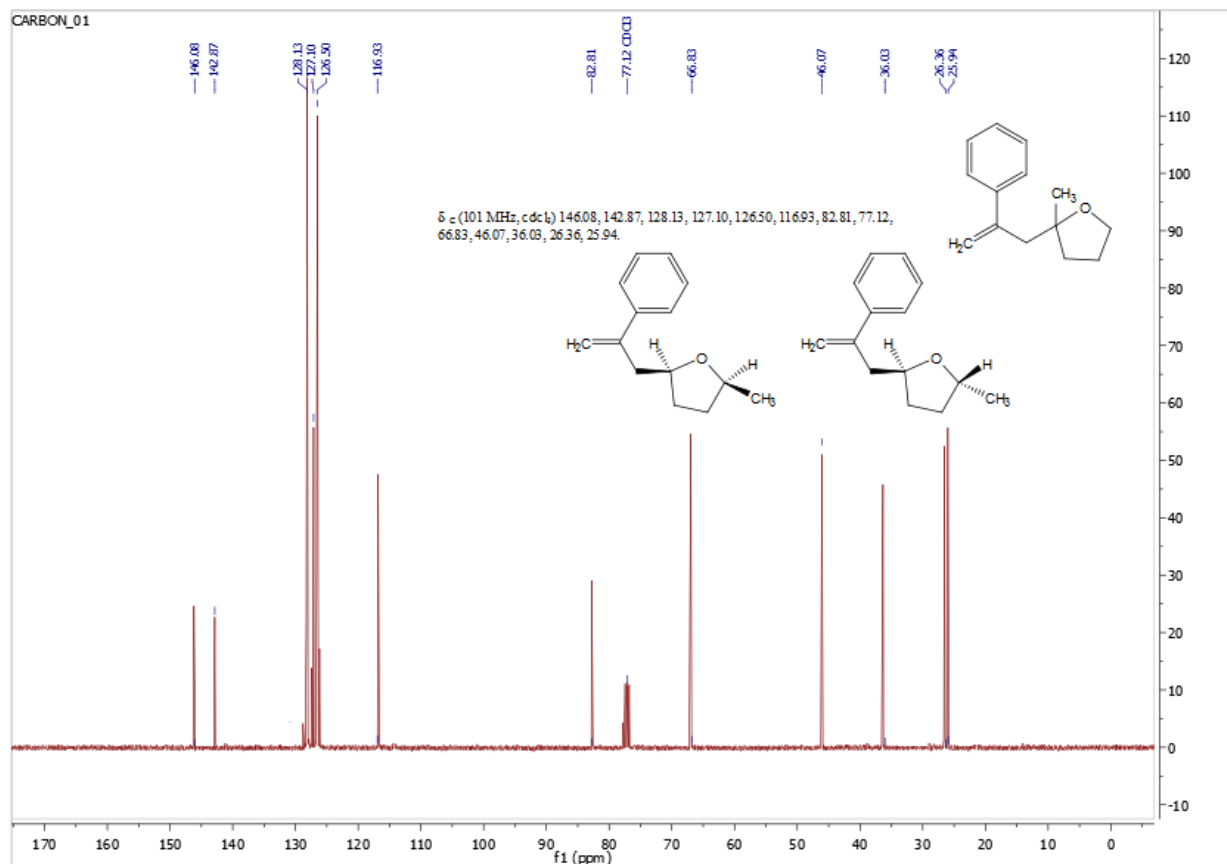
**2-(2-phenylallyl)tetrahydrofuran (3-80):**  $^1\text{H}$  NMR (400 MHz,  $\text{CDCl}_3$ ) 7.49 – 7.23 (4 H, m), 5.36 (1 H, d,  $J$  1.3), 5.18 (1 H, d,  $J$  1.2), 3.99 – 3.86 (1 H, m), 3.75 – 3.67 (1 H, m), 2.91 (1 H, ddd,  $J$  14.3, 6.4, 1.1), 2.62 (1 H, ddd,  $J$  14.3, 6.9, 0.9), 1.98 – 1.75 (3 H, m), 1.53 (1 H, td,  $J$  7.5, 3.0).  $^{13}\text{C}$  NMR (101 MHz,  $\text{CDCl}_3$ ) 145.49, 141.22, 128.39, 127.61, 126.19, 114.41, 77.54, 67.80, 41.58, 31.14, 25.54. **HRMS:** Calculated for  $\text{C}_{13}\text{H}_{16}\text{O}$  189.1274, observed  $[\text{M}+\text{H}]$  189.1259 (-7.71 ppm).



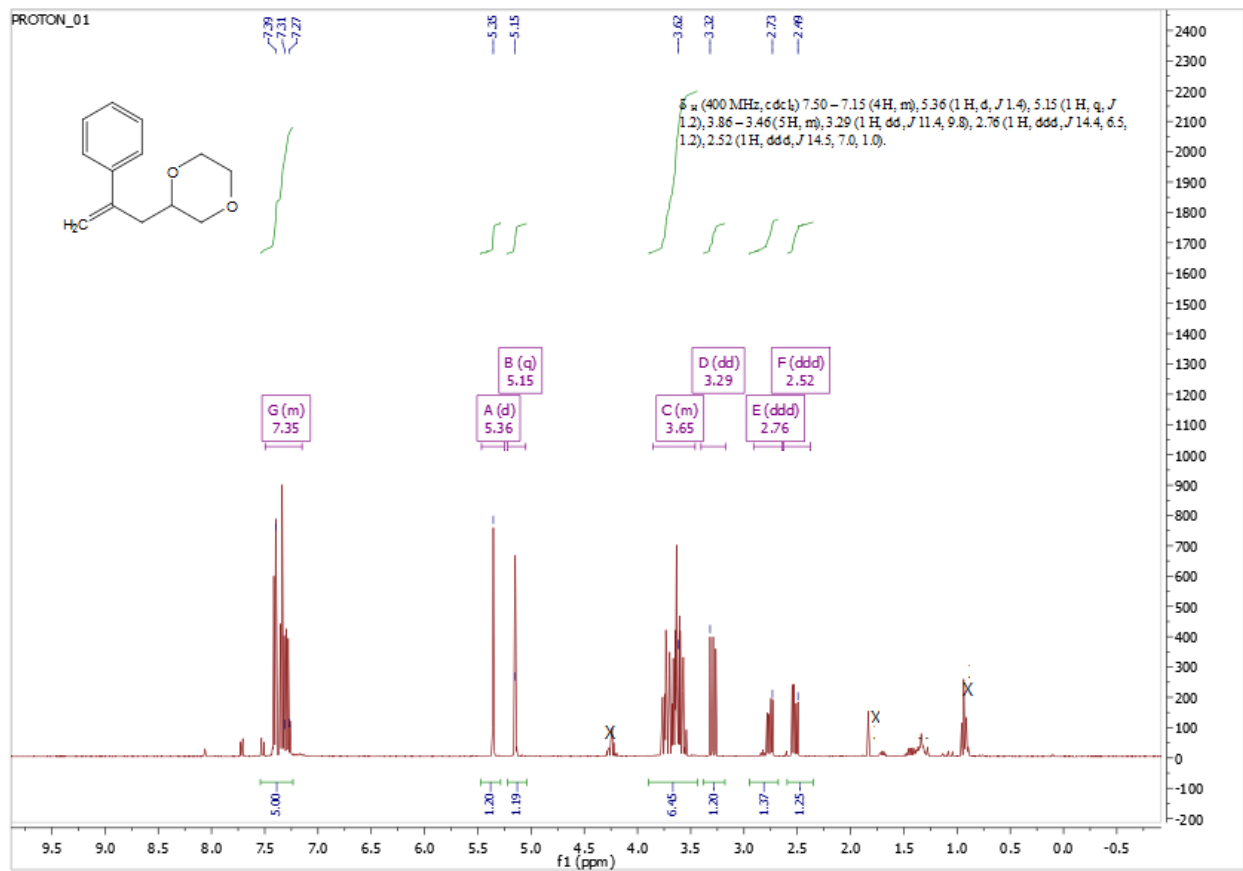


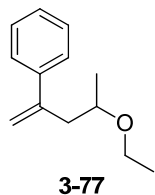
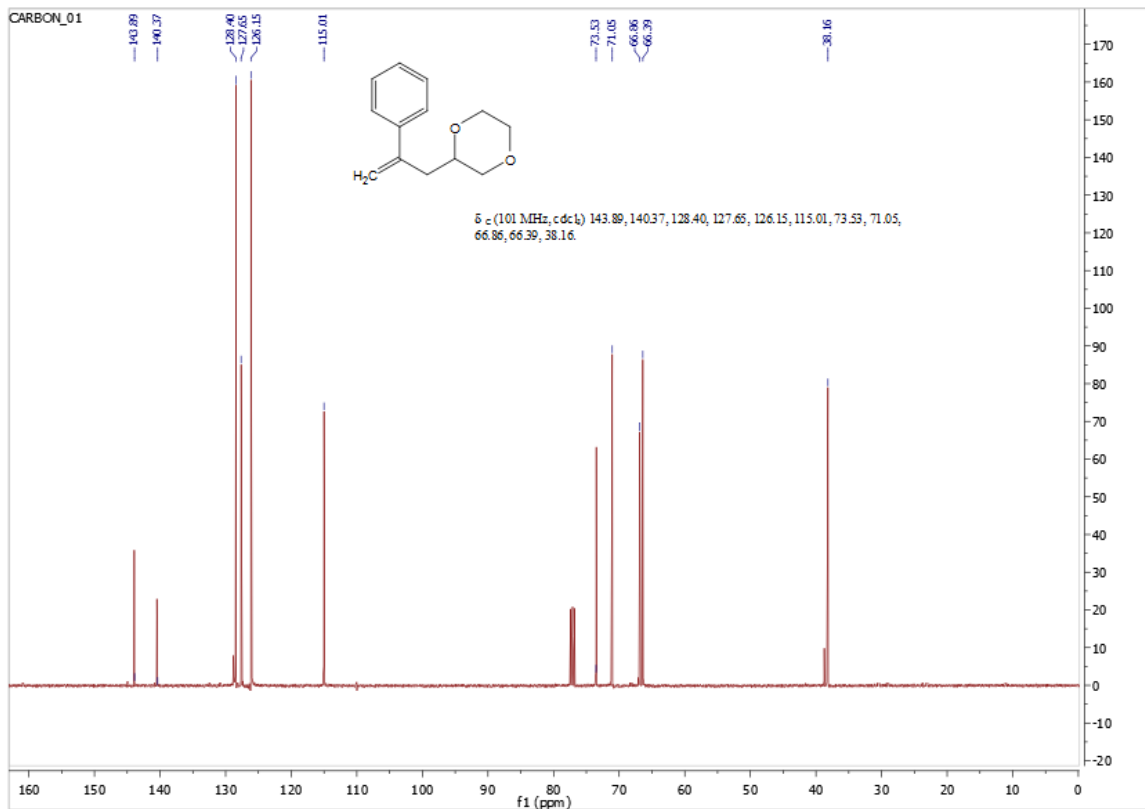
**2-methyl-2-(2-phenylallyl)tetrahydrofuran (3-96 + 3-98):**  $^1\text{H NMR}$  (400 MHz,  $\text{CDCl}_3$ ) 7.36 (2 H, d,  $J$  50.6), 5.34 (1 H, s), 5.17 (1 H, s), 3.75 (1 H, ddt,  $J$  21.9, 8.2, 6.8), 2.78 (1 H, s), 1.85 (2 H, s), 1.12 (1 H, s).  $^{13}\text{C NMR}$  (101 MHz,  $\text{CDCl}_3$ ) 146.08, 142.87, 128.13, 127.10, 126.50, 116.93, 82.81, 66.83, 46.07, 36.03, 26.36, 25.94. **HRMS:** Calculated for  $\text{C}_{14}\text{H}_{18}\text{O}$  203.143, observed  $[\text{M}+\text{H}]$  203.1414 (- 7.86 ppm).



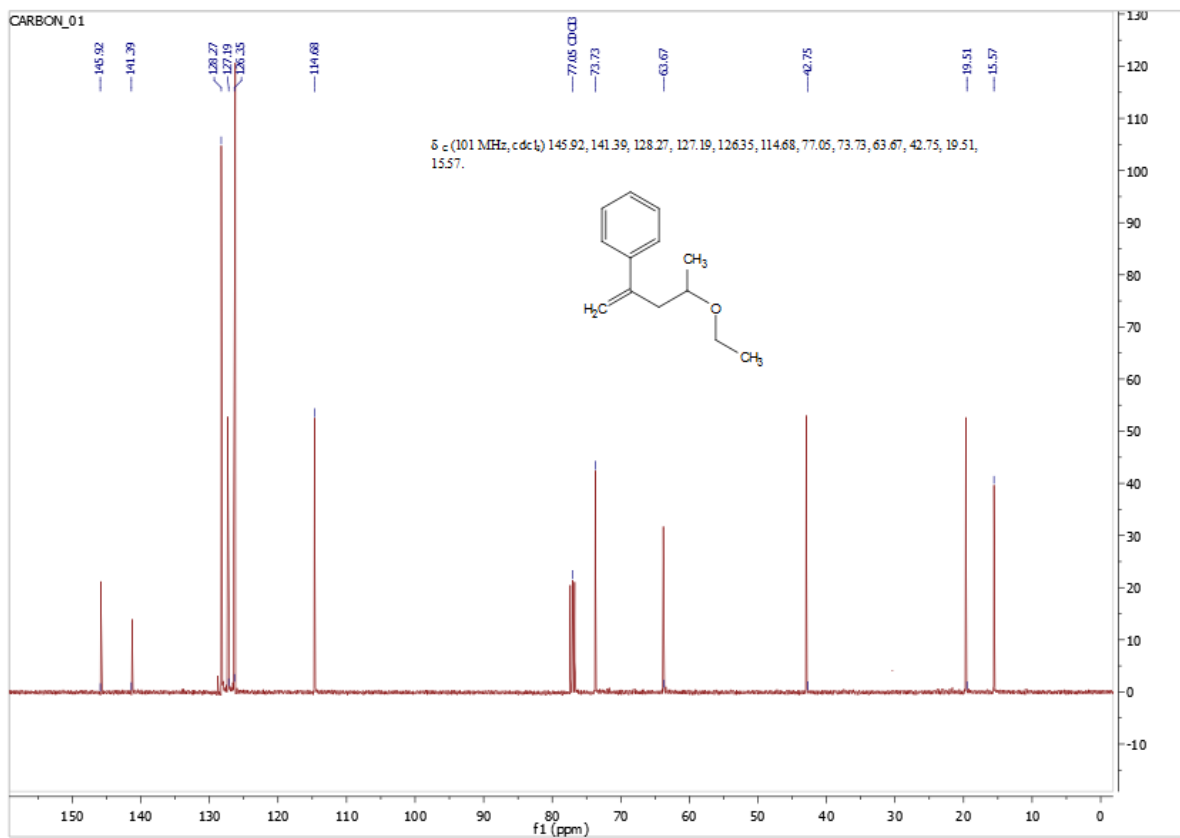
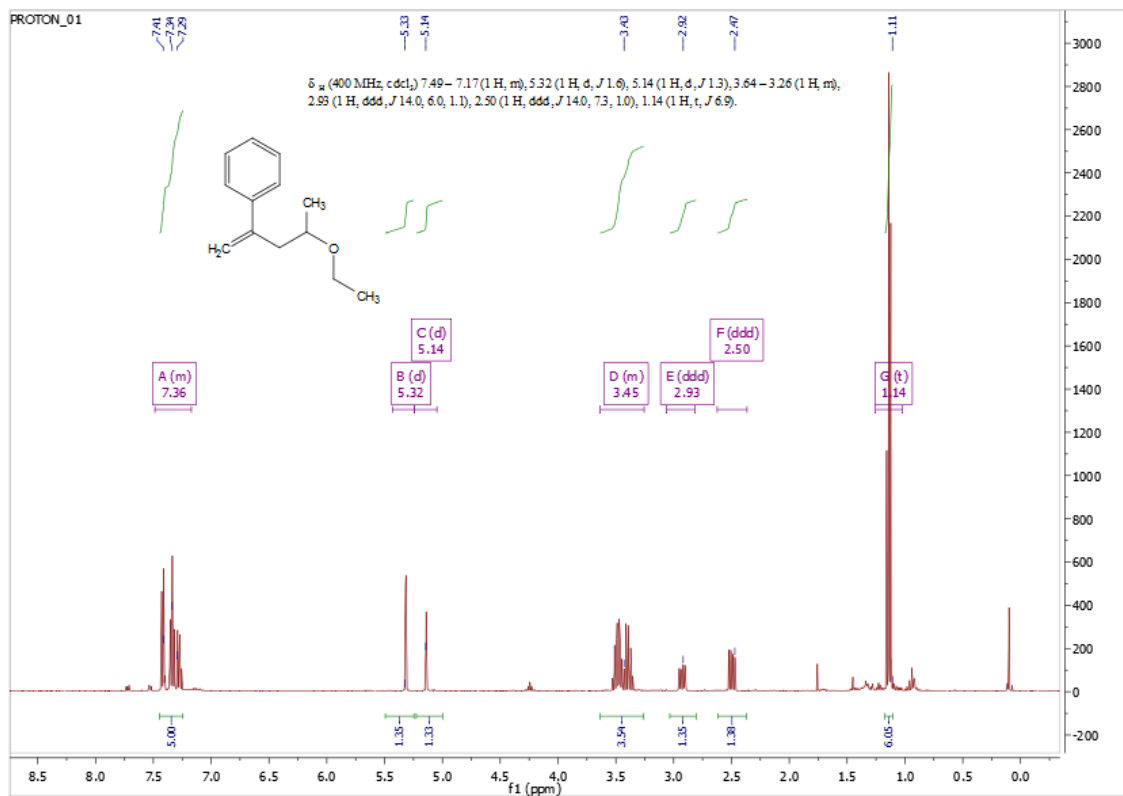


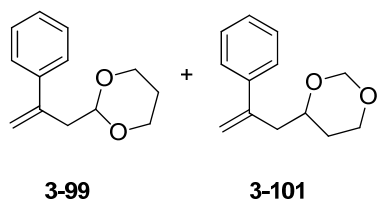
**2-(2-phenylallyl)-1,4-dioxane (3-84):**  $^1\text{H NMR}$  (400 MHz,  $\text{CDCl}_3$ ) 7.50 – 7.15 (4 H, m), 5.36 (1 H, d,  $J$  1.4), 5.15 (1 H, q,  $J$  1.2), 3.86 – 3.46 (5 H, m), 3.29 (1 H, dd,  $J$  11.4, 9.8), 2.76 (1 H, ddd,  $J$  14.4, 6.5, 1.2), 2.52 (1 H, ddd,  $J$  14.5, 7.0, 1.0).  $^{13}\text{C NMR}$  (101 MHz,  $\text{CDCl}_3$ ) 143.89, 140.37, 128.40, 127.65, 126.15, 115.01, 73.53, 71.05, 66.86, 66.39, 38.16. **HRMS:** Calculated for  $\text{C}_{13}\text{H}_{16}\text{O}_2$  205.1225, observed  $[\text{M}+\text{H}]$  205.1229 (+0.87 ppm).





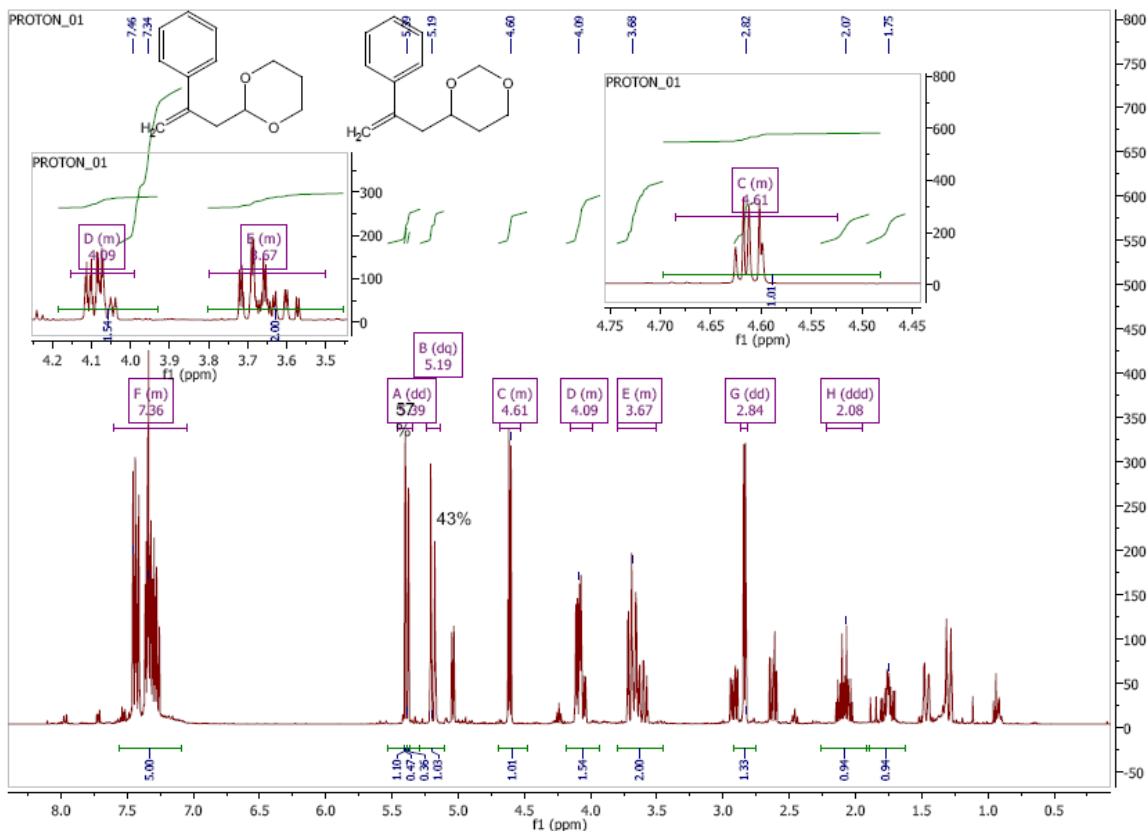
**(4-ethoxypent-1-en-2-yl)benzene (3-77):**  $^1H$  NMR (400 MHz,  $CDCl_3$ ) 7.49 – 7.17 (1 H, m), 5.32 (1 H, d,  $J$  1.6), 5.14 (1 H, d,  $J$  1.3), 3.64 – 3.26 (1 H, m), 2.93 (1 H, ddd,  $J$  14.0, 6.0, 1.1), 2.50 (1 H, ddd,  $J$  14.0, 7.3, 1.0), 1.14 (1 H, t,  $J$  6.9).  $^{13}C$  NMR (101 MHz,  $CDCl_3$ ) 145.92, 141.39, 128.27, 127.19, 126.35, 114.68, 73.73, 63.67, 42.75, 19.51, 15.57. **HRMS:** Calculated for  $C_{13}H_{18}O$  191.143, observed  $[M+H]$  191.1427 (-1.72 ppm)

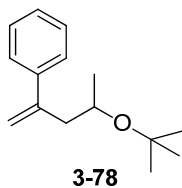
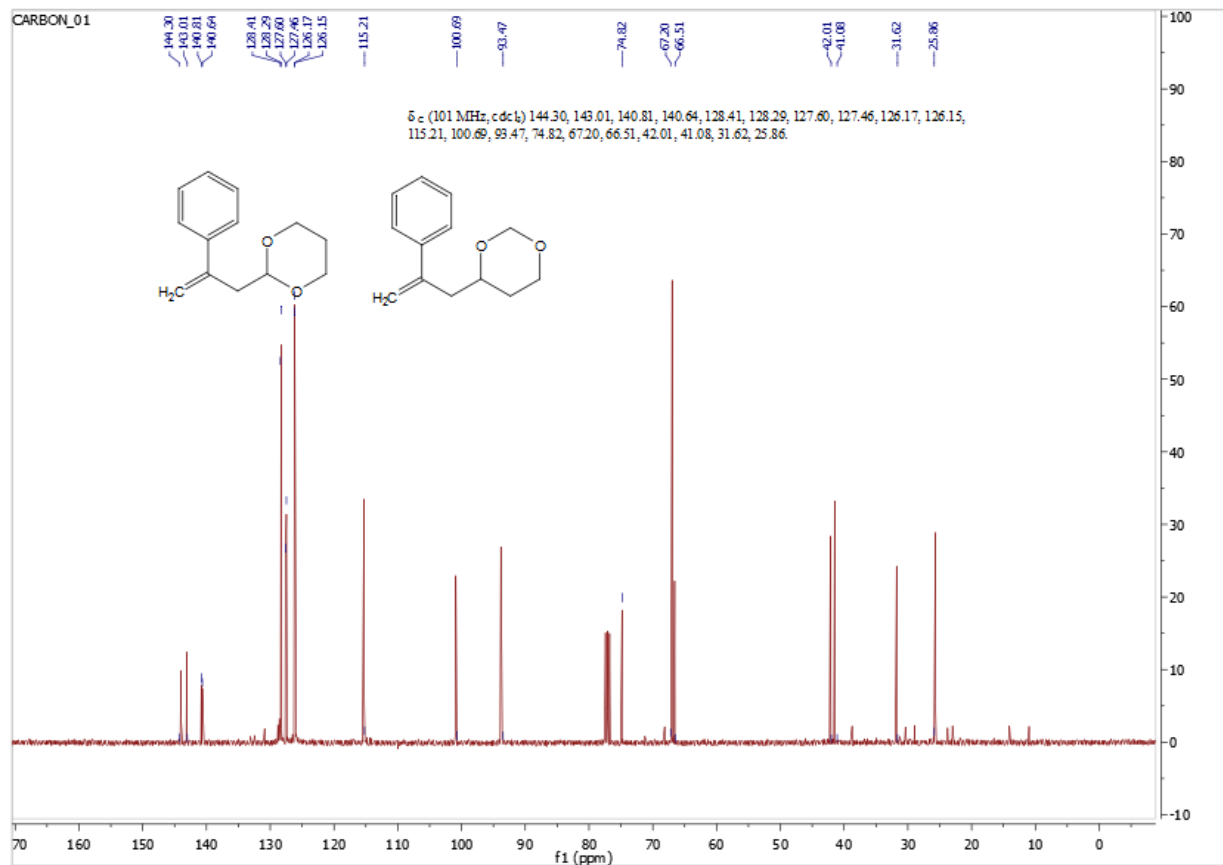




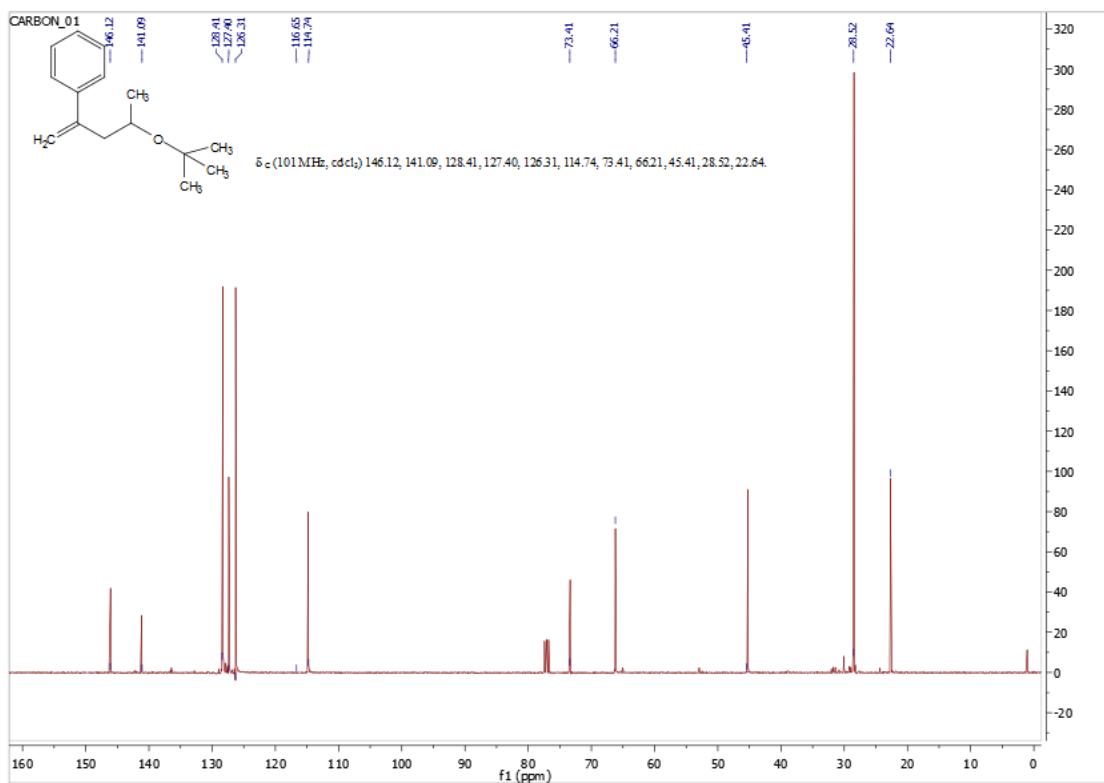
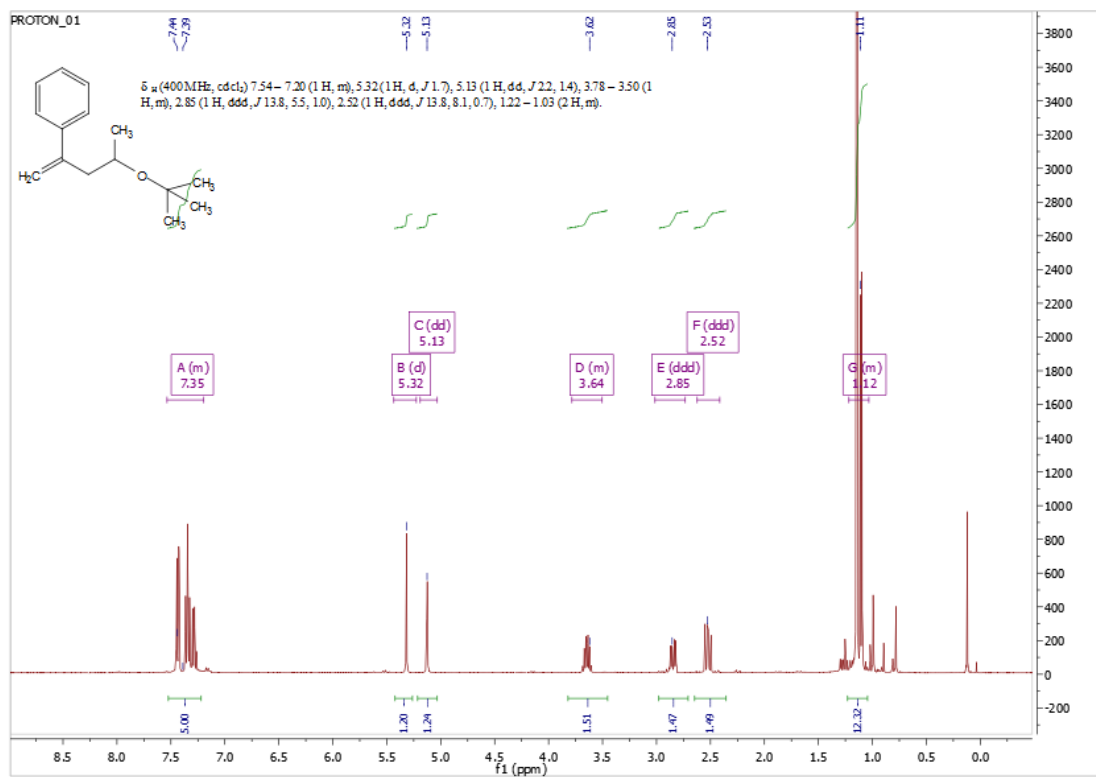
**2-(2-phenylallyl)-1,3-dioxane (major:60%) and 4-(2-phenylallyl)-1,3-dioxane(minor:40%)**

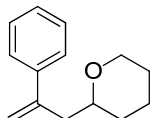
**<sup>1</sup>H NMR** (400 MHz, CDCl<sub>3</sub>) 7.61 – 7.04 (5 H, m), 5.39 (1 H, dd, *J* 9.5, 1.4), 5.19 (1 H, dq, *J* 12.3, 1.3), 4.68 – 4.52 (1 H, m), 4.15 – 3.99 (1 H, m), 3.80 – 3.50 (2 H, m), 2.84 (1 H, dd, *J* 5.3, 1.1), 2.08 (1 H, ddd, *J* 13.4, 13.0, 10.0). **<sup>13</sup>C NMR** (101 MHz, CDCl<sub>3</sub>) 144.30, 143.01, 140.81, 140.64, 128.41, 128.29, 127.60, 127.46, 126.17, 126.15, 115.21, 100.69, 93.47, 74.82, 67.20, 66.51, 42.01, 41.08, 31.62, 25.86. **HRMS:** Calculated for C<sub>13</sub> H<sub>16</sub> O<sub>2</sub> 205.1223, observed [M+H] 205.1225 (+0.89 ppm).





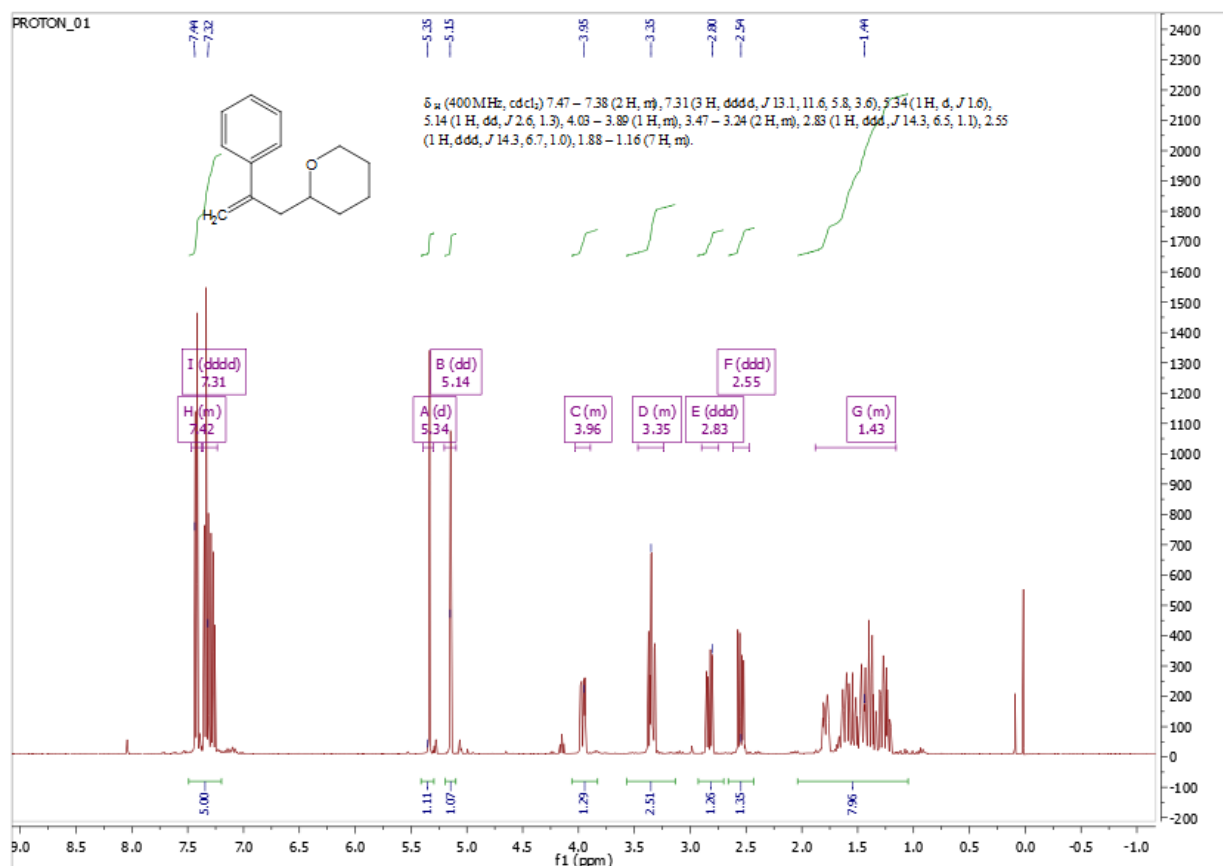
**(4-(tert-butoxy)pent-1-en-2-yl)benzene (3-78):**  $^1\text{H NMR}$  (400 MHz,  $\text{CDCl}_3$ ) 7.54 – 7.20 (1 H, m), 5.32 (1 H, d,  $J$  1.7), 5.13 (1 H, dd,  $J$  2.2, 1.4), 3.78 – 3.50 (1 H, m), 2.85 (1 H, ddd,  $J$  13.8, 5.5, 1.0), 2.52 (1 H, ddd,  $J$  13.8, 8.1, 0.7), 1.22 – 1.03 (2 H, m).  $^{13}\text{C NMR}$  (101 MHz,  $\text{CDCl}_3$ ) 146.12, 141.09, 128.41, 127.40, 126.31, 114.74, 73.41, 66.21, 45.41, 28.52, 22.64. **HMRS:** Difficult to ionize using ESI or APCI ionization methods. (GC-MS analysis in section 5.5)

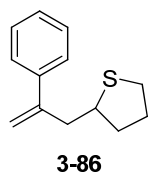
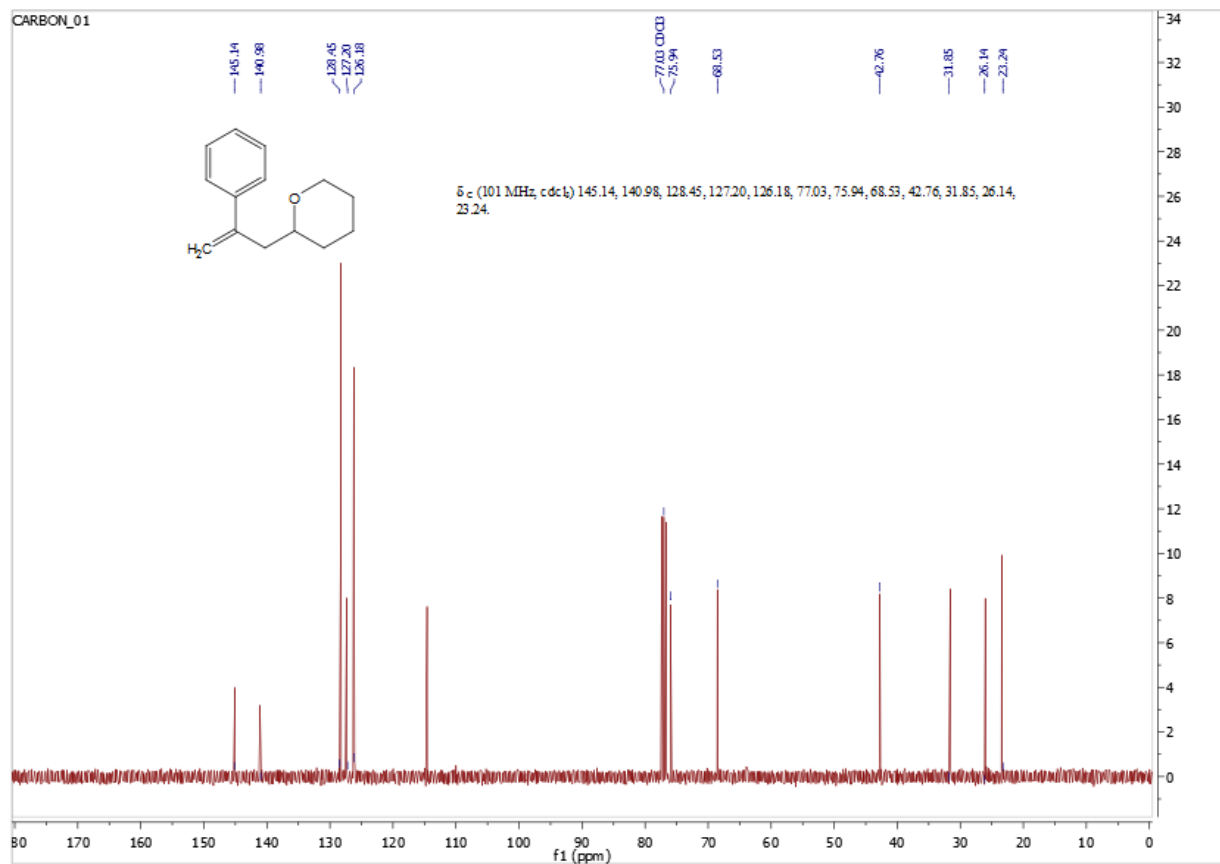




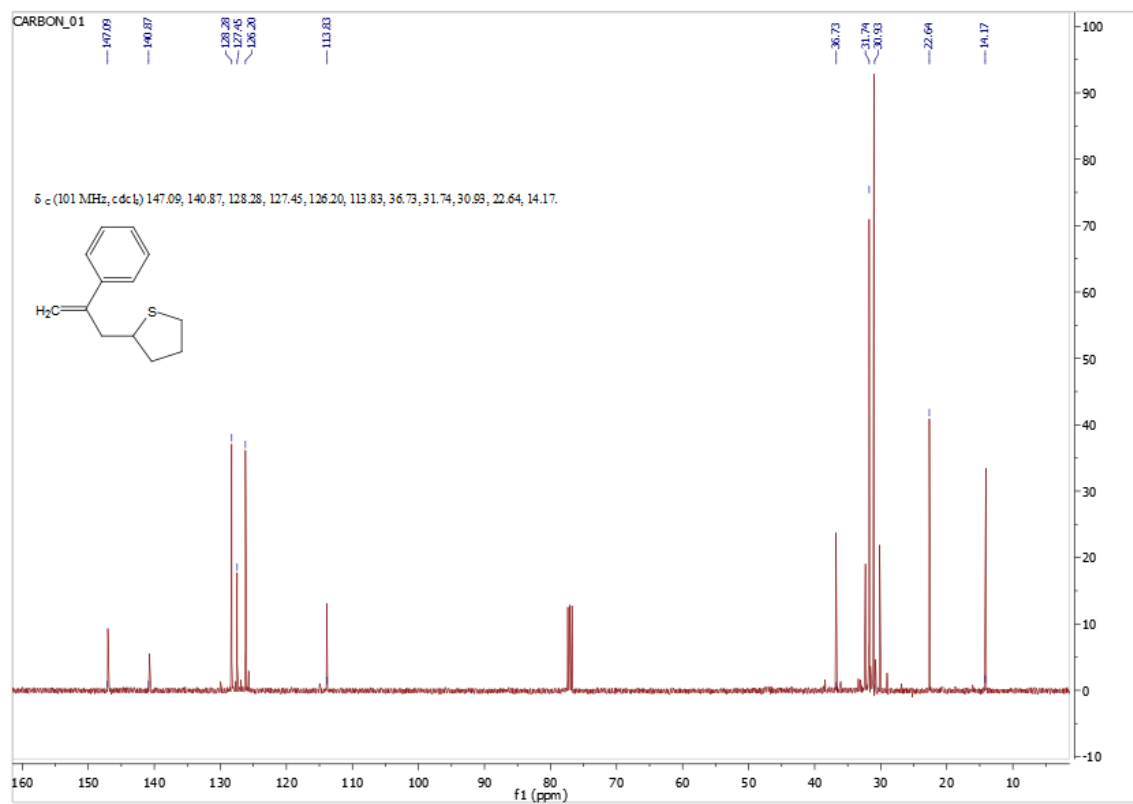
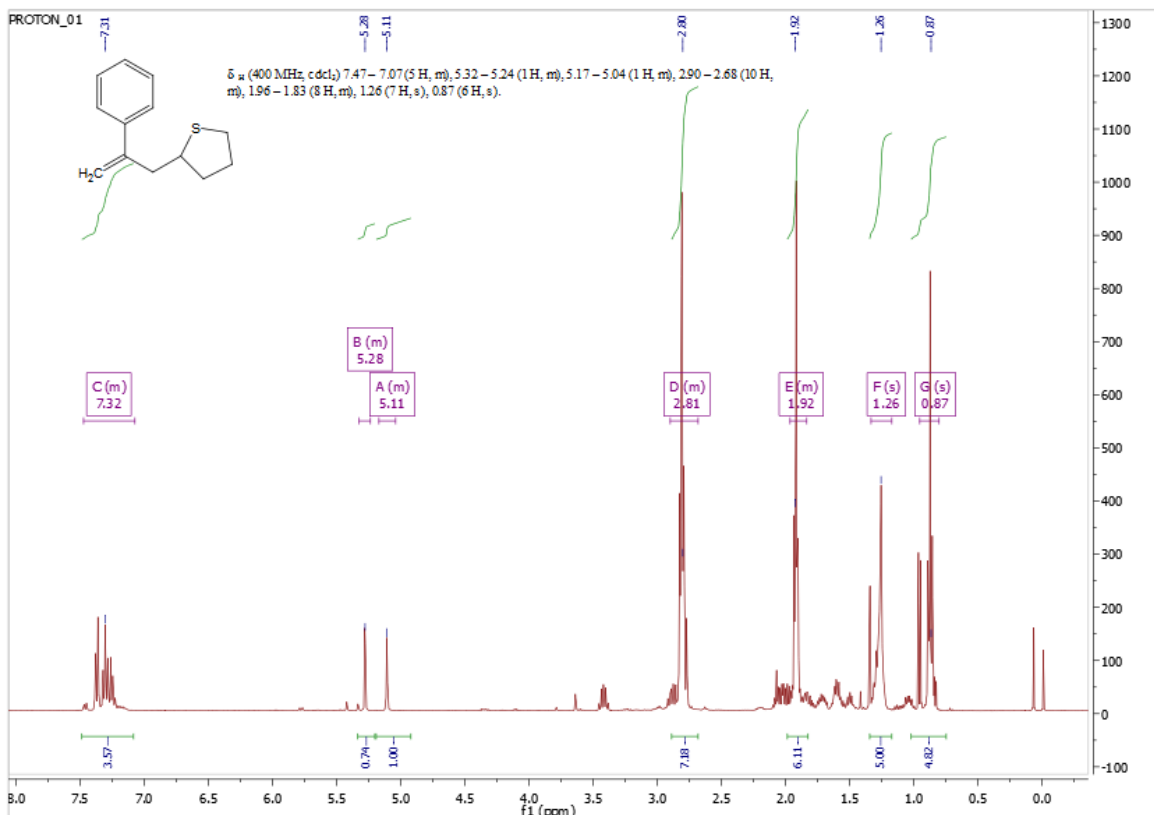
**3-82**

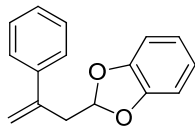
**2-(2-phenylallyl)tetrahydro-2H-pyran (3-82):**  $^1\text{H}$  NMR (400 MHz,  $\text{CDCl}_3$ ) 7.47 – 7.38 (2 H, m), 7.31 (3 H, dddd,  $J$  13.1, 11.6, 5.8, 3.6), 5.34 (1 H, d,  $J$  1.6), 5.14 (1 H, dd,  $J$  2.6, 1.3), 4.03 – 3.89 (1 H, m), 3.47 – 3.24 (2 H, m), 2.83 (1 H, ddd,  $J$  14.3, 6.5, 1.1), 2.55 (1 H, ddd,  $J$  14.3, 6.7, 1.0), 1.88 – 1.16 (7 H, m).  $^{13}\text{C}$  NMR (101 MHz,  $\text{CDCl}_3$ ) 145.14, 140.98, 128.45, 127.20, 126.18, 75.94, 68.53, 42.76, 31.85, 26.14, 23.24. **HMRS:** Calculated for  $\text{C}_{14}\text{H}_{18}\text{O}$  203.143, observed  $[\text{M}+\text{H}]$  203.1436 (+2.54 ppm).





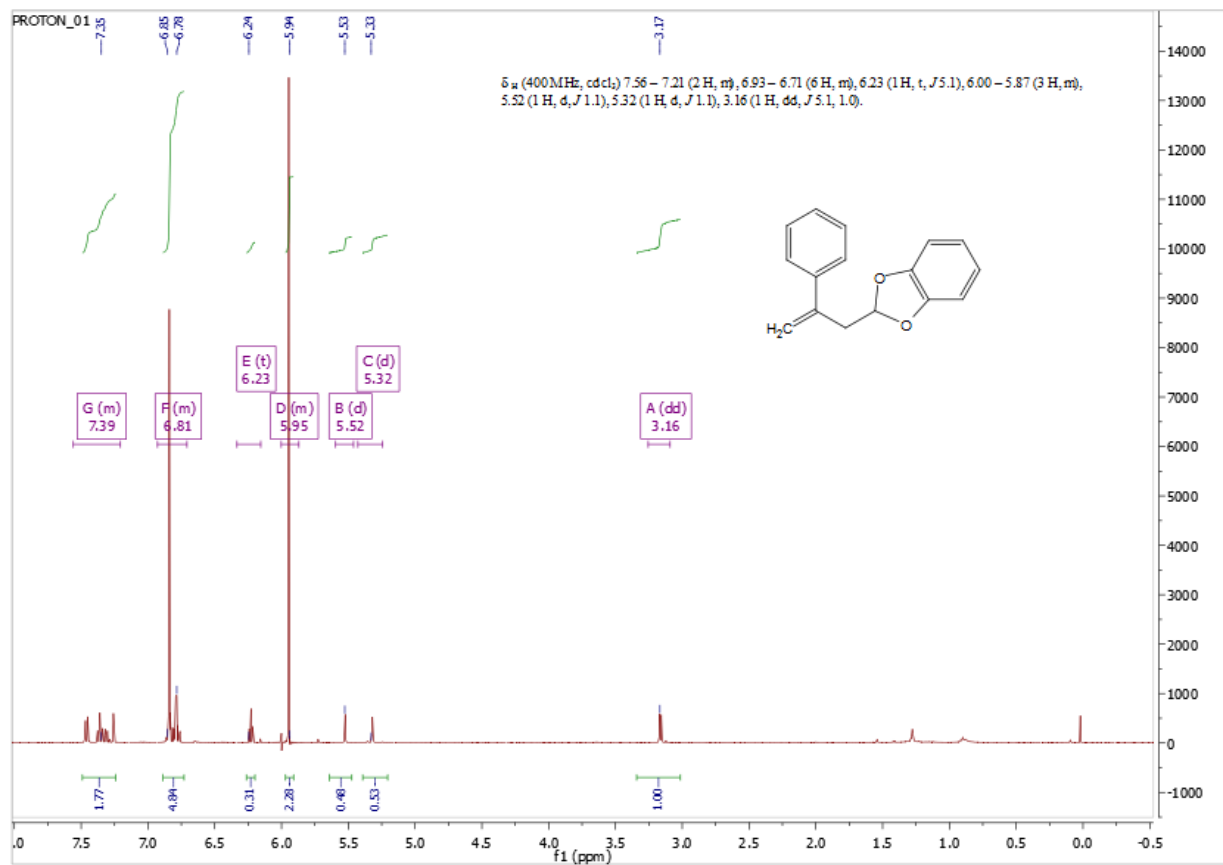
**2-(2-phenylallyl)tetrahydrothiophene (3-86):**  $^1\text{H NMR}$  (400 MHz,  $\text{CDCl}_3$ ) 7.47 – 7.07 (5 H, m), 5.32 – 5.24 (1 H, m), 5.17 – 5.04 (1 H, m), 2.90 – 2.68 (10 H, m), 1.96 – 1.83 (8 H, m), 1.26 (7 H, s), 0.87 (6 H, s).  $^{13}\text{C NMR}$  (101 MHz,  $\text{CDCl}_3$ ) 147.09, 140.87, 128.28, 127.45, 126.20, 113.83, 36.73, 31.74, 30.93, 22.64, 14.17. **HRMS:** Calculated for  $\text{C}_{13}\text{H}_{16}\text{S}$ : 205.1045, observed  $[\text{M}+\text{H}]$  205.1052 (+3.27 ppm)

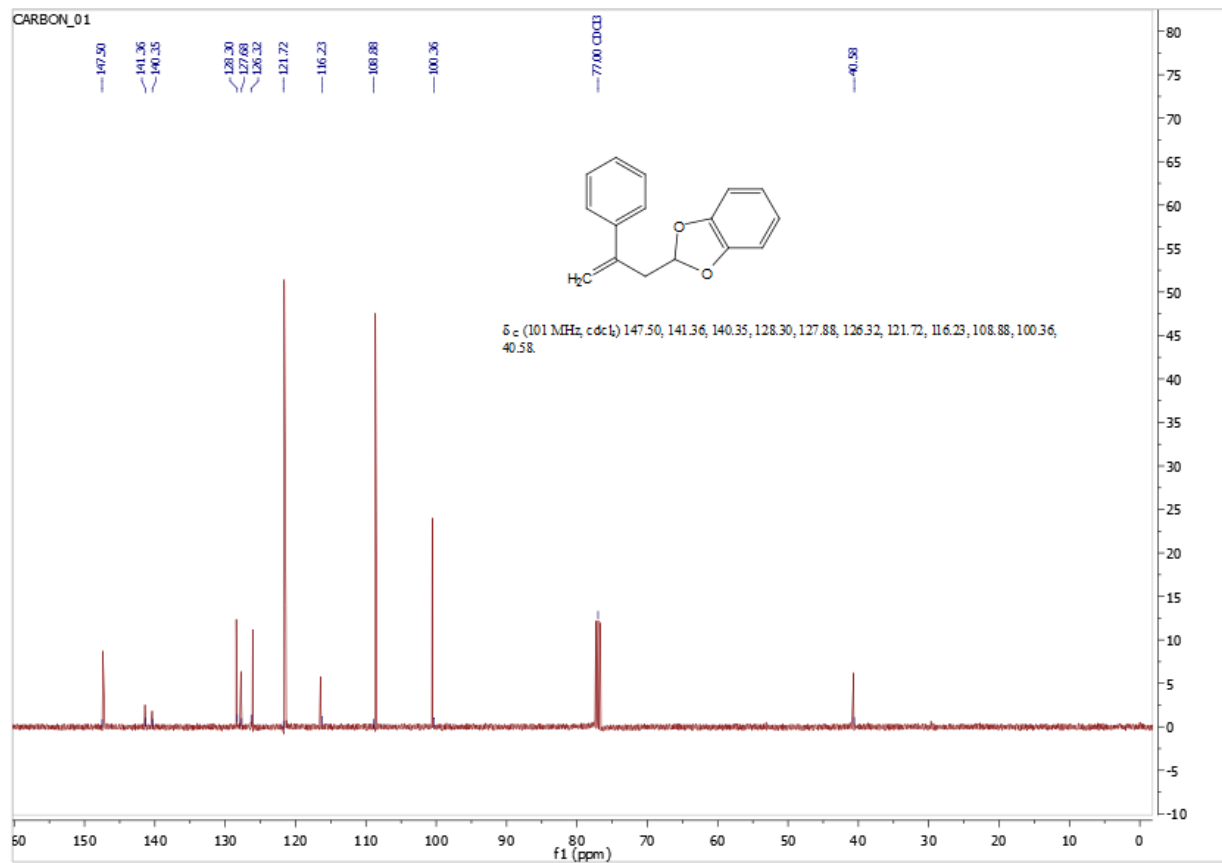


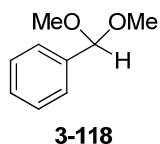


**3-88**

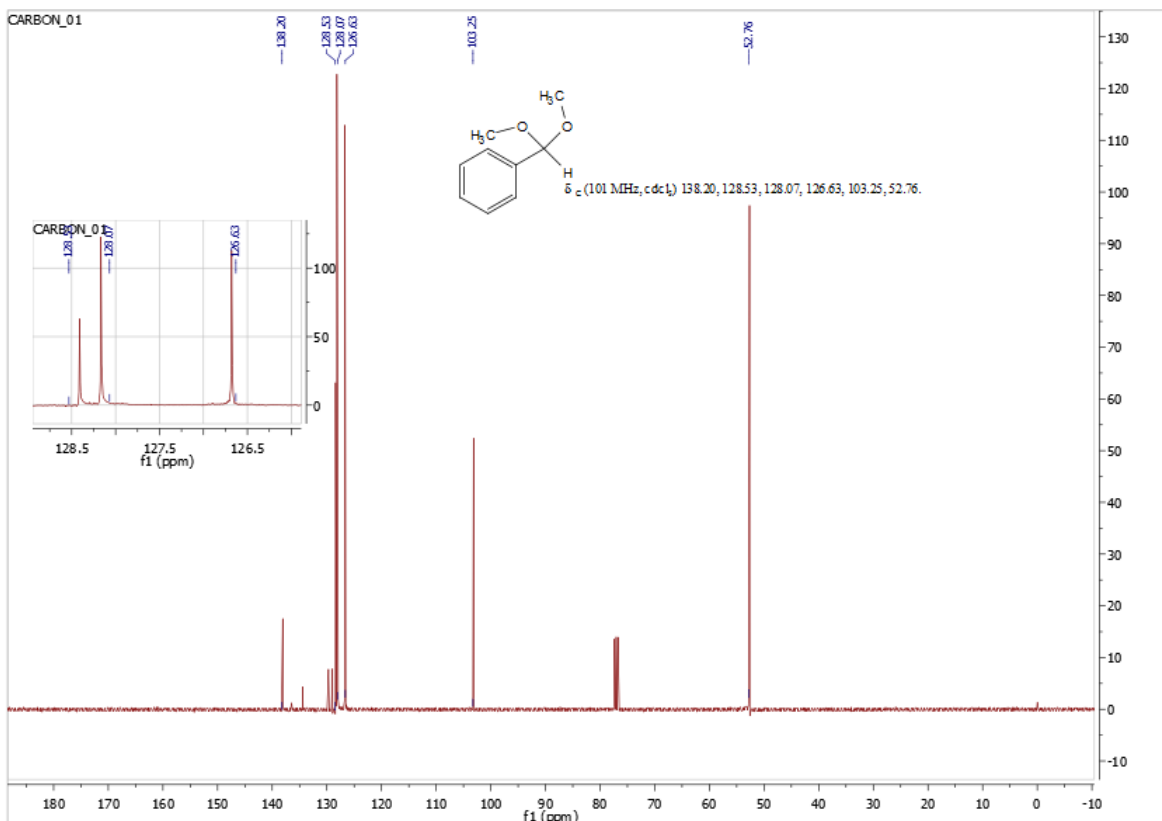
**2-(2-phenylallyl)benzo[1,3]dioxole (3-88):**  $^1\text{H NMR}$  (400 MHz,  $\text{CDCl}_3$ ) 7.56 – 7.21 (2 H, m), 6.93 – 6.71 (6 H, m), 6.23 (1 H, t,  $J$  5.1), 6.00 – 5.87 (3 H, m), 5.52 (1 H, d,  $J$  1.1), 5.32 (1 H, d,  $J$  1.1), 3.16 (1 H, dd,  $J$  5.1, 1.0).  $^{13}\text{C NMR}$  (101 MHz,  $\text{CDCl}_3$ ) 147.50, 141.36, 140.35, 128.30, 127.88, 126.32, 121.72, 116.23, 108.88, 100.36, 40.58. **HMRS:** Calculated for  $\text{C}_{16}\text{H}_{12}\text{O}_2$  237.0910, observed  $[\text{M}+\text{H}]$  237.0927 (+7.1)

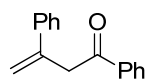






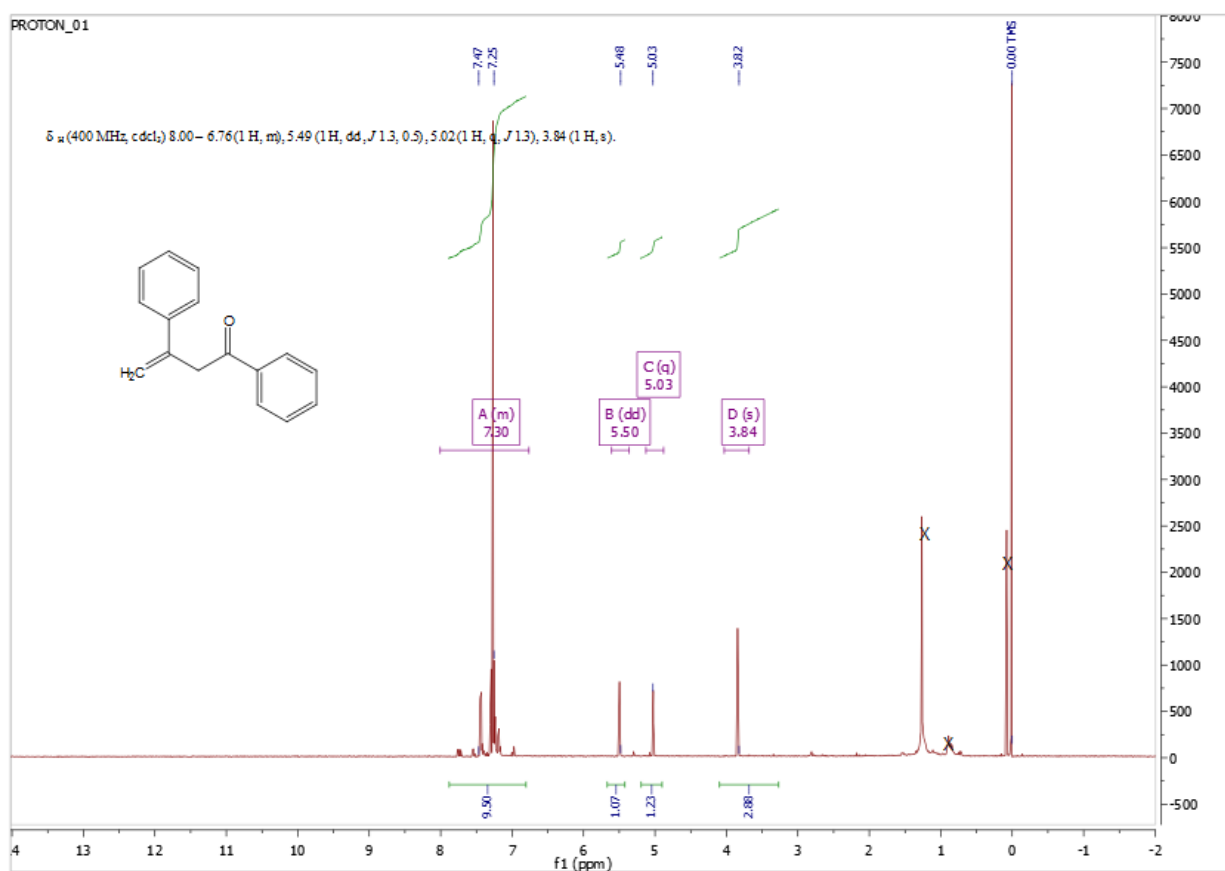
**(dimethoxymethyl)benzene (3-118):** Based on a literature procedure<sup>1</sup>. A mixture of benzaldehyde (2 g, 0.01886 mol), CoCl<sub>2</sub> (dry, 0.121 g, 0.000943 mol) and dry methanol (80 mL) were refluxed at 110 °C for 3 h, using CaCl<sub>2</sub> guard tube over reflux condenser. Methanol was evaporated under reduced pressure. Ethyl acetate (5 mL) was added to the residue. Co(II) salt was filtered and filtrate was passed through a short column of alumina (basic) using 5% ethyl acetate in hexane. Procedure yielded pure dimethyl acetal product which was characterized by NMR. <sup>1</sup>H NMR (400 MHz, CDCl<sub>3</sub>) 7.50 – 7.30 (4 H, m), 5.41 (1 H, s), 3.34 (6 H, s). <sup>13</sup>C NMR (101 MHz, CDCl<sub>3</sub>) 138.20, 128.53, 128.07, 126.63, 103.25, 52.76.

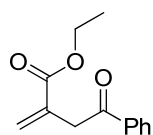
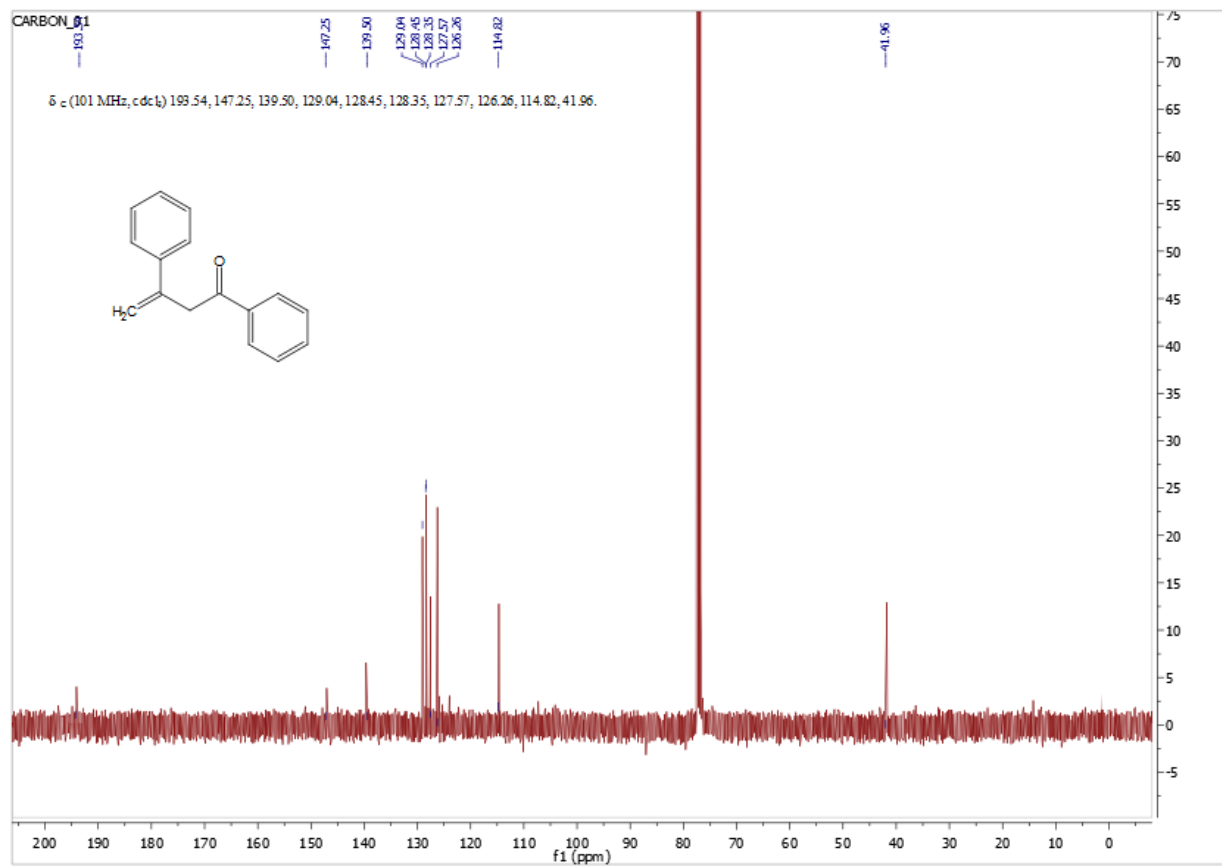




**3-119 (Z=Ph)**

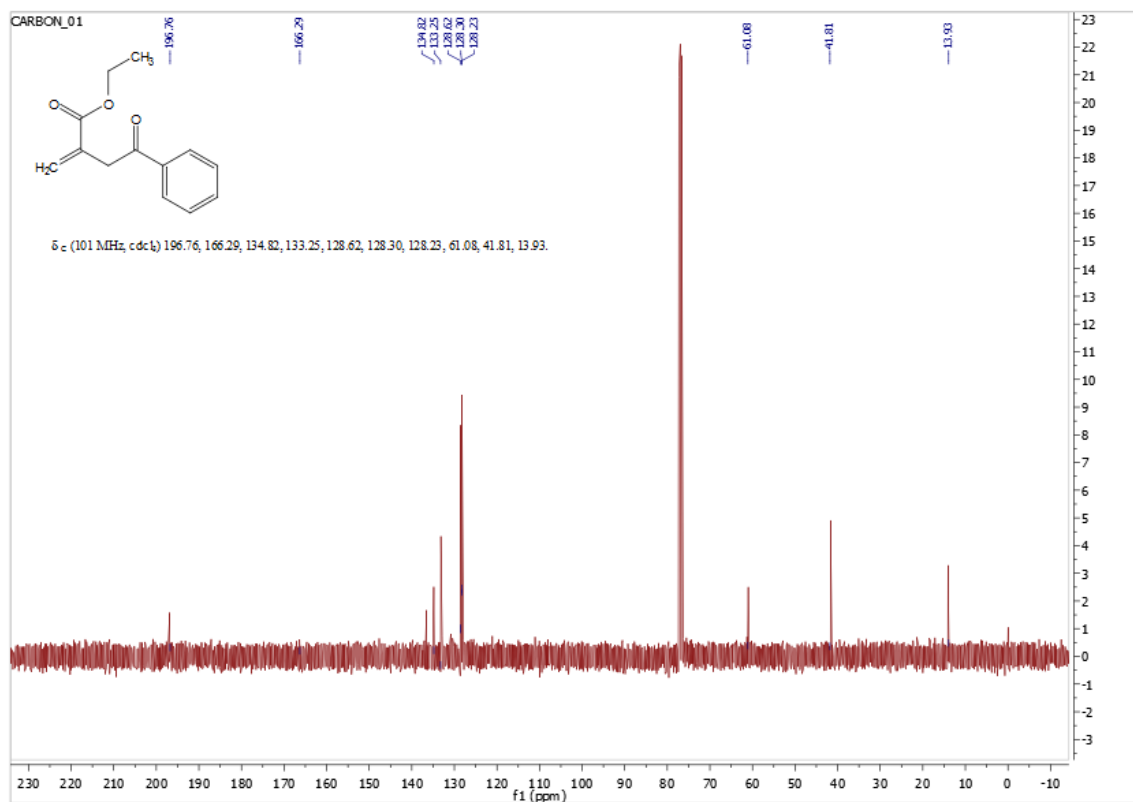
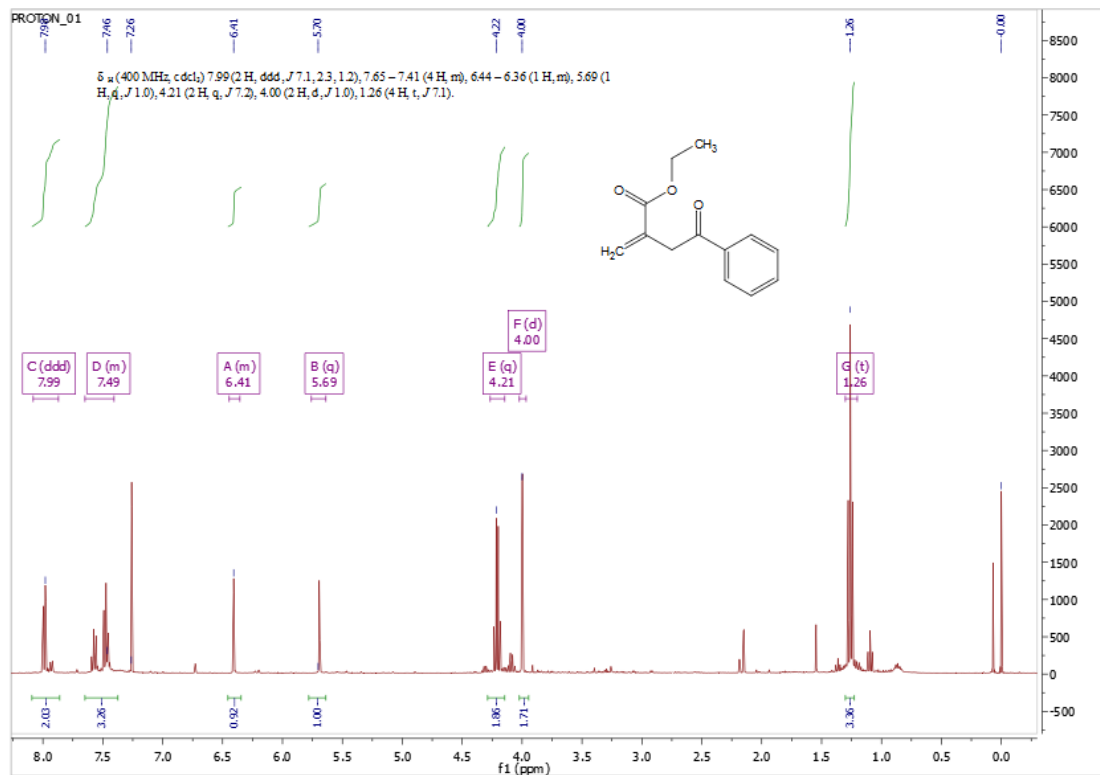
**1,3-diphenylbut-3-en-1-one (3-119, Z=Ph):**  $^1\text{H NMR}$  (400 MHz,  $\text{CDCl}_3$ ) 8.00 – 6.76 (1 H, m), 5.49 (1 H, dd,  $J$  1.3, 0.5), 5.02 (1 H, q,  $J$  1.3), 3.84 (1 H, s).  $^{13}\text{C NMR}$  (101 MHz,  $\text{CDCl}_3$ ) 193.54, 147.25, 139.50, 129.04, 128.45, 128.35, 127.57, 126.26, 114.82, 41.96. **HRMS:** Calculated for  $\text{C}_{16}\text{H}_{14}\text{O}$ , 223.2811, observed 223.1112 (+5.69 ppm)





**3-119 Z=CO<sub>2</sub>Et**

**Ethyl 2-methylene-4-oxo-4-phenylbutanoate (3-119, Z=CO<sub>2</sub>Et):** <sup>1</sup>H NMR (400 MHz, CDCl<sub>3</sub>) 7.99 (2 H, ddd, *J* 7.1, 2.3, 1.2), 7.65 – 7.41 (4 H, m), 6.44 – 6.36 (1 H, m), 5.69 (1 H, q, *J* 1.0), 4.21 (2 H, q, *J* 7.2), 4.00 (2 H, d, *J* 1.0), 1.26 (4 H, t, *J* 7.1). <sup>13</sup>C NMR (101 MHz, CDCl<sub>3</sub>) 196.76, 166.29, 134.82, 133.25, 128.62, 128.30, 128.23, 61.08, 41.81, 13.93. **HRMS:** Calculated for C<sub>13</sub>H<sub>15</sub>O<sub>3</sub> 219.1016, observed 219.101 (-2.63).



### 5.3 Kinetic chain length calculations- Allyl transfer reactions of ethers

Time (min)	Log P/R
15	2.99
30	2.78
60	2.09
120	2.24
180	1.96
360	0.14

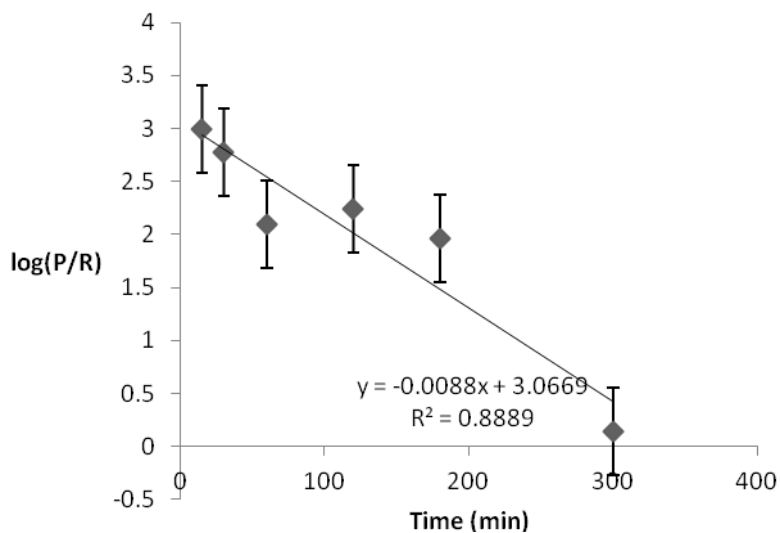


**Figure 5-1: Reaction of 2-10 with THF**

Initial chain length 1200 ( $\pm 60$ ) (120 °C, (2-10) 0.022 M, 0.00053 M, THF 4 mL)

Time (min)	Log P/R
15	1.94
60	1.65
300	1.15

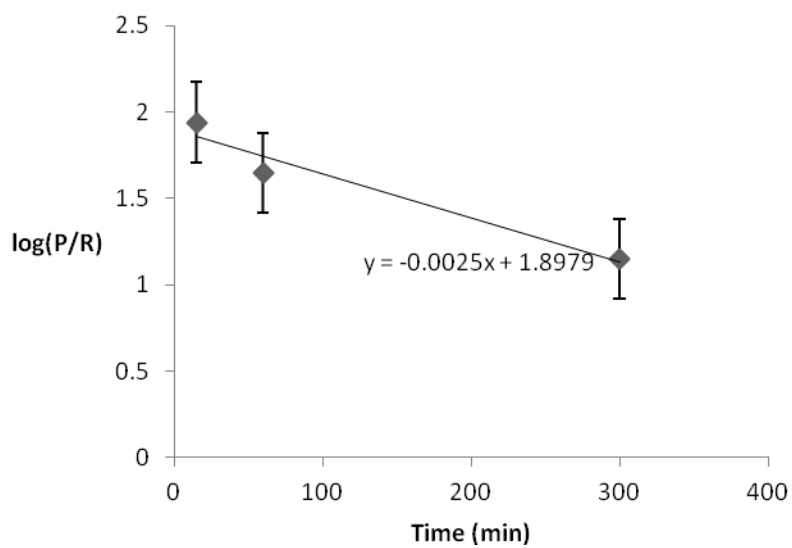


**Figure 5-2: Reaction of 2-10 with 2-MeTHF (for major product)**

Initial chain length= 80 ( $\pm 18$ ) (120 °C, (2-10 0.022 M, 0.00053 M, 2-MeTHF 4 mL)

Time (min)	Log P/R
15	2.97
30	2.75
60	2.64
120	2.24
180	1.94
360	0.51

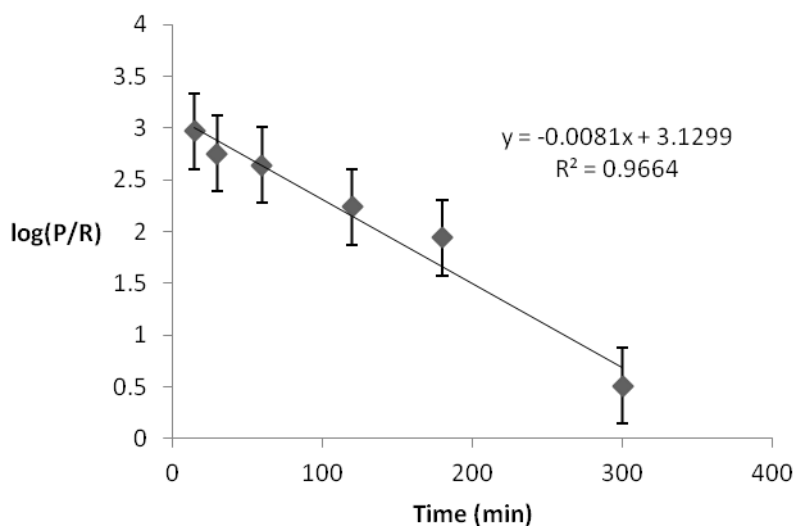


**Figure 5-3: Reaction of 2-10 with 1,4-dioxane**

Initial chain length= 1300 ( $\pm 360$ ) (120 °C, (2-10 0.022 M, 0.00053 M, 1,4-dioxane 4 mL)

Time (min)	Log P/R
5	4.02
10	3.48
15	3.44
25	2.86

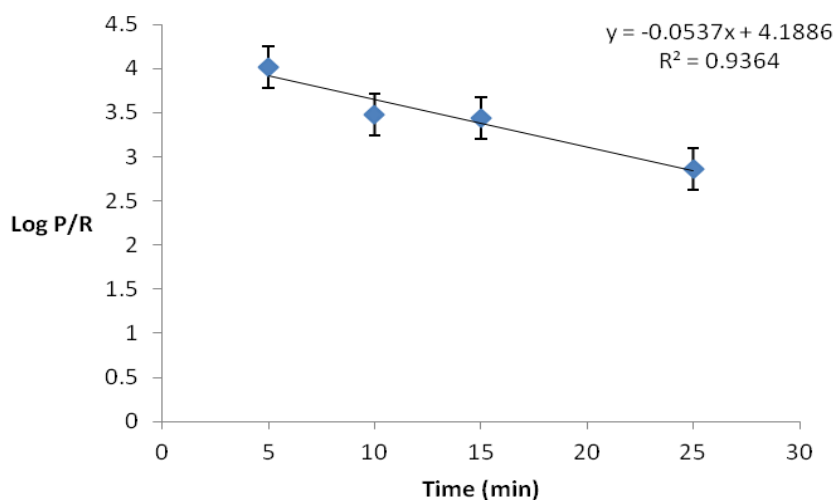


**Figure 5-4: Reaction of 2-11 with THF**

Initail chain length= 15000 ( $\pm 5000$ ) (120 °C, (2-11 0.022 M, 0.00053 M, THF 4 mL)

Time (min)	Log P/R
30	2.03
45	1.99
60	1.75
90	1.34

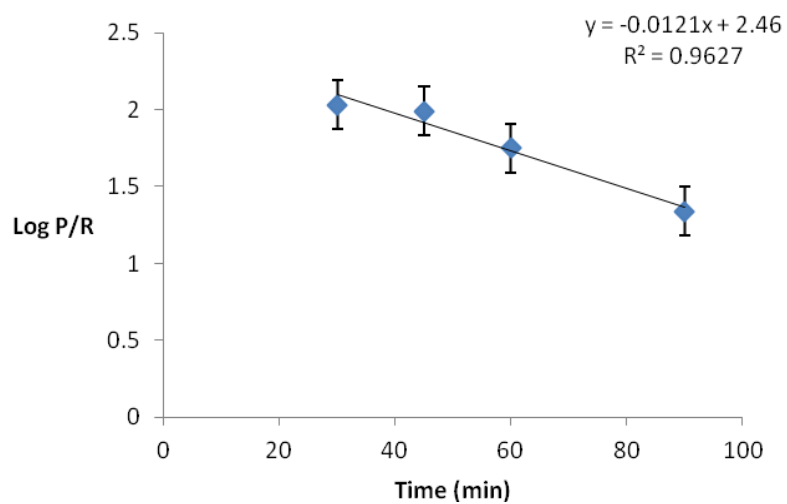


**Figure 5-5: Reaction of 2-11 with 2-MeTHF (for major product)**

Initial chain length= 300 ( $\pm 70$ ) (For major product **3-95**) (120 °C, (**2-11** 0.022 M, 0.00053 M, 2-MeTHF 4 mL)

Time (min)	Log P/R
30	2.61
45	2.14
60	1.82
90	1.43

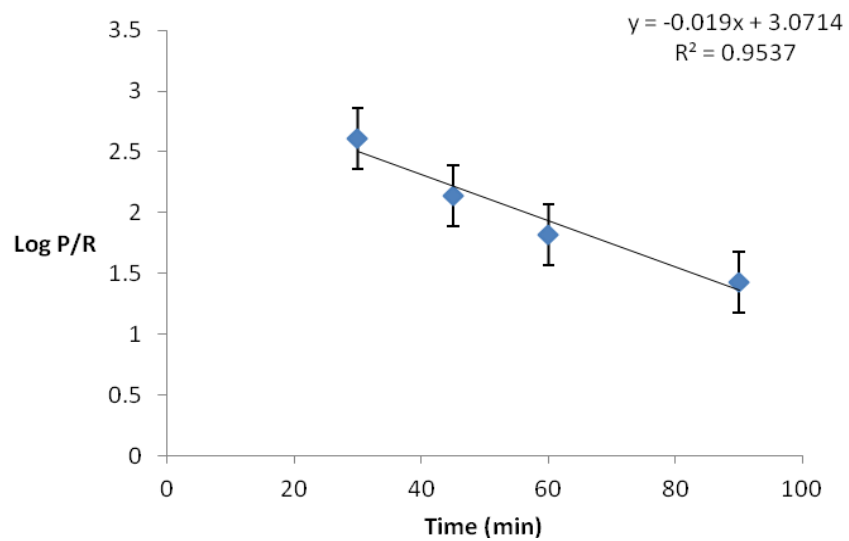


**Figure 5-6: Reaction of 2-11 with 2-MeTHF**

Initial chain length= 1200 ( $\pm 490$ ) (for mixture of all regioisomeric product: **3-95+3-97**) (120 °C,  
**(2-11** 0.022 M, 0.00053 M, 2-MeTHF 4 mL)

Time (min)	Log P/R
15	3.81
30	3.32
45	3.39
60	2.94
90	2.73

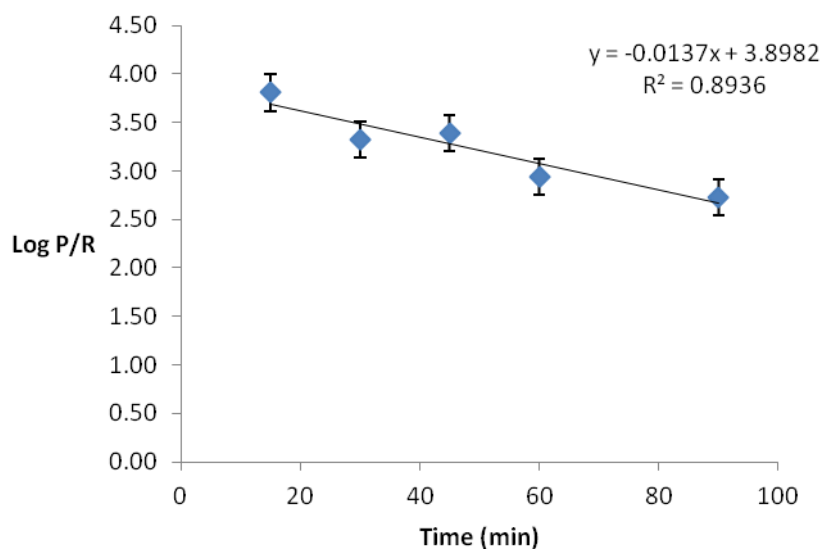


**Figure 5-7: Reaction of 2-11 with 1,4-dioxane**

Initial chain length= 8000 ( $\pm 2700$ ) (120 °C, (2-11 0.022 M, 0.00053 M, 1,4-dioxane 4 mL)

Time (min)	Log P/R
10	1.66
15	0.99
20	1.01
30	0.91
45	0.62

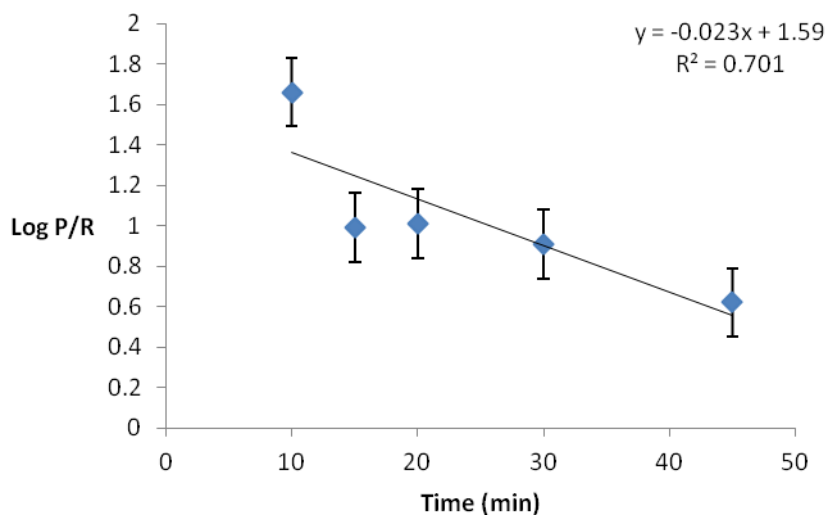


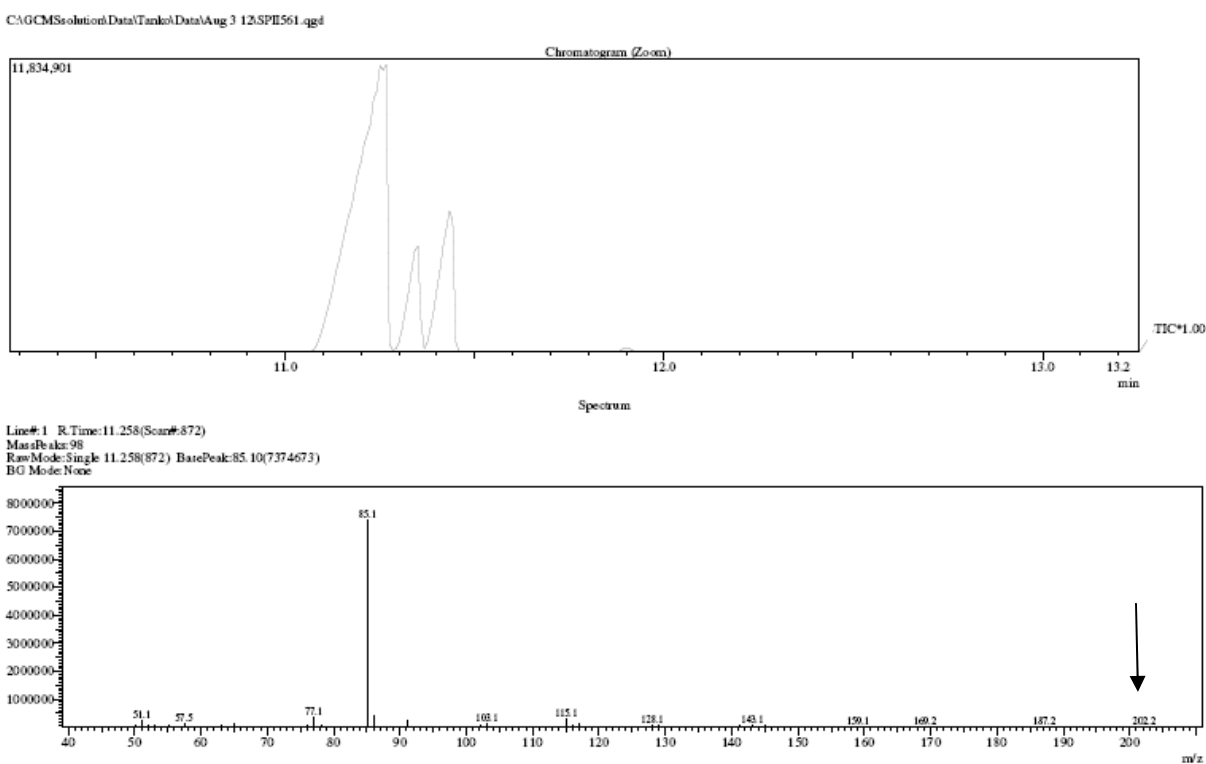
**Figure 5-8: Reaction of 2-11 with THF (3 eq.) in acetonitrile (0.8 M)**

Initial chain length= 40 ( $\pm 20$ ) (120 °C, (2-11 0.022 M, 0.00053 M, THF 0.06 M)

## 5.4 GC-MS evidences for regioisomers (3-96 and 3-98) in allyl transfer reaction of 2-MeTHF with 2-10

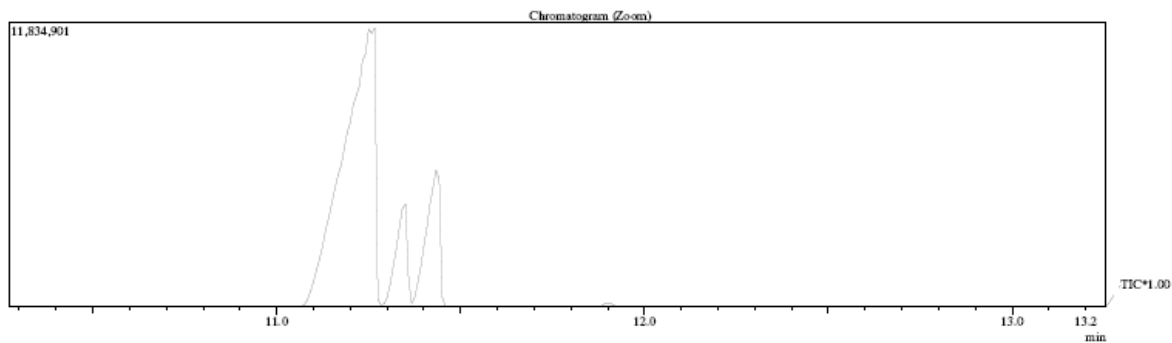
**Figure 5-9:** GC-MS chromatogram showing products of the allyl transfer reaction of **2-10** with 2-MeTHF.

### 1) Compound at retention time 11.25 (Fragments: 202.2, 187.2, 115.1, 85.1)



## 2) Compound at retention time 11.34 (Fragments: 202.3, 187.6, 115.1, 85.1)

C:\GCMSolution\Data\tank\1\Aug 3 12.5PE561.qgd

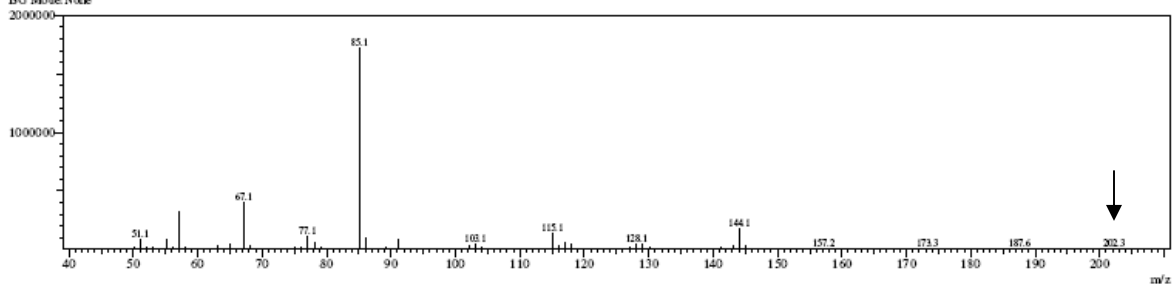


Line# 1 R-Time:11.342(Scan#882)

MassPeak: 73

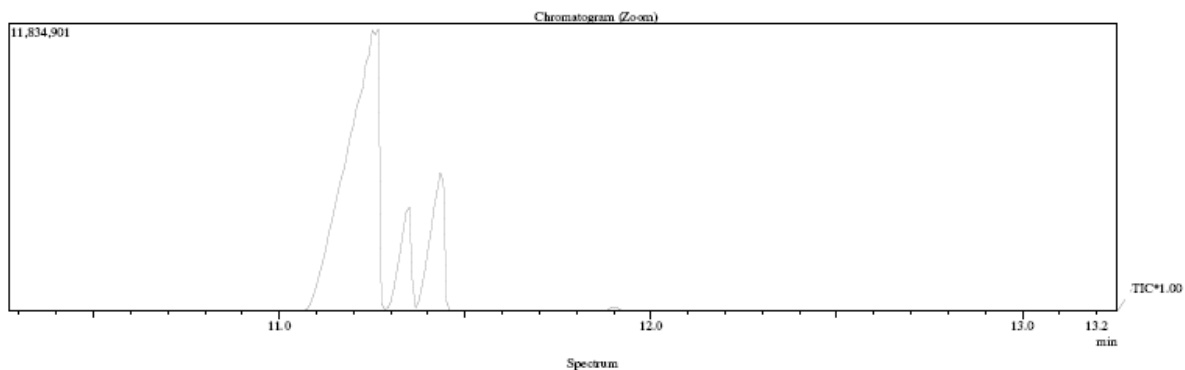
Raw Mode: Single 11.342(882) BasePeak: 85.10(1717582)

BG Mode: None

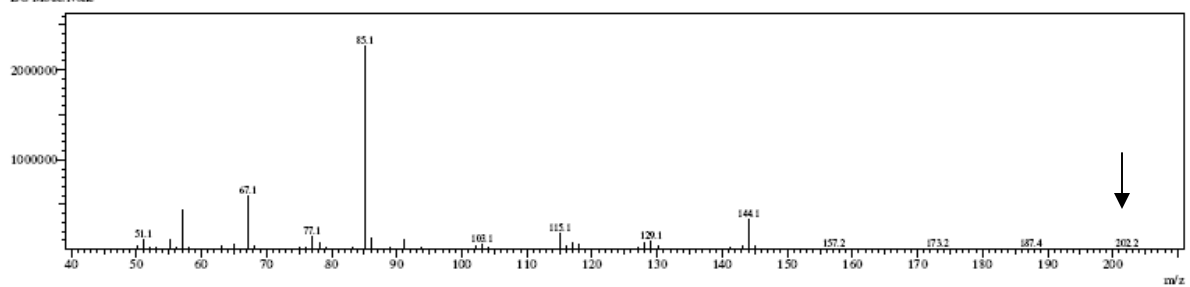


### 3) Compound at retention time 11.43 (Fragments 202.2, 187.4, 115.1, 85.1)

C:\GCMSolution\Data\tankol\data\Aug 3 12\SPI551.qgd



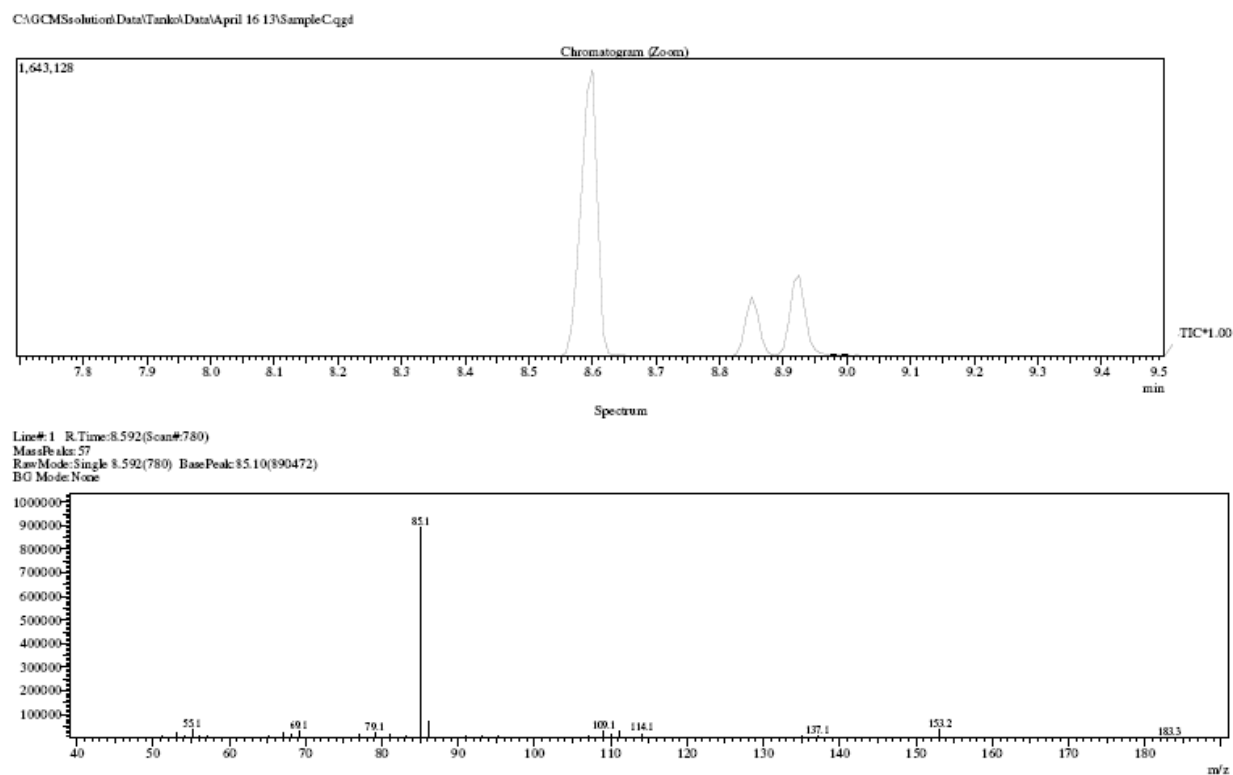
Line# 1 R Time: 11.433 (Scan#: 893)  
Mass Peaks: 78  
Raw Mode: Single 11.433 (893) Base Peak: 85.10 (2259320)  
BG Mode: None



## 5.4.1 GC-MS evidences for regioisomers (3-97 and 3-99) in allyl transfer reaction of 2-MeTHF with 2-11

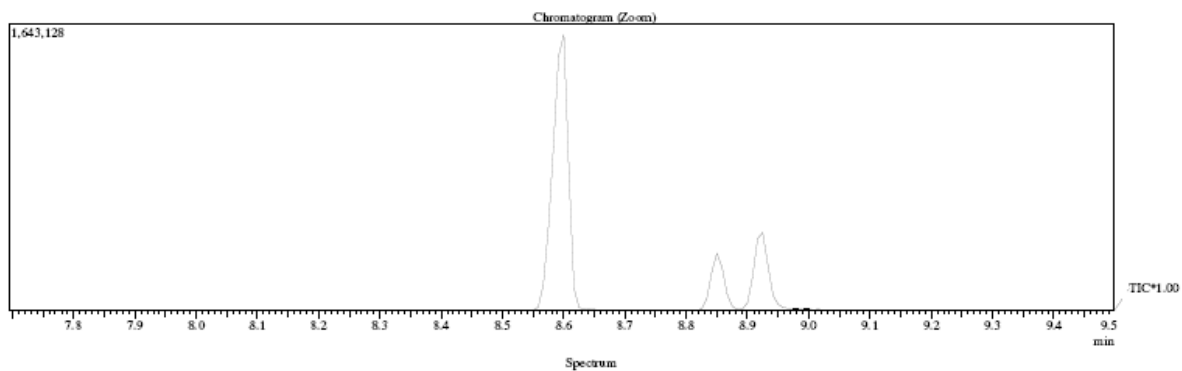
**Figure 5-10:** GC-MS chromatogram showing products from the allyl transfer reaction of **2-11** with 2-MeTHF

### 1) Compound at retention time **8.59** (Fragment 153.2, 85.1, 79.1, 69.1, 55.1)

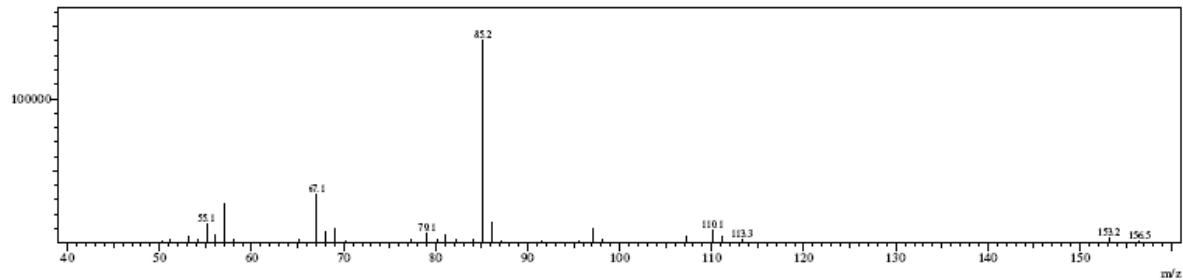


## 2) Compound at retention time 8.85 (Fragments 153.2, 85.2, 79.1, 67.1, 55.1)

C:\GCMSolution\Data\tank\data\April 16 13\Sample C.qgd

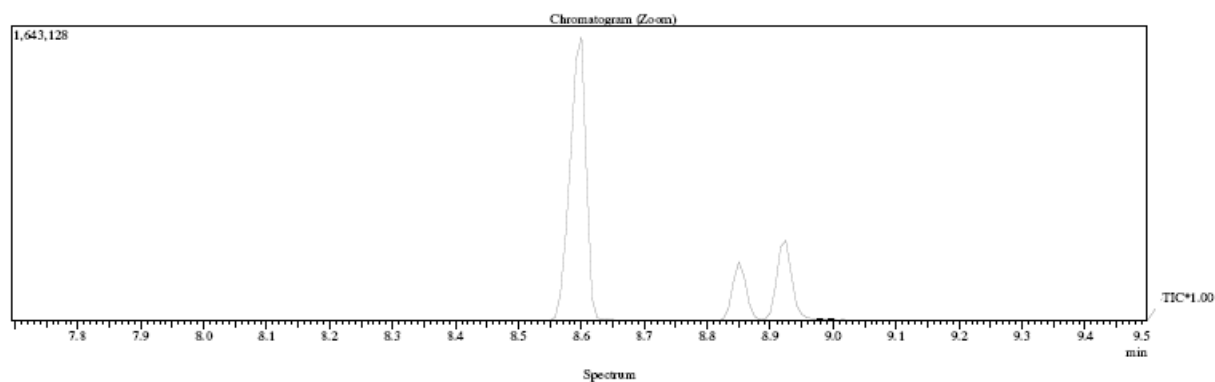


Line# 1 R.Time:8.850(Scan#811)  
MassPeak:32  
RawMode:Single 8.850(811) BasePeak:85.15(140095)  
BG Mode:None

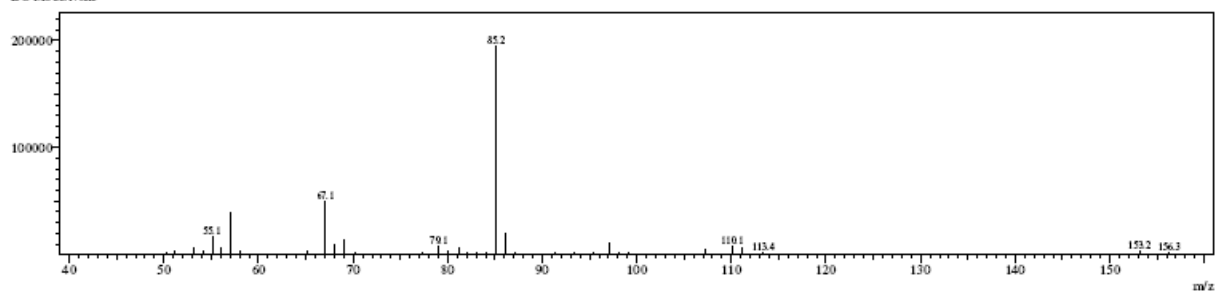


### 3) Compound at retention time 8.92 (Fragment 153.2, 85.2, 79.1, 67.1, 55.1)

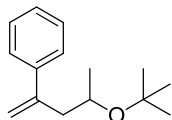
C:\GCMS\data\Tankol\Data\April 16 13\Sample C.ggd



Line# 1 R.Time: 8.925 (Scan# 820)  
MassReak: 36  
RawMode: Single 8.925(820) BasePeak: 85.15(194415)  
BG Mode: None



## 5.5 GC-MS analysis of 3-78 (Note: This product was difficult to ionize via ESI or APCI ionization methods)



**3-78**

Chemical Formula: C<sub>15</sub>H<sub>22</sub>O  
Molecular Weight: 218.33

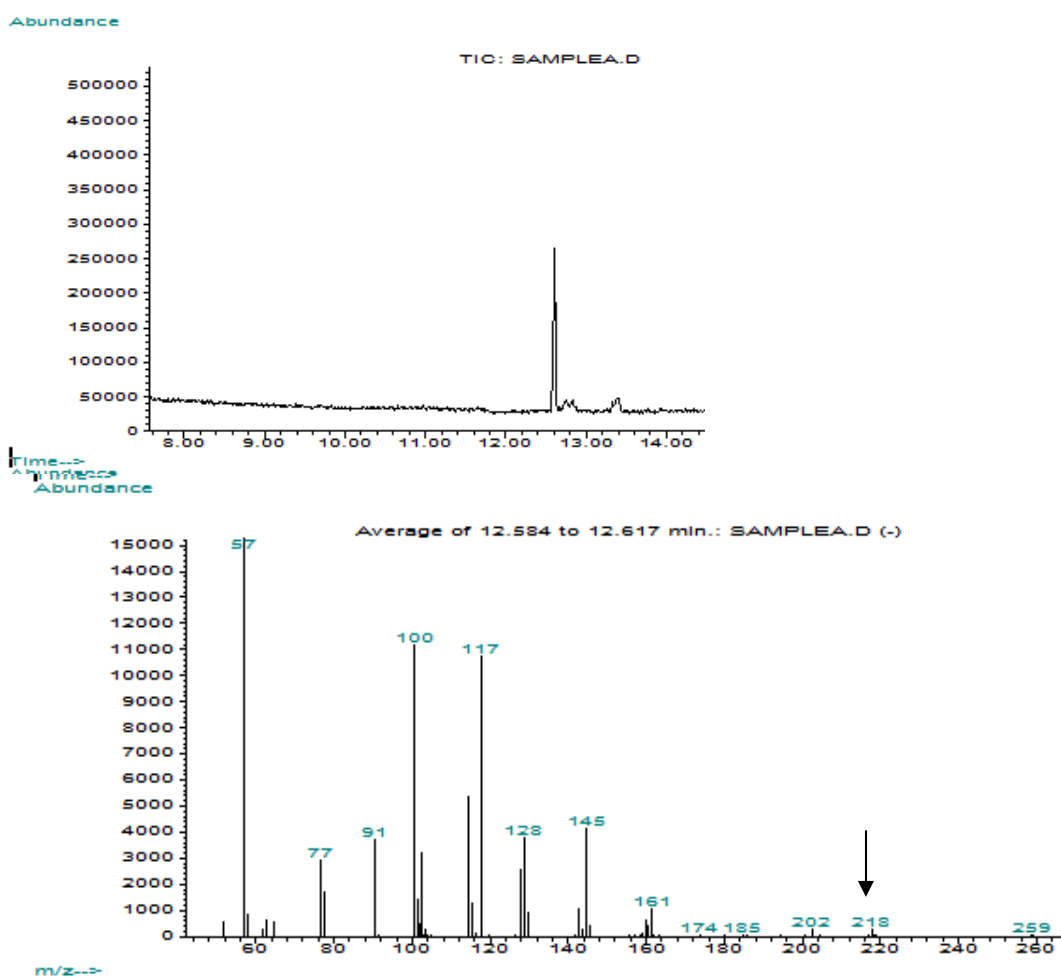


**Figure 5-11:** GC-MS analysis of **3-78** (Base peak = fragment for *t*-butyl group= 57, Fragment 202=from loss of methyl group)

## 5.6 References

1. Punniyamurthy, T.; Velusamy, S.; Iqbal, J., Recent Advances in Transition Metal Catalyzed Oxidation of Organic Substrates with Molecular Oxygen. *Chem. Rev.*, **2005**, *105* (6), 2329-2364.